國家同步輻射研究中心
National Synchrotron Radiation Research Center

Angle-resolved photoemission spectroscopy of quantum materials

Cheng-Maw Cheng (鄭澄懋)
makalu@nsrrc.org.tw

National Synchrotron Radiation Research Center
Department of Physics, NSYSU

Outline

- Introduction to angle-resolved photoemission spectroscopy (ARPES)
  - Band structure of solids
  - How to probe the electronic structure
  - Scientific cases
- The electronic structure of emergent materials
  - Graphene based materials
  - Beyond graphene : 2D materials
  - Topological insulators (TIs)
  - Toward future electronic devices : nano-focus ARPES
- Summary

100 Years of Photoemission

X-ray[1] Photoelectron spectroscopy, based on the photoelectric effect,[2,3] was developed in the mid-1960's as a practical technique by Kai Siegbahn and his research group at the University of Uppsala, Sweden.[4]

Wilhelm Conrad Röntgen

Heinrich Rudolf Hertz

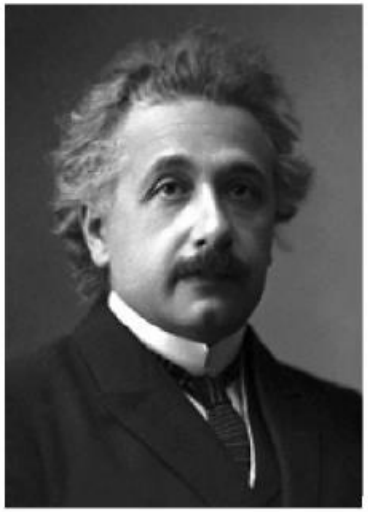

Albert Einstein

Kai M. Siegbahn

1. W. Röntgen, 1901 Nobel Prize in Physics "in recognition of the extraordinary services he has rendered by the discovery of the remarkable rays subsequently named after him."
2. H. Hertz, *Ann. Physik* ***31,983 (1887).***
3. A. Einstein, *Ann. Physik* ***17,132 (1905). 1921 Nobel Prize in Physics "for his services to Theoretical Physics, and especially for his discovery of the*** law of the photoelectric effect."
4. K. Siegbahn, Et. Al.,*Nova Acta Regiae Soc.Sci., Ser. IV, Vol. 20 (1967). 1981 Nobel Prize in Physics "for his contribution to the development of* high resolution electron spectroscopy."

What is photoemission?

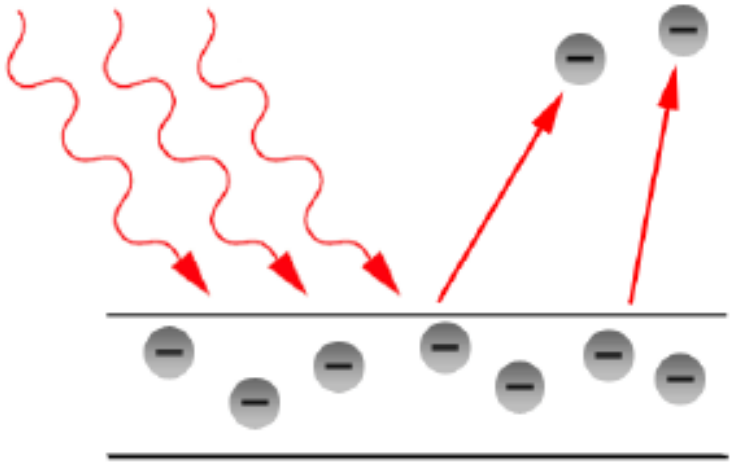

Photon in –> electron out (emission)

What is photoemission spectroscopy? (photoelectron spectroscopy) (PES)

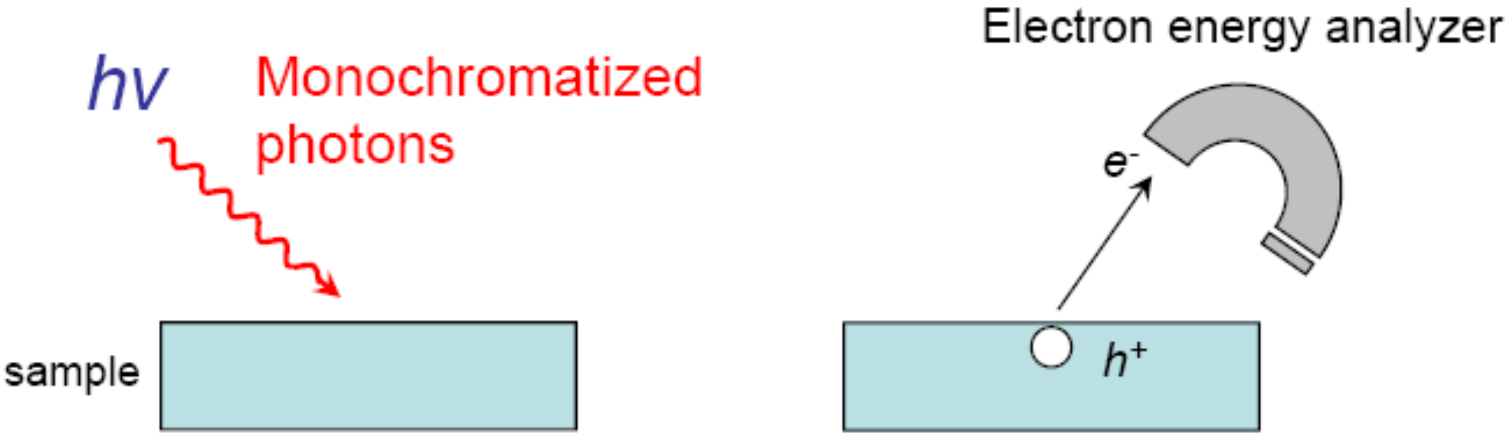

Initial state: ground (neutral) state

Final state: hole (excited) state

Conservation of energy

$E_k = h\nu + E_i - E_f$ (most general expression)

E_k : photoelectron kinetic energy
$E_i(N)$: total initial state system energy
$E_f(N\text{-}1)$: total final state system energy

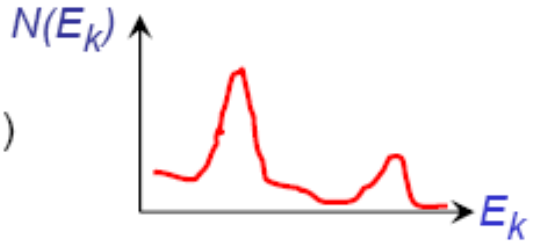

Energy Distribution Curve (EDC) (Spectrum)

The energy level of hydrogen atom

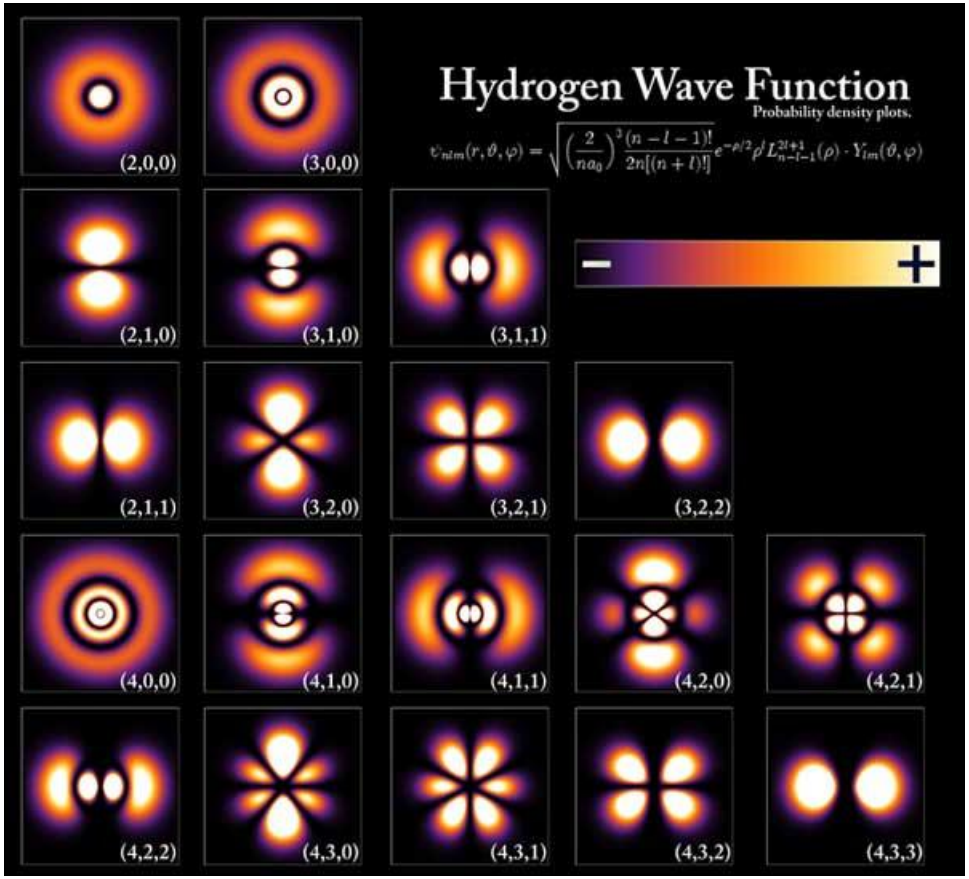

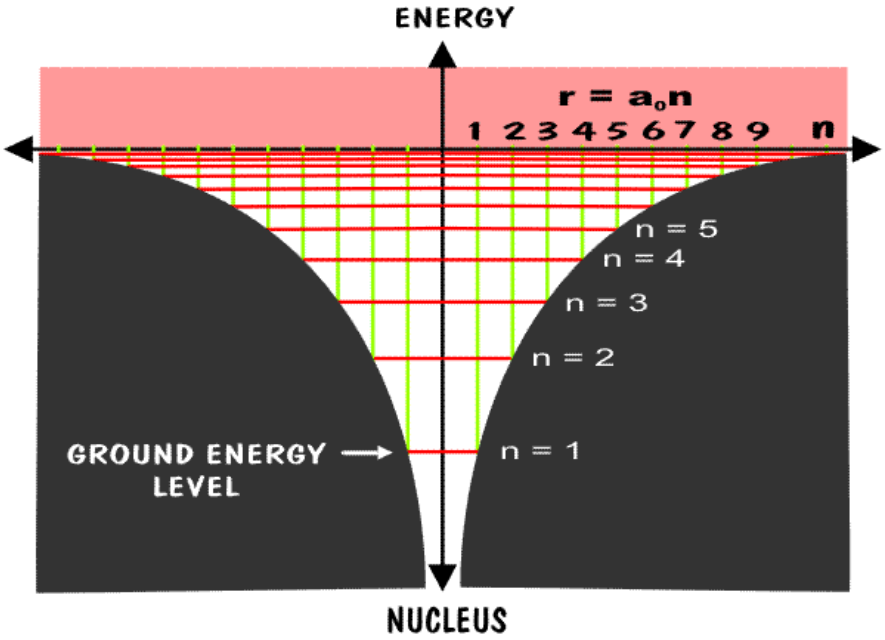

Electron ionization levels are formed from *discrete levels* in an atom

Energy conservation : $h\nu - E_I = KE$

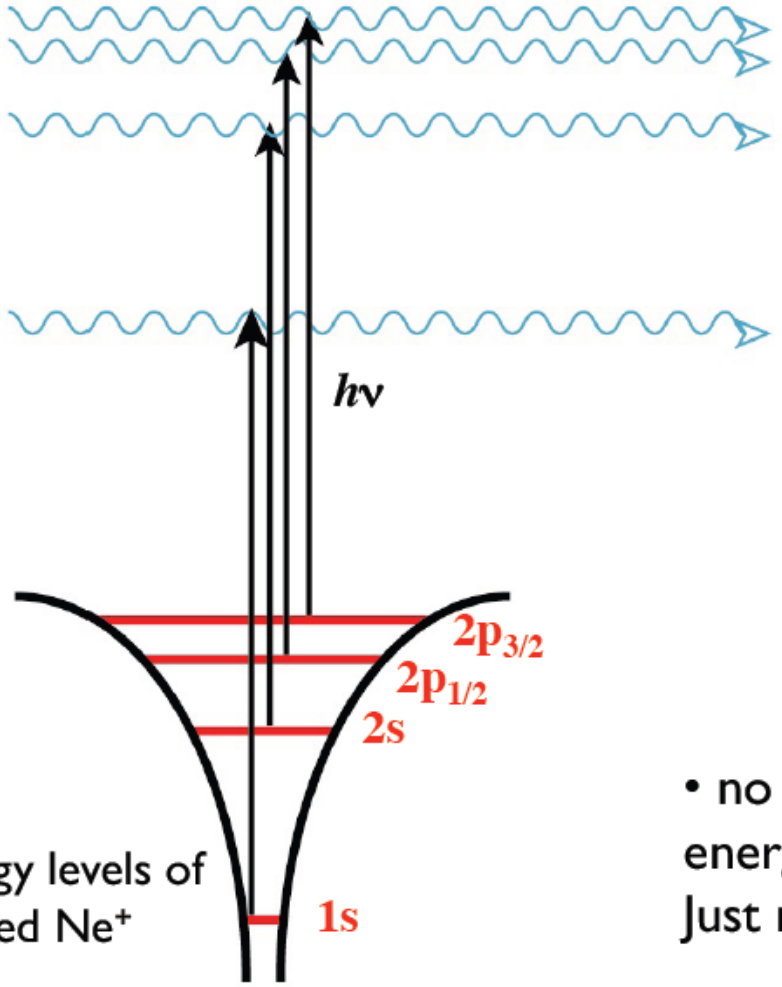

Energy levels of ionized Ne^+

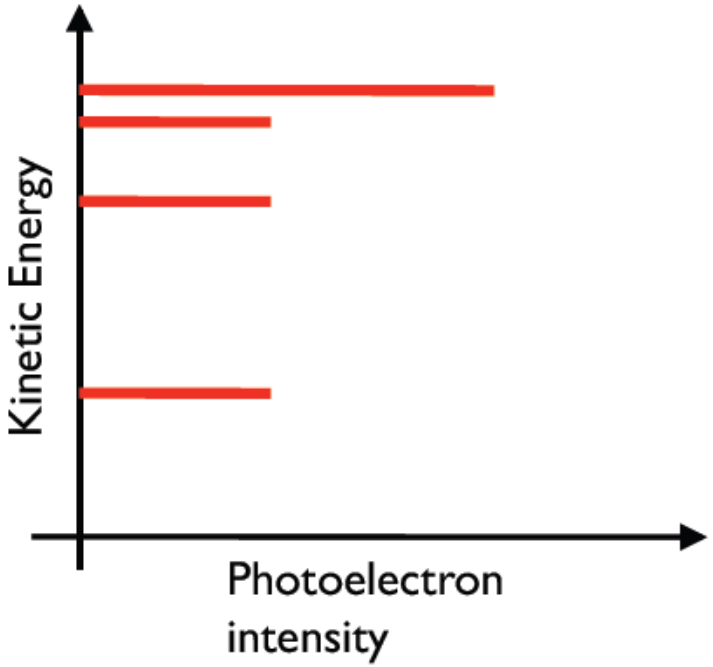

- no need to be on resonance or scan photon energies (e.g. NMR, optical measurements). Just need photons to have high enough energy!

Kyle Shen, IGERT Lecture 2008

Hydrogen atom spectrum

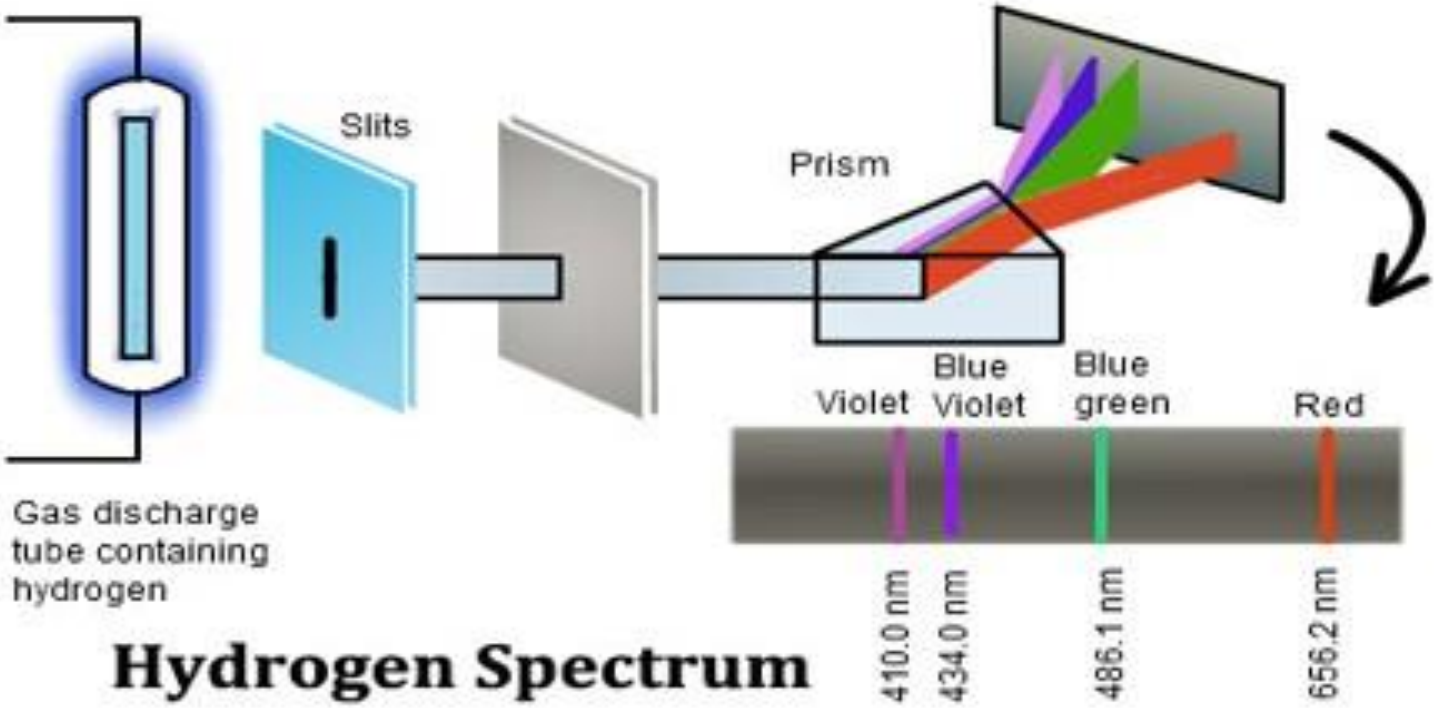

http://www.assignmentpoint.com/science/physics/introduction-of-hydrogen-spectrum.html

Gas phase test

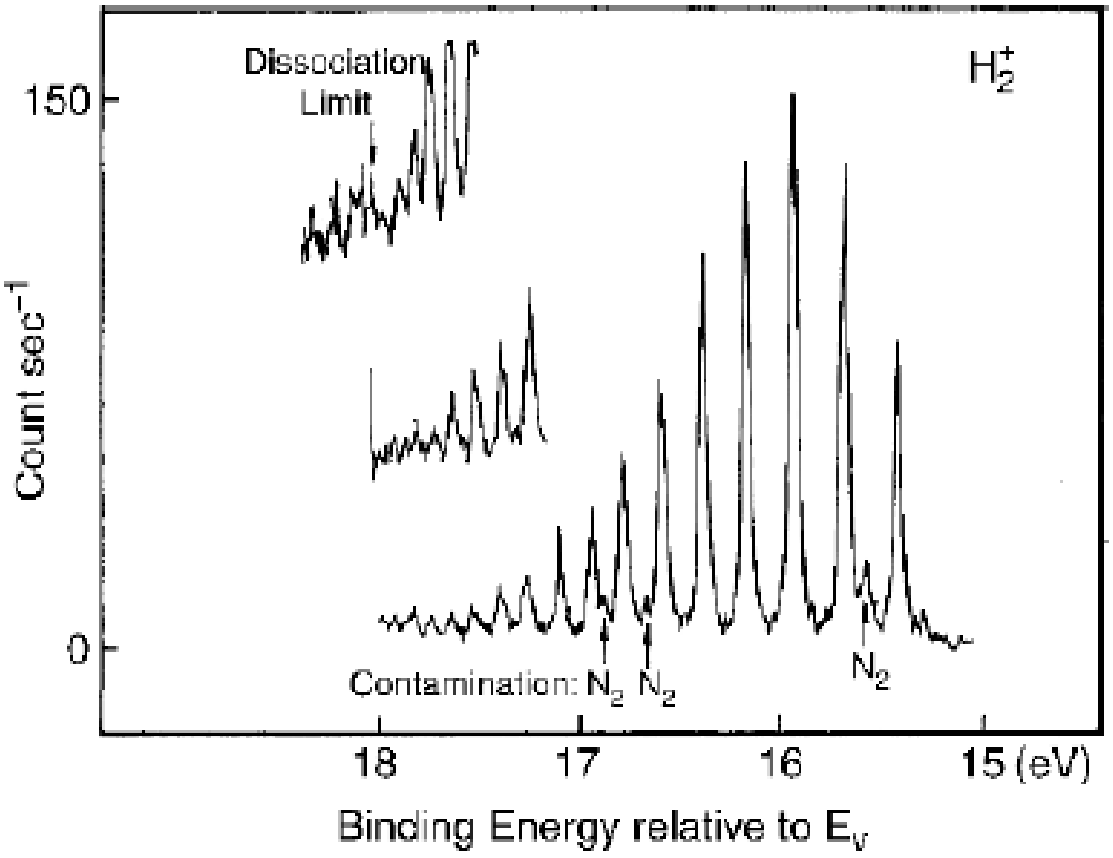

what we are interested in .....

HTSC's

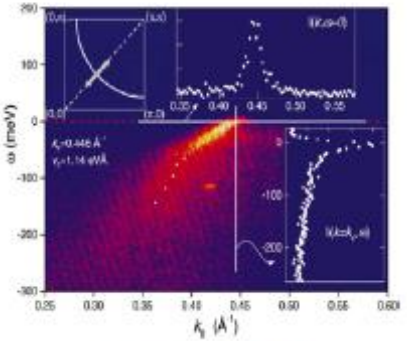

Science 1999

CMR's

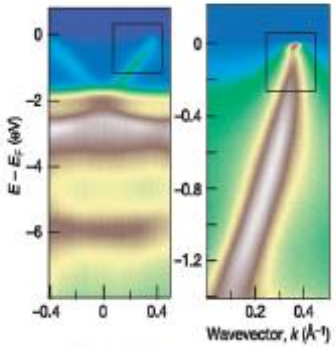

Nature 2005

CDW's

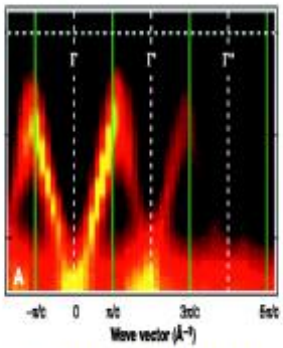

Science 2000

Quasicrystals

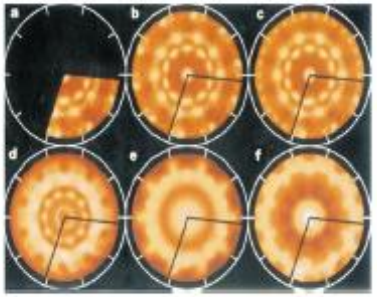

Nature 2000

Quantum Wells

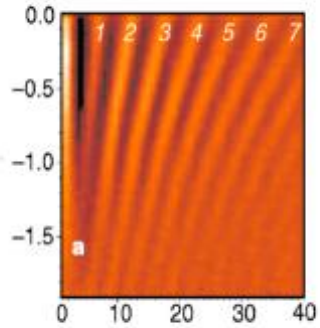

Nature 1999

C_{60}

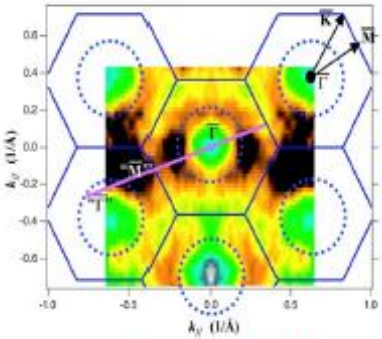

Science 2003

Nanotubes

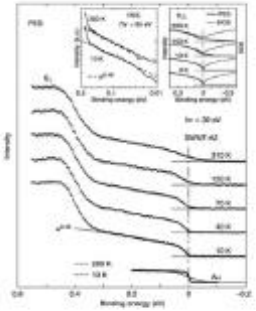

Nature 2003

Diamond

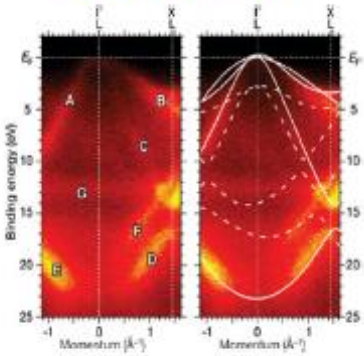

Nature 2005

National Synchrotron Radiation Research Center

The crystal structure and momentum space

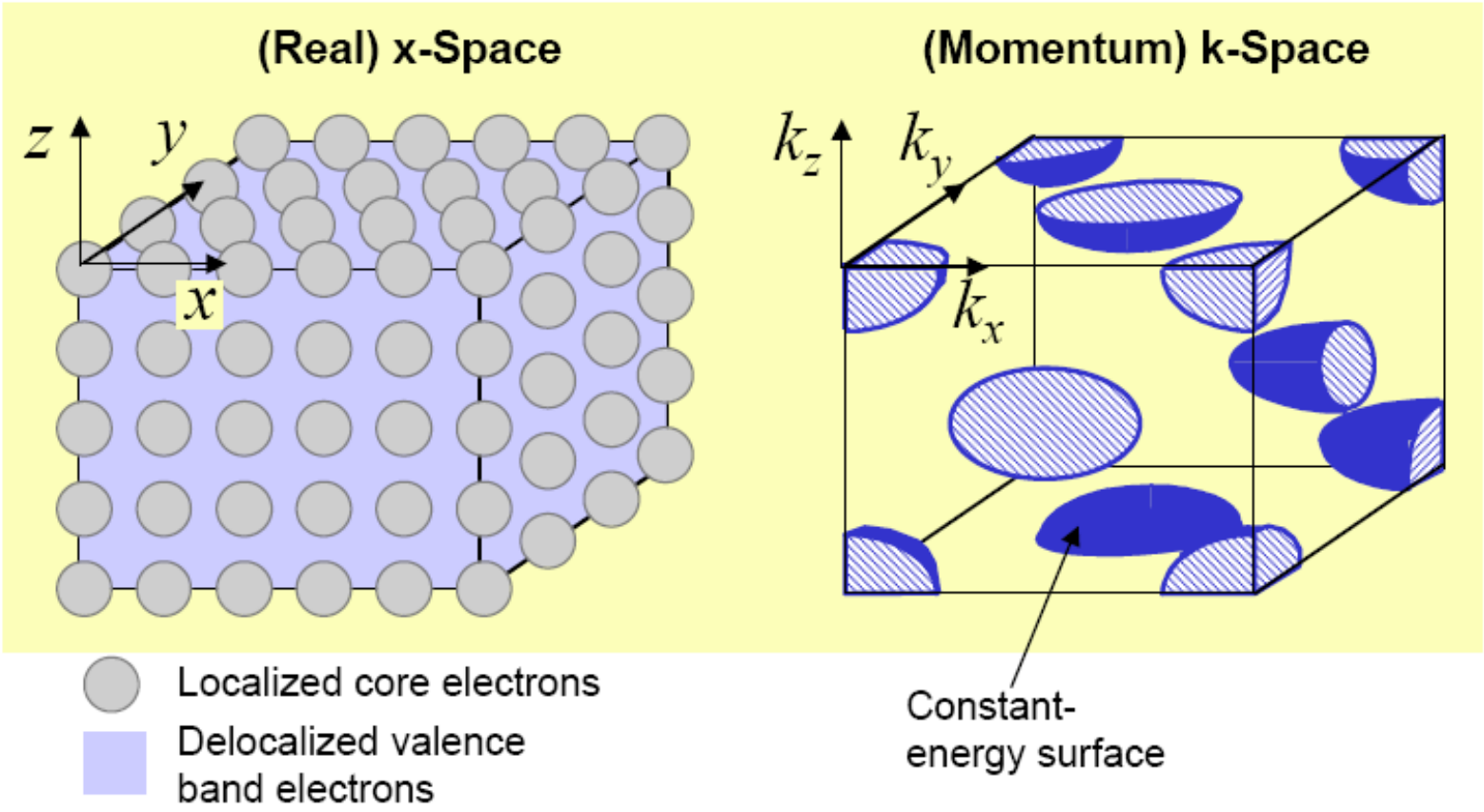

Z. Hussain, ALS summer school

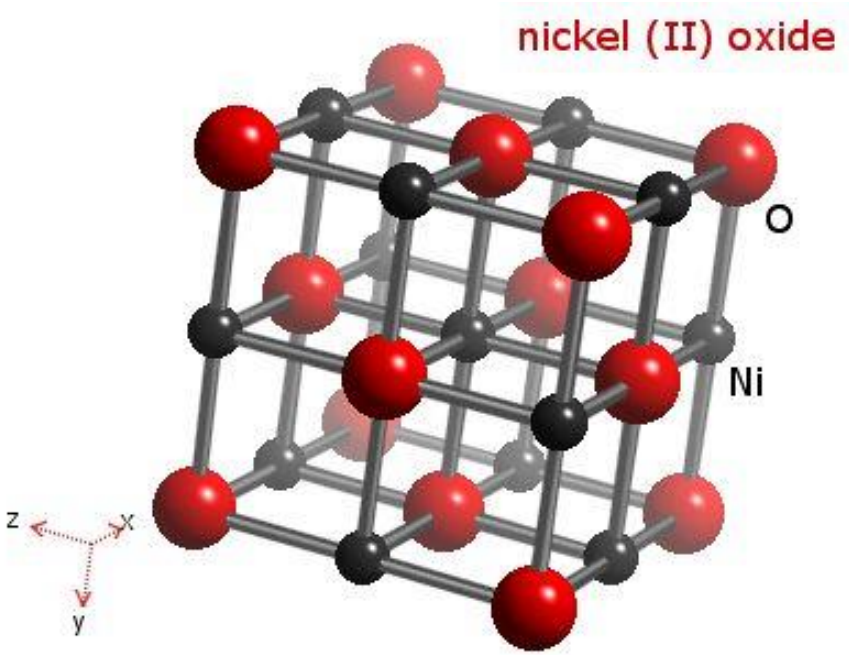

primitive vectors $\mathbf{a_1}$, $\mathbf{a_2}$, $\mathbf{a_3}$

reciprocal lattice vector $\mathbf{b_1}$,$\mathbf{b_2}$,$\mathbf{b_3}$

$$\vec{b}_1 = 2\pi \frac{\vec{a}_2 \times \vec{a}_3}{V}$$

$$\vec{b}_2 = 2\pi \frac{\vec{a}_3 \times \vec{a}_1}{V}$$

$$\vec{b}_3 = 2\pi \frac{\vec{a}_1 \times \vec{a}_2}{V}$$

$$V = \vec{a}_1 \cdot \vec{a}_2 \times \vec{a}_3$$

reciprocal lattice **G** :

$$\vec{G} = l\vec{b}_1 + m\vec{b}_2 + n\vec{b}_3$$

l,*m*,*n* are any integers

- Deeply bound "*core*" electrons remain basically unchanged
- Outermost "*valence*" electrons hybridize forming continuous "*energy bands*"

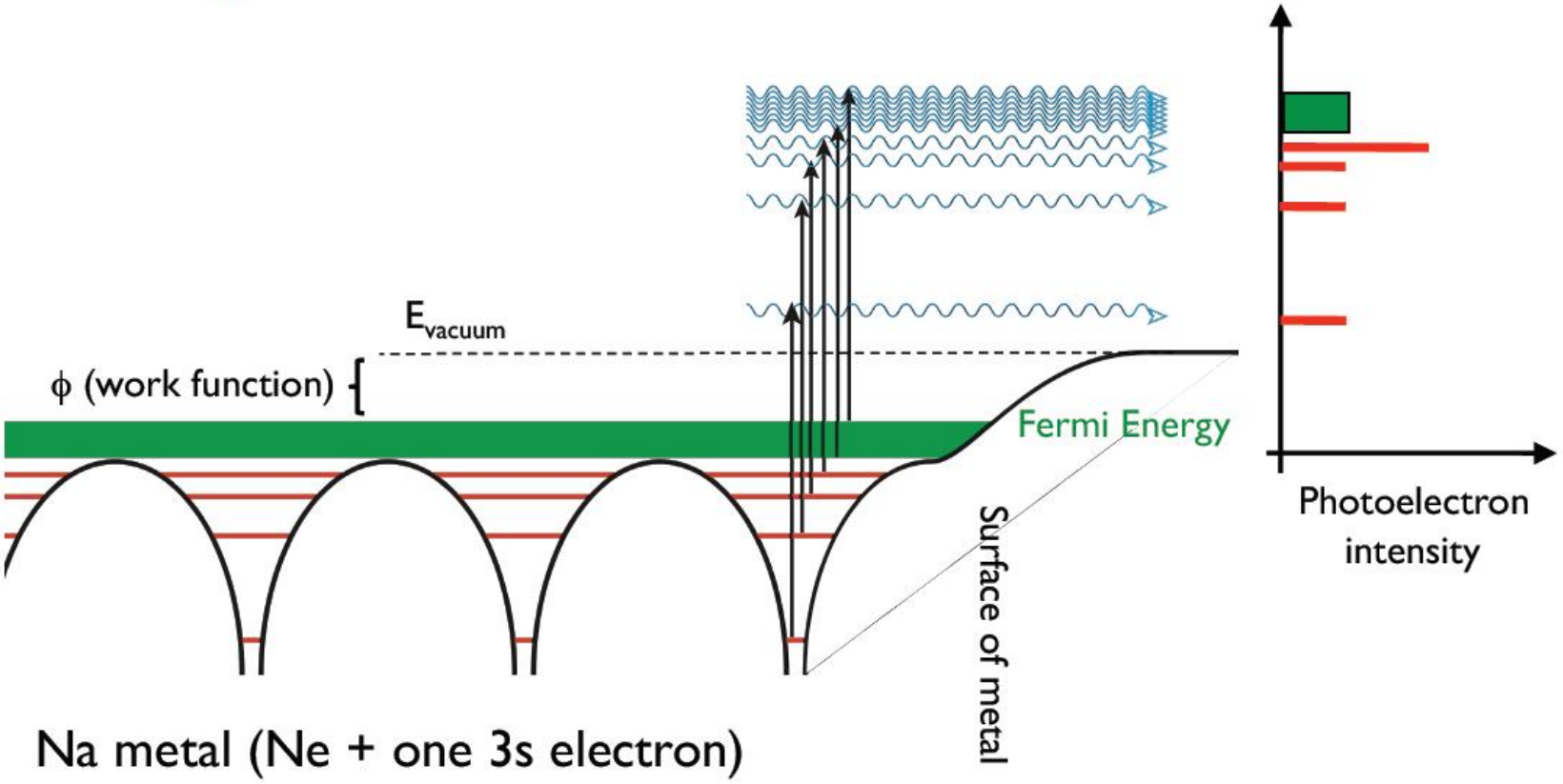

Kyle Shen, IGERT Lecture 2008

Band theory

Two approximations

Nearly free electrons. Electrons are non-interacting in a periodic crystal potential which is relatively weak and can be treated as a perturbation. As in the free-electron-gas model, they are still subject to the Pauli exclusion principle.

Free electron gas :
The interactions between electrons and between electrons and nuclei are turned off, subject only to the Pauli exclusion principle.

Tightly-bonding approximation

Electrons are tightly bound to particular atoms, overlapping only weakly with neighbors.

what we are interested in .....

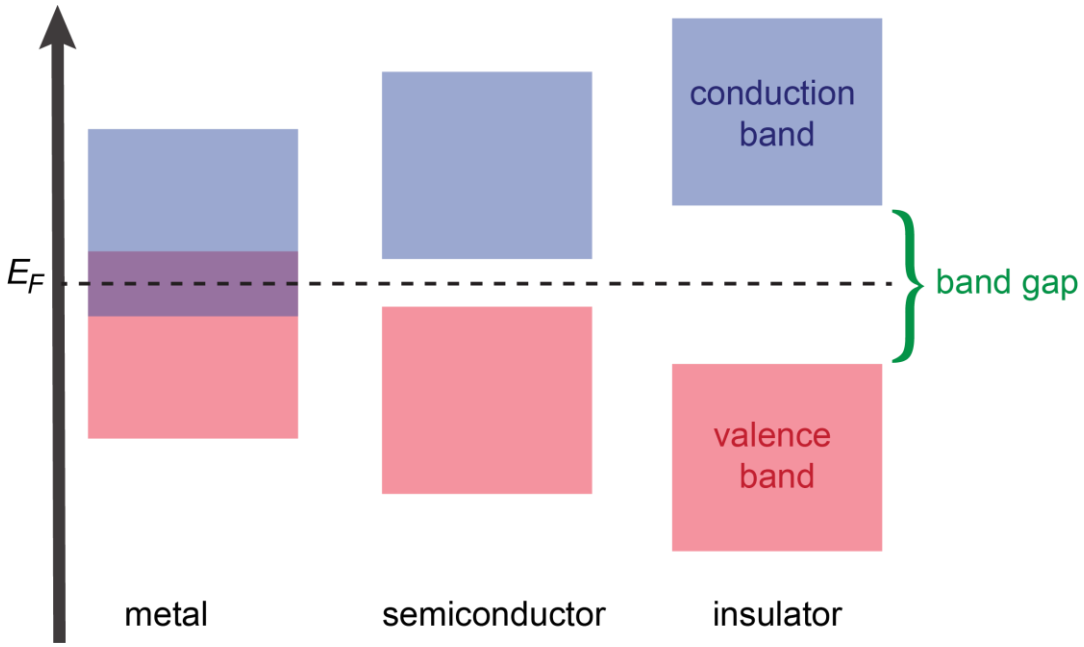

Many properties of a solids are determined by electrons near E_F
(conductivity, magnetoresistance, superconductivity, magnetism)

Fermi-Dirac Distribution

Almost every electronic transport property of solids is proportional to $D(\mathcal{E}_F)$.

Thermal Properties of Free Electron Gas:

Fermi function (Fermi-Dirac distribution)

$$f(\mathcal{E}) = \frac{1}{e^{(\mathcal{E}-\mu)/k_B T} + 1}$$

RT ~ 25 meV

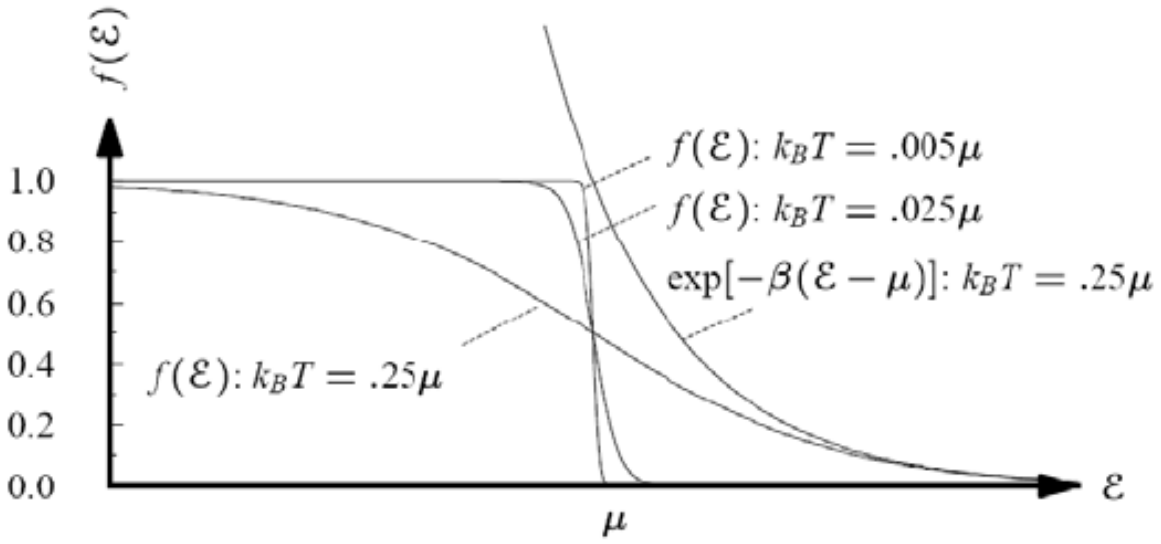

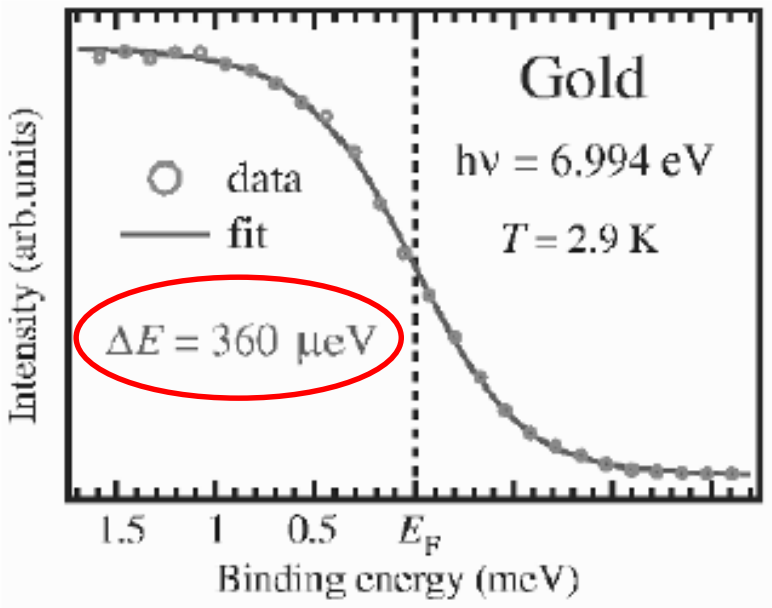

Fig. 2.3. Ultra-high resolution photoemission spectrum on a polycrystalline gold sample (evaporated Au film) for the determination of the energy resolution. The Fermi edge was measured at $T = 2.9\,\mathrm{K}$ using a frequency tripled ($KBe_2BO_3F_2$ crystal, KBBF) YVO_3 laser for the photoexcitation ($h\nu = 6.994\,\mathrm{eV}$) [15]

Hufner, Very high resolution photoelectron spectroscopy

Fermi Surface

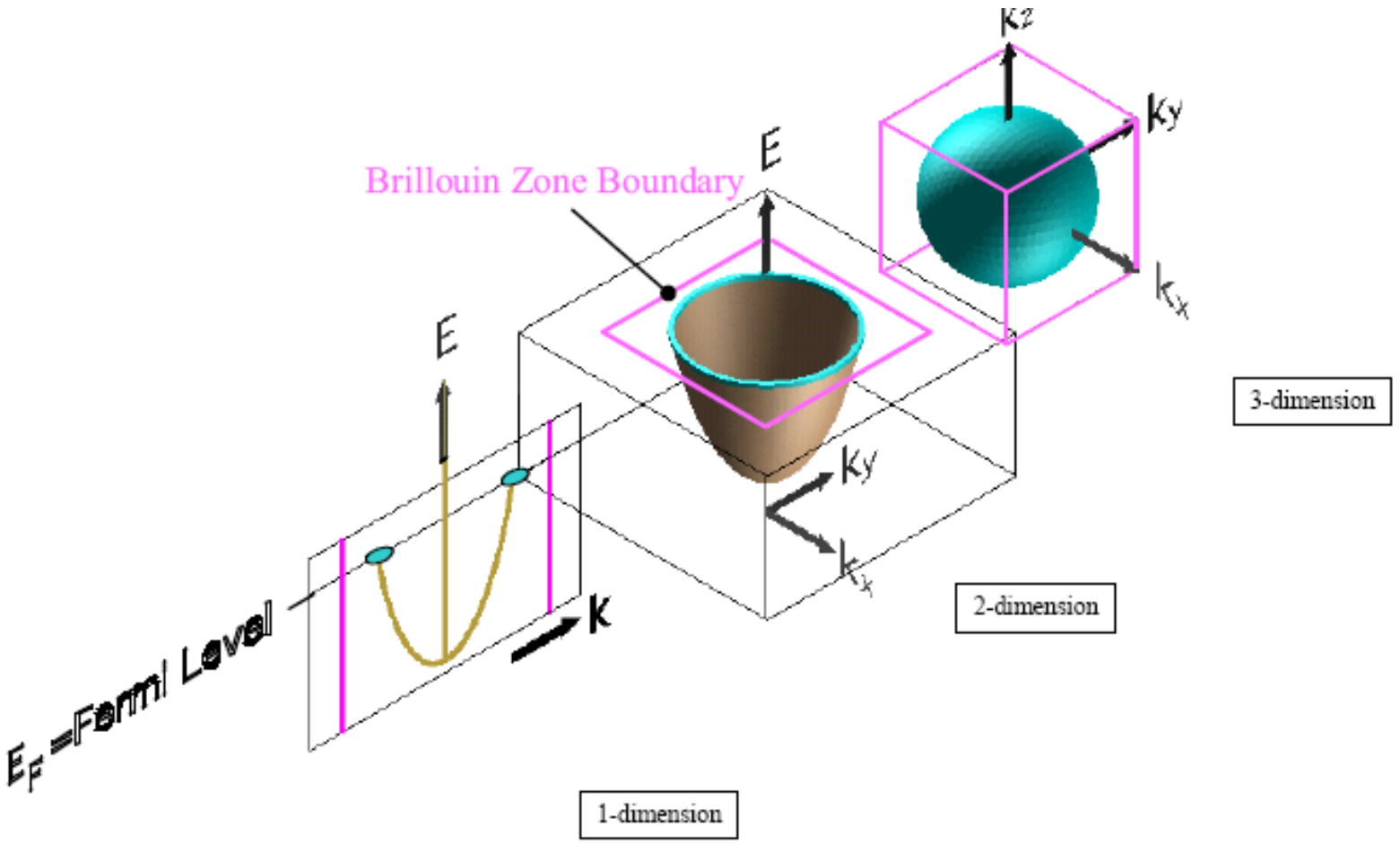

Example: the electronic structure of graphene

研究中心
Research Center

The unit cell of graphene

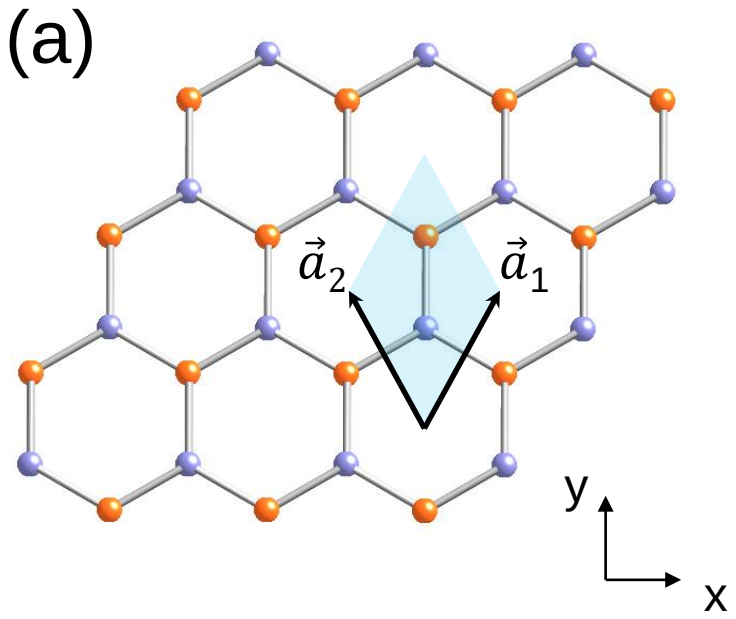

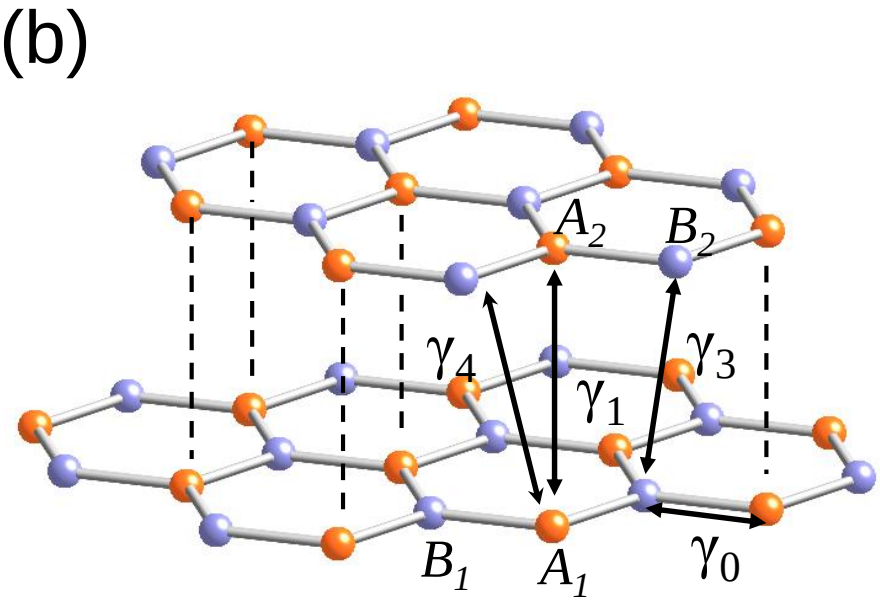

SWMc Hamiltonian of bilayer graphene

$$\mathrm{H}(\vec{k}) = \begin{pmatrix} E_0 + \Delta & \gamma_0 f(\vec{k}) & \gamma_1 & \gamma_4 f^*(\vec{k}) \\ \gamma_0 f^*(\vec{k}) & E_0 & \gamma_4 f^*(\vec{k}) & \gamma_3 f(\vec{k}) \\ \gamma_1 & \gamma_4 f(\vec{k}) & E_0 + \Delta & \gamma_0 f^*(\vec{k}) \\ \gamma_4 f(\vec{k}) & \gamma_3 f^*(\vec{k}) & \gamma_0 f(\vec{k}) & E_0 \end{pmatrix}$$

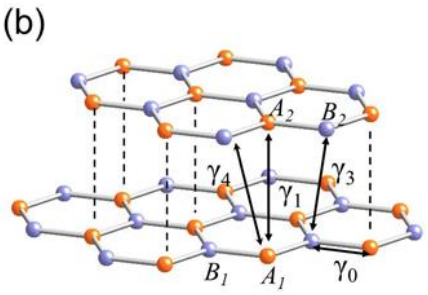

$$f(\vec{k}) = \exp(ik_x a_0/2\sqrt{3}) + 2\exp(-ik_x a_0/2\sqrt{3})\cos(k_y/2)$$

$$\vec{k} = (k_x, k_y)$$

A. Gruneis et al., PRB (2008)

Pure 2D material : graphene

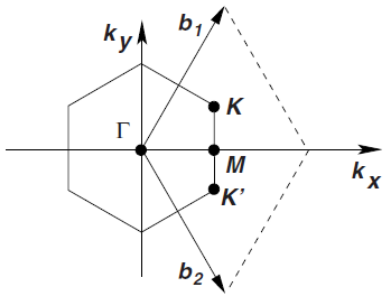

$$\boldsymbol{b}_1 = \frac{2\pi}{3a}(1,\sqrt{3}), \quad \boldsymbol{b}_2 = \frac{2\pi}{3a}(1,-\sqrt{3})$$

$$\boldsymbol{K} = \left(\frac{2\pi}{3a},\frac{2\pi}{3\sqrt{3}a}\right), \quad \boldsymbol{K}' = \left(\frac{2\pi}{3a},-\frac{2\pi}{3\sqrt{3}a}\right)$$

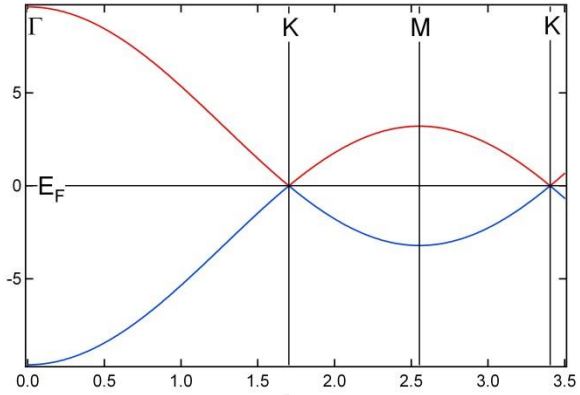

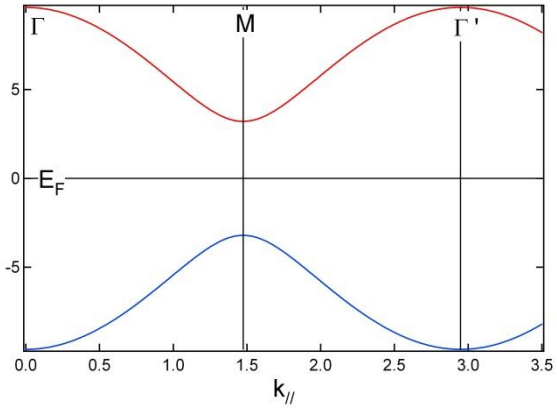

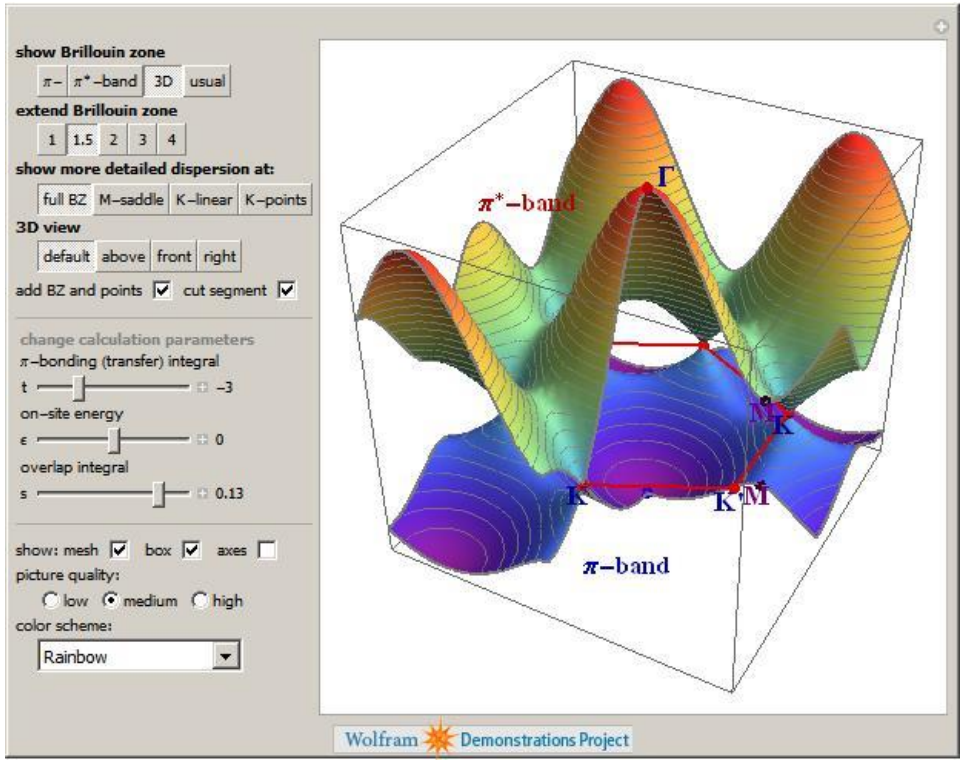

Pure 2D material : graphene

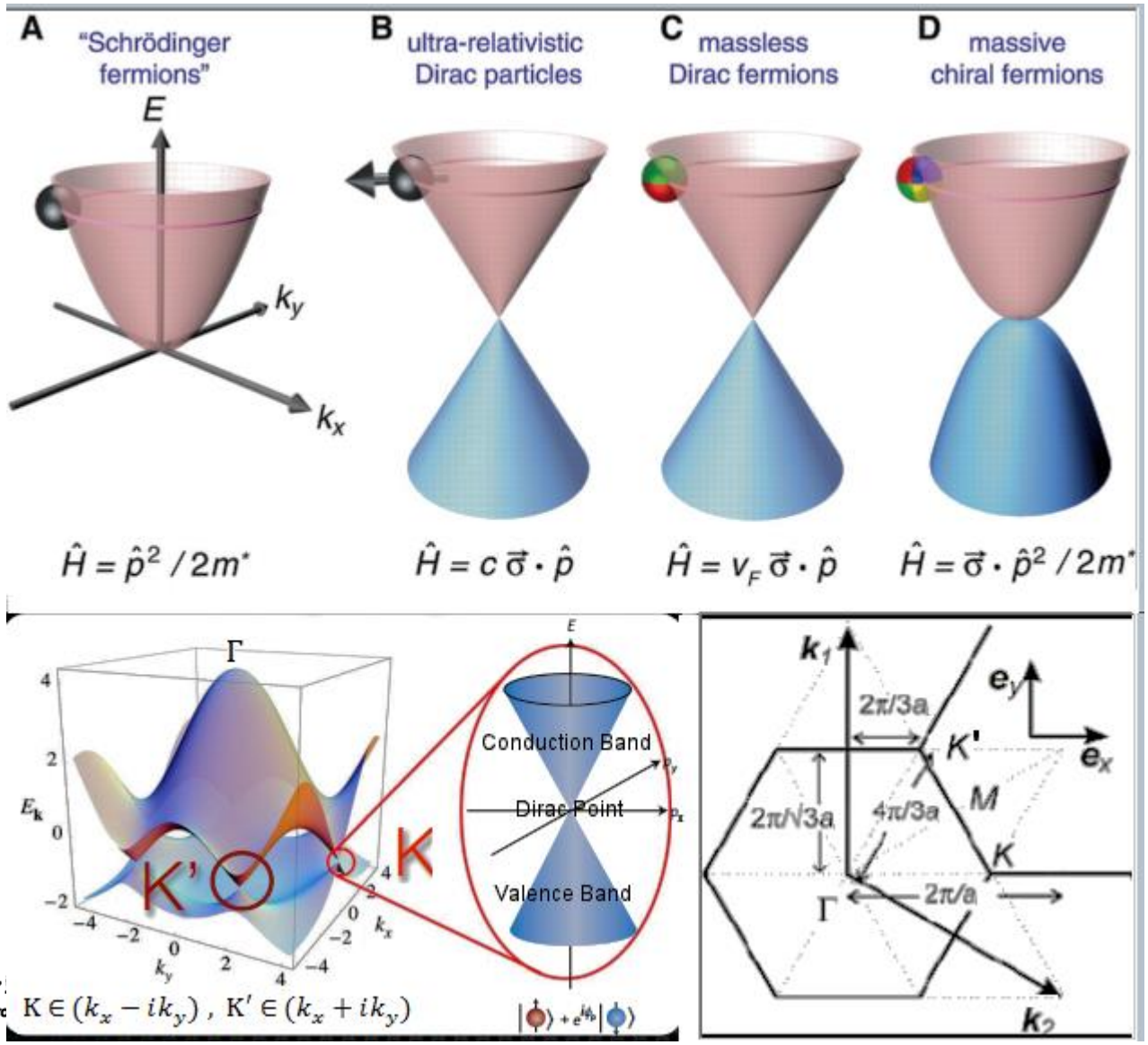

The band structure of graphene/SiC

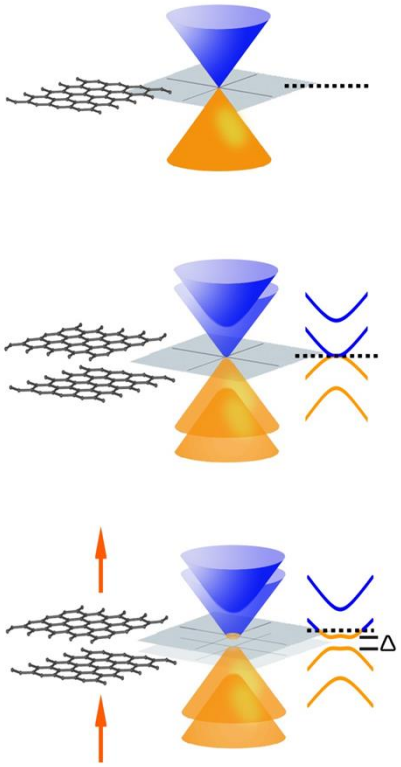

1400 °C 2min
SLG+BLG

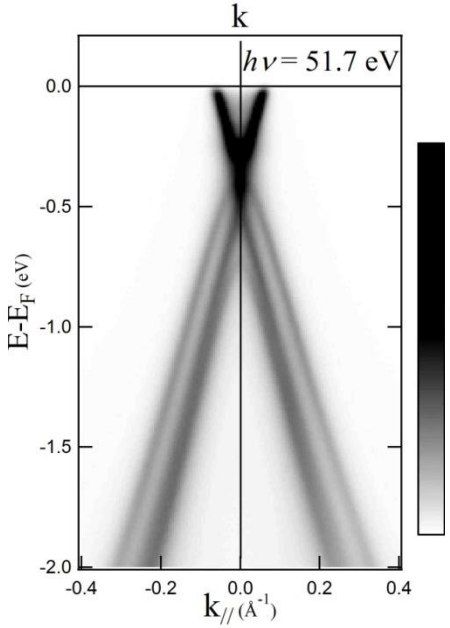

1400 °C 6 min
SLG+BLG

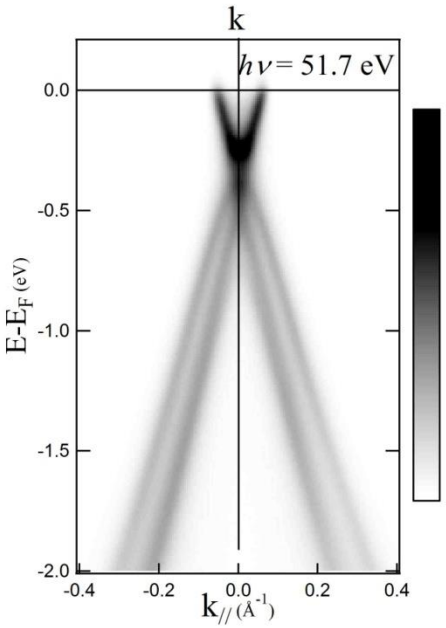

1400 °C 10 min
SLG+BLG

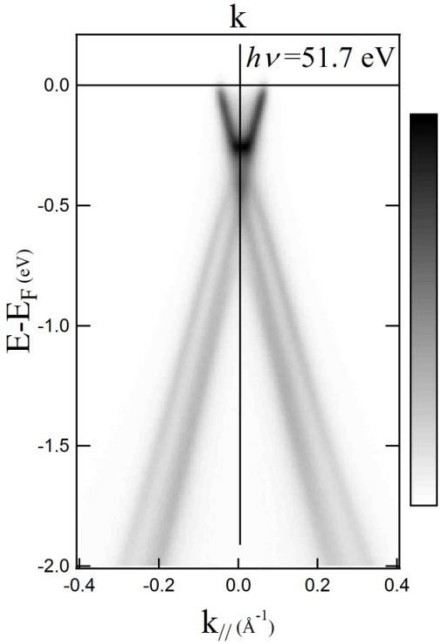

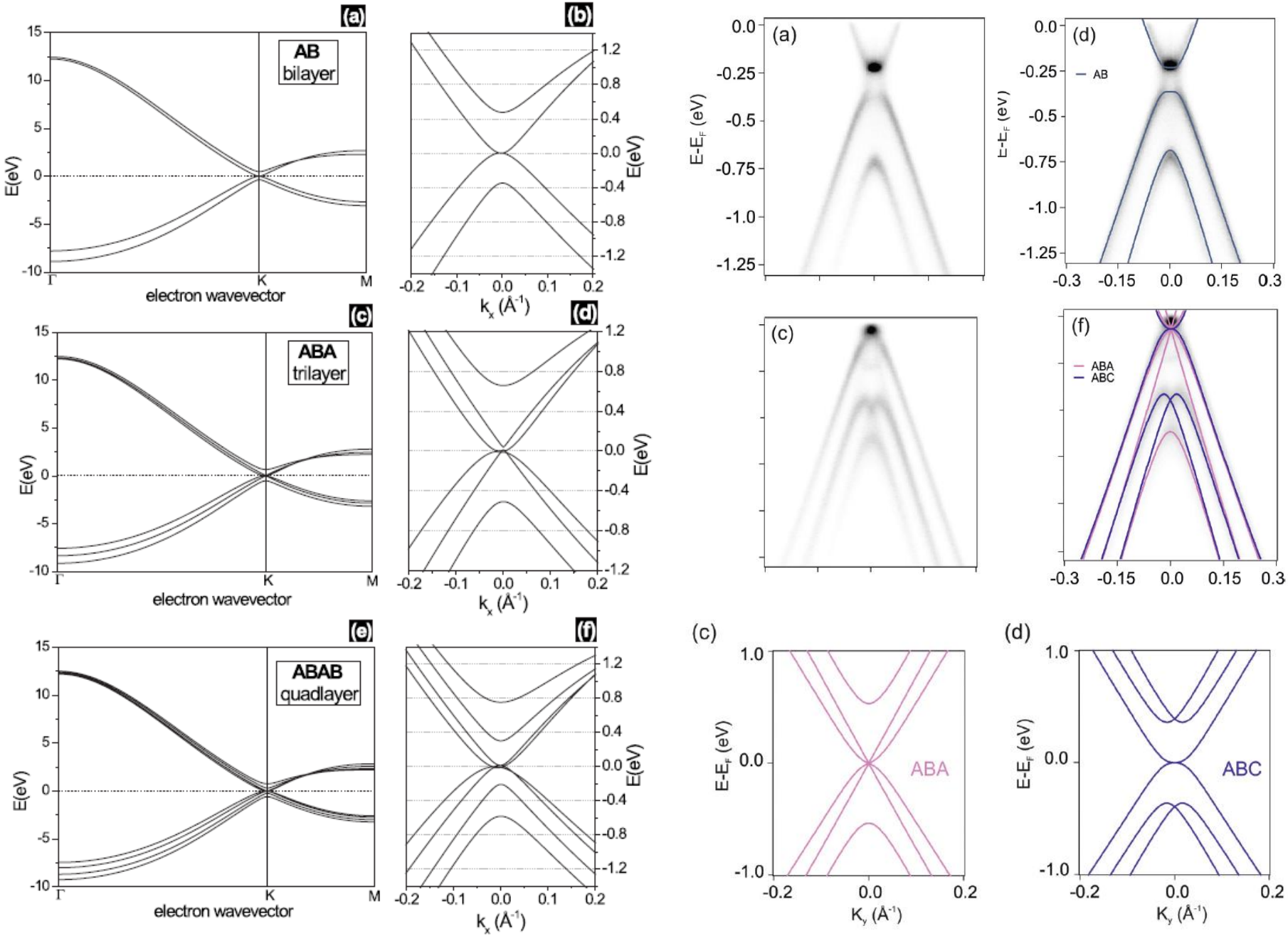

Coletti et al., PRB (2013)

Why orientation of solid so important

conventional ARPES on a large, pure single crystal

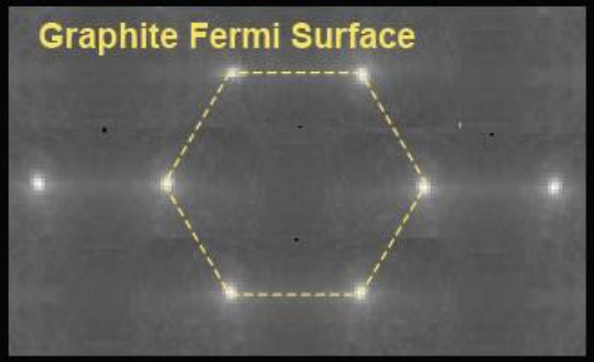

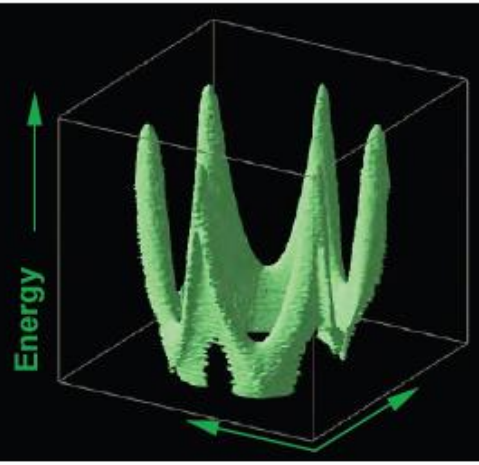

Energy Bands

conventional ARPES of polycrystalline graphite

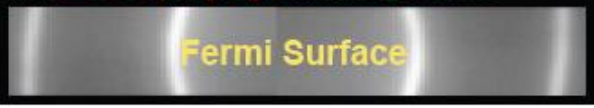

most of the momentum information is lost
as our spot size is much larger than the grain size.

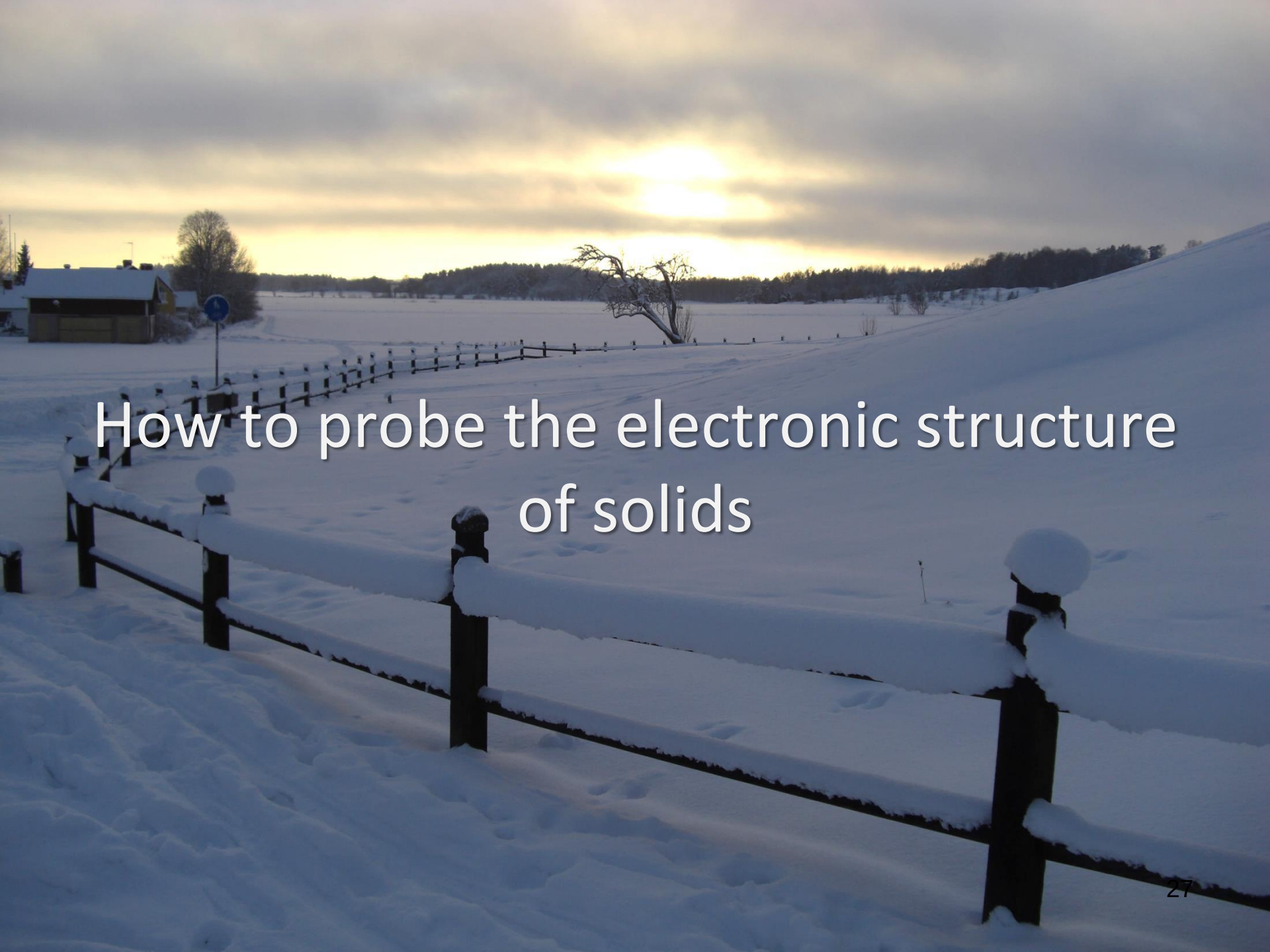
How to probe the electronic structure of solids

The principle of photoemission spectroscopy

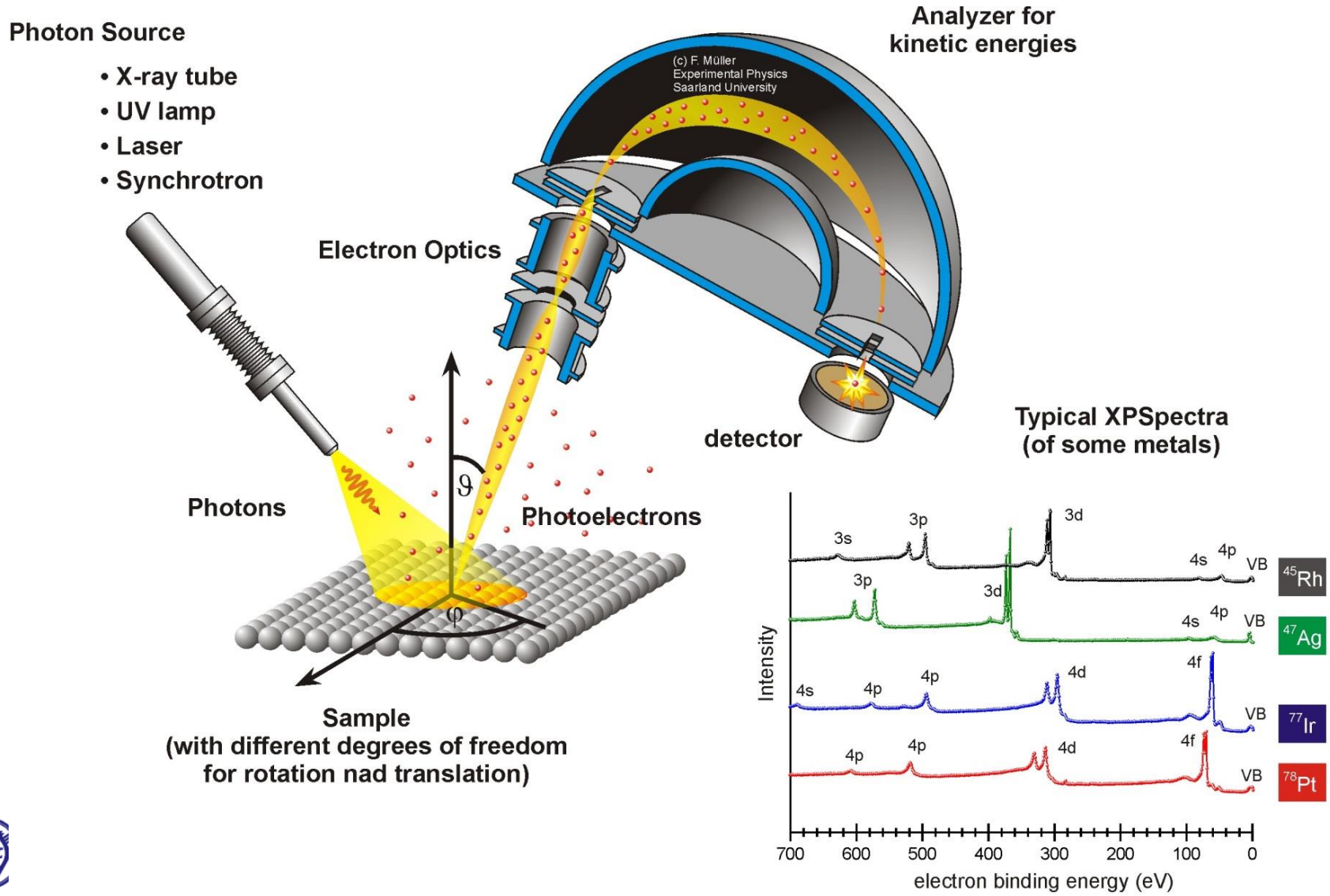

What is photoemission spectroscopy? (photoelectron spectroscopy) (PES)

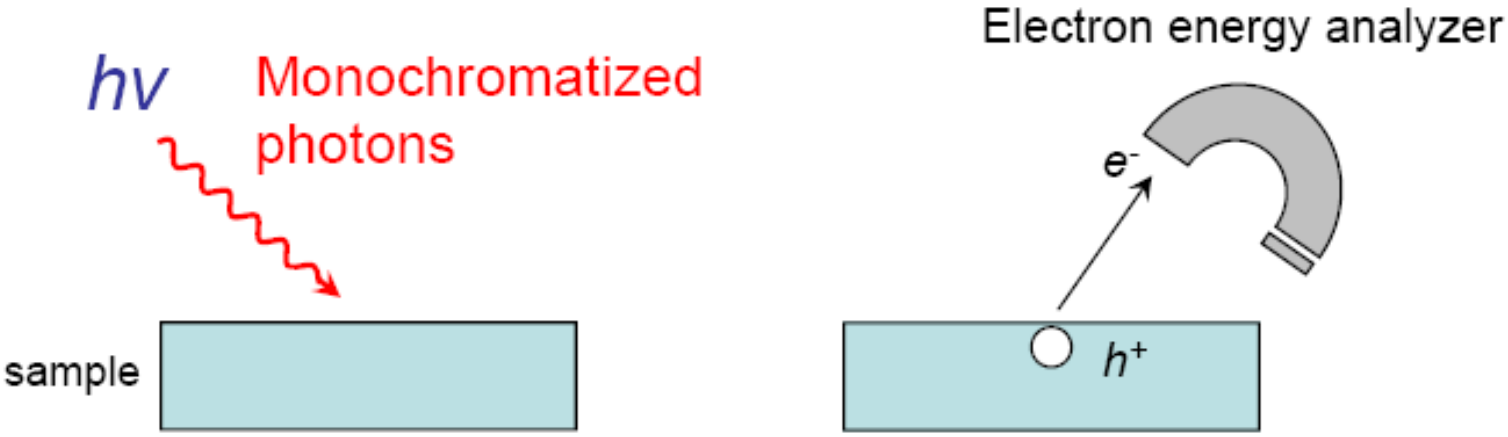

Initial state: ground (neutral) state

Final state: hole (excited) state

Conservation of energy

$E_k = h\nu + E_i - E_f$ (most general expression)

E_k : photoelectron kinetic energy
$E_i(N)$: total initial state system energy
$E_f(N\text{-}1)$: total final state system energy

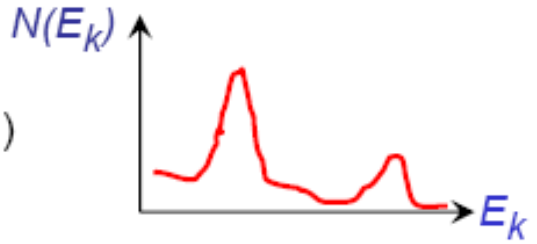

Energy Distribution Curve (EDC) (Spectrum)

The principle of photoemission spectroscopy

- Deeply bound "*core*" electrons remain basically unchanged
- Outermost "*valence*" electrons hybridize forming continuous "*energy bands*"

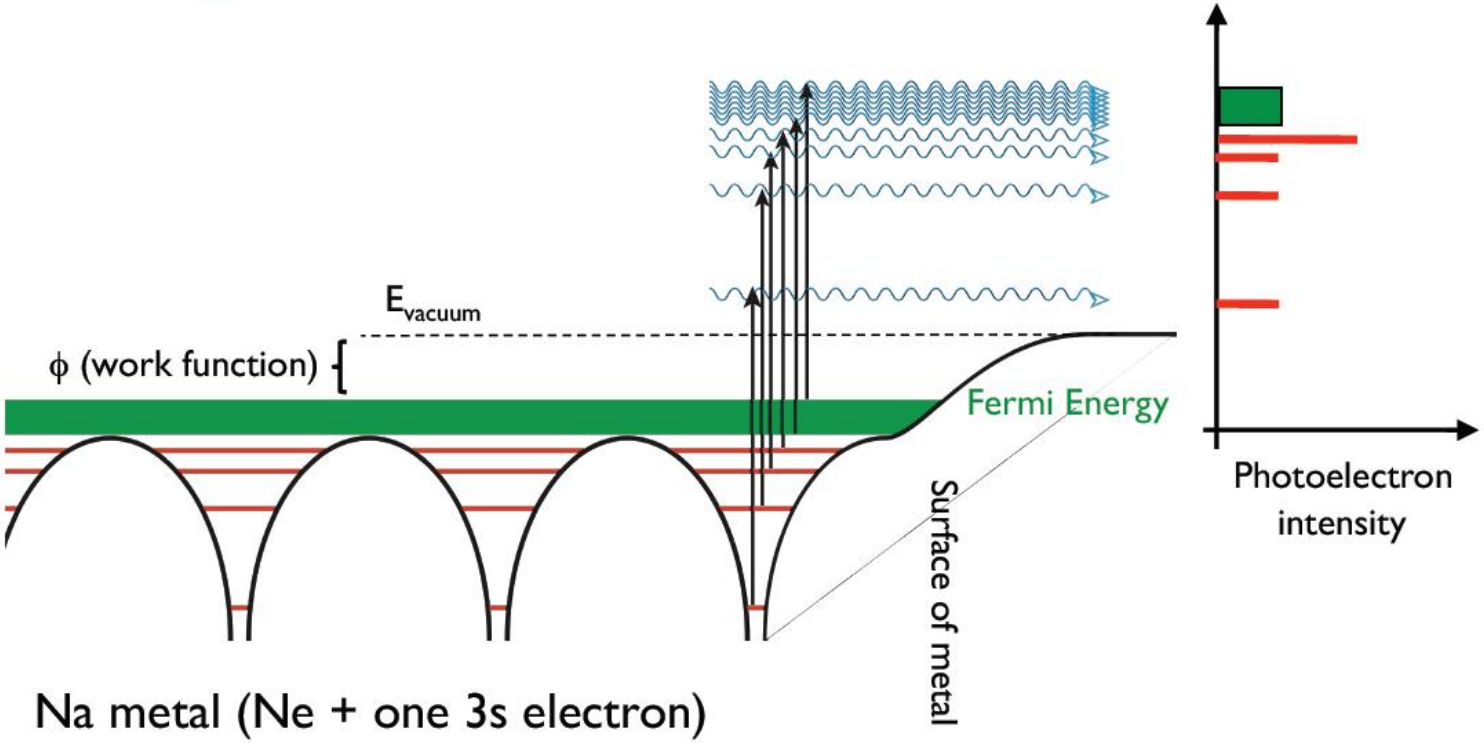

Kyle Shen, IGERT Lecture 2008

What are the samples and probed states?

• Atoms	atomic orbitals (states)
• Molecules	molecular orbitals
	core level states (atomic like)
• Nanoparticles	valence bands/states
	core level states (atomic like)
• Solids	valence bands
	core level states (atomic like)

Kai Seigbahn: Development of X-ray Photoelectron Spectroscopy

C. Nordling E. Sokolowski and K. Siegbahn, *Phys. Rev.* **1957**, *105*, 1676.

Precision Method for Obtaining Absolute Values of Atomic Binding Energies

CARL NORDLING, EVELYN SOKOLOWSKI, AND KAI SIEGBAHN
Department of Physics, University of Uppsala, Uppsala, Sweden
(Received January 10, 1957)

WE have recently developed a precision method of investigating atomic binding energies, which we believe will find application in a variety of problems in atomic and solid state physics. In principle, the method

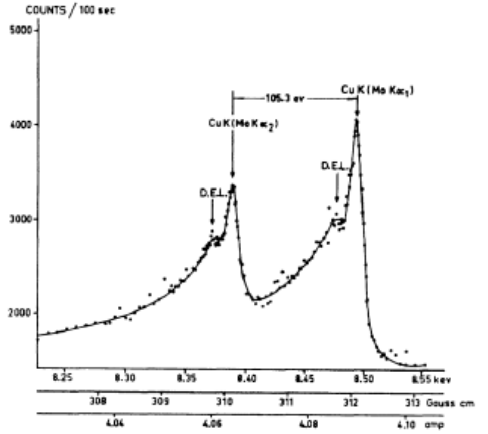

FIG. 1. Lines resulting from photoelectrons expelled from Cu by Mo $K\alpha_1$ and Mo $K\alpha_2$ x-radiation. The satellites marked D.E.L. are interpreted as due to electrons which have suffered a discrete energy loss when scattered in the source.

Nobel Prize in Physics 1981
(His father, Manne Siegbahn, won the Nobel Prize in Physics in 1924 for the development of X-ray spectroscopy)

Photoemission Core Level Spectroscopy

Table 1-1. Electron binding energies, in electron volts, for the elements in their natural forms.

Element	K 1s	L_1 2s	L_2 $2p_{1/2}$	L_3 $2p_{3/2}$	M_1 3s	M_2 $3p_{1/2}$	M_3 $3p_{3/2}$	M_4 $3d_{3/2}$	M_5 $3d_{5/2}$	N_1 4s	N_2 $4p_{1/2}$	N_3 $4p_{3/2}$
1 H	13.6											
2 He	24.6*											
3 Li	54.7*											
4 Be	111.5*											
5 B	188*											
6 C	284.2*											
7 N	409.9*	37.3*										
8 O	543.1*	41.6*										
9 F	696.7*											
10 Ne	870.2*	48.5*	21.7*	21.6*								
11 Na	1070.8†	63.5†	30.65	30.81								
12 Mg	1303.0†	88.7	49.78	49.50								
13 Al	1559.6	117.8	72.95	72.55								
14 Si	1839	149.7*b	99.82	99.42								
15 P	2145.5	189*	136*	135*								
16 S	2472	230.9	163.6*	162.5*								
17 Cl	2822.4	270*	202*	200*								
18 Ar	3205.9*	326.3*	250.6†	248.4*	29.3*	15.9*	15.7*					
19 K	3608.4*	378.6*	297.3*	294.6*	34.8*	18.3*	18.3*					
20 Ca	4038.5*	438.4†	349.7†	346.2†	44.3 †	25.4†	25.4†					
23 V	5465	626.7†	519.8†	512.1†	66.3†	37.2†	37.2†					
24 Cr	5989	696.0†	583.8†	574.1†	74.1†	42.2†	42.2†					
25 Mn	6539	769.1†	649.9†	638.7†	82.3†	47.2†	47.2†					
26 Fe	7112	844.6†	719.9†	706.8†	91.3†	52.7†	52.7†					
27 Co	7709	925.1†	793.2†	778.1†	101.0†	58.9†	59.9†					
28 Ni	8333	1008.6†	870.0†	852.7†	110.8†	68.0†	66.2†					
29 Cu	8979	1096.7†	952.3†	932.7	122.5†	77.3†	75.1†					
30 Zn	9659	1196.2*	1044.9*	1021.8*	139.8*	91.4*	88.6*	10.2*	10.1*			
31 Ga	10367	1299.0*b	1143.2*	1116.4†	159.5†	103.5†	100.0†	18.7†	18.7†			
32 Ge	11103	1414.6*b	1248.1*b	1217.0*b	180.1*	124.9*	120.8*	29.8	28.2			
33 As	11867	1527.0*b	1359.1*b	1323.6*b	204.7*	146.2*	141.2*	41.7*	41.7*			
34 Se	12658	1652.0*b	1474.3*b	1433.9*b	229.6*	166.5*	160.7*	55.5*	54.6*			
35 Br	13474	1782*	1596*	1550*	257*	189*	182*	70*	68*			
36 Kr	14326	1921	1730.9*	1678.4*	292.8*	222.2*	214.4	95.0*	93.8*	27.5*	14.1*	14.1*
37 Rb	15200	2065	1864	1804	326.7*	248.7*	239.1*	113.0*	112*	30.5*	16.3*	15.3 *
38 Sr	16105	2216	2007	1940	358.7†	280.3†	270.0†	136.0†	134.2†	38.9†	21.3	20.1†
39 Y	17038	2373	2156	2080	392.0*b	310.6*	298.8*	157.7†	155.8†	43.8*	24.4*	23.1*
40 Zr	17998	2532	2307	2223	430.3†	343.5†	329.8†	181.1†	178.8†	50.6†	28.5†	27.1†
41 Nb	18986	2698	2465	2371	466.6†	376.1†	360.6†	205.0†	202.3†	56.4†	32.6†	30.8†
42 Mo	20000	2866	2625	2520	506.3†	411.6†	394.0†	231.1†	227.9†	63.2†	37.6†	35.5†
43 Tc	21044	3043	2793	2677	544*	447.6	417.7	257.6	253.9*	69.5*	42.3*	39.9*
44 Ru	22117	3224	2967	2838	586.1*	483.5†	461.4†	284.2†	280.0†	75.0†	46.3†	43.2†
45 Rh	23220	3412	3146	3004	628.1†	521.3†	496.5†	311.9†	307.2†	81.4*b	50.5†	47.3†
46 Pd	24350	3604	3330	3173	671.6†	559.9†	532.3†	340.5†	335.2†	87.1*b	55.7†a	50.9†
47 Ag	25514	3806	3524	3351	719.0†	603.8†	573.0†	374.0†	368.3	97.0†	63.7†	58.3†

Core level binding energies are characteristic of each orbital of each element

Finger prints

Core level BE independent of photon energy used

Auger Electron Spectroscopy

Core electron ionized by photons or high energy electrons
Non-radiative core hole decay
→ Auger electron emission
Radiative decay
→ Fluorescent x-ray emission

Comparison between PES and AES
PES: constant BE, Ek shift with changing photon energy
AES: constant Ek, apparent BE shift with changing photon energy
(synchrotron)

(a) Photoelectric absorption

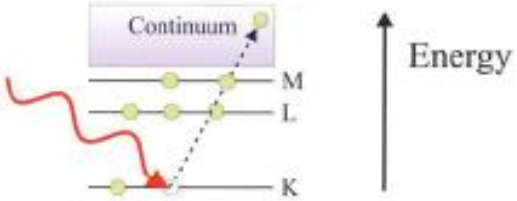

(b) Fluorescent X-ray emission

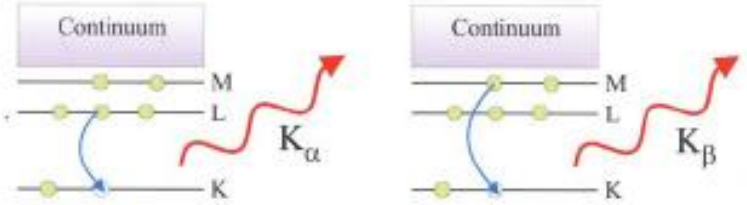

(c) Auger electron emission

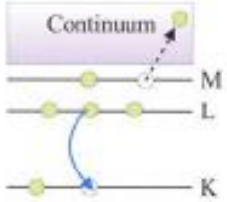

Photoelectron probing Depth

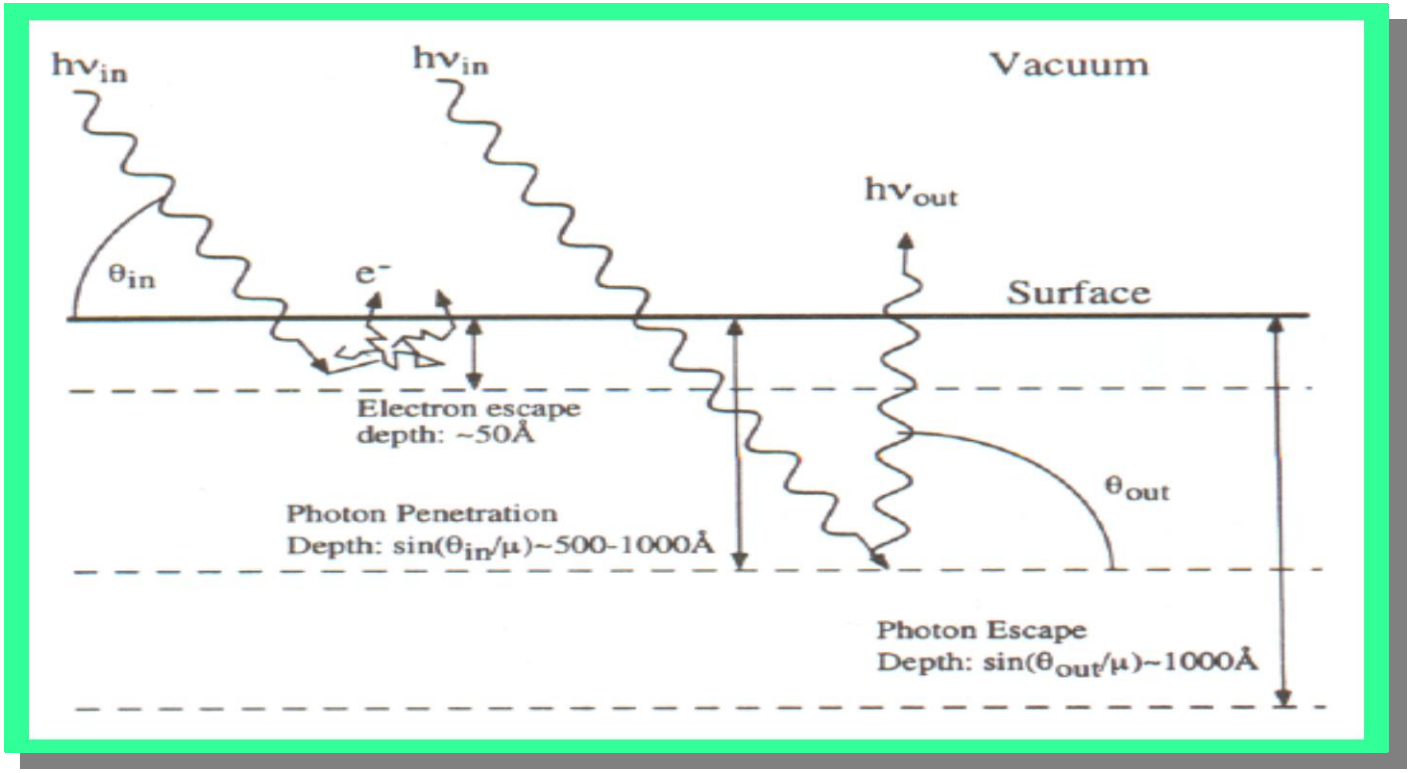

The powerful spectroscopic tools such as XPS and UPS might be limited in in-situ chemical analysis because of the short penetration depth of electrons.

Electron Escape Depth : Surface Sensitivity

Why are electrons so useful as probes of surfaces?

or

Not so useful for studying bulk properties !!

Minimum due to electron-electron scattering, mainly plasmons

PES is a surface sensitive technique! (requires UHV)

High energy photoemission: several keV to increase bulk sensitivity

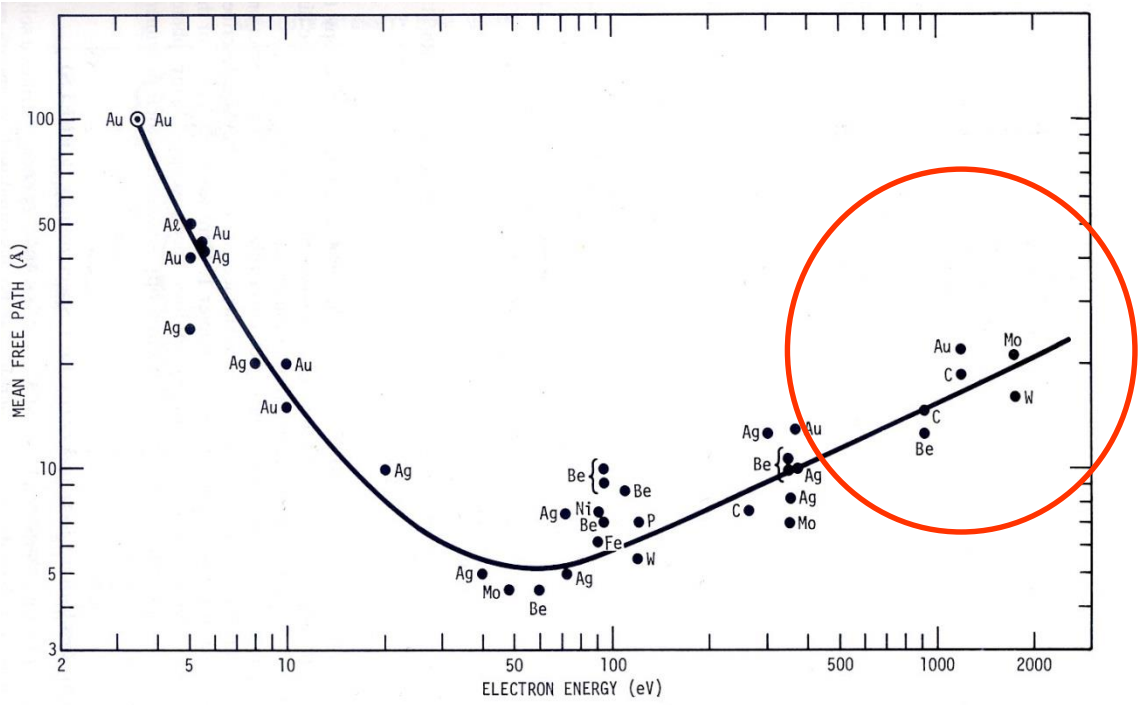

Why ARPES - key technique for the electronic structure mapping

- Angle-resolved photoemission spectroscopy (ARPES) is the most general tool to probe band structure, electronic interactions or spectral function mapping.

- Broad applications: surfaces, thin films, bulk materials, superconductors, magnetic/spin systems, complex materials, topological insulators, graphene based materials, charge density wave materials, low-dimensional systems, artificial stacks, device configurations, etc.

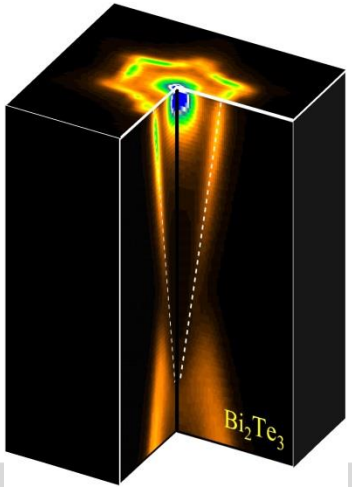

what is ARPES?

Angle-resolved Photoemission Spectroscopy

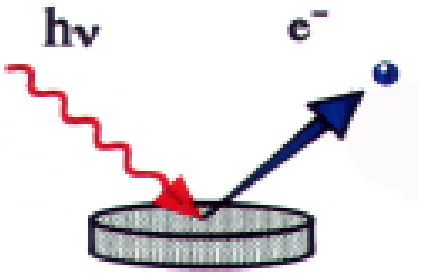

PES

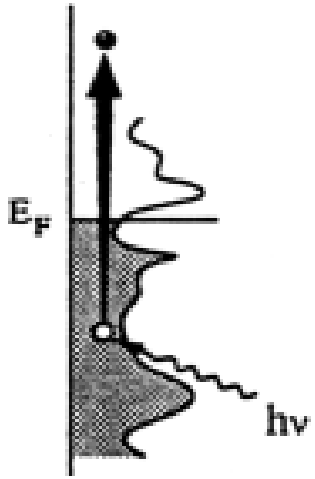

Occupied DOS

Conservation of Energy

$$E_{ph} = E_b + \Phi + E_k$$

Angle-resolved Photoemission Spectroscopy

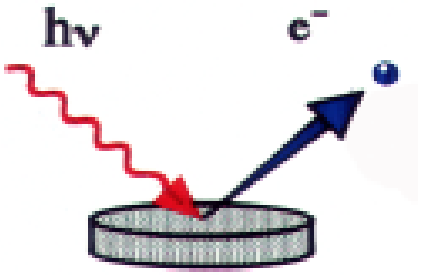

Conservation of Energy

$$E_{ph} = E_b + \Phi + E_k$$

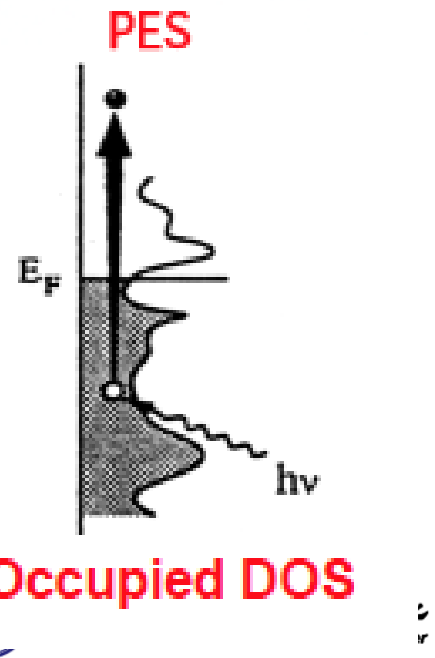

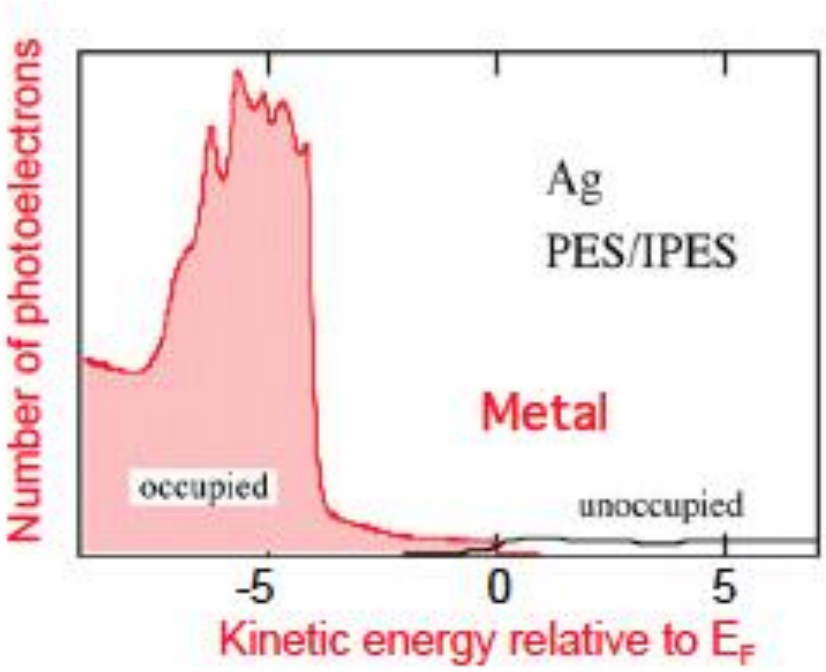

Angular Resolved Photoemission Spectroscopy(ARPES)

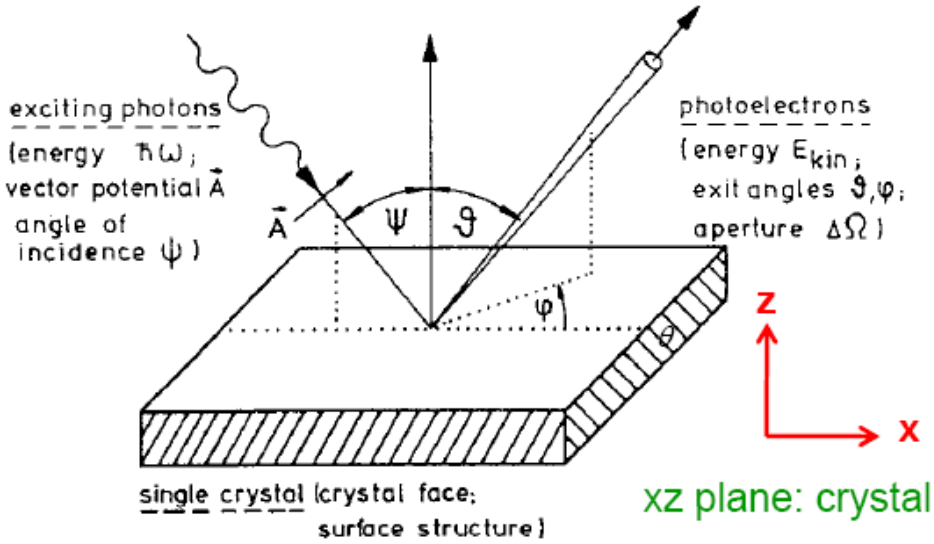

xz plane: crystal symmetry plane

Electron emission angle: θ

Photon incident angle: ψ, *s*- and *p*-polarization

$$k_{//} = \sqrt{\frac{2m}{\hbar^2} E_k} \cdot \sin\theta$$

$$k_{//}(\text{Å}^{-1}) = 0.5123\sqrt{E_k(eV)} \cdot \sin\theta$$

$k_{||}$(inside) = $k_{||}$(outside)

Conservation of liner momentum

Important for 3D and 2D band mapping

$$k_{\perp} = 0.5123\sqrt{(E_{kin}\cos^2\theta + V_0)}$$

Conservation of linear momentum parallel to the surface

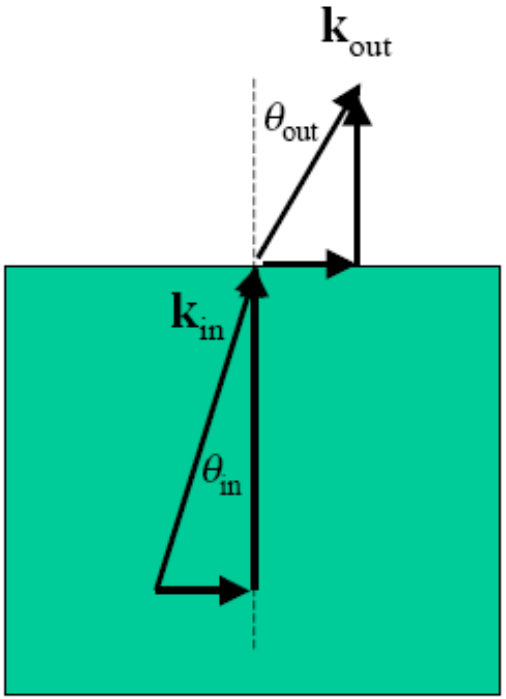

Kinematic relations

$$k_{out} = \sqrt{\frac{2m}{\hbar^2} E_{kin}}$$

$$k_{in} = \sqrt{\frac{2m}{\hbar^2} (E_{kin} + V_0)}$$

$$k_{out,\parallel} = k_{in,\parallel} \equiv k_{\parallel}$$

"Snell's Law"

$$k_{\parallel} = \sin\theta_{out} \sqrt{\frac{2m}{\hbar^2} E_{kin}} = \sin\theta_{in} \sqrt{\frac{2m}{\hbar^2} (E_{kin} + V_0)}$$

Critical angle for emission

$$(\sin\theta_{out})_{\max} = \sqrt{\frac{E_{kin}}{E_{kin} + V_0}}$$

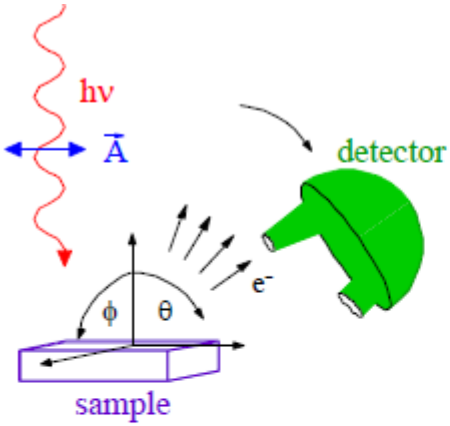

Intensity $\propto \sum_{i,f} \left| \langle f | \vec{p} \cdot \vec{A} | i \rangle \right|^2 A(\vec{k}, E) f(E)$

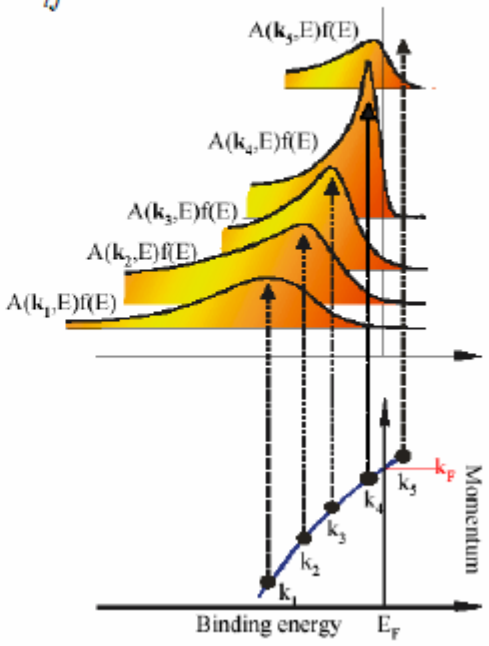

Electron momentum Parallel to the surface is conserved

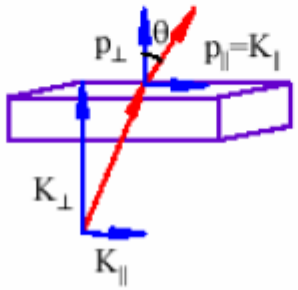

$$k_{\perp} = 0.5123\sqrt{(E_{kin}\cos^2\theta + V_0)}$$

$$k_{//} = 0.5123\sqrt{E_{kin}}\sin\theta$$

- **Low photon energy provides better momentum resolution, but the covering range of BZ is also small.**
- **We expect to study the electronic structure of solids at VUV region (10 eV~ 100 eV).**

Early ARPES experimental result

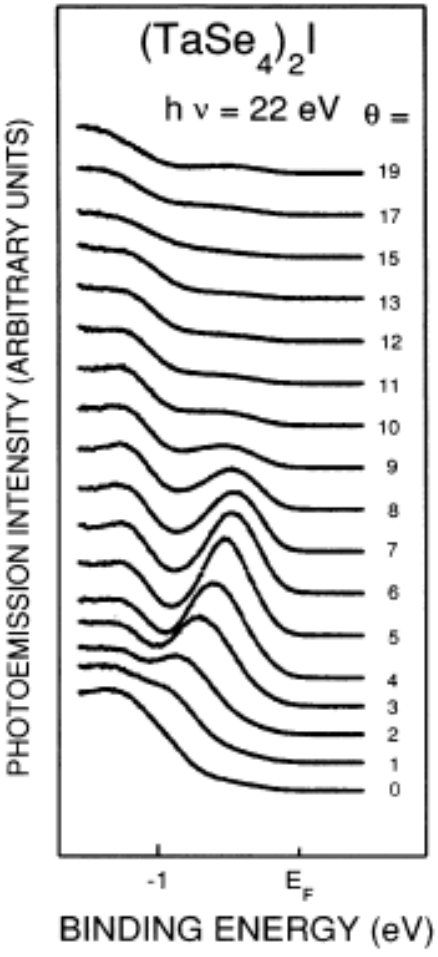

FIG. 1. A series of high-energy-resolution angle-resolved photoemission spectra, taken along the direction of the sample and for different values of the azimuthal angle.

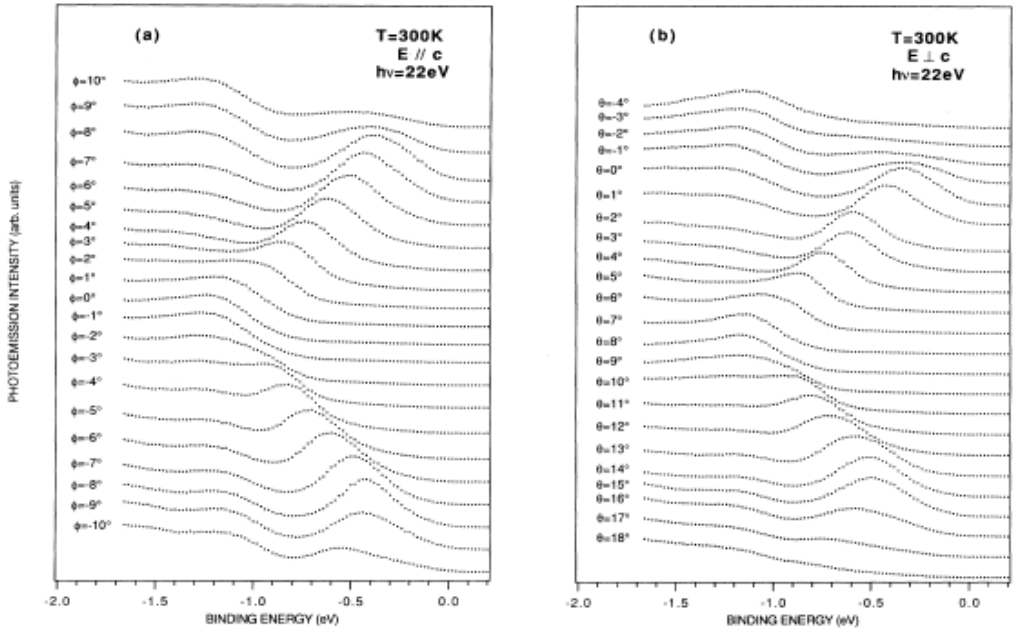

FIG. 1. Angle-resolved photoemission spectra taken using 22-eV photon energy, at room temperature, for photon electric field (a) parallel and (b) perpendicular to the conducting axis. The emission angle is along the conducting axis, with the surface normal defined as 0°.

Now a 2-D detector with $\pm 30^{\circ}$ and 0.1° angular resolution can be obtained.

Au(111) : The inversion symmetry is broken at the surface

$$H = \frac{\hbar}{\quad}(\vec{\nabla}V \wedge \vec{p})\cdot\vec{\sigma}$$

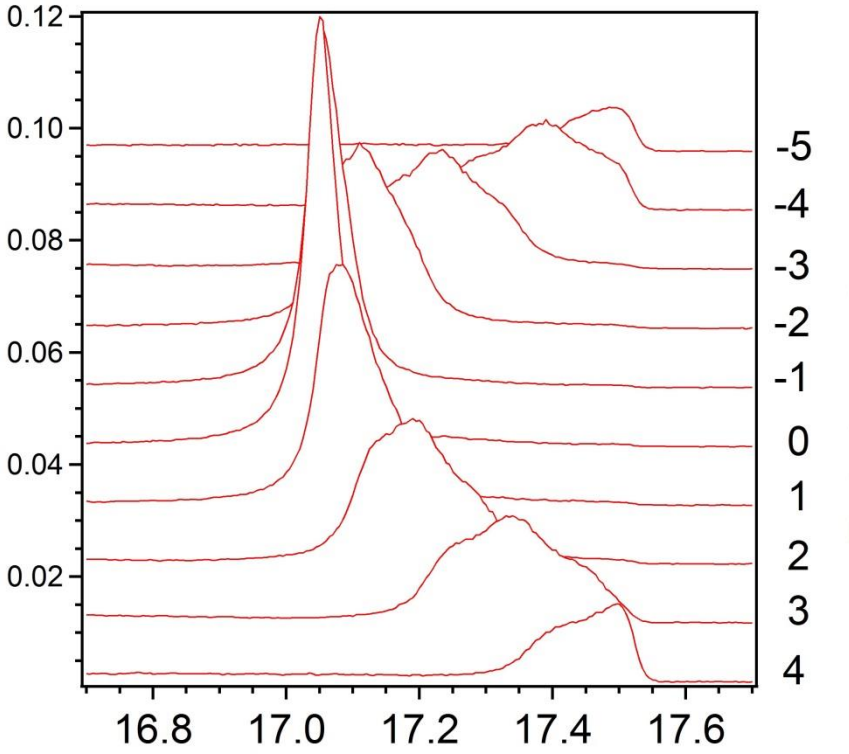

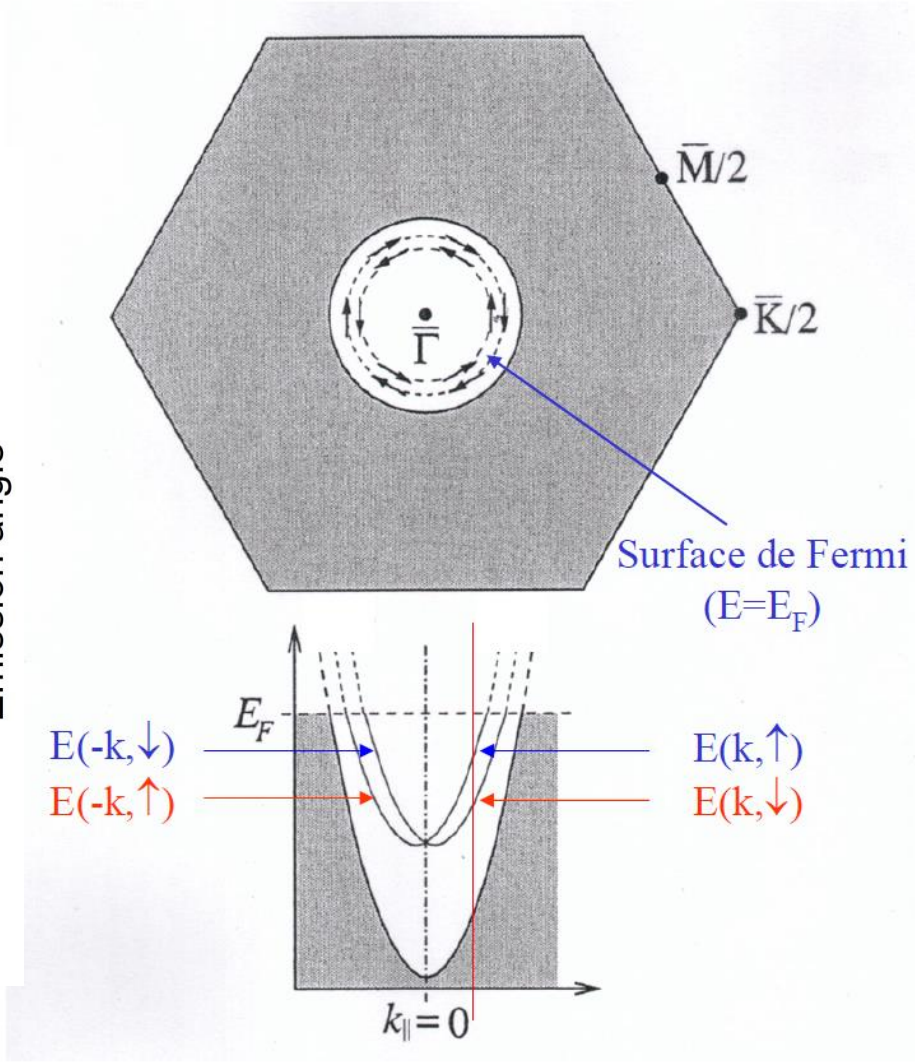

two spin polarized SS bands

Typical Experimental Result with 2D detector

Accumulate spectra of Rashba effect on Au(111) as the angle is scanned

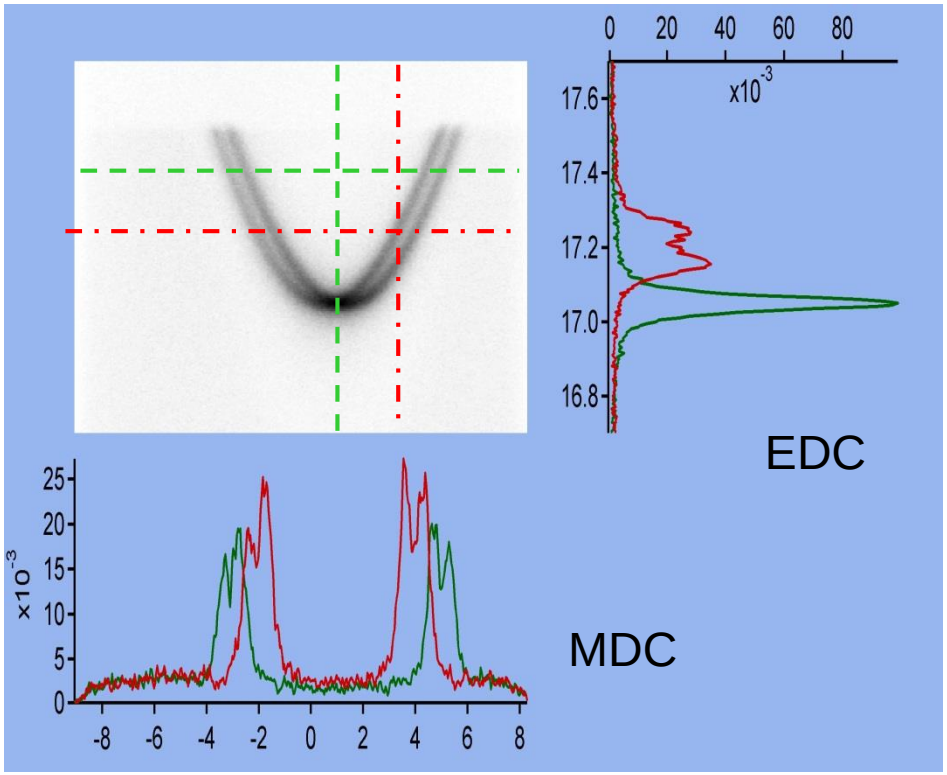

Emission angle

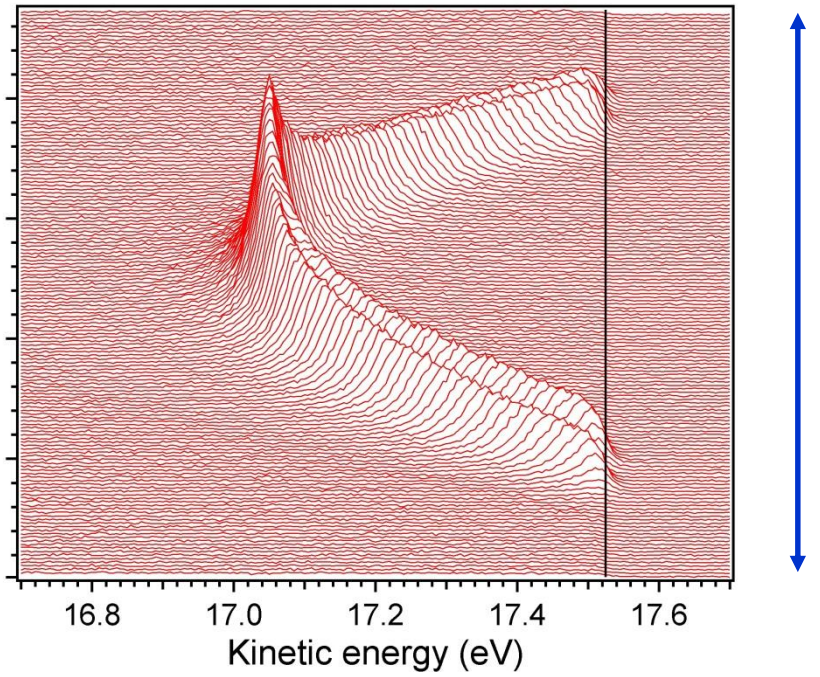

國家同步輻射研究中心
National Synchrotron Radiation Research Center

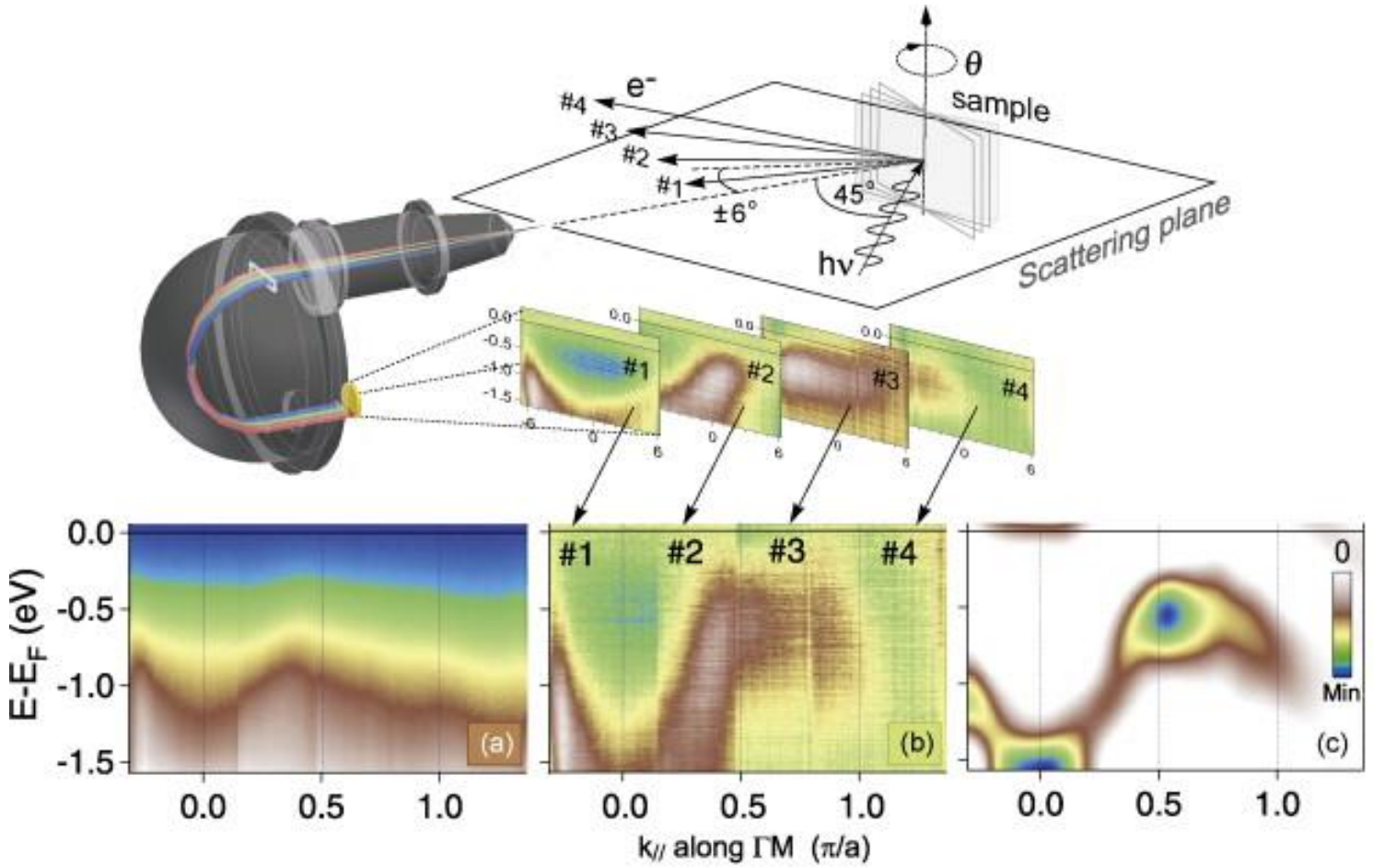

國家同步輻射研究中心
National Synchrotron Radiation Research Center

Krempasky et al., JESRP (2010)

Typical experimental result on graphene/SiC

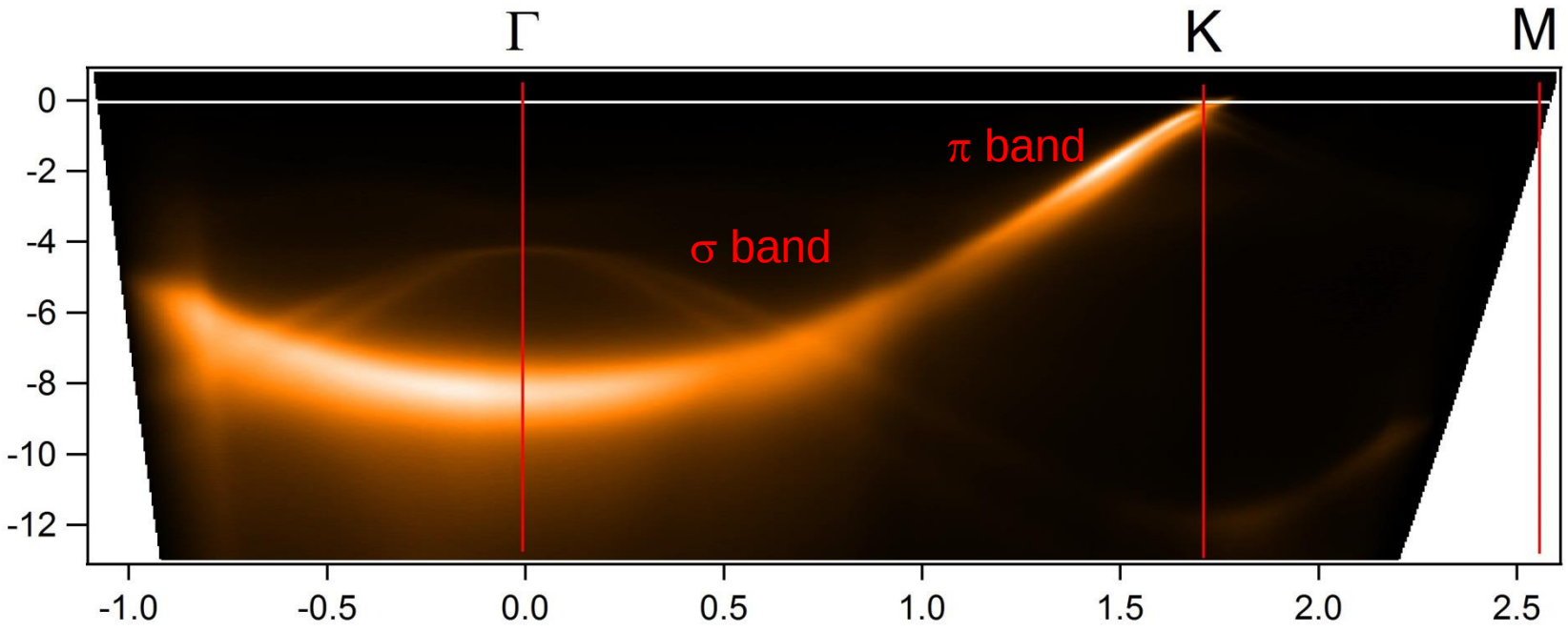

Experimental geometry

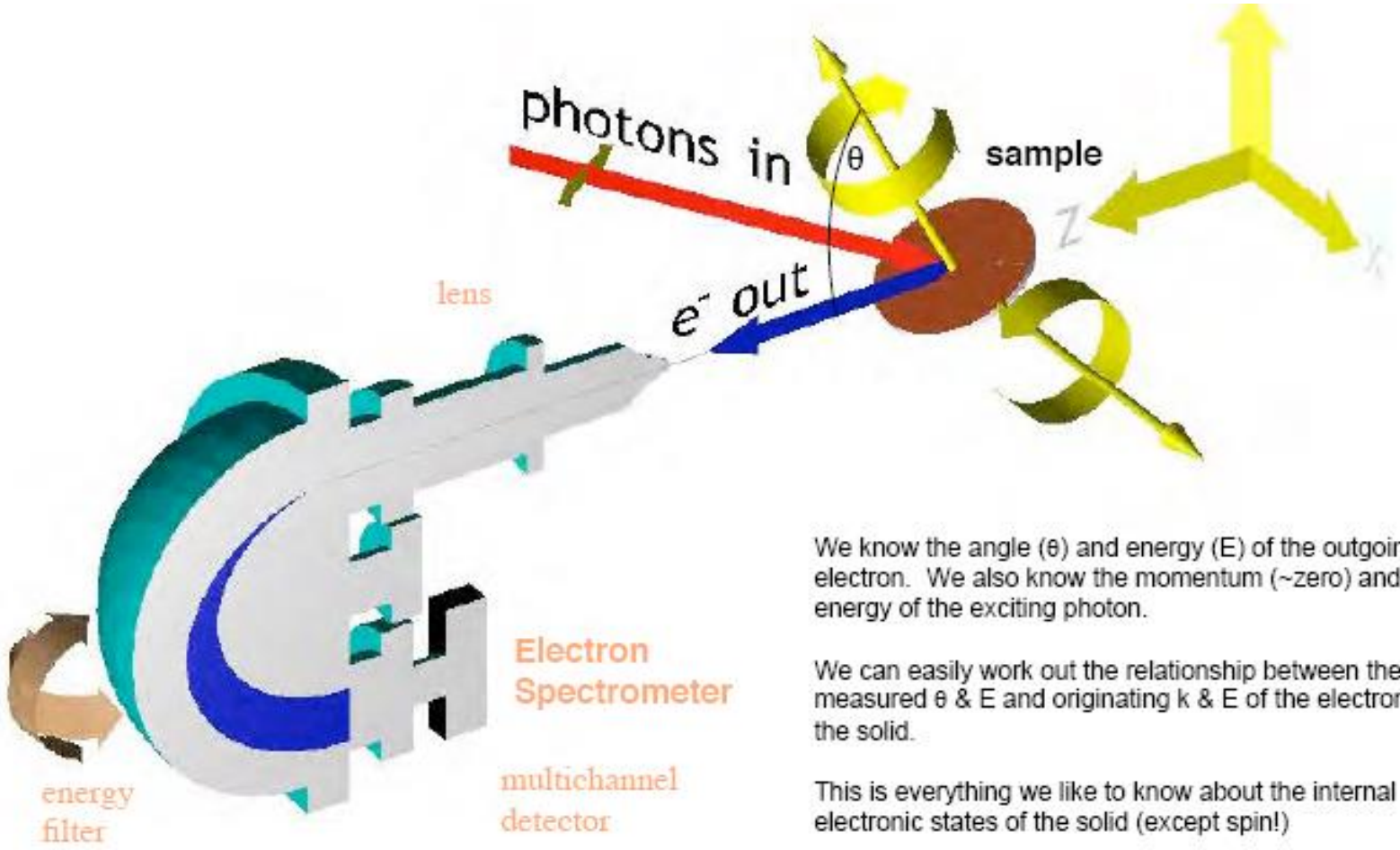

We know the angle (θ) and energy (E) of the outgoing electron. We also know the momentum (~zero) and the energy of the exciting photon.

We can easily work out the relationship between the measured θ & E and originating k & E of the electrons in the solid.

This is everything we like to know about the internal electronic states of the solid (except spin!)

Rashba splitting on Au(111) surface

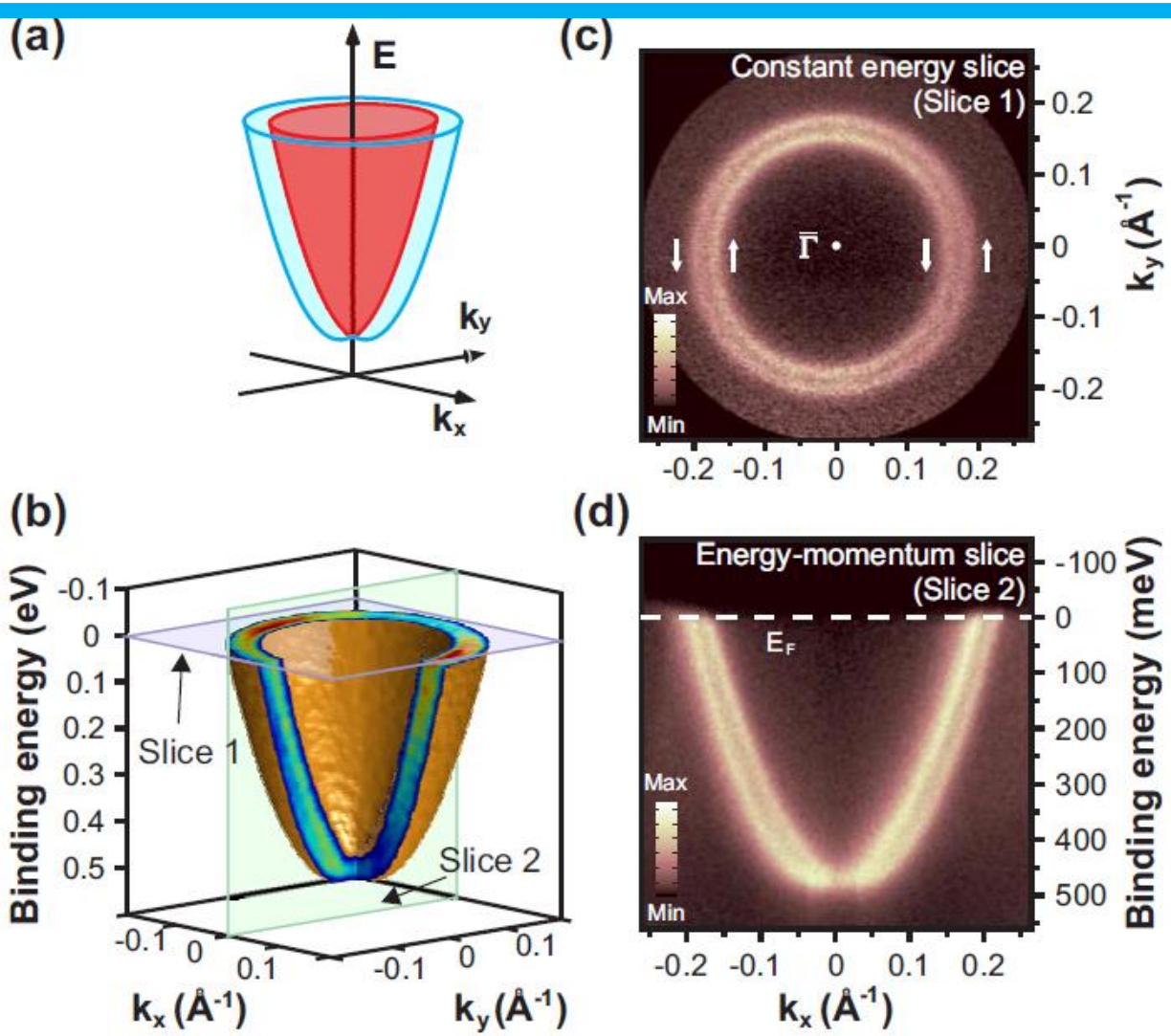

Surface state of Au(111)

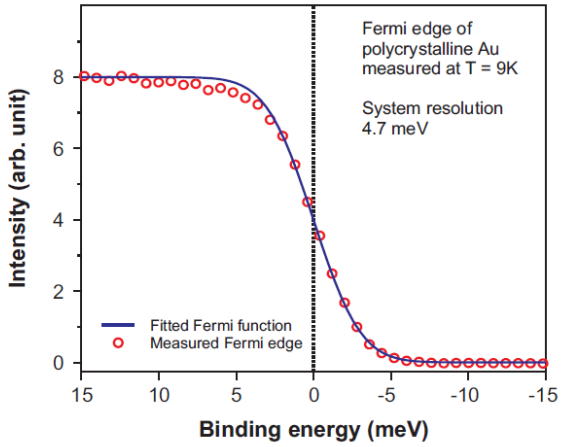

National Synchrotron Radiation Research Center

Courtesy of M. Berndsen and O. Tjernberg, KTH, Stockholm

Quick Band Mapping with ARPES

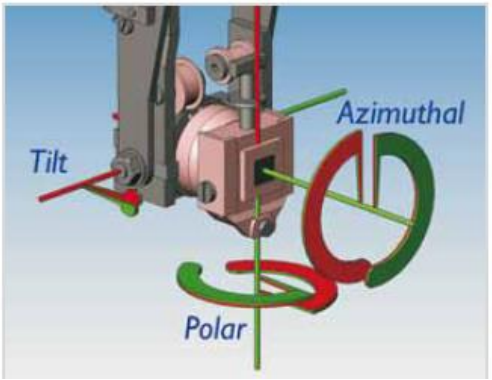

Azimuthal angle scan

Tilt angle scan

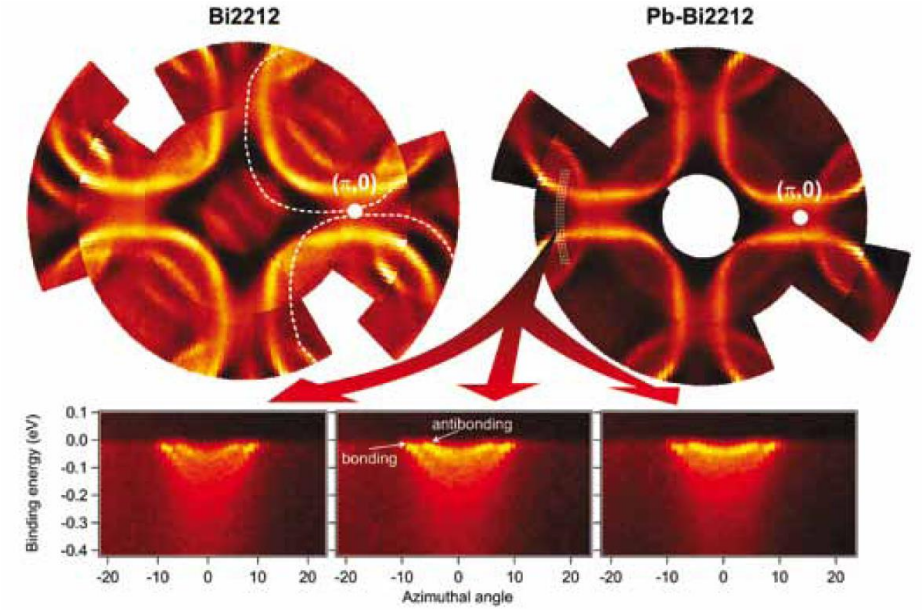

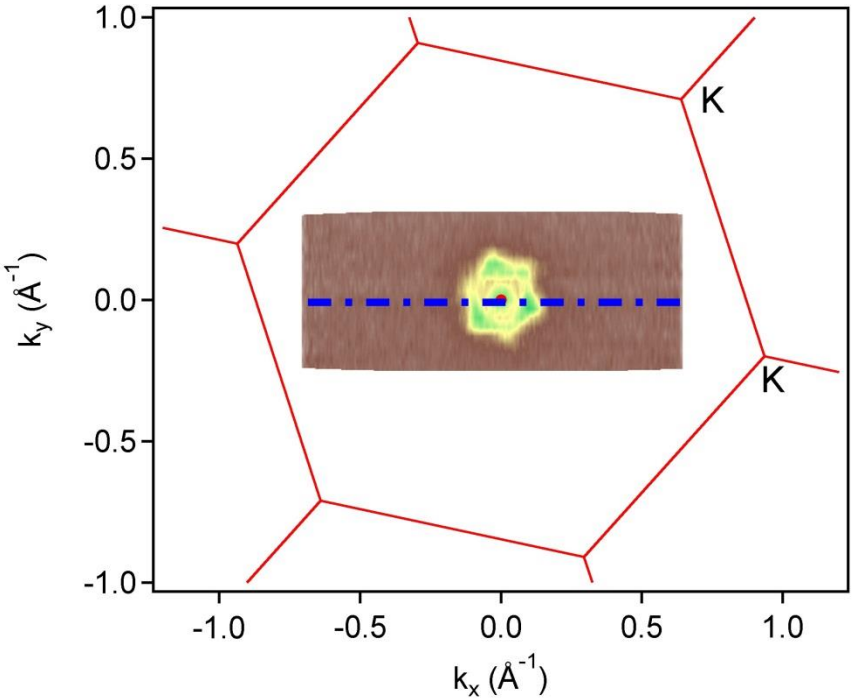

國家同步輻射研究中心
National Synchrotron Radiation Research Center

Map the band structure over all BZ

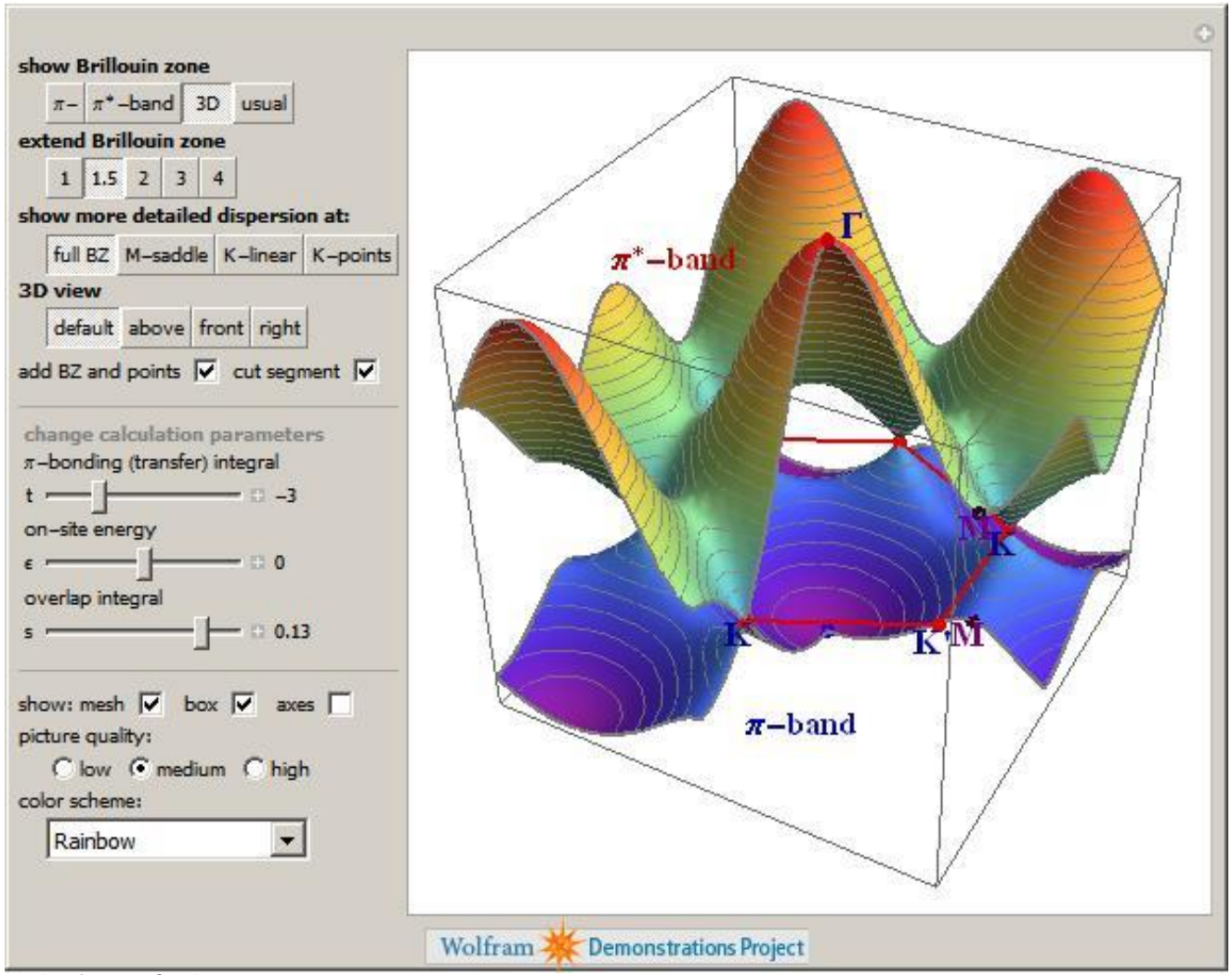

Requests before ARPES experiment

- You need to understand the crystal structure of solids.
- The sample characterization, such as the orientation and crystalline, is quite important before conducting ARPES experiment.
- XRD, Laue diffraction and LEED are required.

Light sources and terminology

- **Ultraviolet Photoemission Spectroscopy (UPS)**
  - UV He lamp (21.2 eV, 40.8 eV)
  - Laser : 6 eV (BBO), 8 eV (KBBF), 11 eV (gas cell) or HHG (High harmonic generation)
  - Valence band PES, direct electronic state info.

- **X-ray Photoemission Spectroscopy (XPS)**
  (Electron Spectroscopy for Chemical Analysis) (ESCA)
  - X-ray gun (Al: 1486.6 eV, Mg: 1253.6 eV)
  - core level PE, indirect electronic state info
  - chemical analysis

- **Synchrotron radiation**
  - continuous tunable wavelength
  - valance band and core level

Light sources and terminology

- **Ultraviolet Photoemission Spectroscopy (UPS)**
  - UV He lamp (21.2 eV, 40.8 eV)
  - Laser : 6 eV (BBO), 8 eV (KBBF), 11 eV (gas cell) or HHG (High harmonic generation)
  - Valence band PES, direct electronic state info.

- X-ray Photoemission Spectroscopy (XPS)
  (Electron Spectroscopy for Chemical Analysis) (ESCA)
  - X-ray gun (Al: 1486.6 eV, Mg: 1253.6 eV)
  - core level PE, indirect electronic state info
  - chemical analysis

- **Synchrotron radiation**
  - continuous tunable wavelength
  - valance band and core level

$$k_{\perp} = 0.5123\sqrt{(E_{kin}\cos^2\theta + V_0)}$$

$$k_{//} = 0.5123\sqrt{E_{kin}}\sin\theta$$

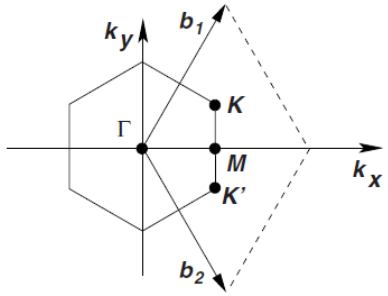

Lattice constant :
Graphene : 2.46 Å
Cu(111) : 2.08 Å
MoS_2 : 3.12 Å

- ✓ Assume the work function is 4.3 eV , please estimate the largest covering range of BZ at the Fermi level at 6 eV, 21.2 eV, 50 eV, 100 eV and 500 eV photon energy.
  Answer: 0.67 $Å^{-1}$, 2.11 $Å^{-1}$,3.46 $Å^{-1}$, 5.01 $Å^{-1}$, 11.4 $Å^{-1}$

- ✓ The angle between the incident beam and spectrometer is 50 degree, please estimate the covering range of BZ at 6 eV, 21.2 eV, 50 eV, 100 eV and 500 eV photon energy.
  Answer: 0.51 $Å^{-1}$, 1.61 $Å^{-1}$, 2.65 $Å^{-1}$, 3.83 $Å^{-1}$, 8.45 $Å^{-1}$

- ✓ The BZ in single layer graphene, the magnitude of ΓK is 1.703 $Å^{-1}$. If you plan to probe the band structure of graphene near the K-point, what are the required angle between the surface normal and spectrometer at 6 eV, 21.2 eV, 50 eV, 100 eV and 500 eV photon energy?
  Answer: mission impossible, 54 degree, 29.5 degree, 19.9 degree, 8.6 degree

Photon energy

- defines the detectable area of Energy

$$E_{kin} = \hbar\nu - \phi$$

- defines the accessible area of BZ

$$k_{//} = \frac{1}{\hbar}\sqrt{2mE_{kin}}\sin\theta$$

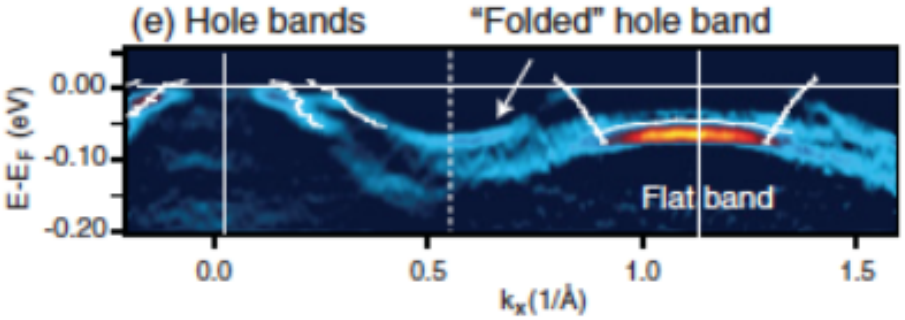

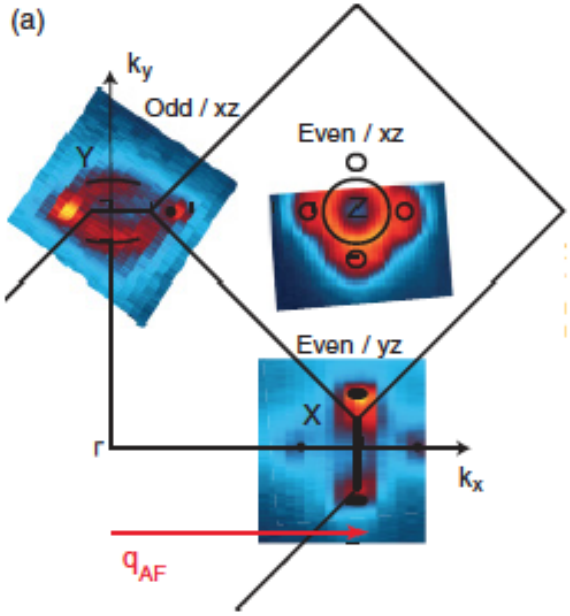

Phys. Rev. B 84, 014509 (2011)

Photon energy

- defines the detectable area of Energy

$$E_{kin} = \hbar\nu - \phi$$

- defines the accessible area of BZ

$$k_{//} = \frac{1}{\hbar}\sqrt{2mE_{kin}}\sin\theta$$

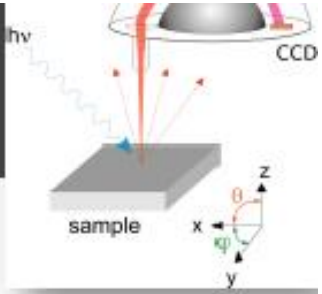

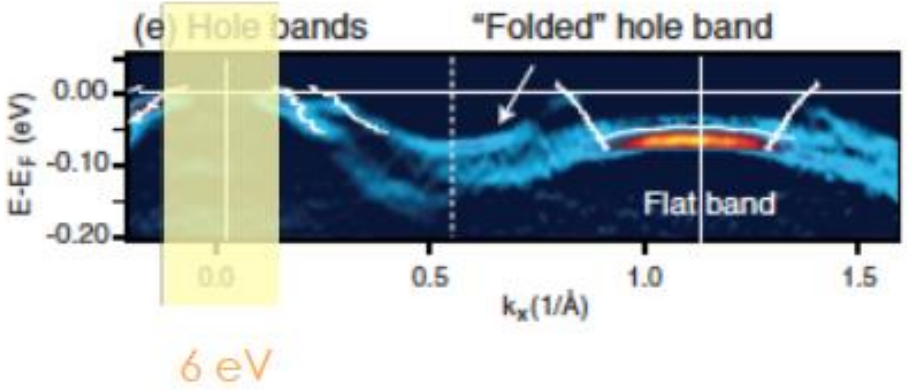

6 eV

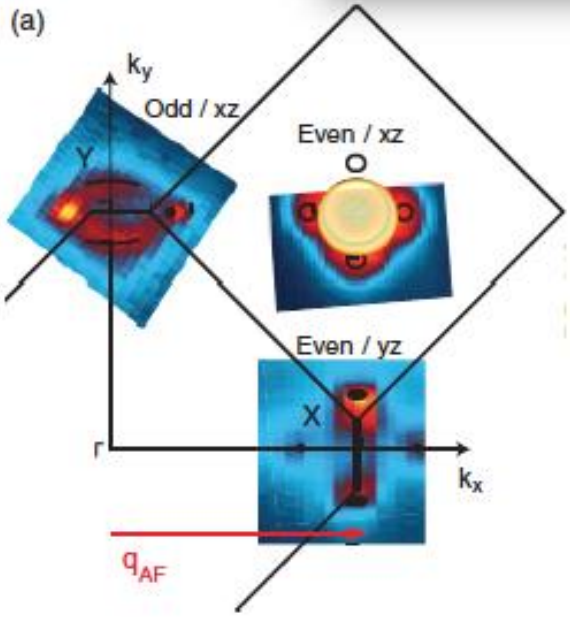

Phys. Rev. B 84, 014509 (2011)

Photon energy

- defines the detectable area of Energy

$$E_{kin} = \hbar\nu - \phi$$

- defines the accessible area of BZ

$$k_{//} = \frac{1}{\hbar}\sqrt{2mE_{kin}}\sin\theta$$

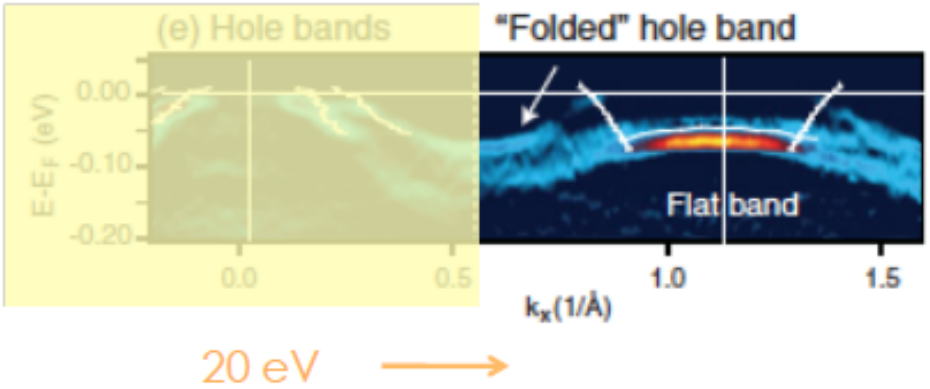

20 eV ⟶

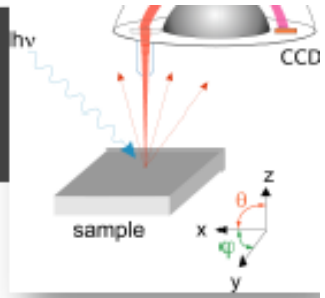

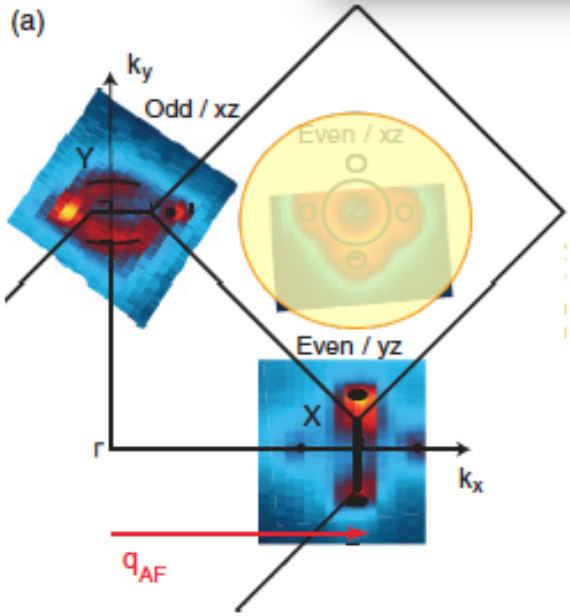

Phys. Rev. B 84, 014509 (2011)

Electron Escape Depth : Surface Sensitivity

Why are electrons so useful as probes of surfaces?

Or

Not so useful for studying bulk properties !!

Minimum due to electron-electron scattering, mainly plasmons

PES is a surface sensitive technique! (requires UHV)

High energy photoemission: several keV to increase bulk sensitivity

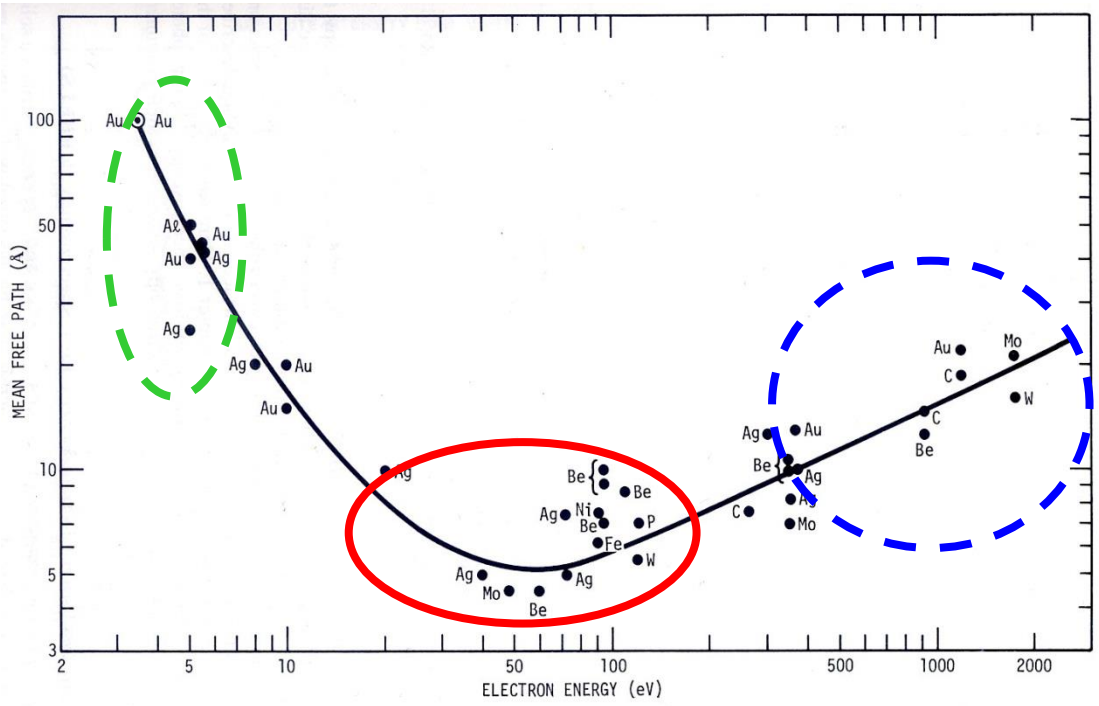

The requirement of ARPES

- UHV environment : better than $1x10^{-10}$ Torr
- Single crystals or *in-situ* growth thin films
- Conductors or semiconductors
- Tunable photon energies

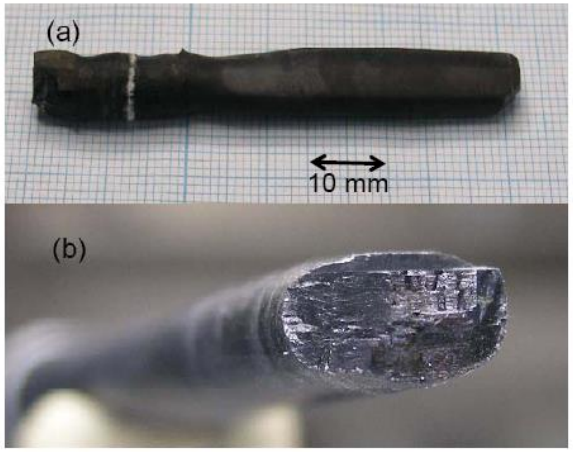

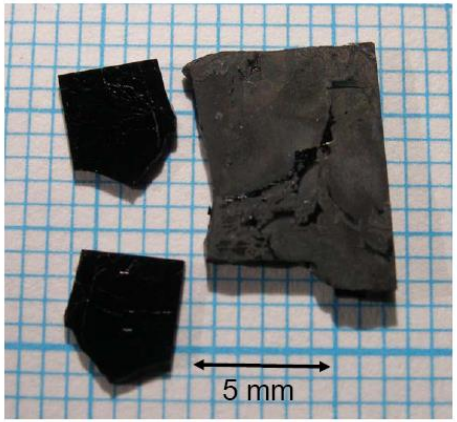

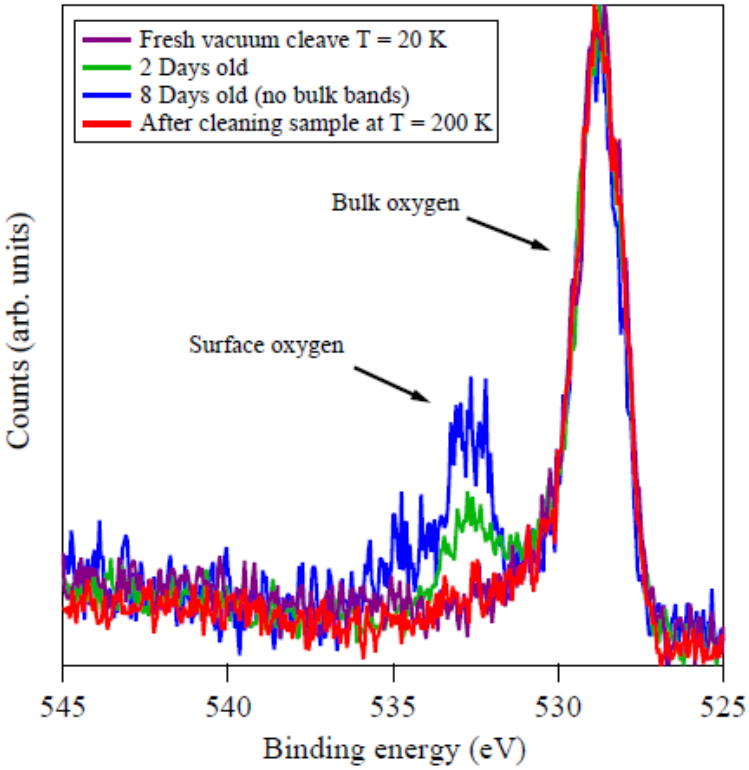

Figure 5.2: (color) The oxygen 1s peaks from Bi2212 at different times after the cleave. A constant background was subtracted from each spectrum to allow direct comparison. The peak derived from bulk oxygen is stable over time, while the surface oxygen peak grows as more oxygen sticks to the cold surface.

國家同步輻射研究中心
National Synchrotron Radiation Research Center

HC Hsu, Ph.D. Thesis NTNU(2010)
Koralek, U. Colorado Ph.D. Thesis (2007)

Single crystals or *in-situ* growth well-ordered thin films are favorable for ARPES measurement

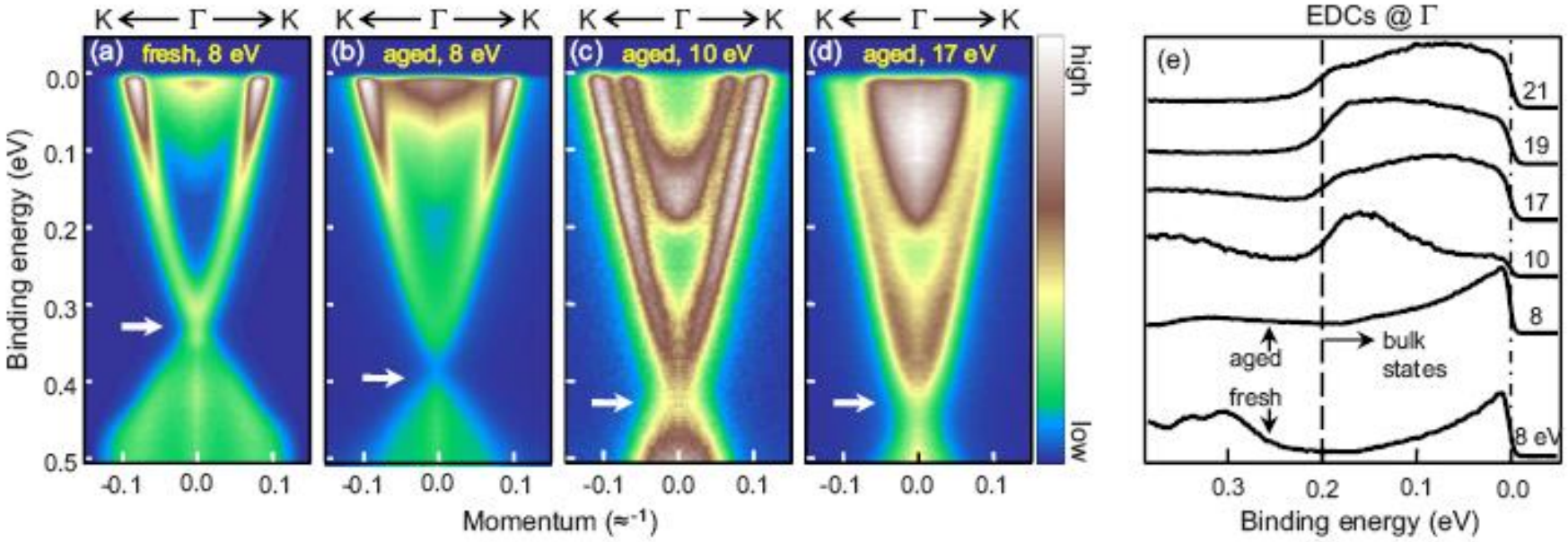

Base pressure : 1×10^{-10} Torr

In-situ cleaved Bi_2Se_3 single crystal

Park et al., PRB (2010)

Current status of ARPES end station at TLS

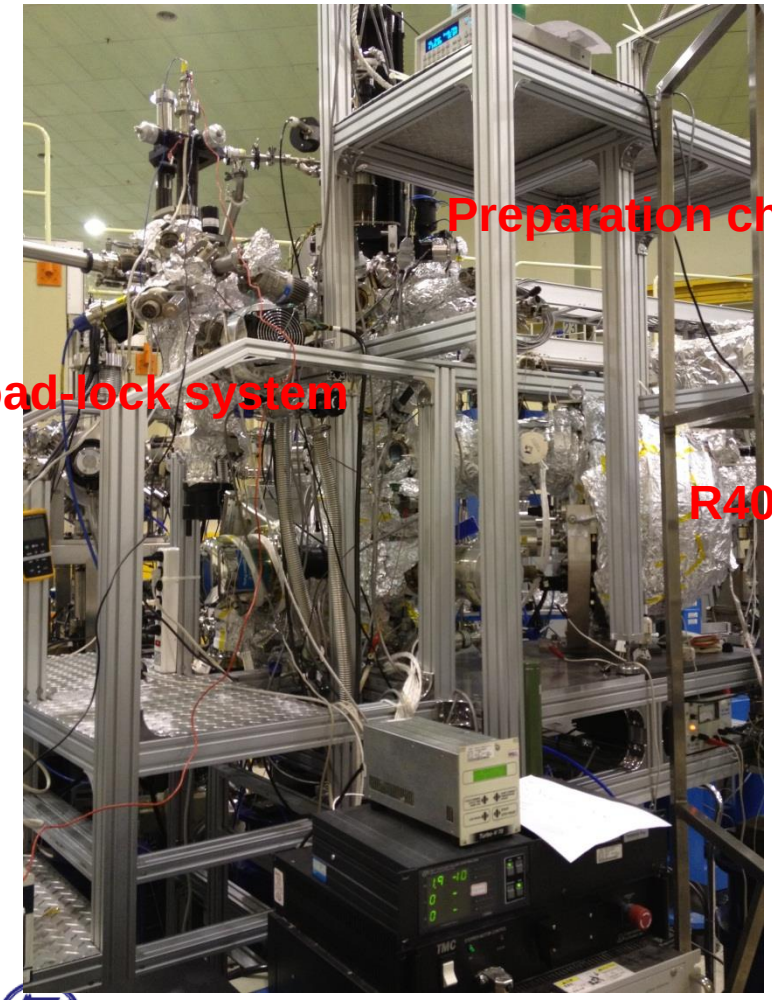

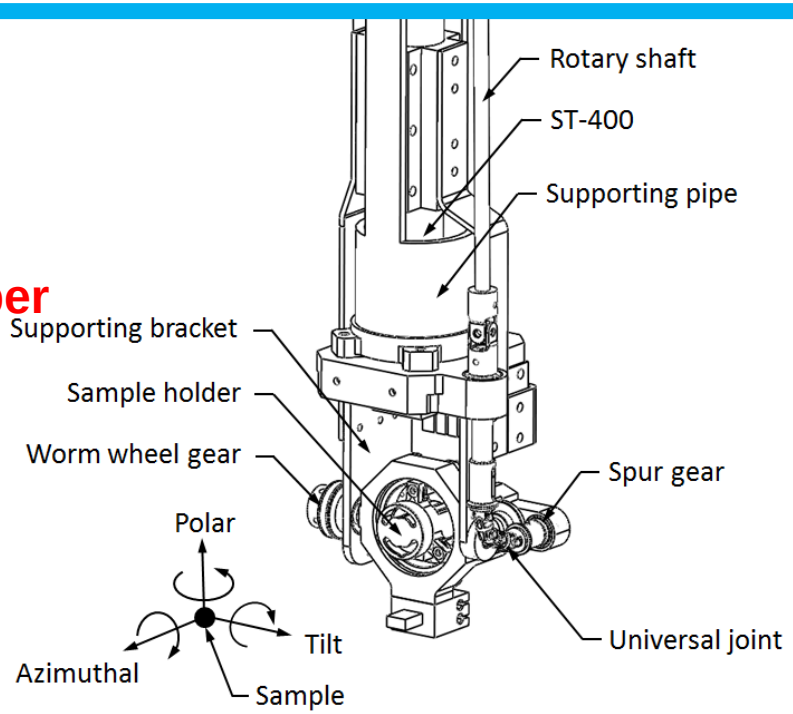

Energy range : 5 eV~120 eV

E/ΔE: 100,000 at 16 eV and 64 eV

Scienta R4000 analyzer

Manipulator : 6-axis motorized manipulator

Sample Preparation: *in-situ* cleave, thin film growth

Measurement temperature range : 10 K~ 350 K

Base pressure : 4.5×10^{-11} torr

國家同步輻射研究中心
National Synchrotron Radiation Research Center

What does ARPES measure

$$I \propto \sum_{f,i,\mathbf{k}} \left| \langle \phi_f | H_{\text{int}} | \phi_i \rangle \right|^2 A(\mathbf{k}, E)$$

Matrix element

Spectra function

ejected photoelectron

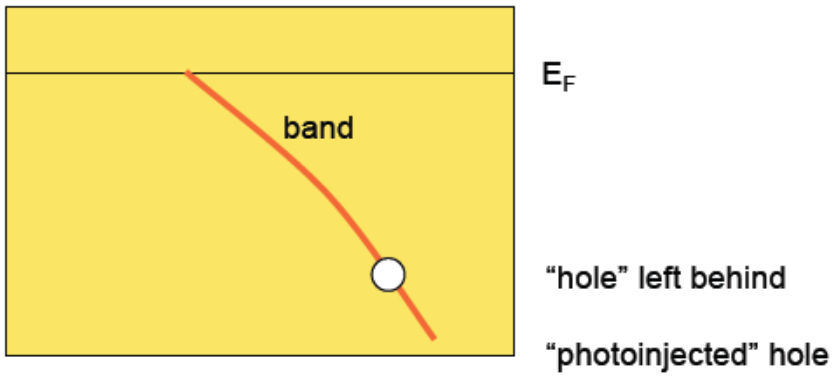

we believe the properties of the photoelectron reflect the properties of the injected hole

namely,

we can learn about the scattering and lifetime of the injected hole

Eli Rotenberg, ALS summer school

The carriers have a finite lifetime due to absorption and emission of phonons and other excitations

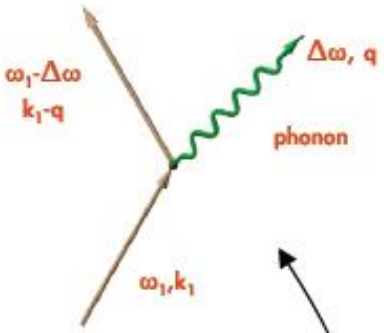

electron emits a phonon : change of energy **ω** and momentum *k*

The measured state is broader in momentum and energy

electron emits and reabsorbs a phonon :Change of mass and slope

The mass of carrier is increased

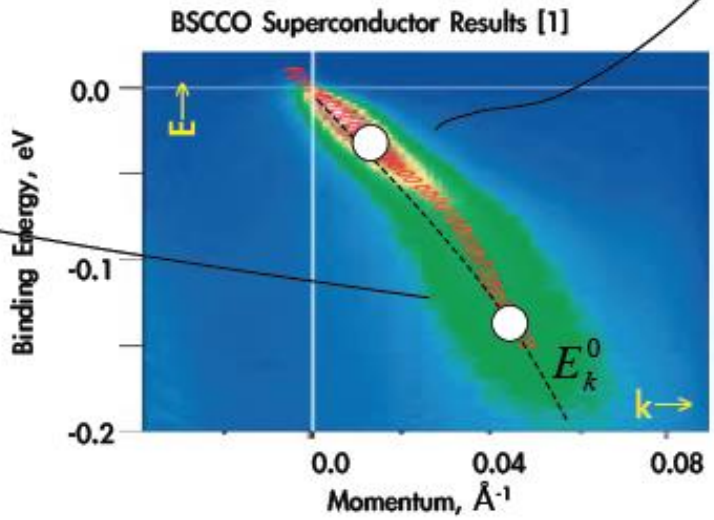

there is no direct way to probe these processes except through ARPES measurments

Self energy in photoemission spectra

The quantity determined in ARPES experiments is the single-particle spectral function

$$G(k,\omega) = \frac{1}{\omega - \varepsilon_k - \Sigma(k,\omega)}$$

$$A(k,\omega) = \frac{\mathrm{Im}\,\Sigma(k,\omega)}{[\omega - \varepsilon_k - \mathrm{Re}\,\Sigma(k,\omega)]^2 + [\mathrm{Im}\,\Sigma(k,\omega)]^2}$$

$$\Sigma = \mathrm{Re}\,\Sigma + i\,\mathrm{Im}\,\Sigma$$

Dispersion:
E-k Relation (Velocity; Effective mass etc.)

Scattering rate (Lifetime)

Optimally doped Bi-2212 cuprate

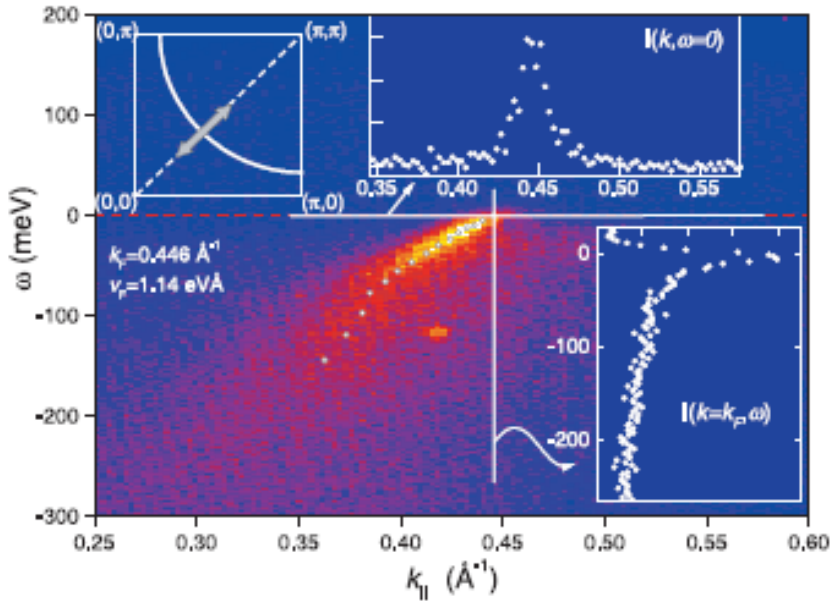

$$\hbar v_k \Delta k = \frac{\hbar v_k}{l} = \left|2\,\mathrm{Im}\,\Sigma(k,\omega)\right|$$

T. Valla et al., Science 285, 2110 (2000)

What does ARPES measure

$$I \propto \sum_{f,i,\mathbf{k}} \left| \langle \phi_f | H_{\text{int}} | \phi_i \rangle \right|^2 A(\mathbf{k}, E)$$

Matrix element

Spectra function

ejected photoelectron

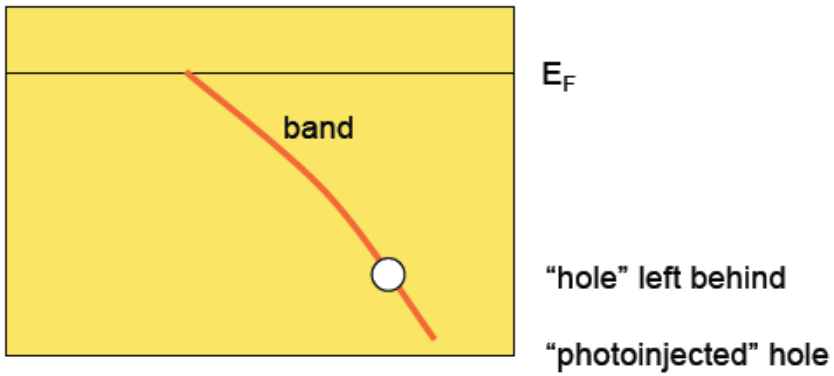

we believe the properties of the photoelectron reflect the properties of the injected hole

namely,

we can learn about the scattering and lifetime of the injected hole

Eli Rotenberg, ALS summer school

The unit cell of graphene

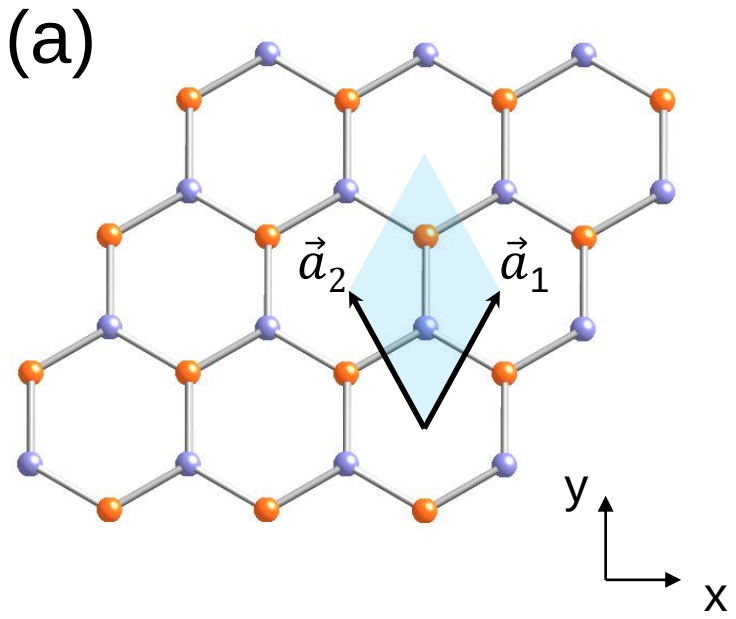

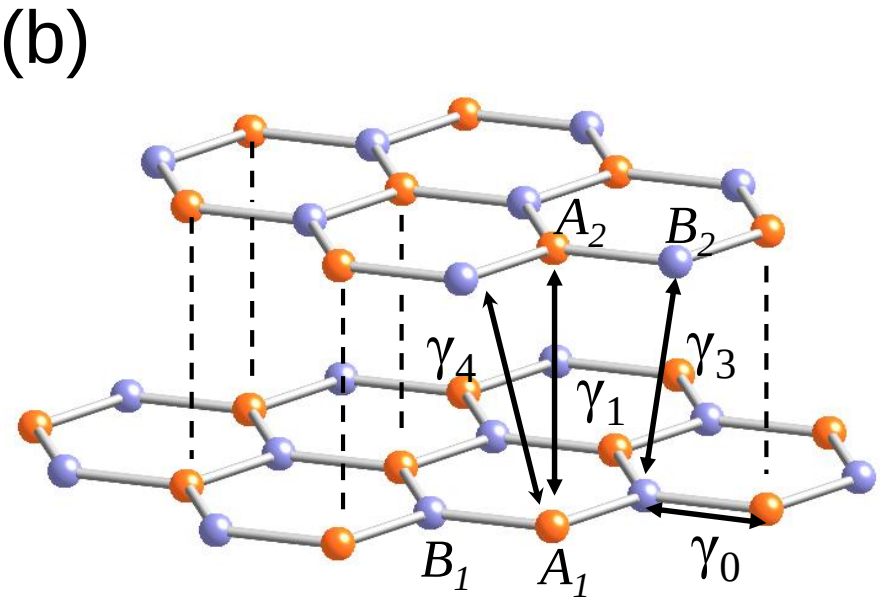

SWMc Hamiltonian of bilayer graphene

$$\mathrm{H}(\vec{k}) = \begin{pmatrix} E_0 + \Delta & \gamma_0 f(\vec{k}) & \gamma_1 & \gamma_4 f^*(\vec{k}) \\ \gamma_0 f^*(\vec{k}) & E_0 & \gamma_4 f^*(\vec{k}) & \gamma_3 f(\vec{k}) \\ \gamma_1 & \gamma_4 f(\vec{k}) & E_0 + \Delta & \gamma_0 f^*(\vec{k}) \\ \gamma_4 f(\vec{k}) & \gamma_3 f^*(\vec{k}) & \gamma_0 f(\vec{k}) & E_0 \end{pmatrix}$$

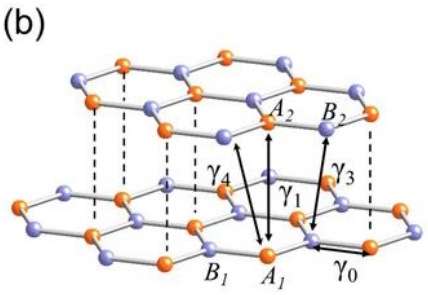

$$f(\vec{k}) = \exp(ik_x a_0/2\sqrt{3}) + 2\exp(-ik_x a_0/2\sqrt{3})\cos(k_y/2)$$

$$\vec{k} = (k_x, k_y)$$

A. Gruneis et al., PRB (2008)

Photon energy dependent in ARPES experiment

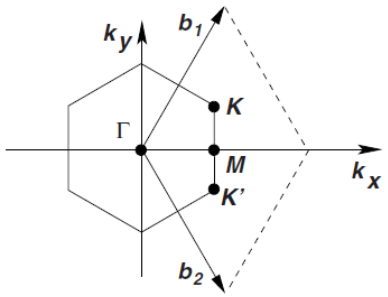

$$\boldsymbol{b}_1 = \frac{2\pi}{3a}(1,\sqrt{3}), \quad \boldsymbol{b}_2 = \frac{2\pi}{3a}(1,-\sqrt{3})$$

$$\boldsymbol{K} = \left(\frac{2\pi}{3a}, \frac{2\pi}{3\sqrt{3}a}\right), \quad \boldsymbol{K}' = \left(\frac{2\pi}{3a}, -\frac{2\pi}{3\sqrt{3}a}\right)$$

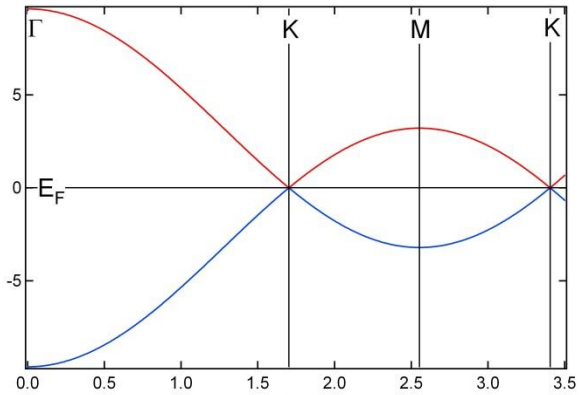

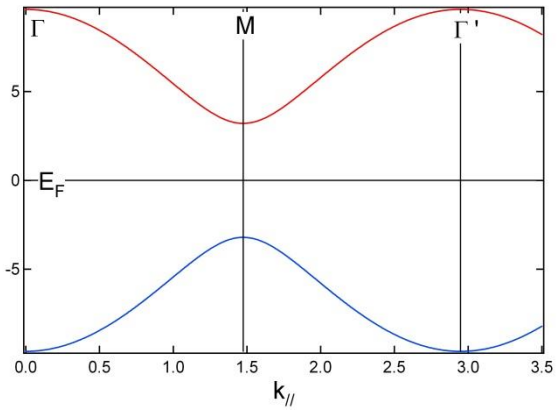

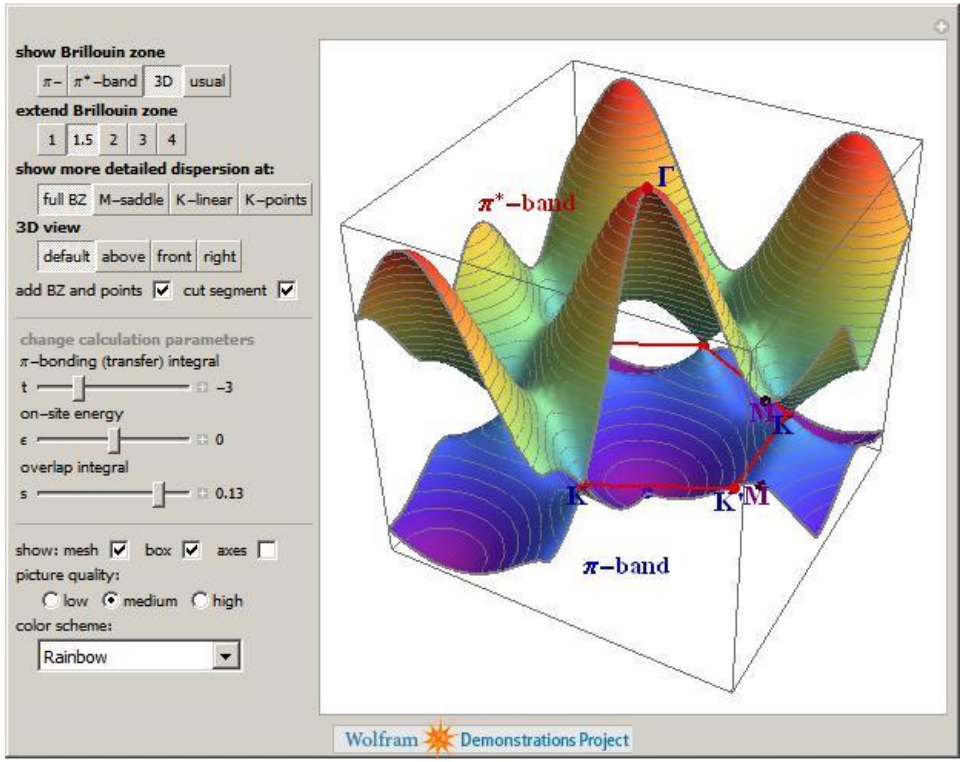

Single layer and bilayer graphene

Single layer graphene

Bilayer graphene

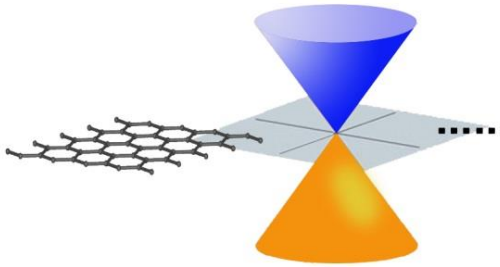

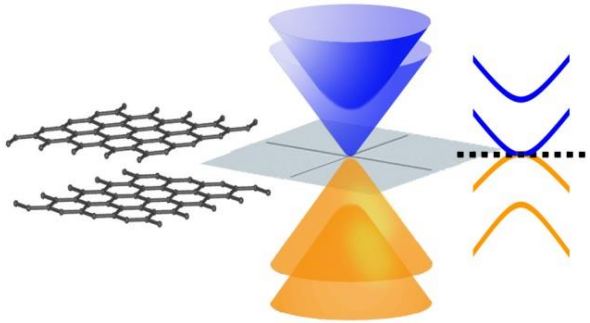

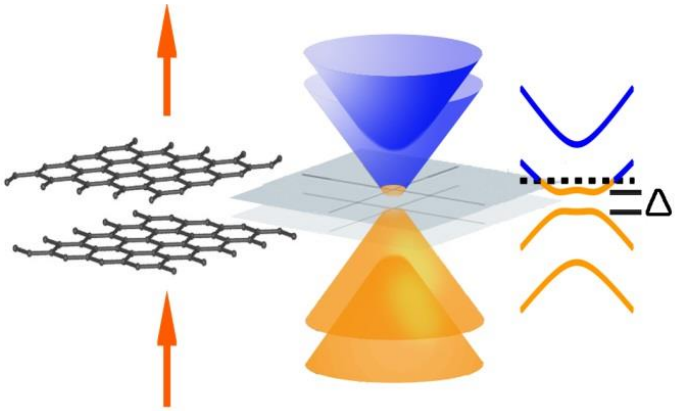

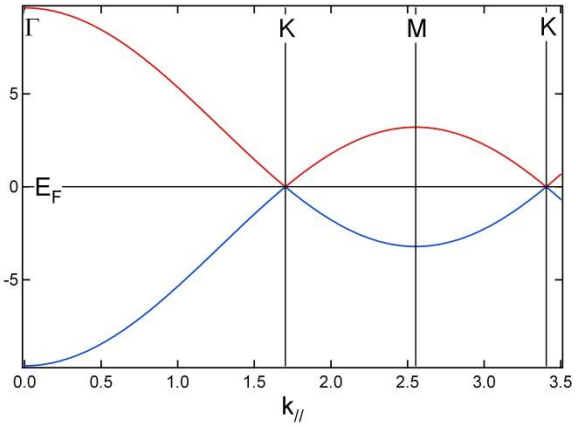

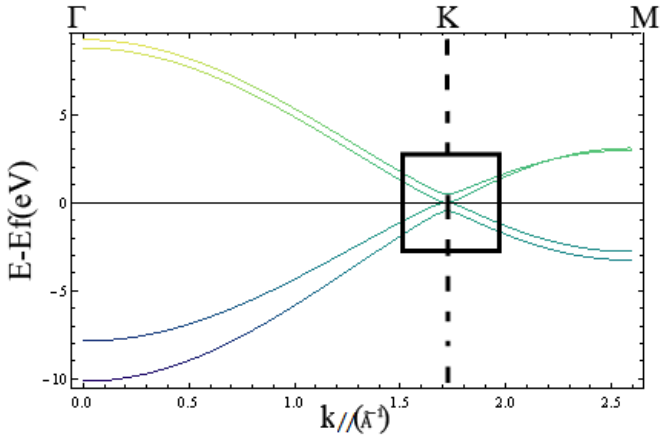

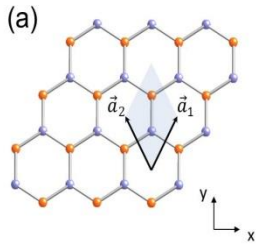

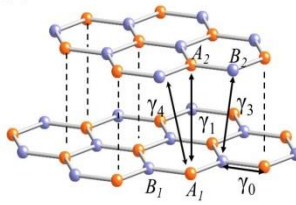

Image : http://infared.lbnl.gov.tw

TBM fitted results for presented BLG/SiC

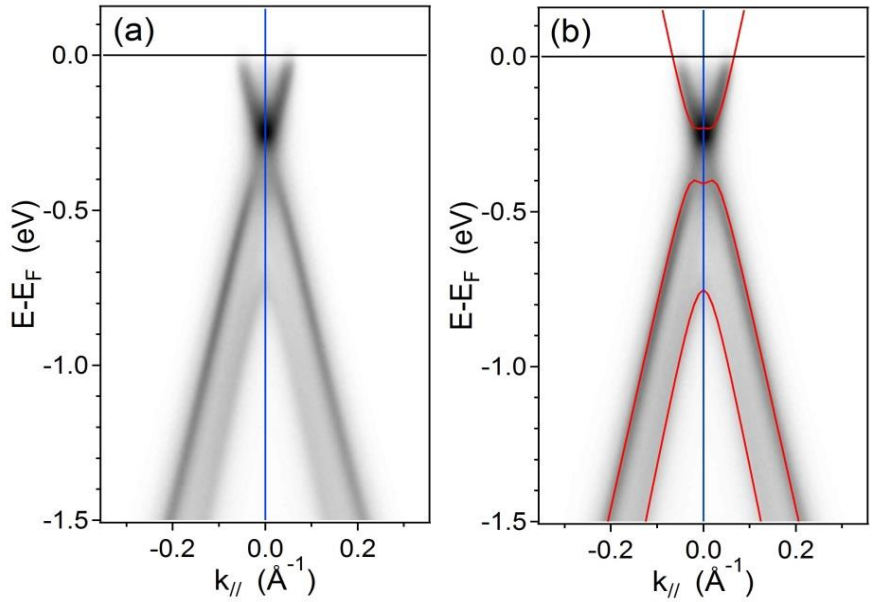

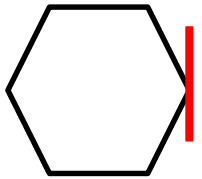

r0= -3.32 ; r1= **0.46** ;
r3= 0.25 ; r4= 0.15

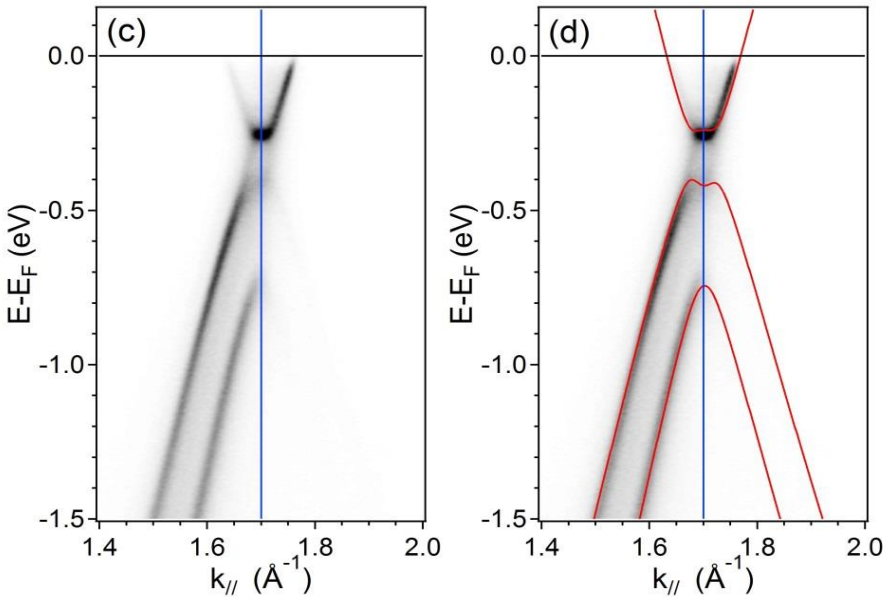

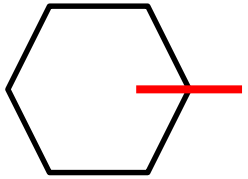

What does ARPES measure

$$I \propto \sum_{f,i,\mathbf{k}} \left| \langle \phi_f | H_{\text{int}} | \phi_i \rangle \right|^2 A(\mathbf{k}, E)$$

Matrix element

Spectra function

ejected photoelectron

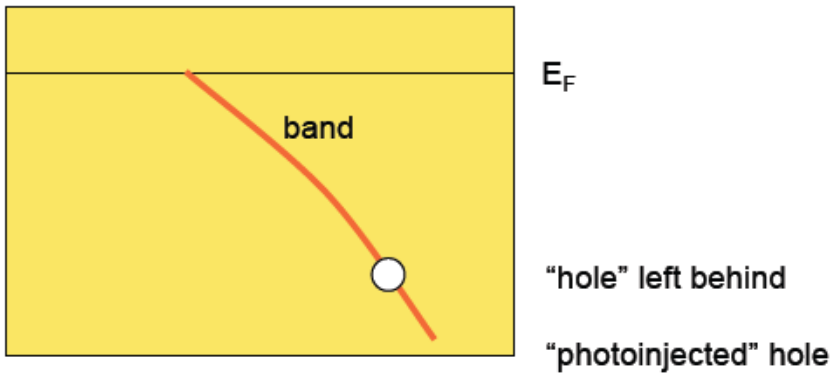

we believe the properties of the photoelectron reflect the properties of the injected hole

namely,

we can learn about the scattering and lifetime of the injected hole

Eli Rotenberg, ALS summer school

SWMc Hamiltonian of bilayer graphene

$$\mathrm{H}(\vec{k}) = \begin{pmatrix} E_0 + \Delta & \gamma_0 f(\vec{k}) & \gamma_1 & \gamma_4 f^*(\vec{k}) \\ \gamma_0 f^*(\vec{k}) & E_0 & \gamma_4 f^*(\vec{k}) & \gamma_3 f(\vec{k}) \\ \gamma_1 & \gamma_4 f(\vec{k}) & E_0 + \Delta & \gamma_0 f^*(\vec{k}) \\ \gamma_4 f(\vec{k}) & \gamma_3 f^*(\vec{k}) & \gamma_0 f(\vec{k}) & E_0 \end{pmatrix}$$

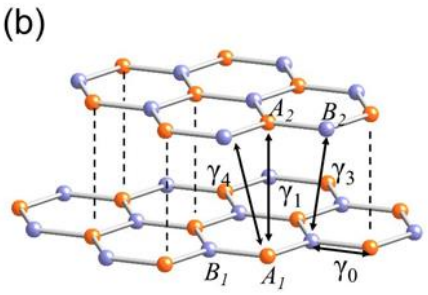

$$f(\vec{k}) = \exp(ik_x a_0/2\sqrt{3}) + 2\exp(-ik_x a_0/2\sqrt{3})\cos(k_y/2)$$

$$\vec{k} = (k_x, k_y)$$

A. Gruneis et al., PRB (2008)

$$\left\langle \Psi_f(\vec{k}_f) \middle| H^{\text{int}} \middle| \Psi_i(\vec{k}_i) \right\rangle = M^k_{f,i}$$

$$M^k_{f,i} \propto \int d^3 r e^{-i\vec{k}_f \cdot \vec{r}} (\vec{A} \cdot \vec{p}) \Psi_i(k)$$

Photoemission intensity and matrix element effect

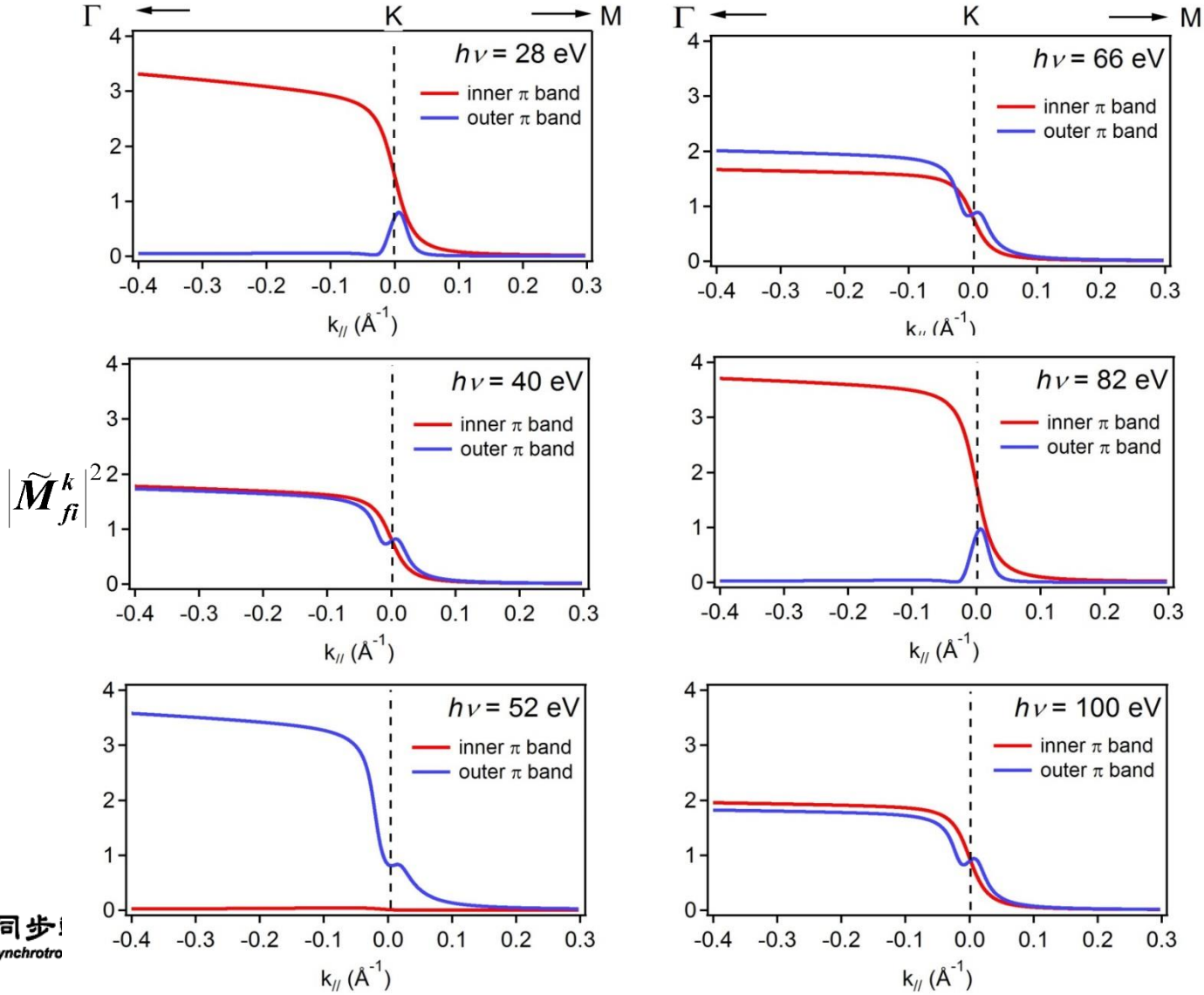

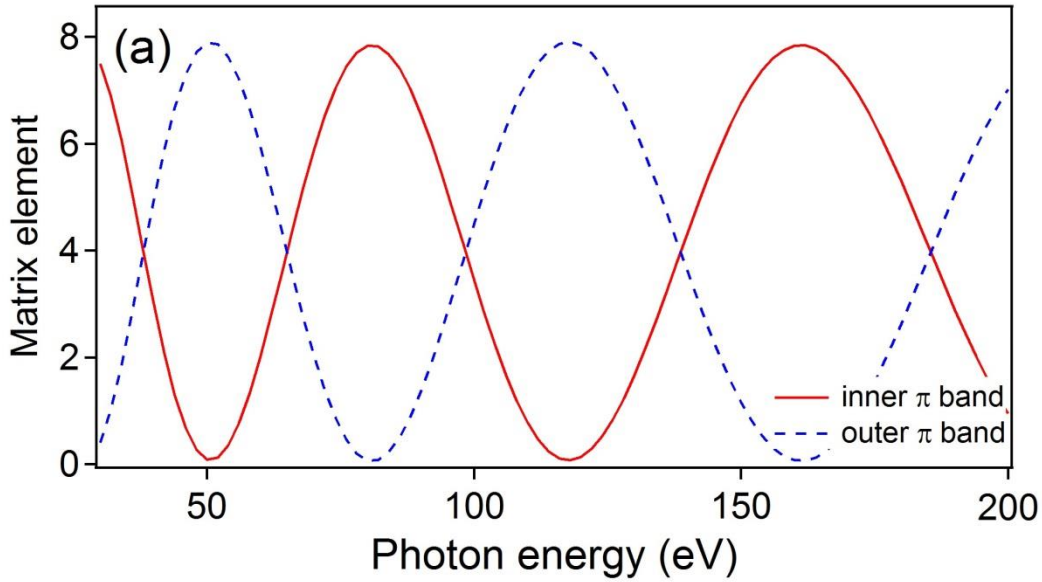

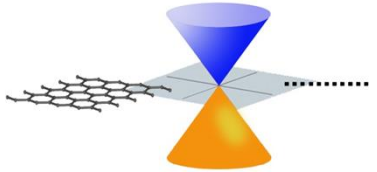

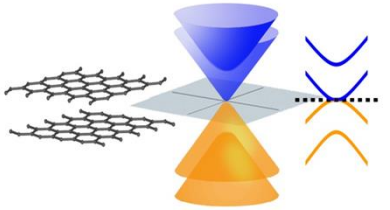

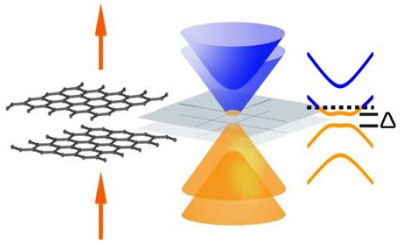

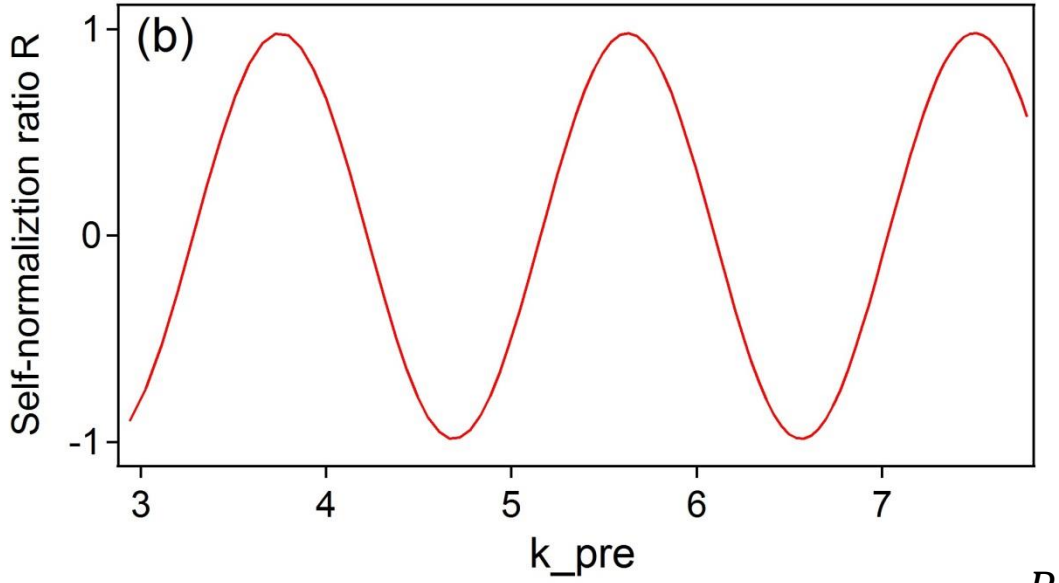

$$k_{\perp} = 0.5123\sqrt{(E_{kin}\cos^2\theta + V_0)}$$

$$k_{//} = 0.5123\sqrt{E_{kin}}\sin\theta$$

$$R = (I_{outer} - I_{inner})/(I_{outer} + I_{inner})$$

ARPES result

Calculation

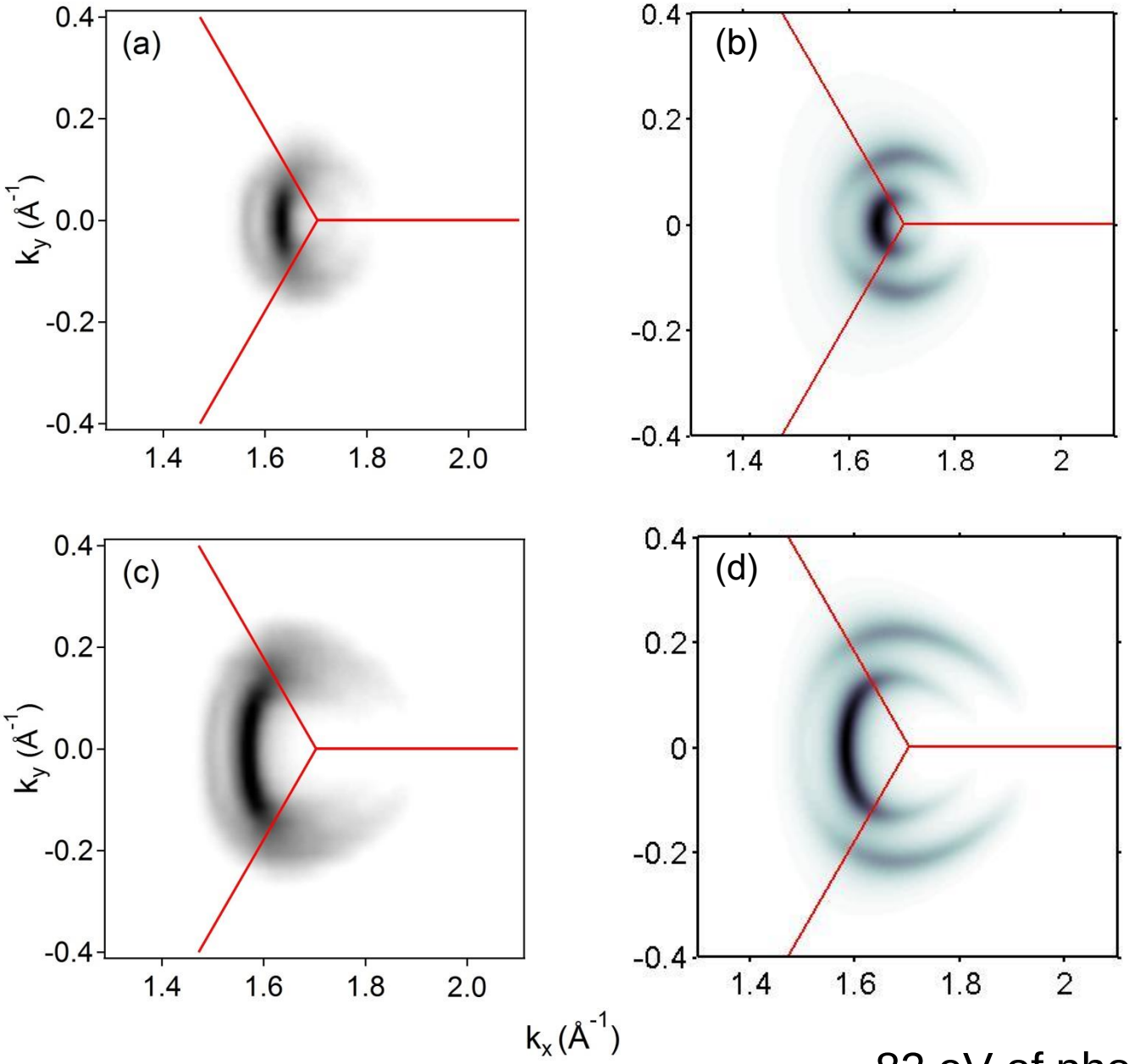

國家同步輻射研究中心 National Synchrotron Radiation Research Center

82 eV of photon energy

Varing incident photon energies to determine the interlayer spacing of BLG/SiC

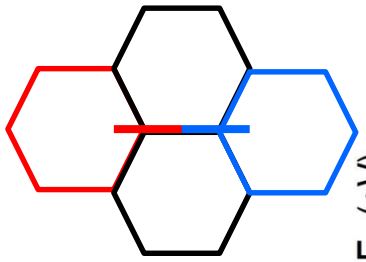

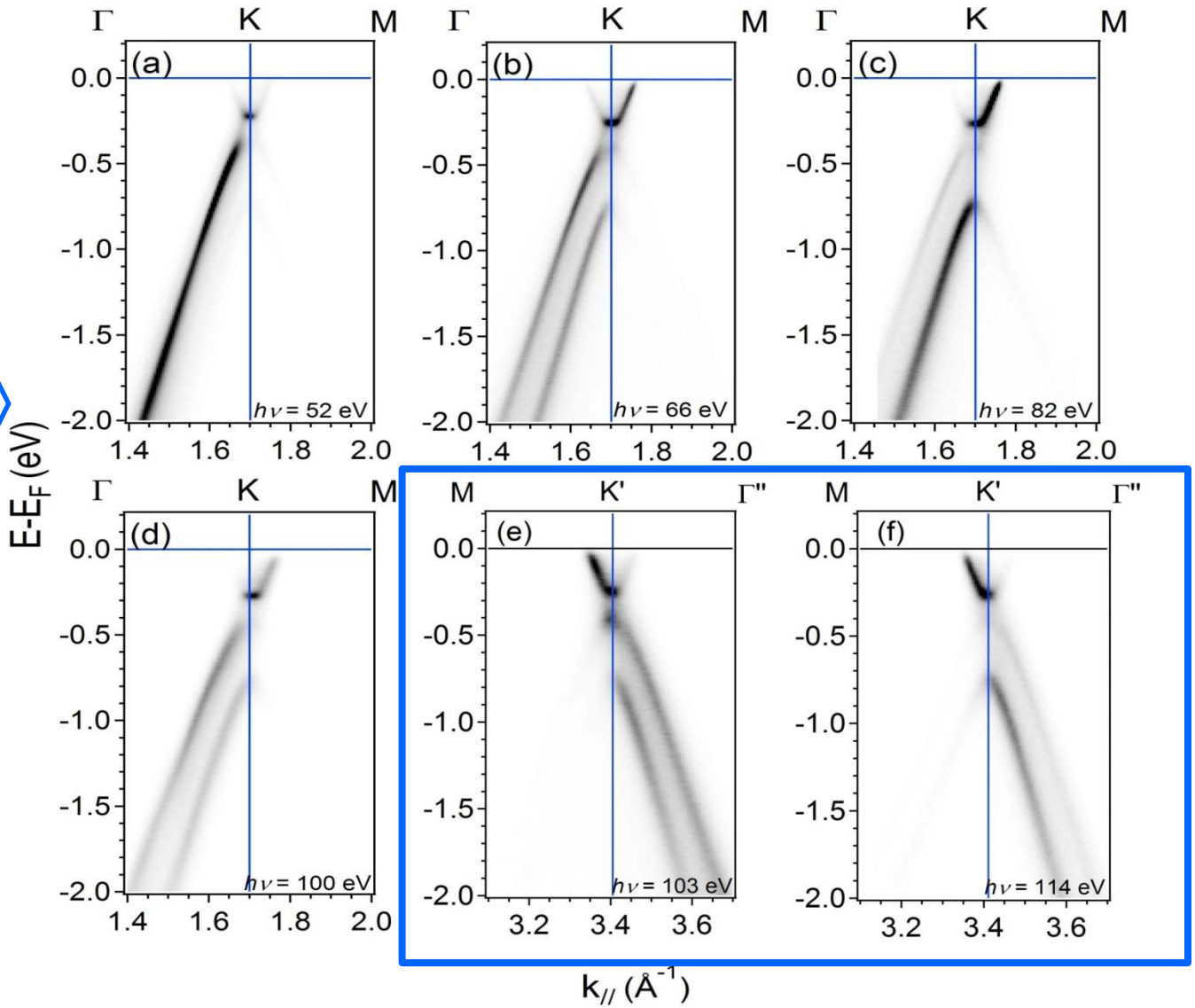

國家同步輻
National Synchrotron Ra

k_z dependent in bulk band mapping

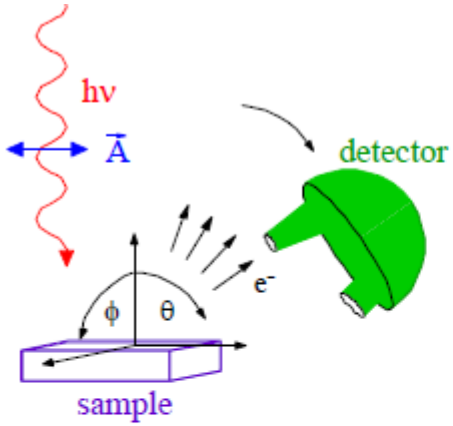

Intensity $\propto \sum_{i,f} \left| \langle f | \vec{p} \cdot \vec{A} | i \rangle \right|^2 A(\vec{k}, E) f(E)$

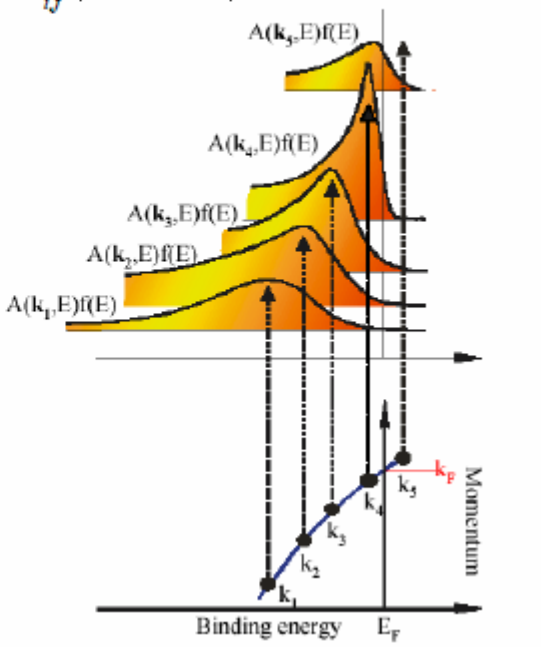

Electron momentum
Parallel to the surface is
conserved

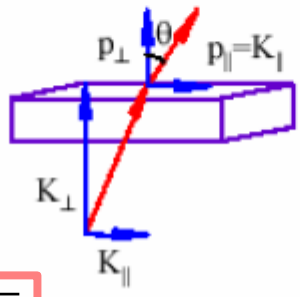

$$k_{\perp} = 0.5123\sqrt{(E_{kin}\cos^2\theta + V_0)}$$

$$k_{//} = 0.5123\sqrt{E_{kin}}\sin\theta$$

k_z dependent in bulk band mapping

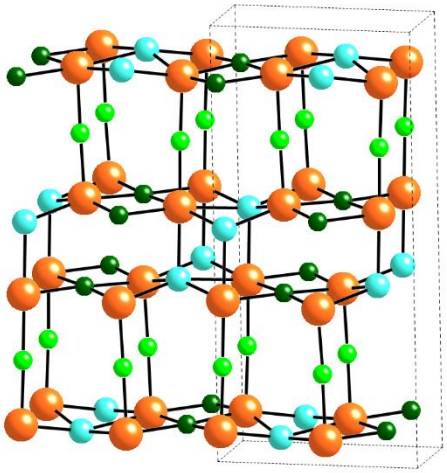

Cu^{2+}
Cu^{+}
Li
O

a~2b

Crystal structure of $LiCu_2O_2$

1. Floating zone technique
2. LEED and X-ray diffraction
3. In-situ cleave at $8x10^{-11}$ torr

CuO_2 chains

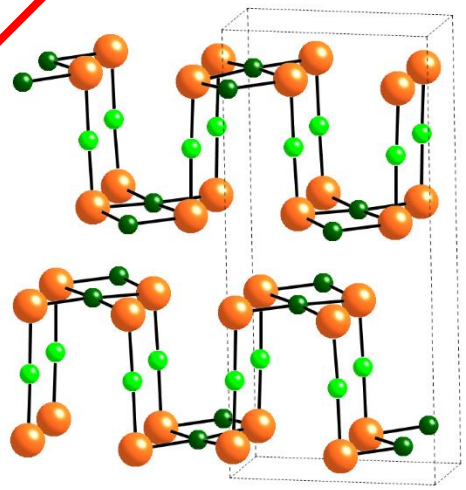

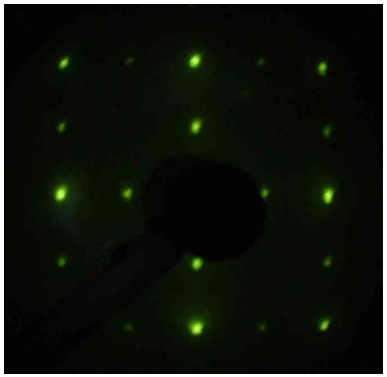

Twin domains

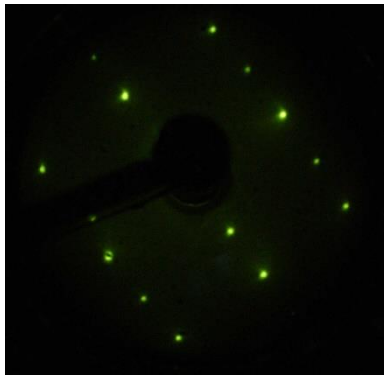

Single domain

Photon energy dependence PES

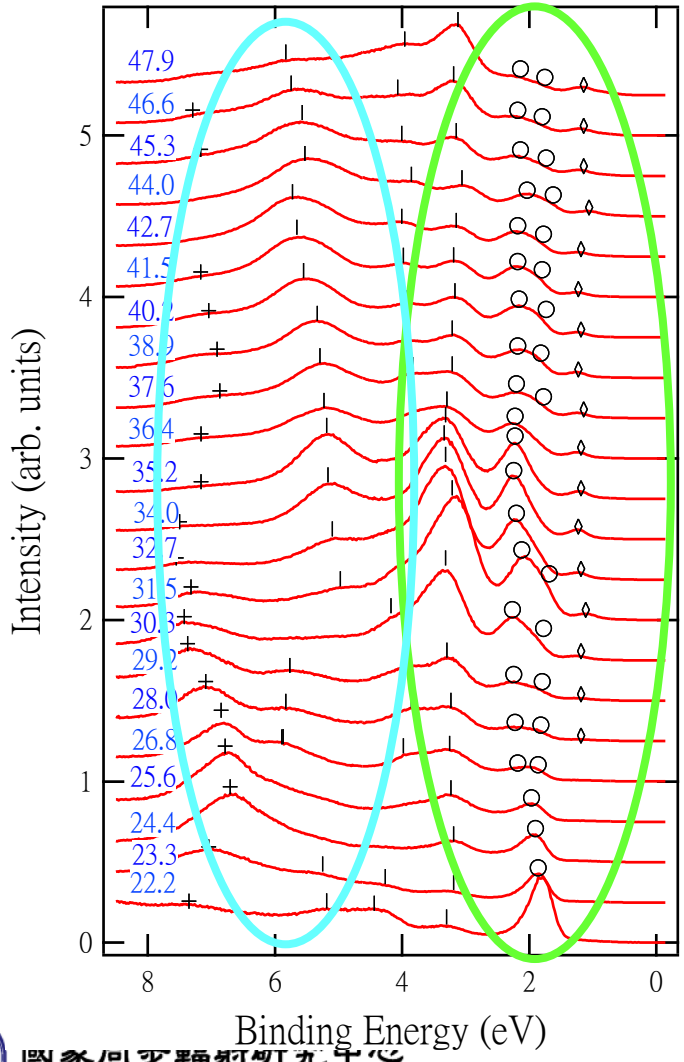

- The bands between about 3.6 eV and 8 eV display a clear dispersion with photon energies disclosing a strong coupling along the *c*-axis,

- The bands above 3.6 eV until E_F: weaker dispersion, more localized character within each electronic bi-layer.

The electronic structure of $BiSbSe_3$ with varied incident photon energies.

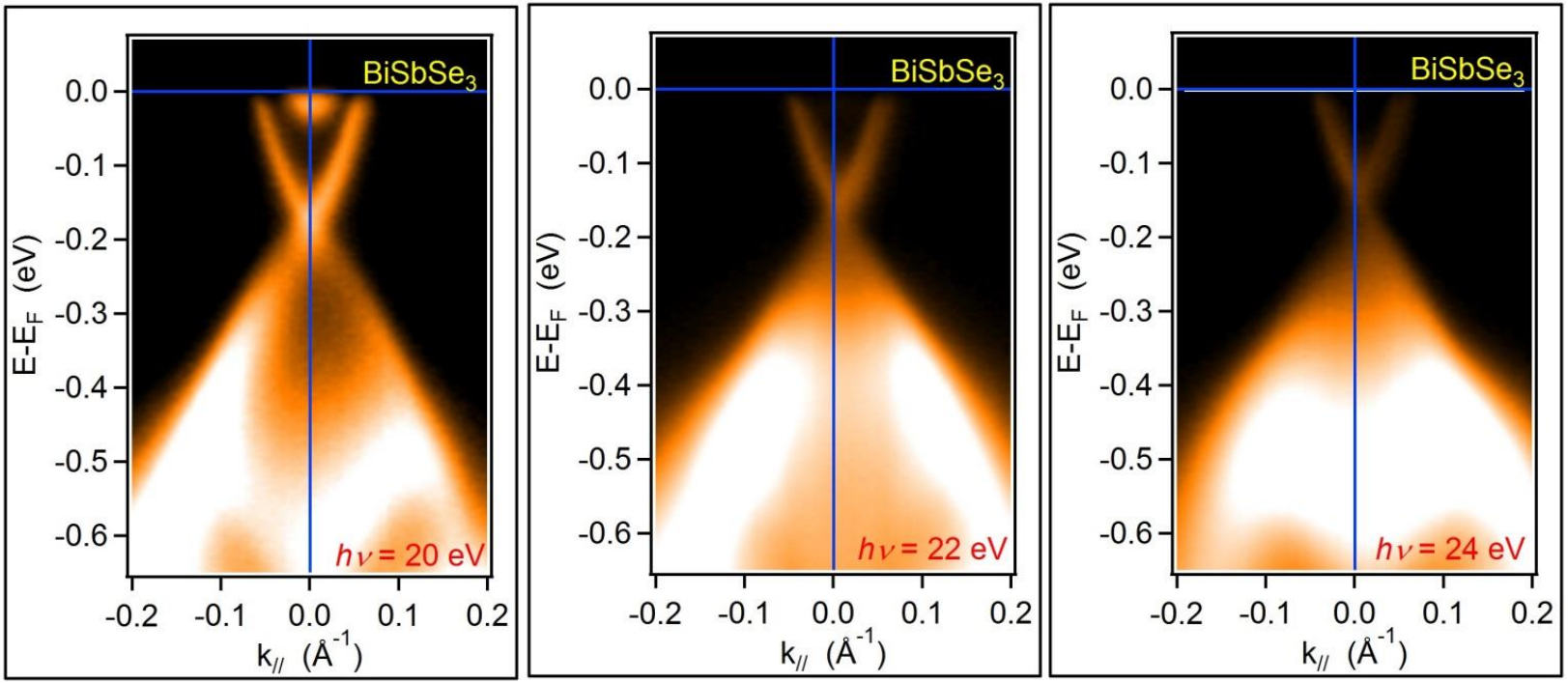

The electronic structure of Sb_2Te_2Se

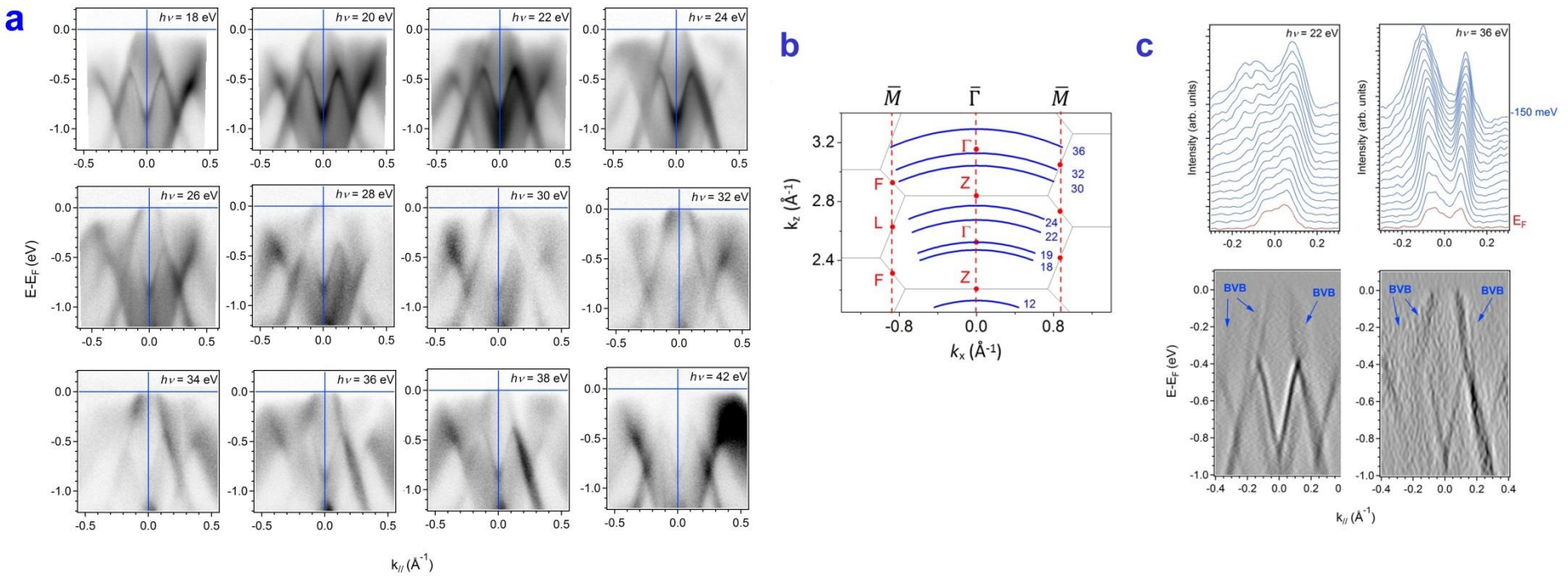

國家同步輻射研究中心
National Synchrotron Radiation Research Center

Lee et al., Scientific Reports (2016)

Using ARPES to study the electronic structure of emergent quantum materials

The rise of emergent quantum materials

Graphene and Beyond Graphene 2D Crystals
Topological Insulators and Their Spintronics Application
for Next Generation Green Electronics

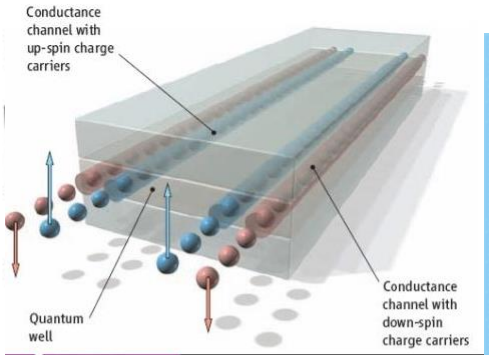

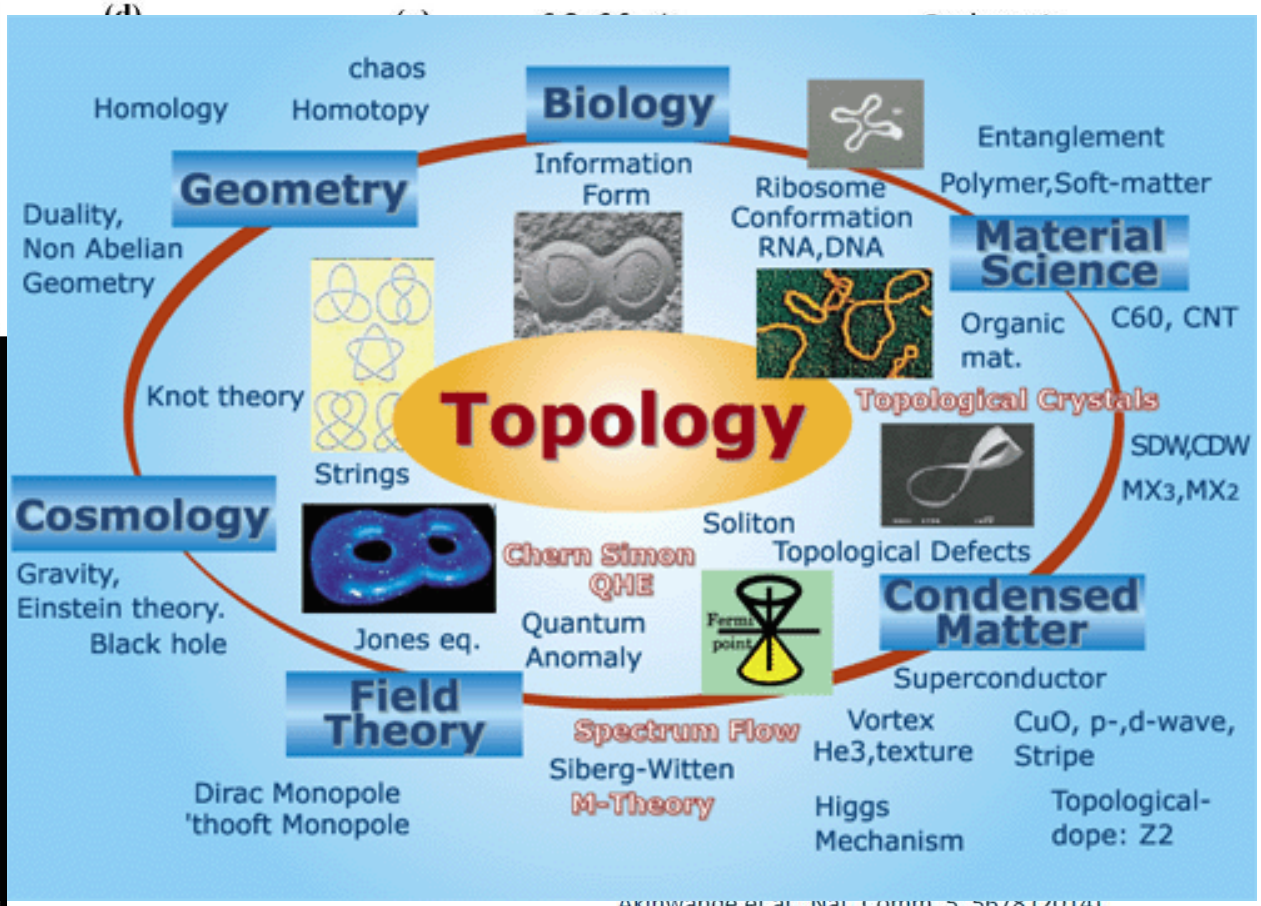

Akinwande et al., Nat. Comm. 5, 5678 (2014).

Kang, Proc. Of SPIE (2014)

What is Topology

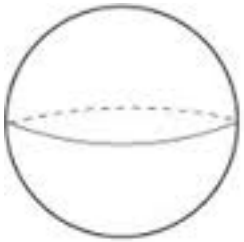

genus 0

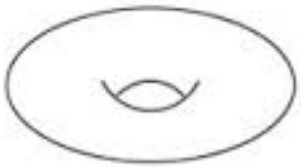

genus 1

genus 2

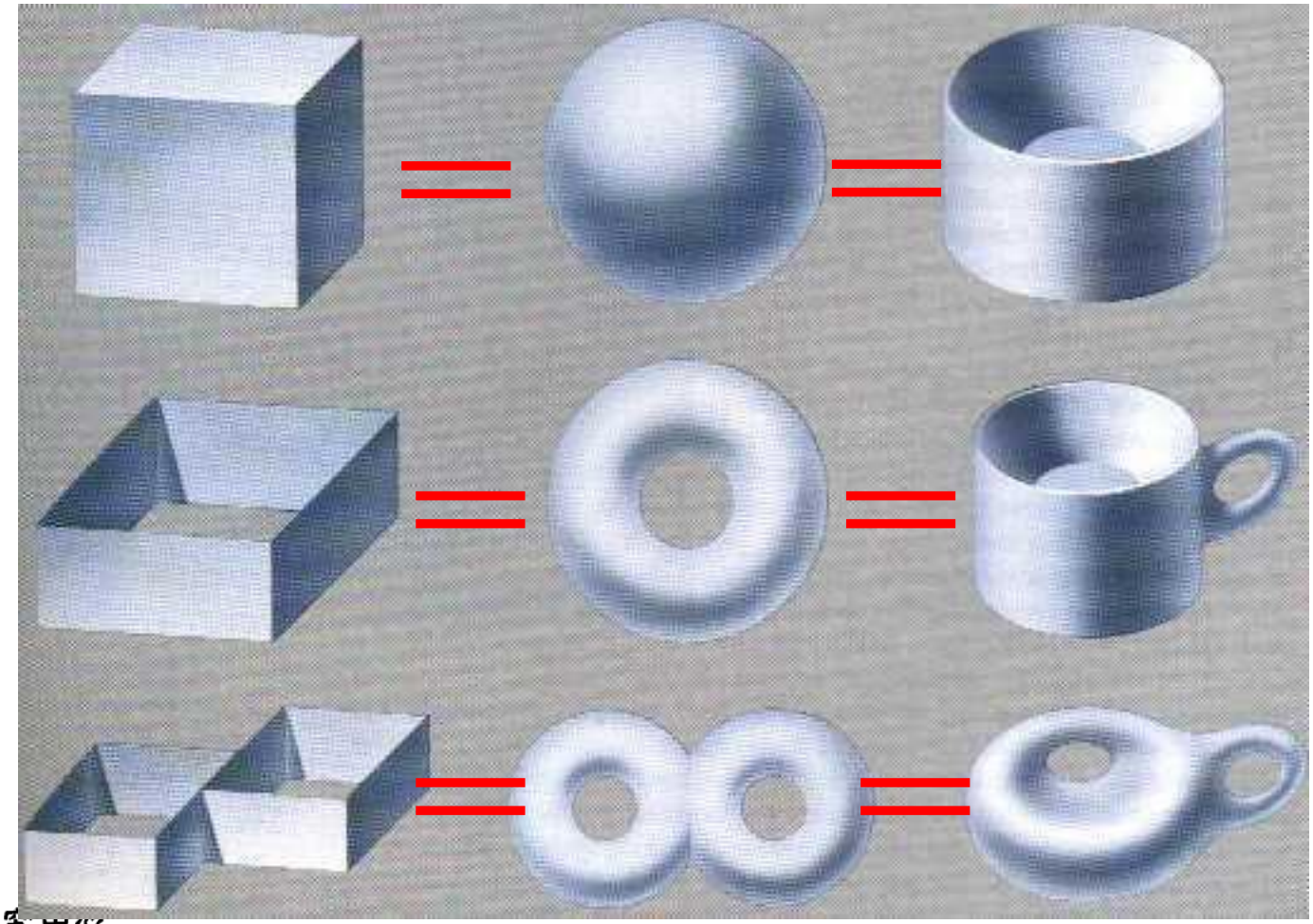

The advantage of electron transport in TIs

- electrons cannot be scattered by defects or other perturbations → **little resistance**

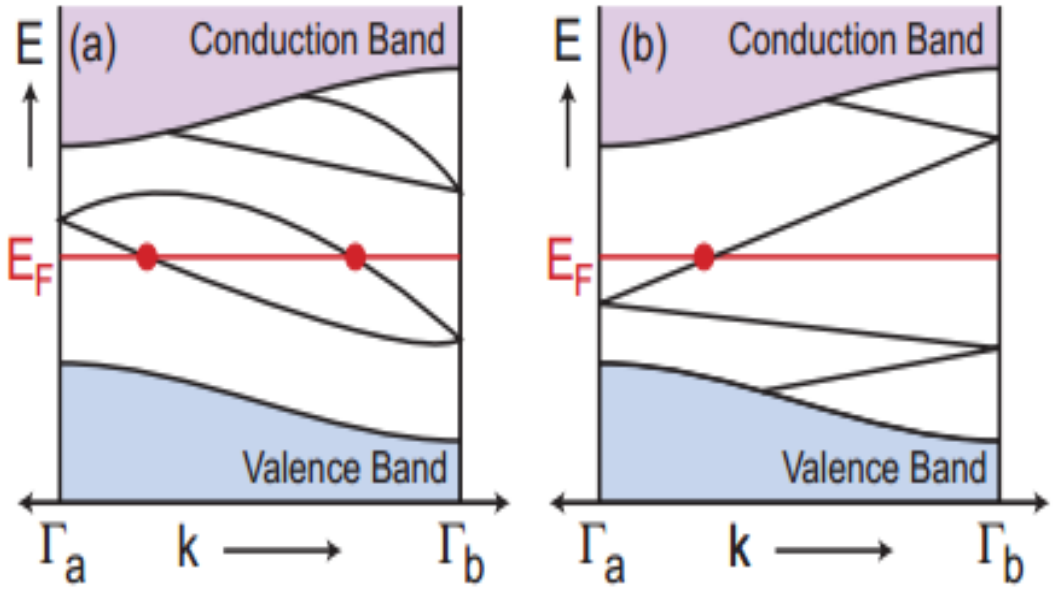

(a) Insulator (b)Topological Insulator

Z. Hasan and C. L. Kane. Reviews of Modern Physics (2010)

Hall Effect

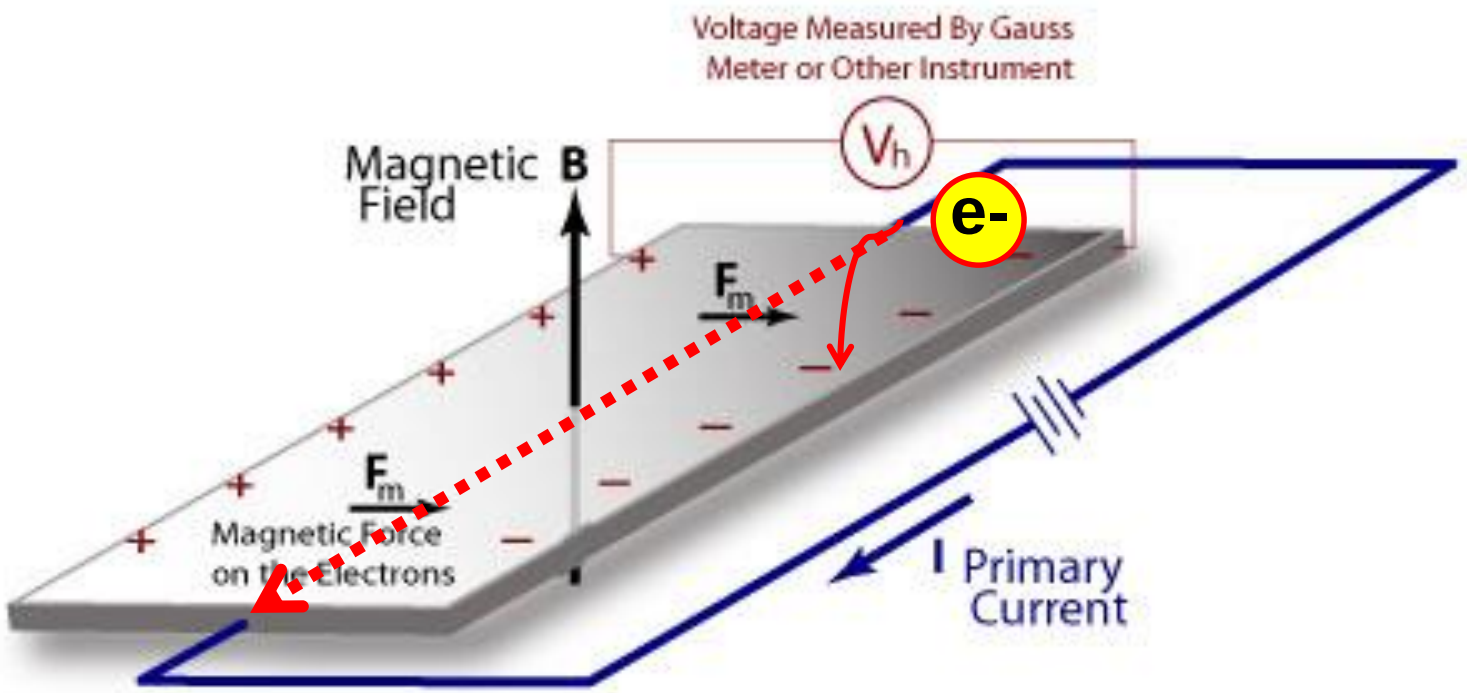
Voltage Measured By Gauss Meter or Other Instrument
Vh
Magnetic Field
B
e-
Fm
Fm
Magnetic Force on the Electrons
I Primary Current

Quantum Hall Effect

High magnetic field
Low temperature

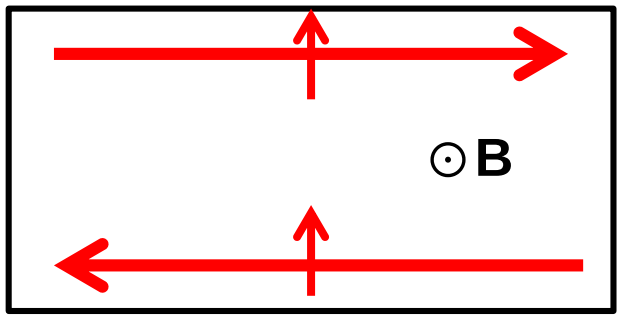

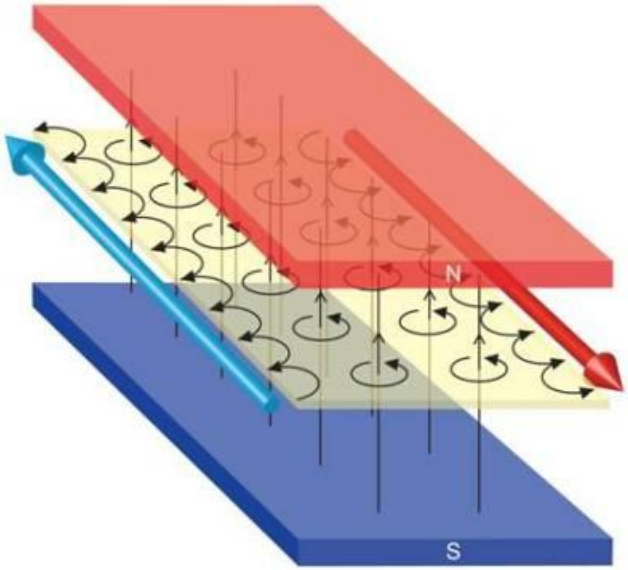

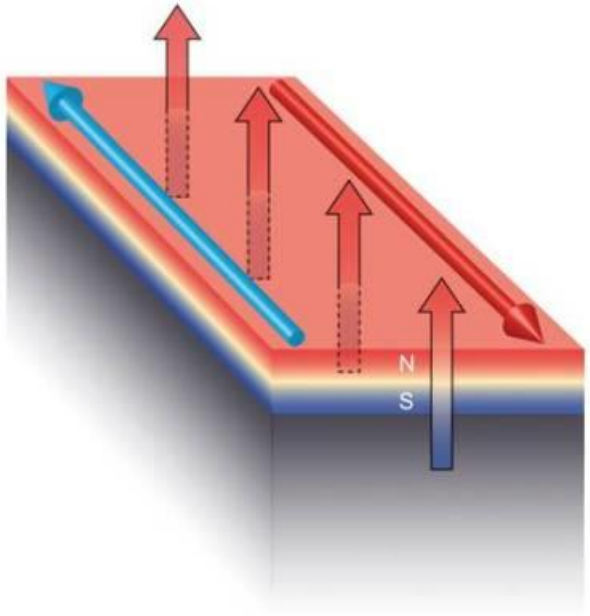

Topological insulator

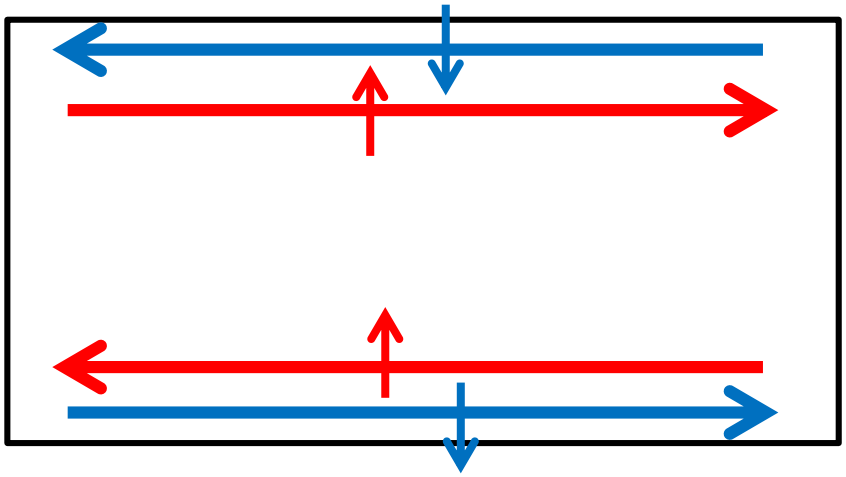

High magnetic field
Low temperature

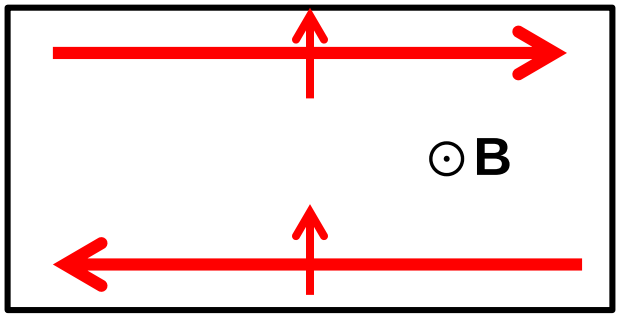

I. no external magnetic field
II. pairs of currents
III. Spin splitting

SO coupling → No external magnetic field → Quantum Spin Hall Effect

The applications of topological insulators

- **Thermoelectric materials**
  - $ZT = S^2\sigma/\kappa$
  - Bi_2Te_3, Sb_2Te_3

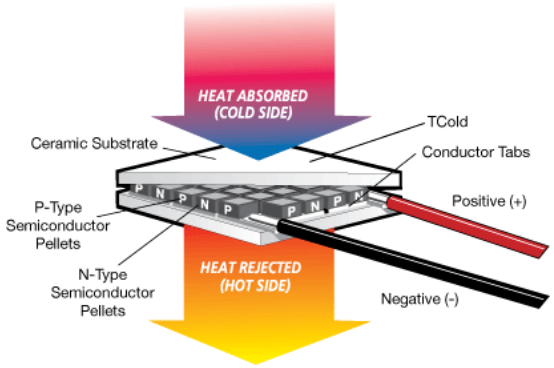

- **Spintronics device**
  - Quantum computing

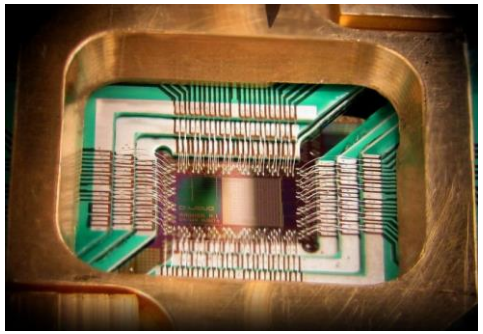

- **Find predicted Majorana fermion**
  - topological superconductor

Band inversion in topological insulator

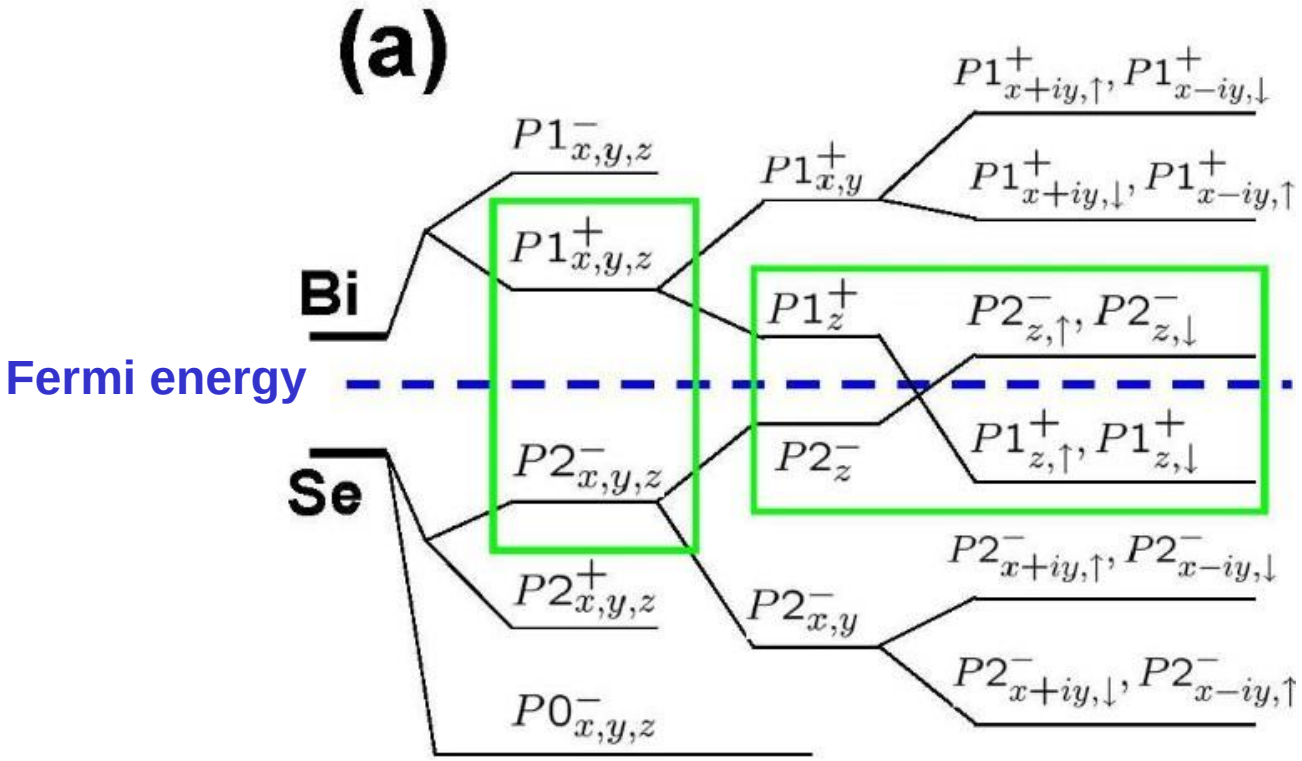

parity difference

crystal field splitting

spin-orbital coupling

Xiao-Liang Qi and Shou-Cheng Zhang, RMP (2011)

The difference of band Structure between insulator and TI

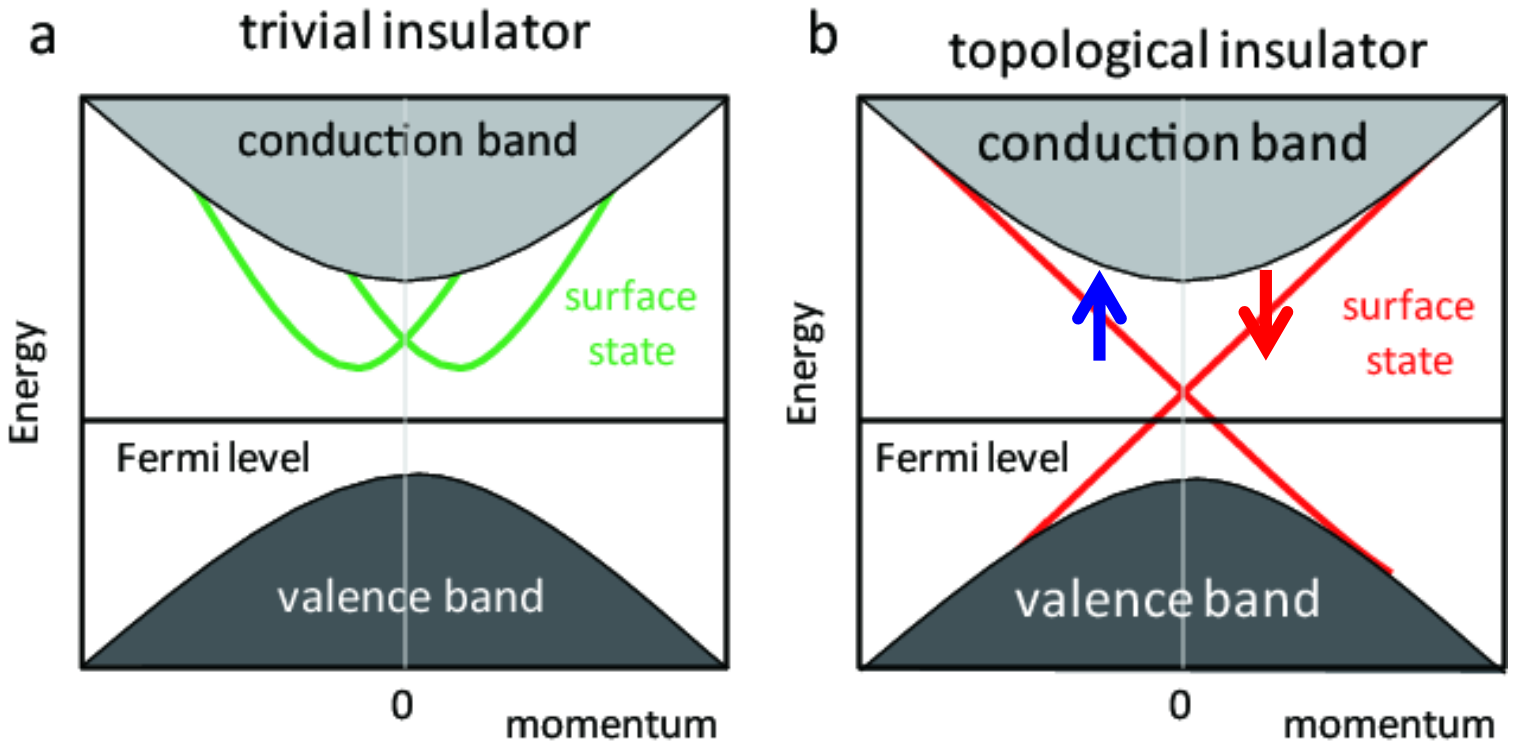

time-reversal symmetry protected

http://www.scholarpedia.org/article/Topological_insulators

The electronic structure of TI

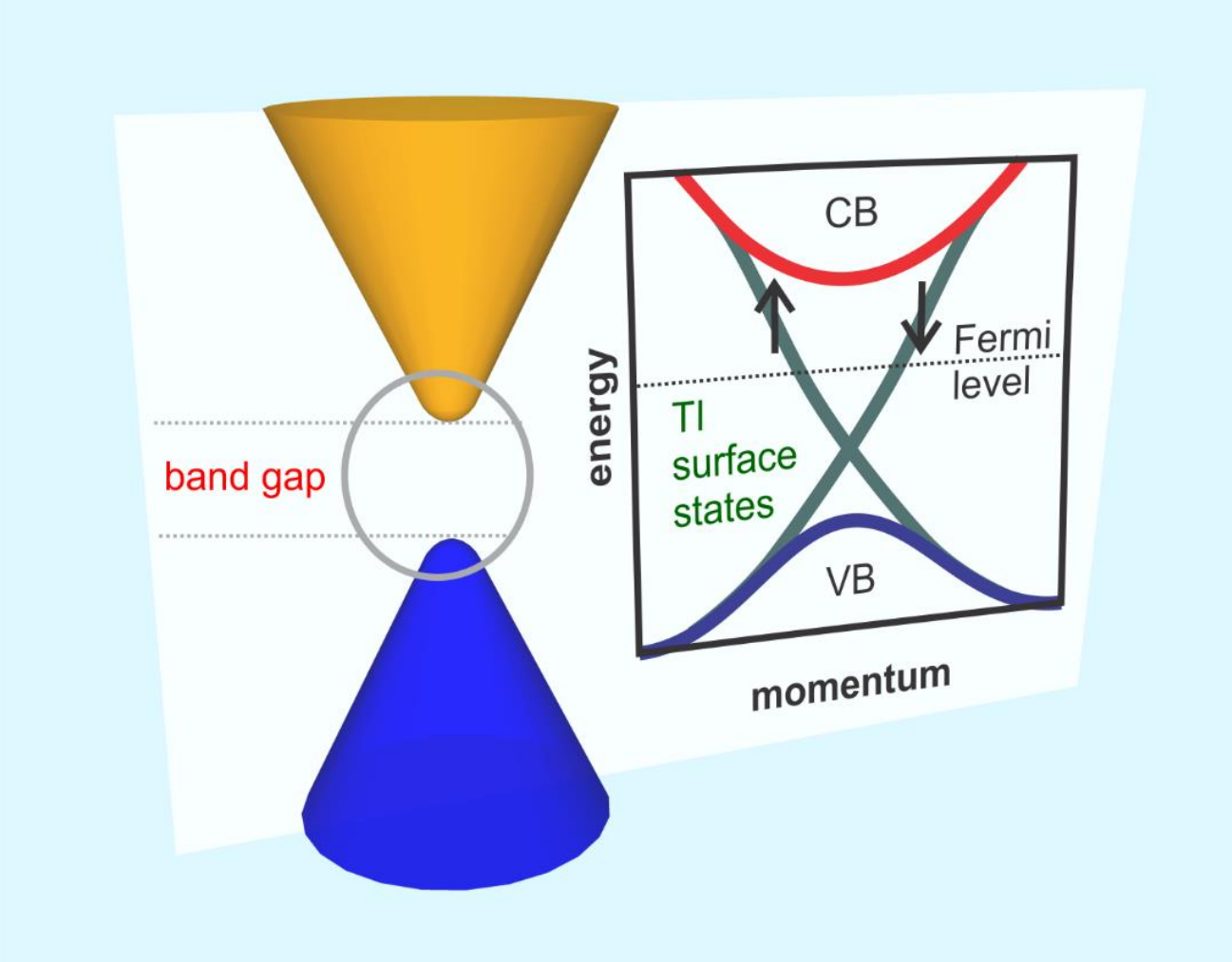

https://www.diamond.ac.uk/Science/Research/Highlights/2015/I10-MSG-TIs.html

Predictions of 3D topological insulators

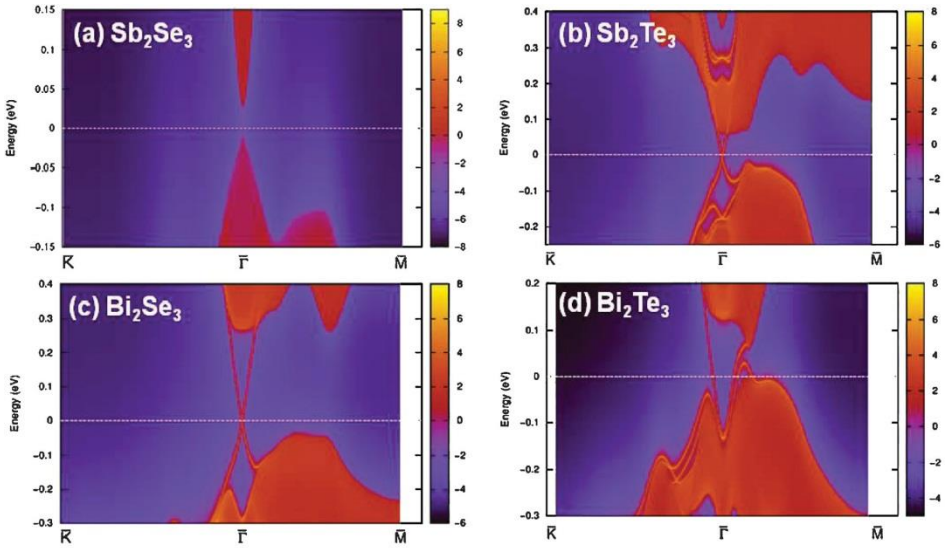

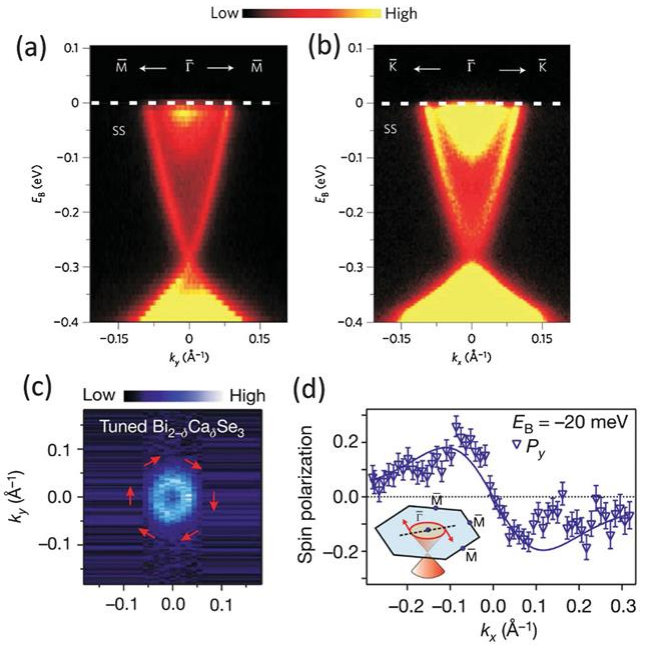

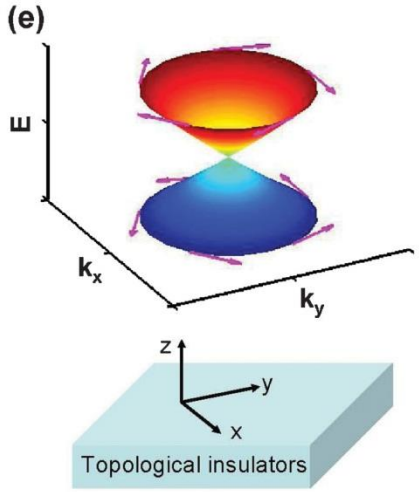

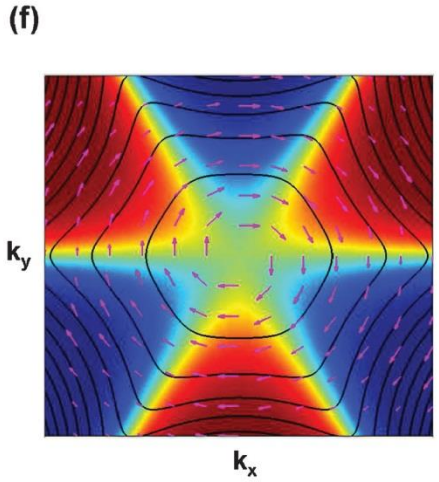

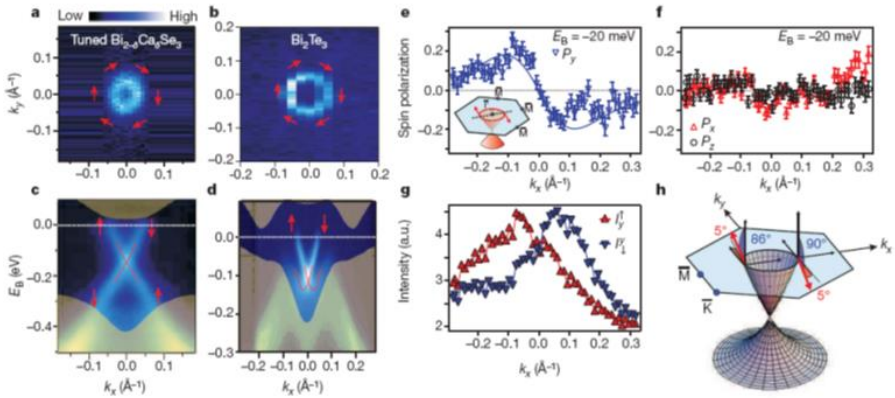

Xia et al., Nature Physics (2009)
Hsieh et al., Nature (2009)

Chen et al, Science (2009)
Xiao-Liang Qi, RMP (2011)

Predictions of 3D topological insulators

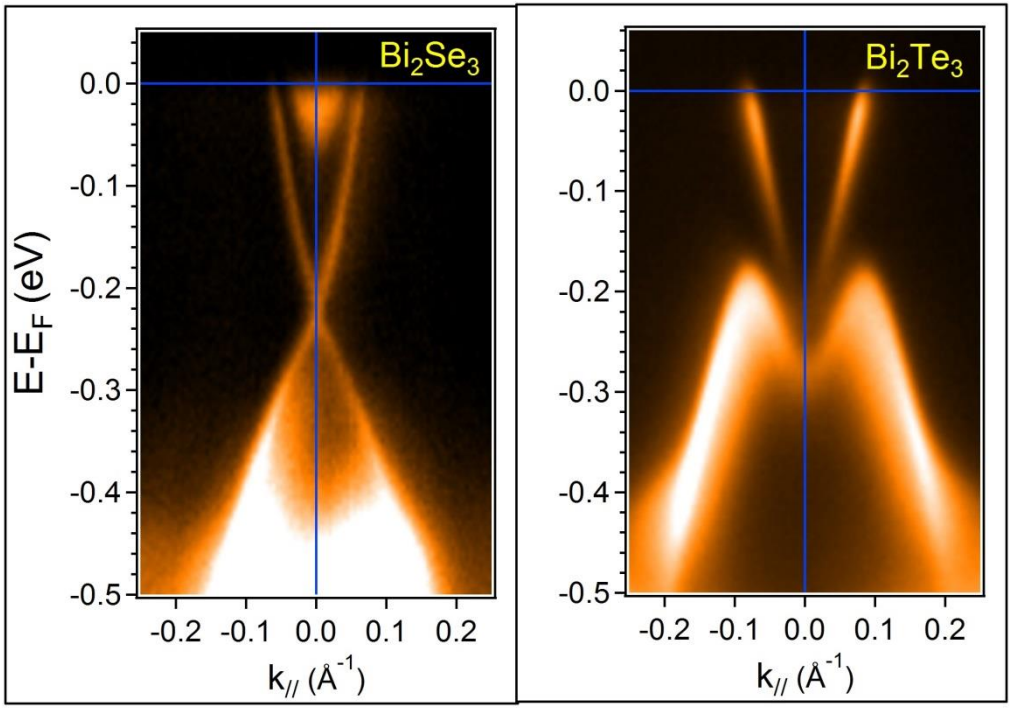

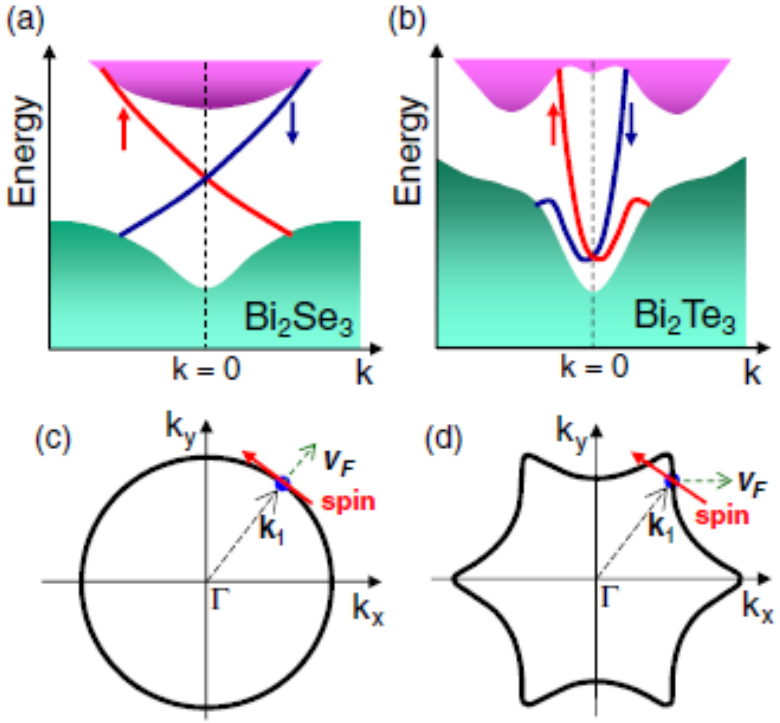

Spectra taken at BL21B1, NSRRC

國家同步輻射研究中心
National Synchrotron Radiation Research Center

Y. Ando, J. Phys. Soc. Japan (2013)

Initial growth condition of Bi family TIs

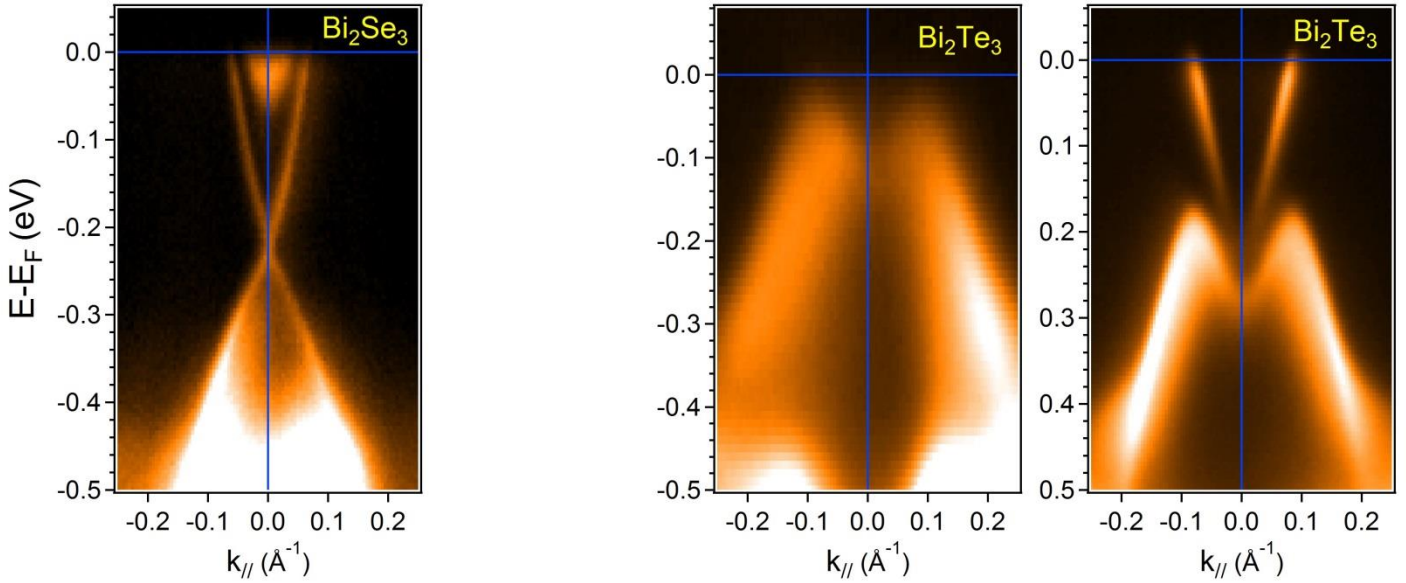

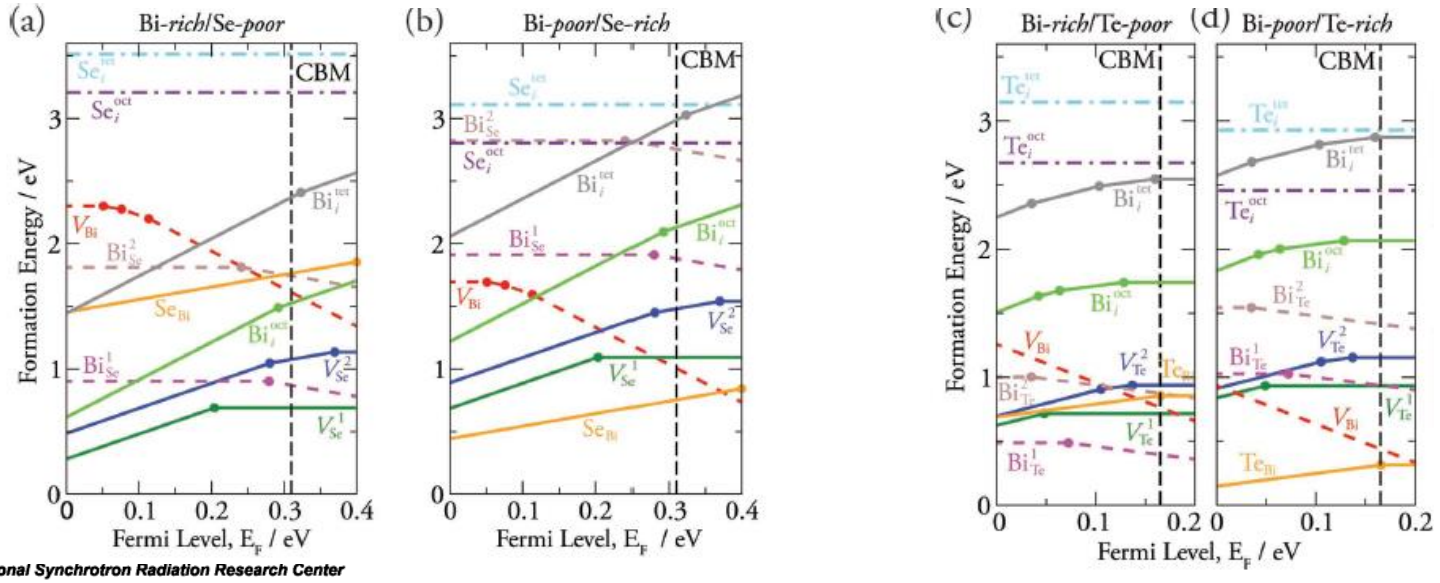

National Synchrotron Radiation Research Center

D.O. Scanlon, Adv. Mat. (2012)

Band mapping of Bi_2Se_3

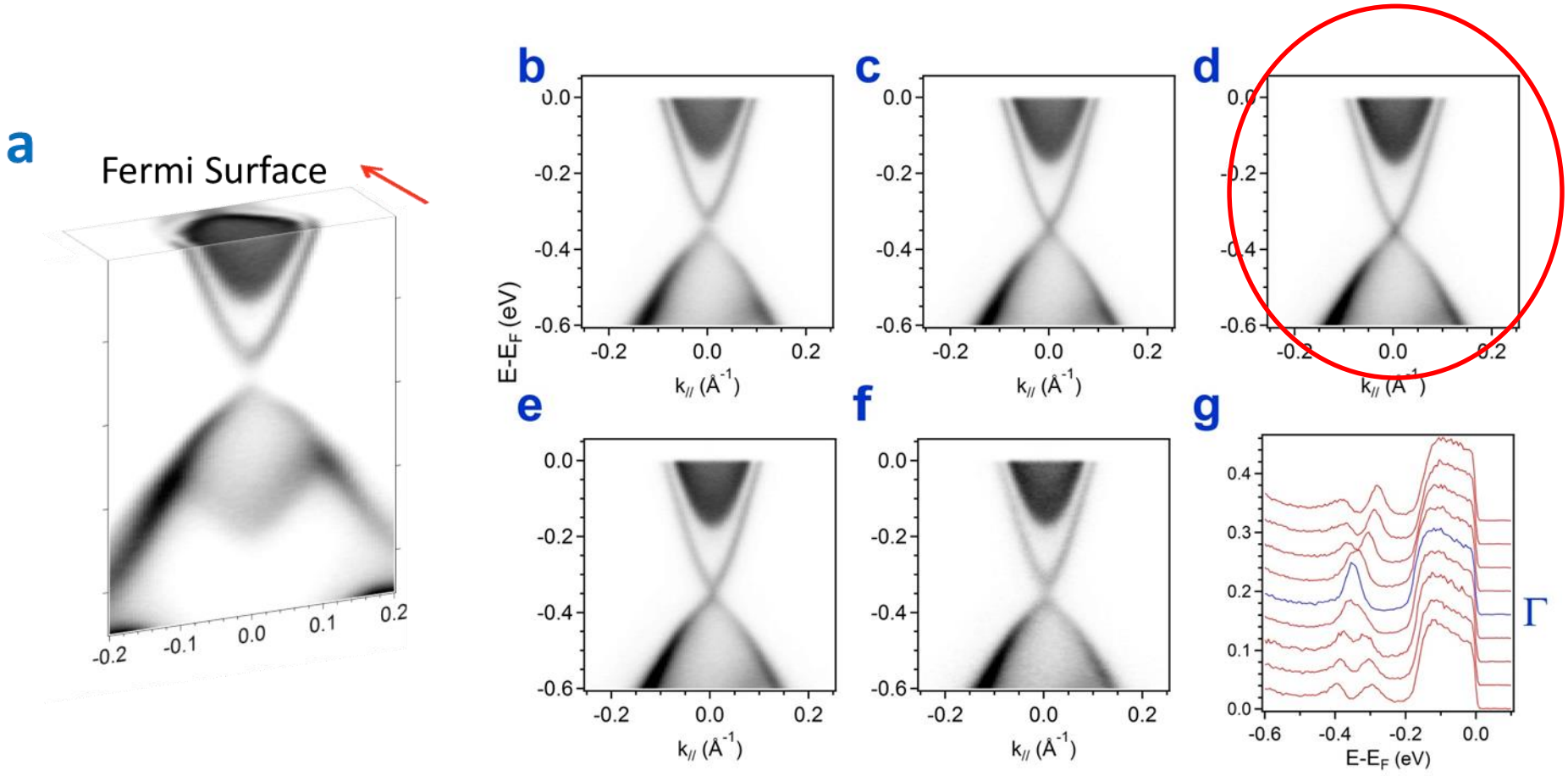

國家同步輻射研究中心
National Synchrotron Radiation Research Center

Band mapping of $Sb_2Te_{3-x}Se_x$ with varied Se content

Along $\overline{\Gamma}\overline{K}$

x=0 x=1 x=2 x=2.4

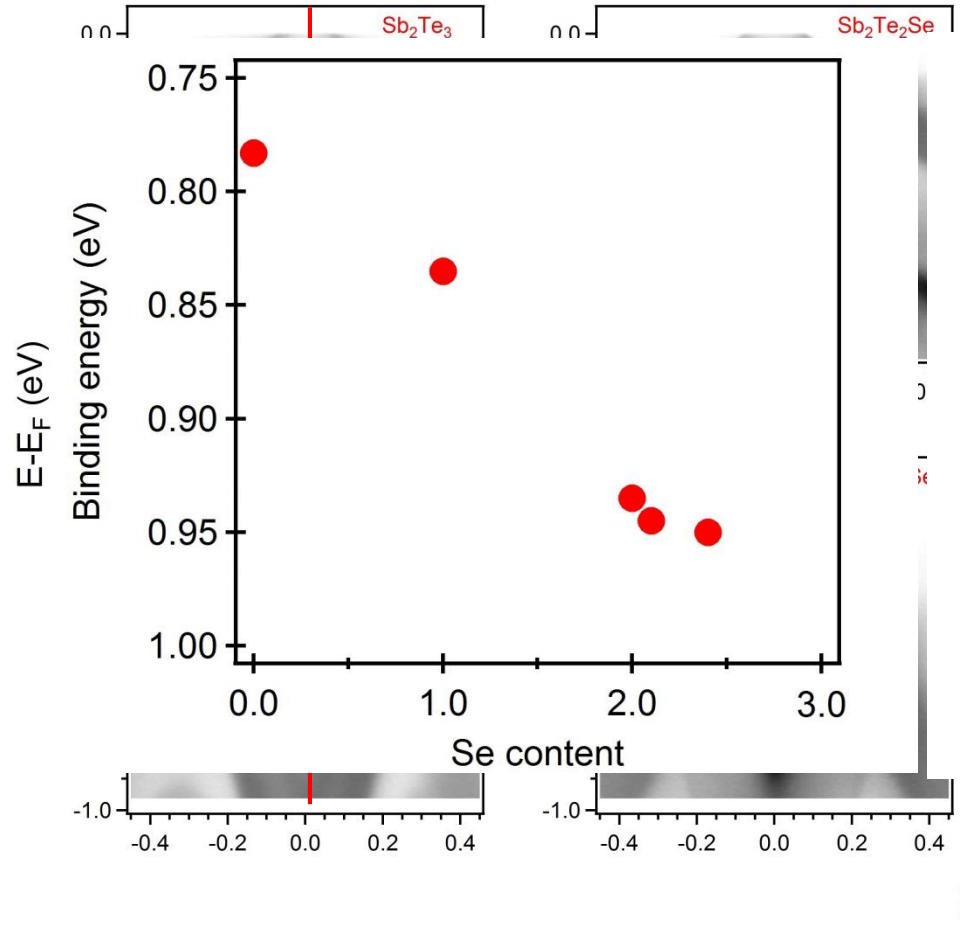

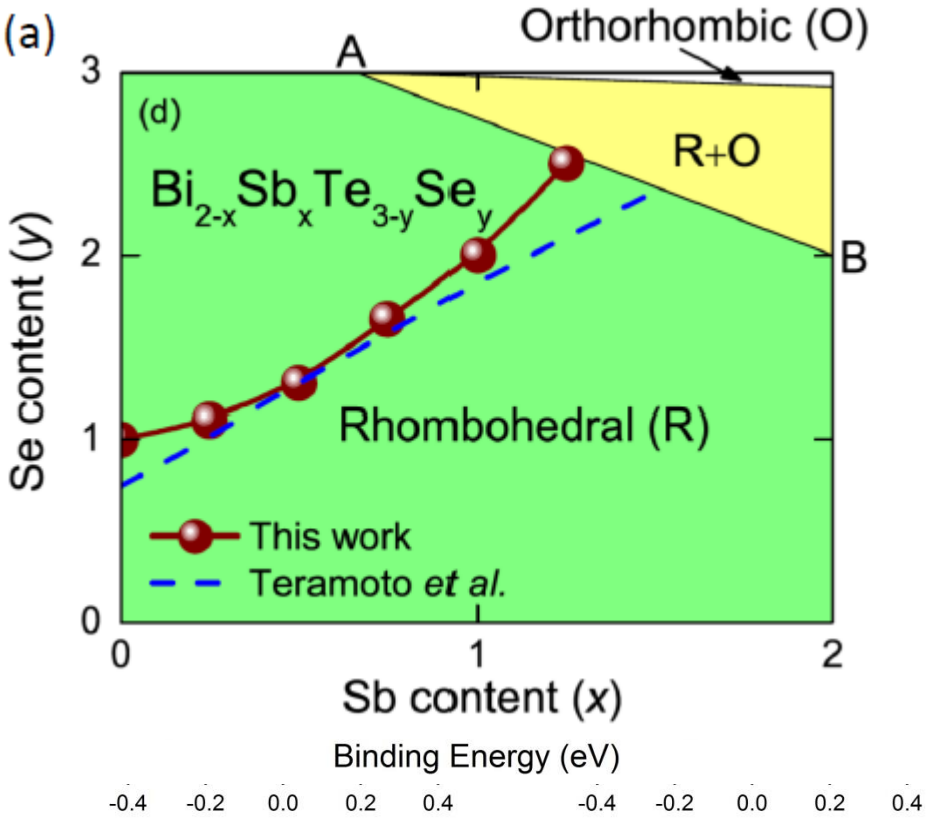

Manuscript in preparation

Tuning the position of the Dirac point in ternary TIs and doped TIs

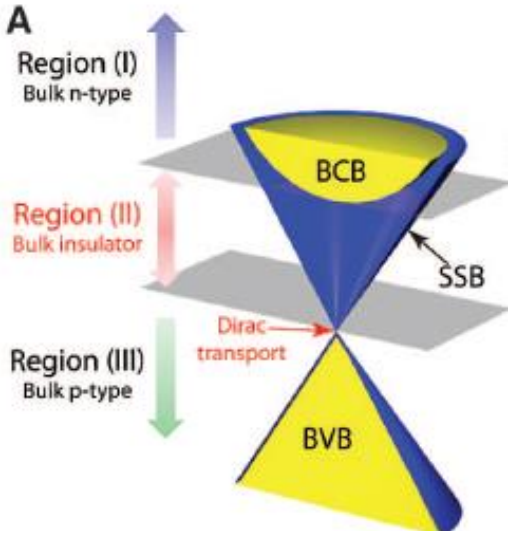

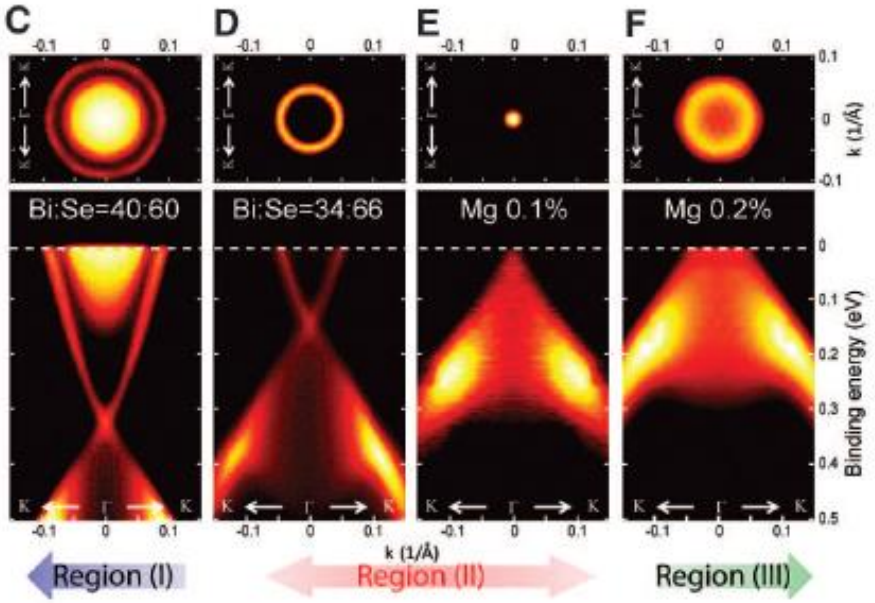

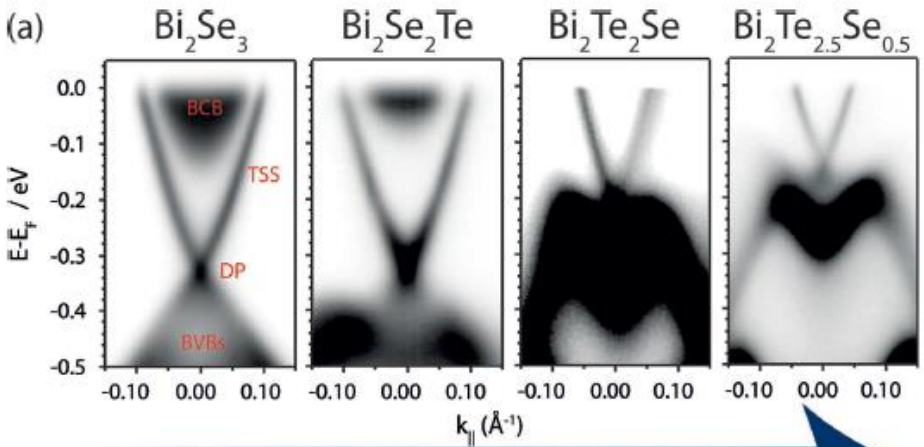

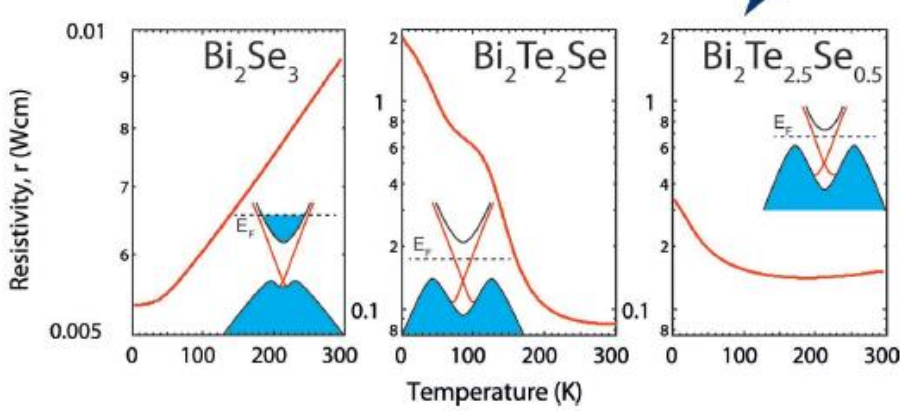

YL Chen, Science (2014)

Reducing the thickness of Sb_2Te_3 thin film

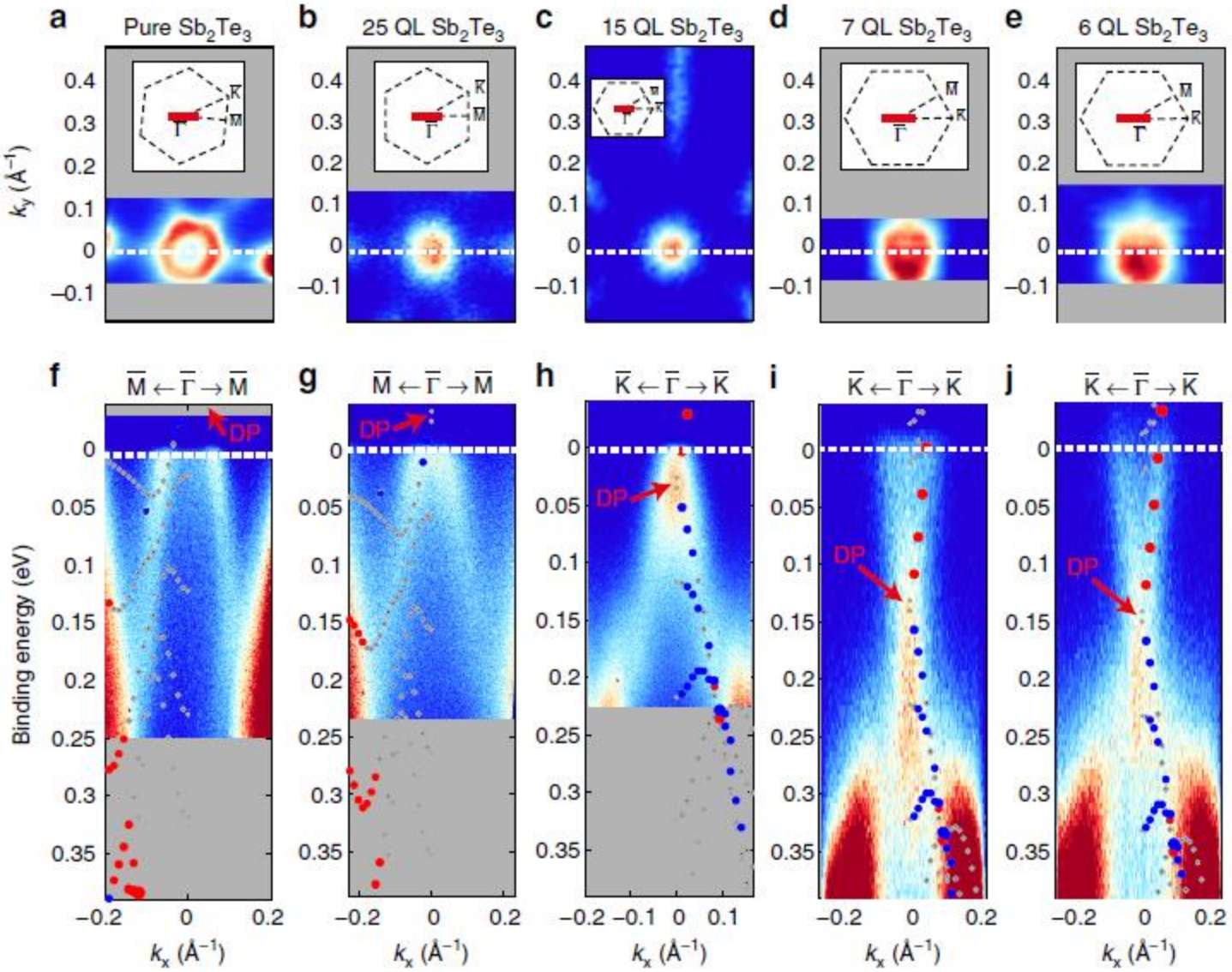

Eschbach et al., Nat. Comm. (2015)

Spin-orbit torque and surface states in topological insulators

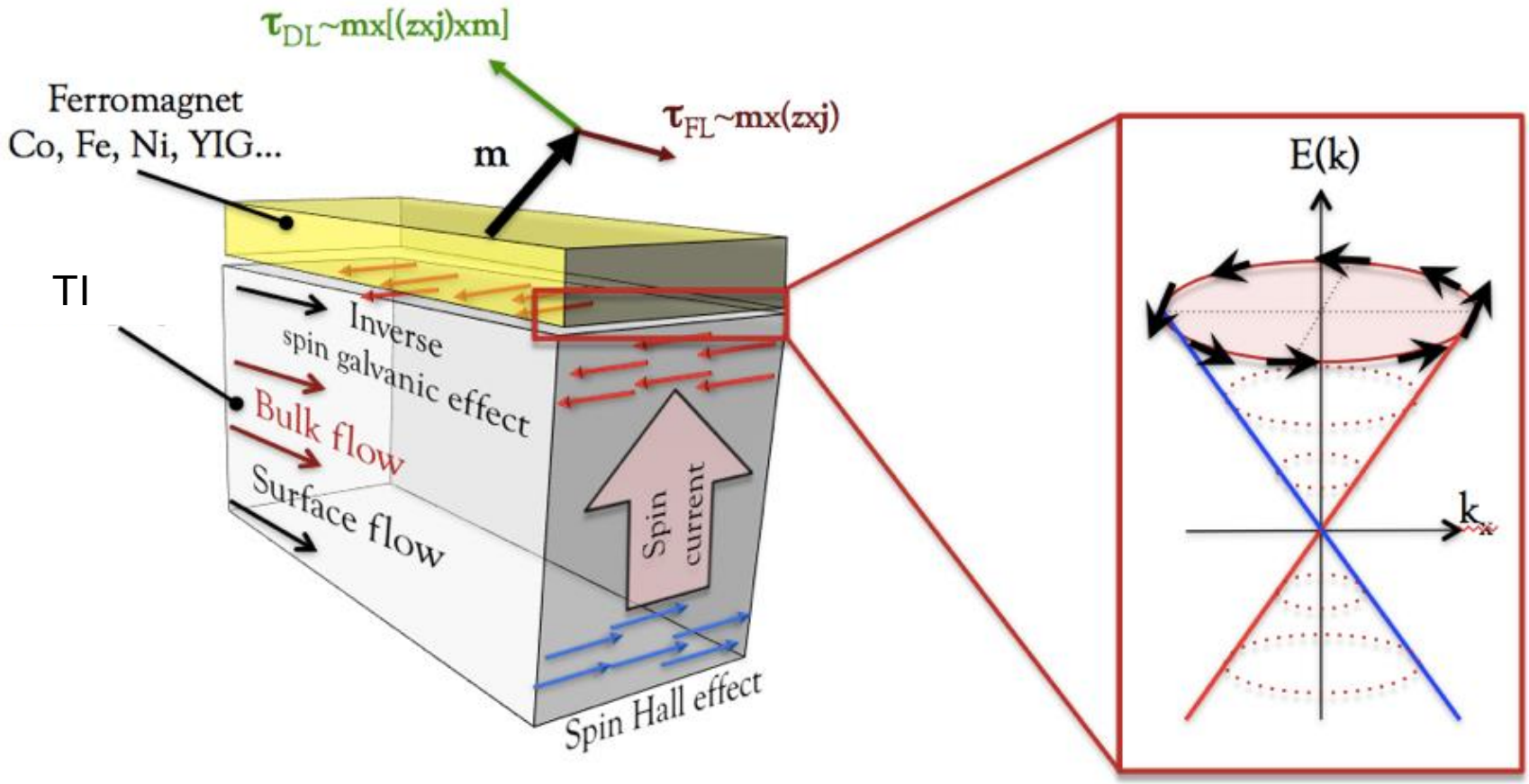

https://spintronics.kaust.edu.sa/Pages/Research_Spin-orbit%20physics.aspx

Spintronics potential at the surface of topological insulators

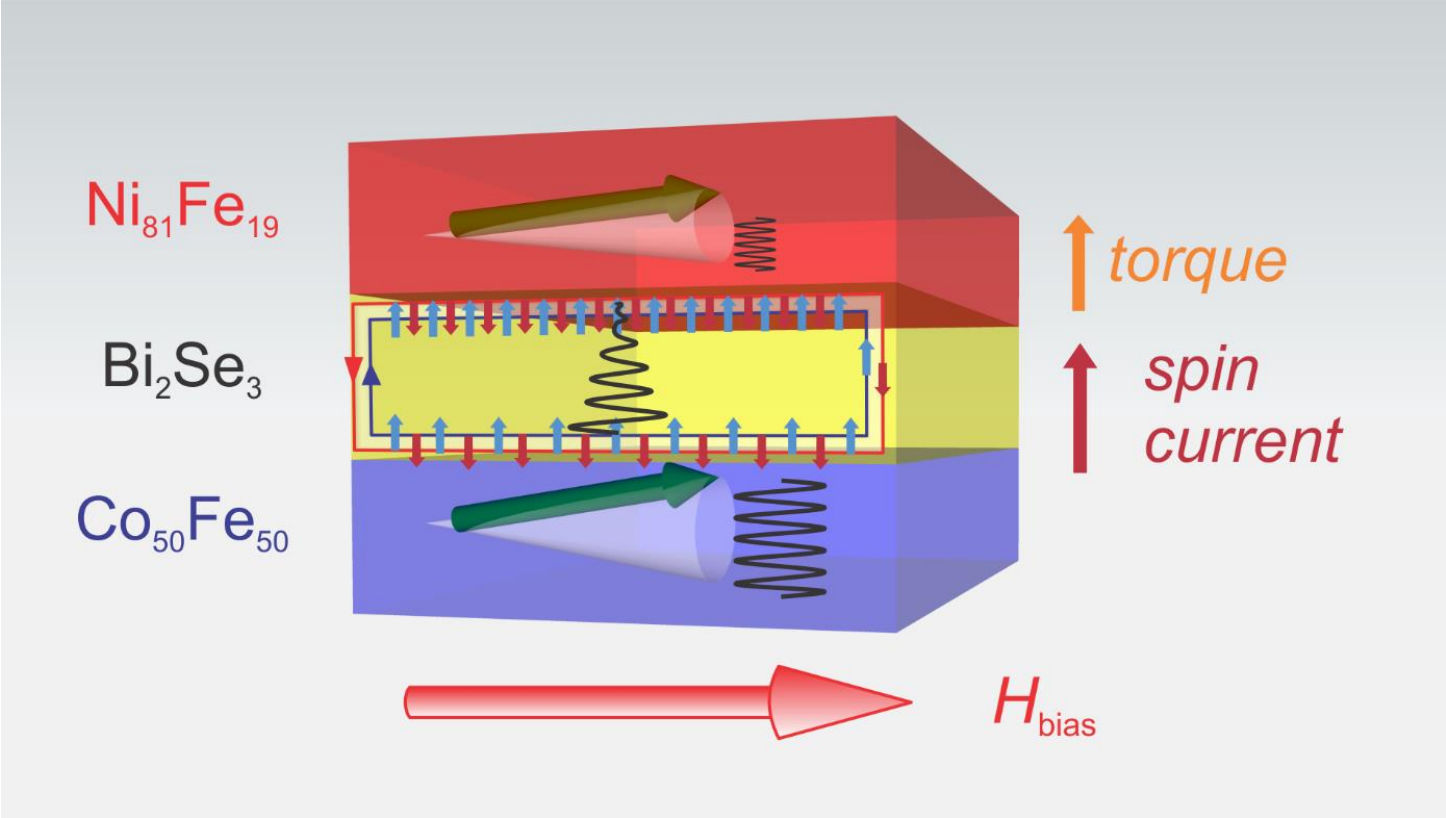

a pure spin current from the CoFe layer through the TI Bi2Se3 into the NiFe layer, exerting a spin transfer torque.

Baker et al., Scientific Reports (2015)

The applications of topological insulators

- **Thermoelectric materials**
  - $ZT = S^2\sigma/\kappa$
  - Bi_2Te_3, Sb_2Te_3

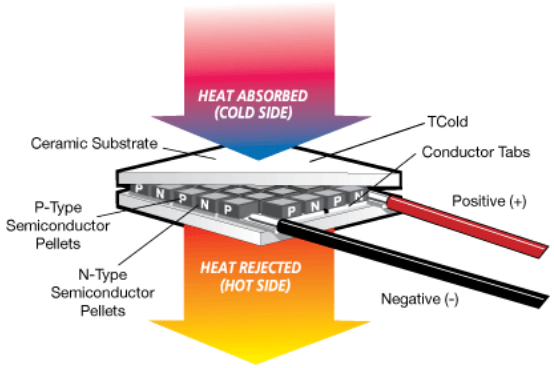

- **Spintronics device**
  - Quantum computing

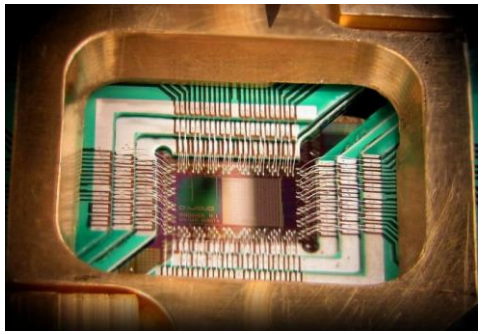

- **Find predicted Majorana fermion**
  - topological superconductor

Superconductivity in Sb_2Te_3

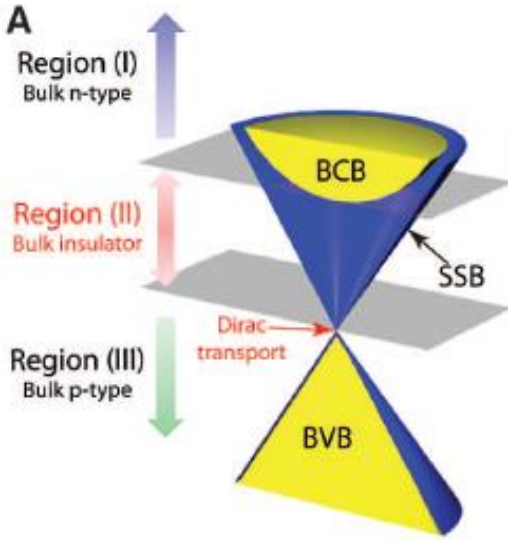

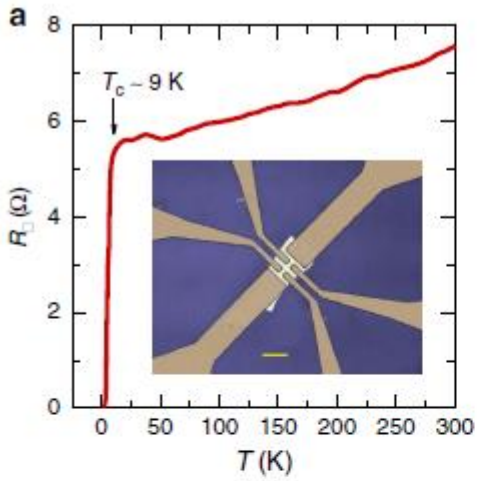

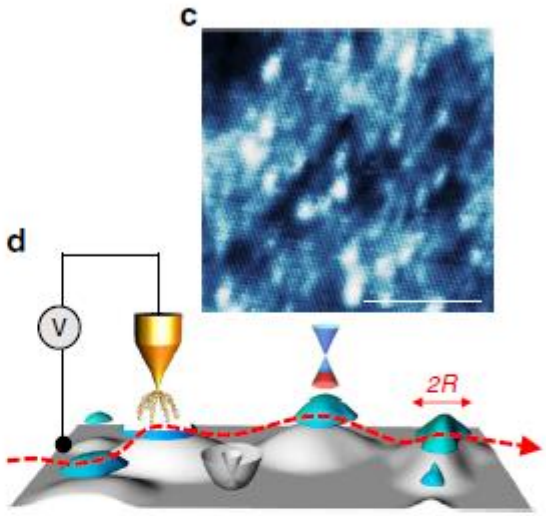

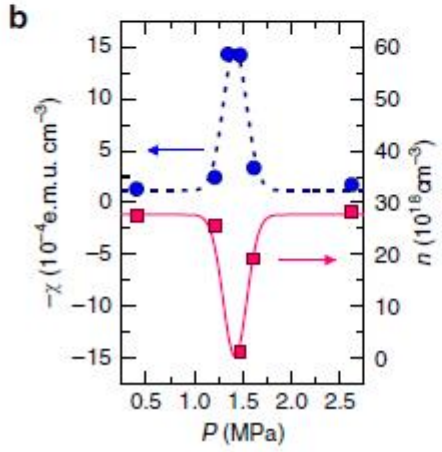

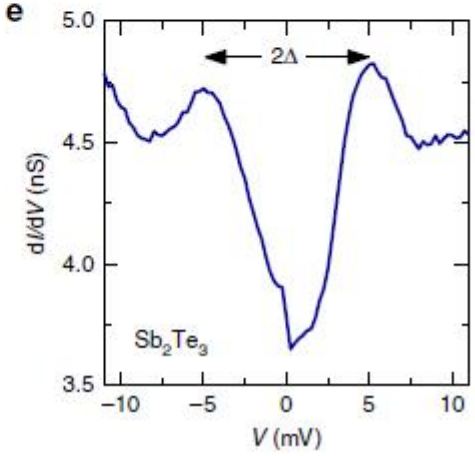

Sb_2Te_3 crystal was synthesized under 1.4 Mpa Te vapour pressure.

Carrier mobility increases to μ ~25,000 due to the upshift of the Fermi energy

Zhao et al., Nat. Comm. (2015)

Superconductivity in Cu doped Bi_2Se_3 compound

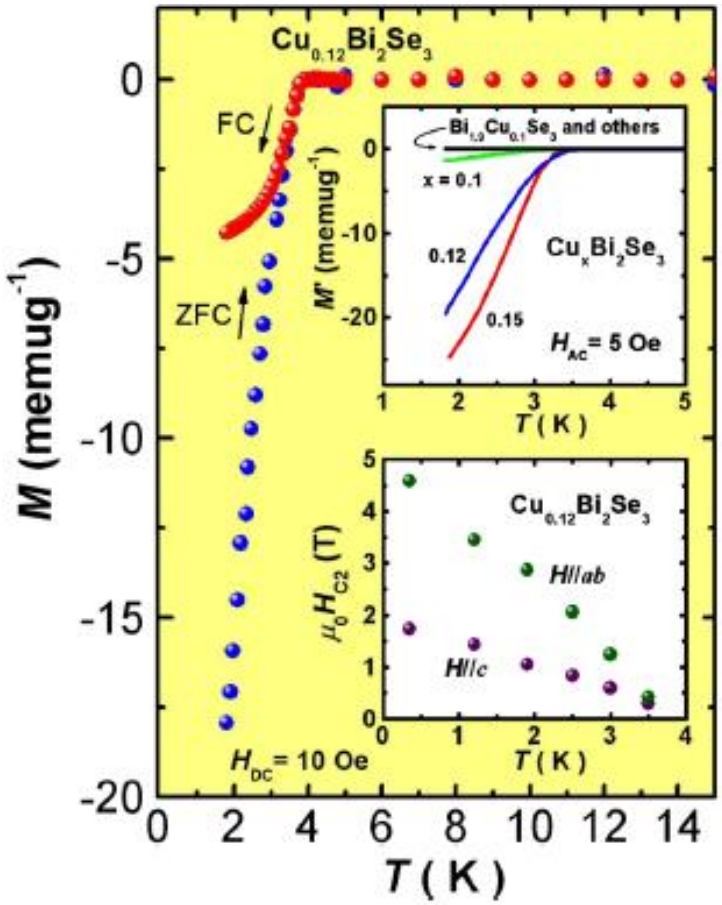

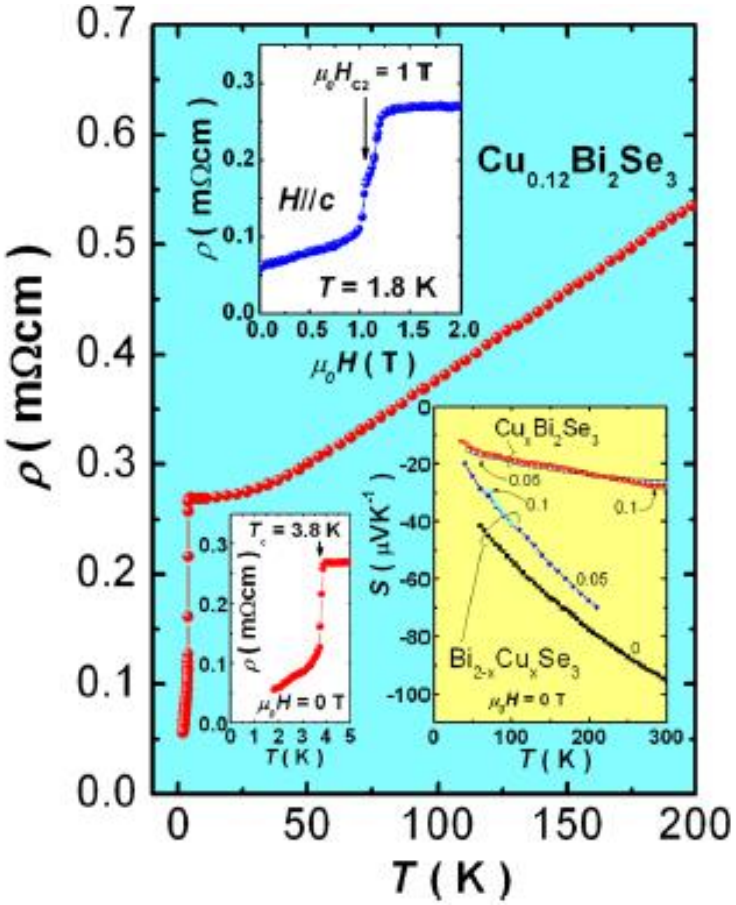

Hor et al., PRL (2010)

$Cu_xBi_2Se_3$ for 0.1<x<0.15

Superconductivity in Cu doped Bi_2Se_3 compound

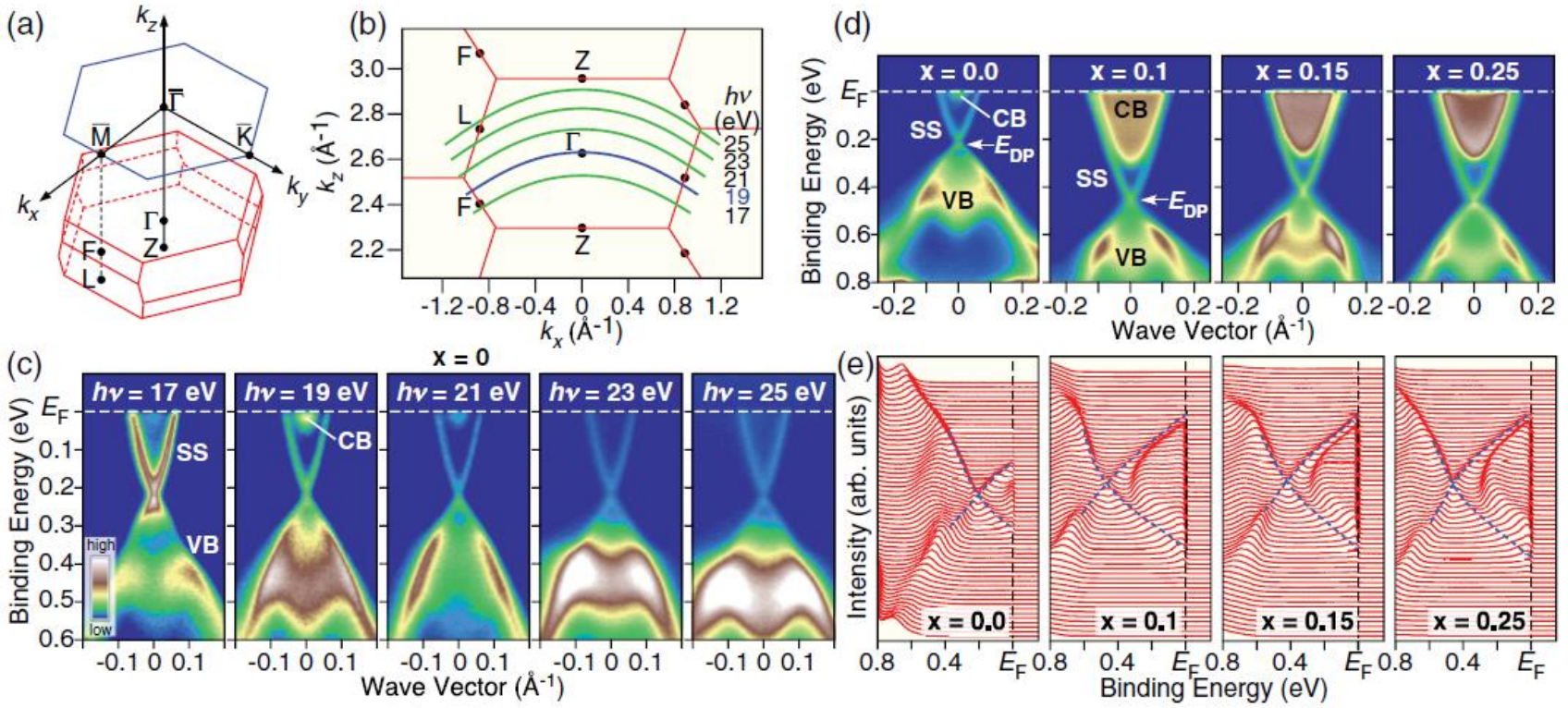

Tanaka et al., PRB (2012)

Superconductivity in Cu doped Bi_2Se_3 compound

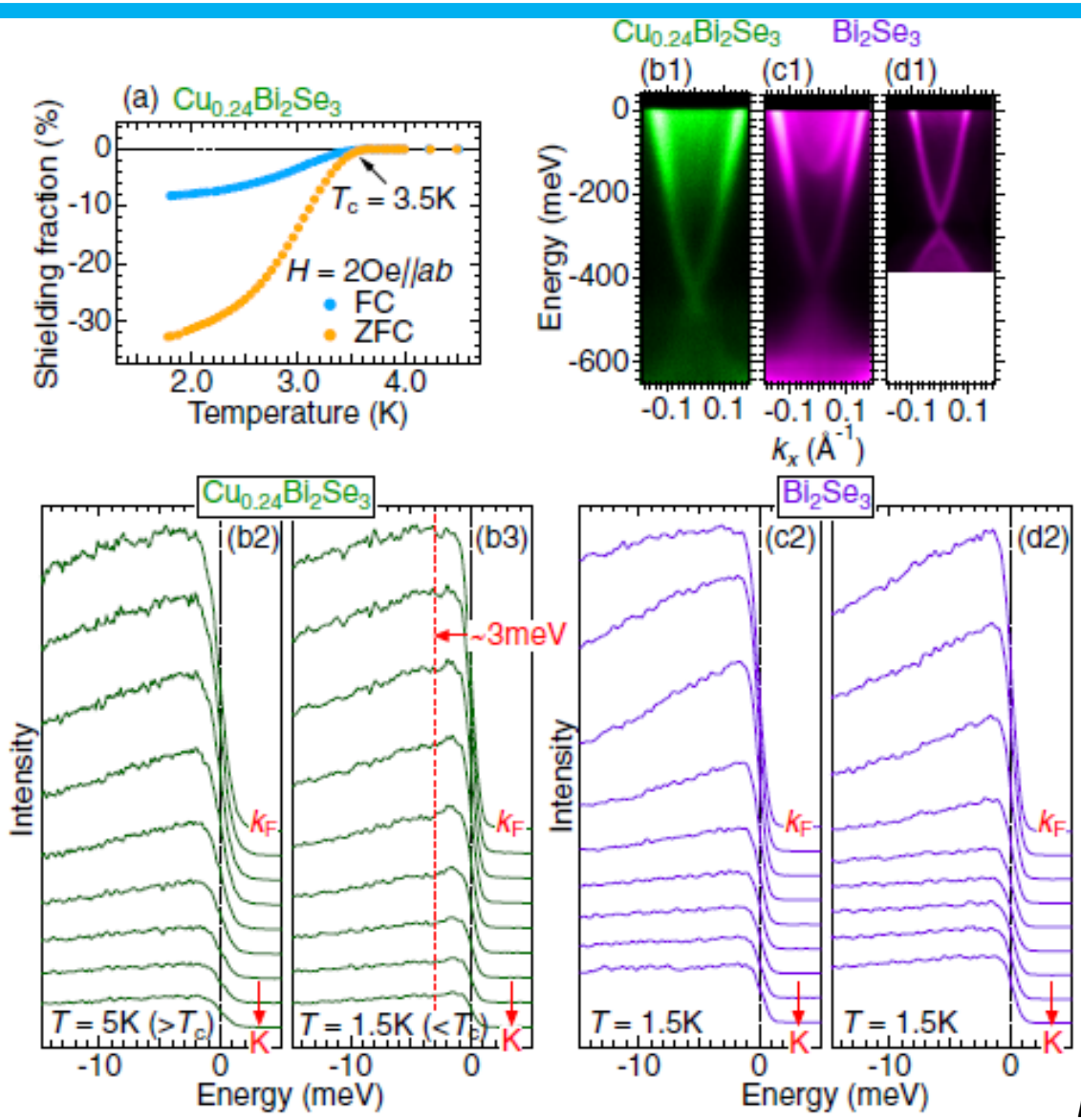

Kondo et al., PRL (2013)

Dirac semimetal and Weyl semimetal

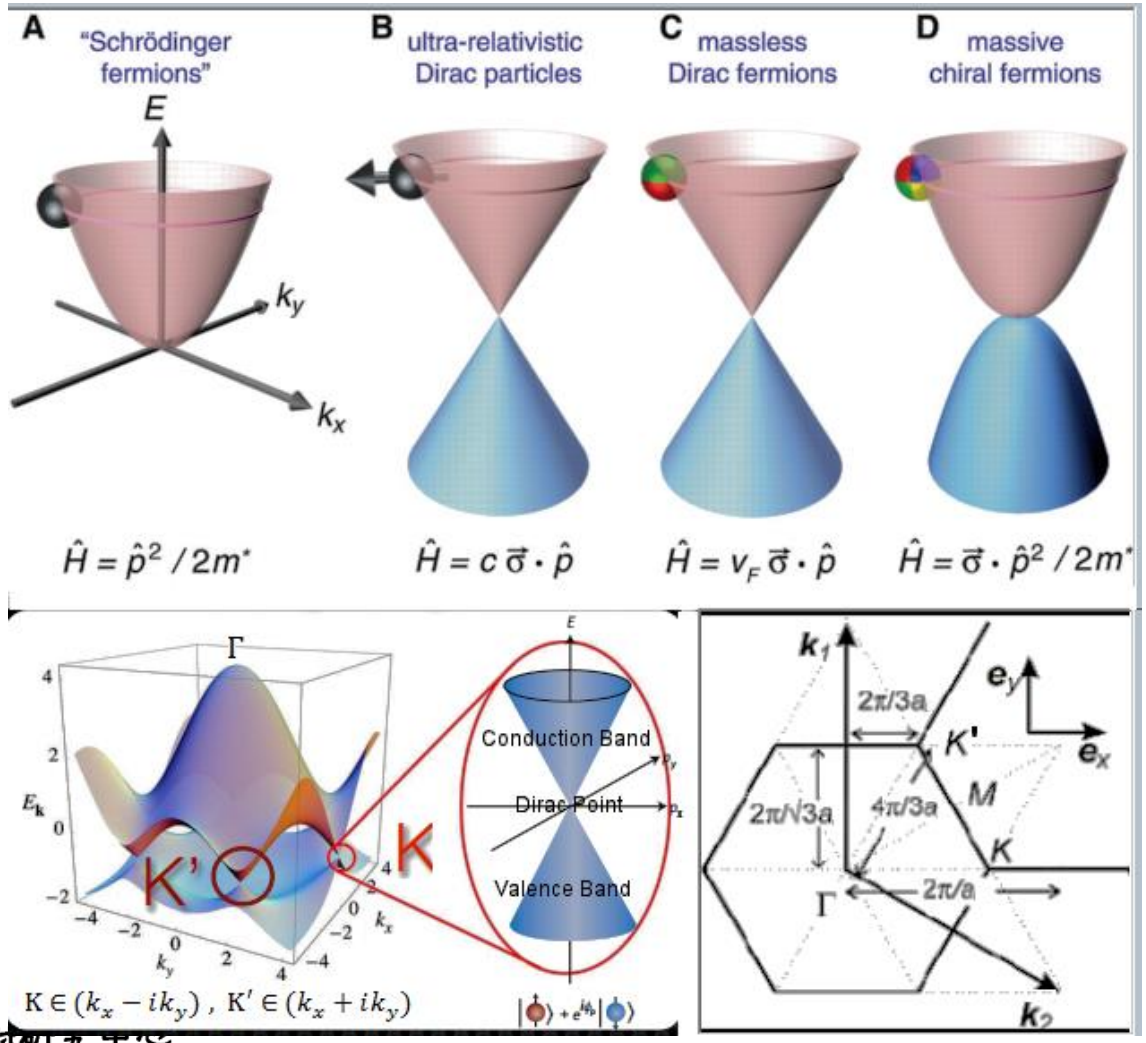

Dirac semimetal and Weyl semimetal

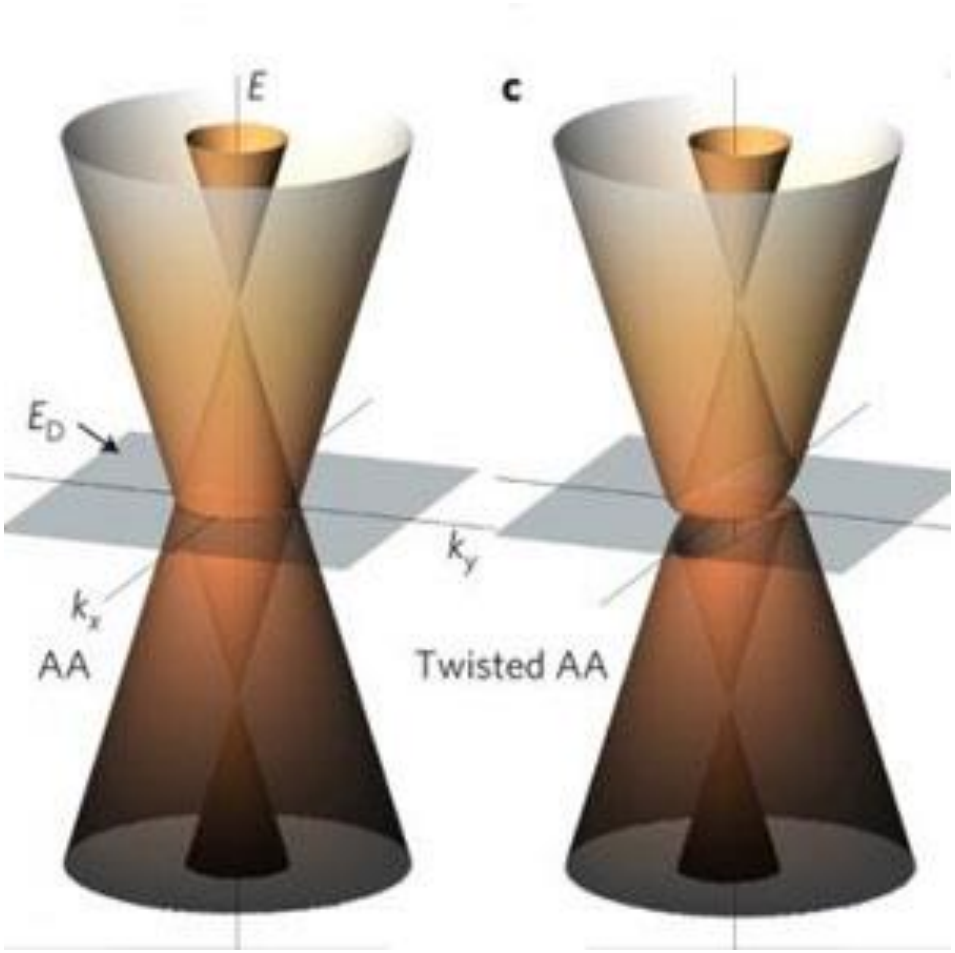

Dirac semimetal and Weyl semimetal

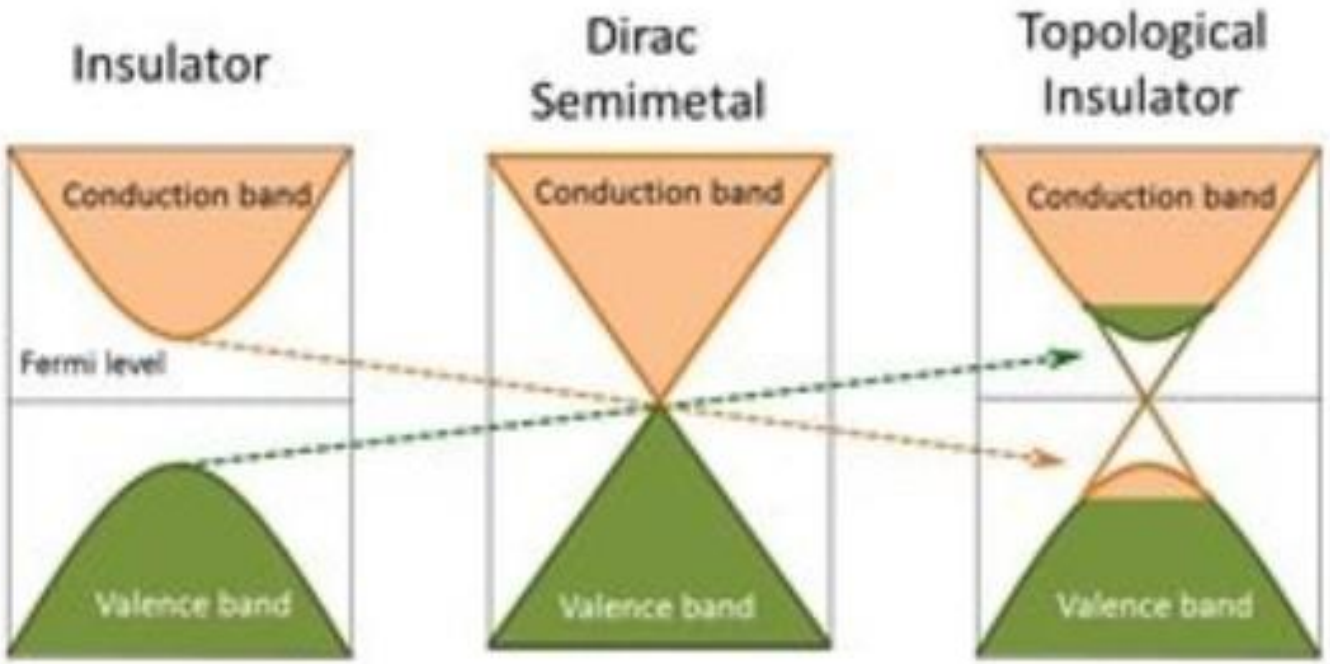

Dirac semimetal and Weyl semimetal

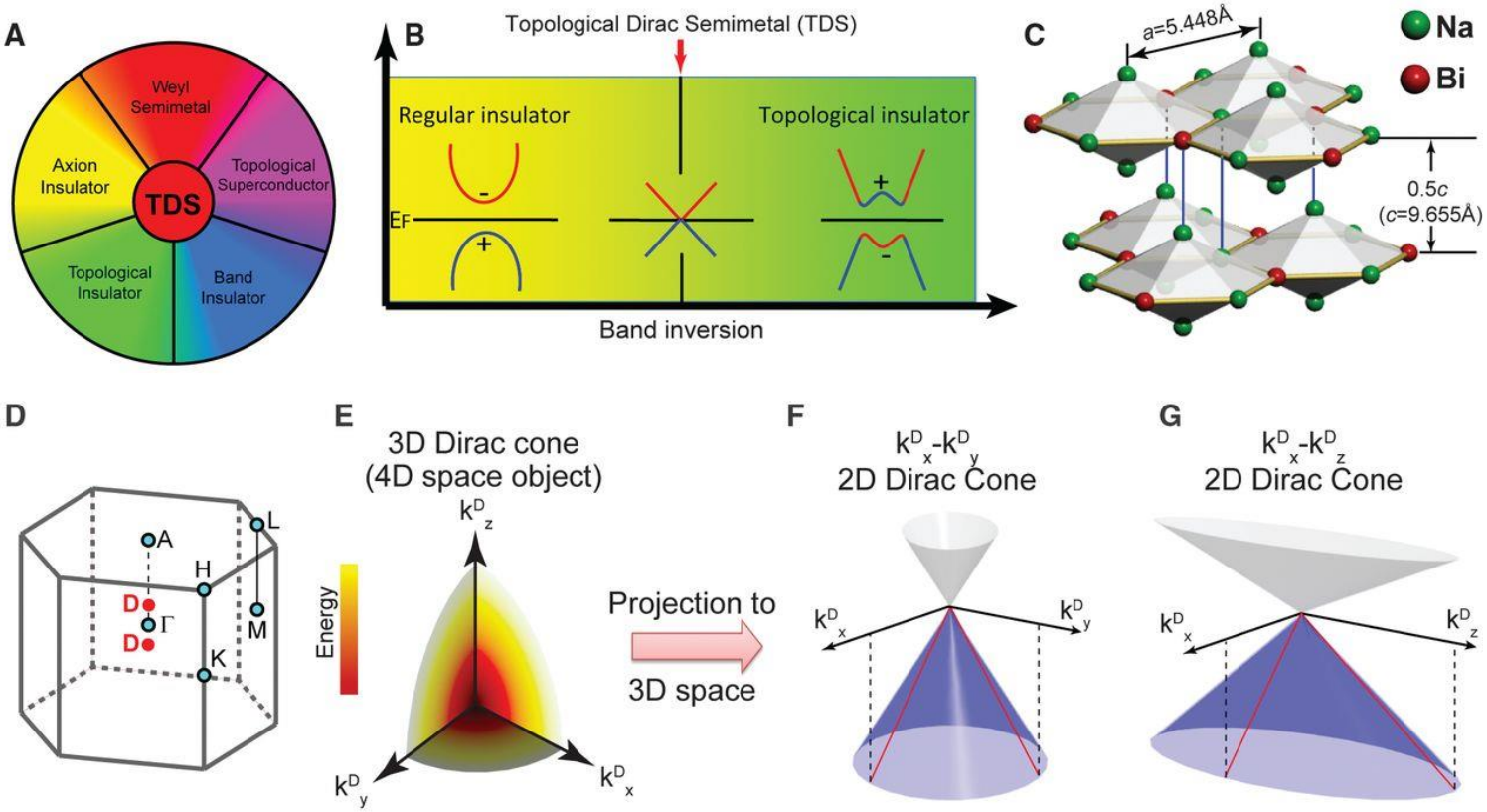

Liu et al., Science (2014)

Dirac semimetal and Weyl semimetal

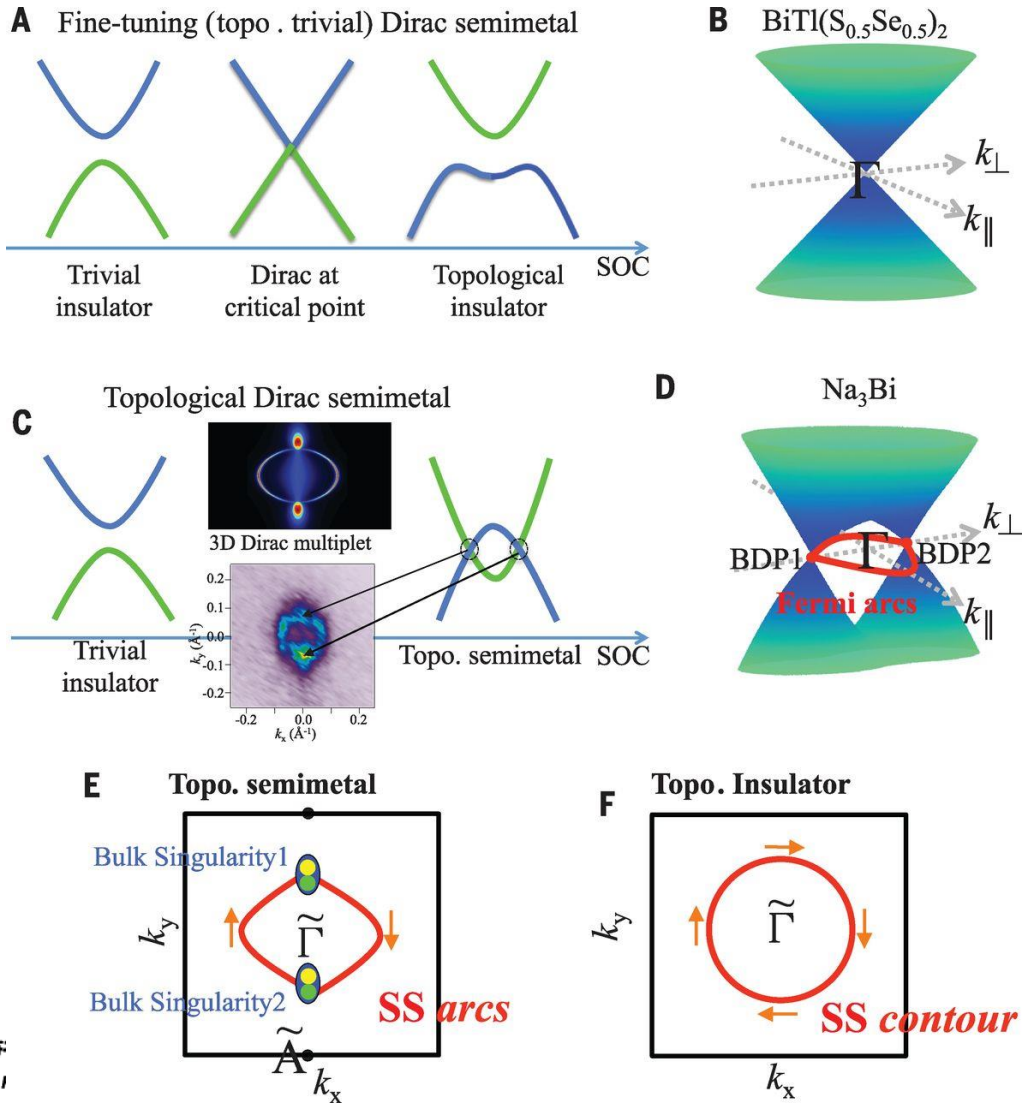

Xu et al., Science (2014)

Dirac semimetal and Weyl semimetal

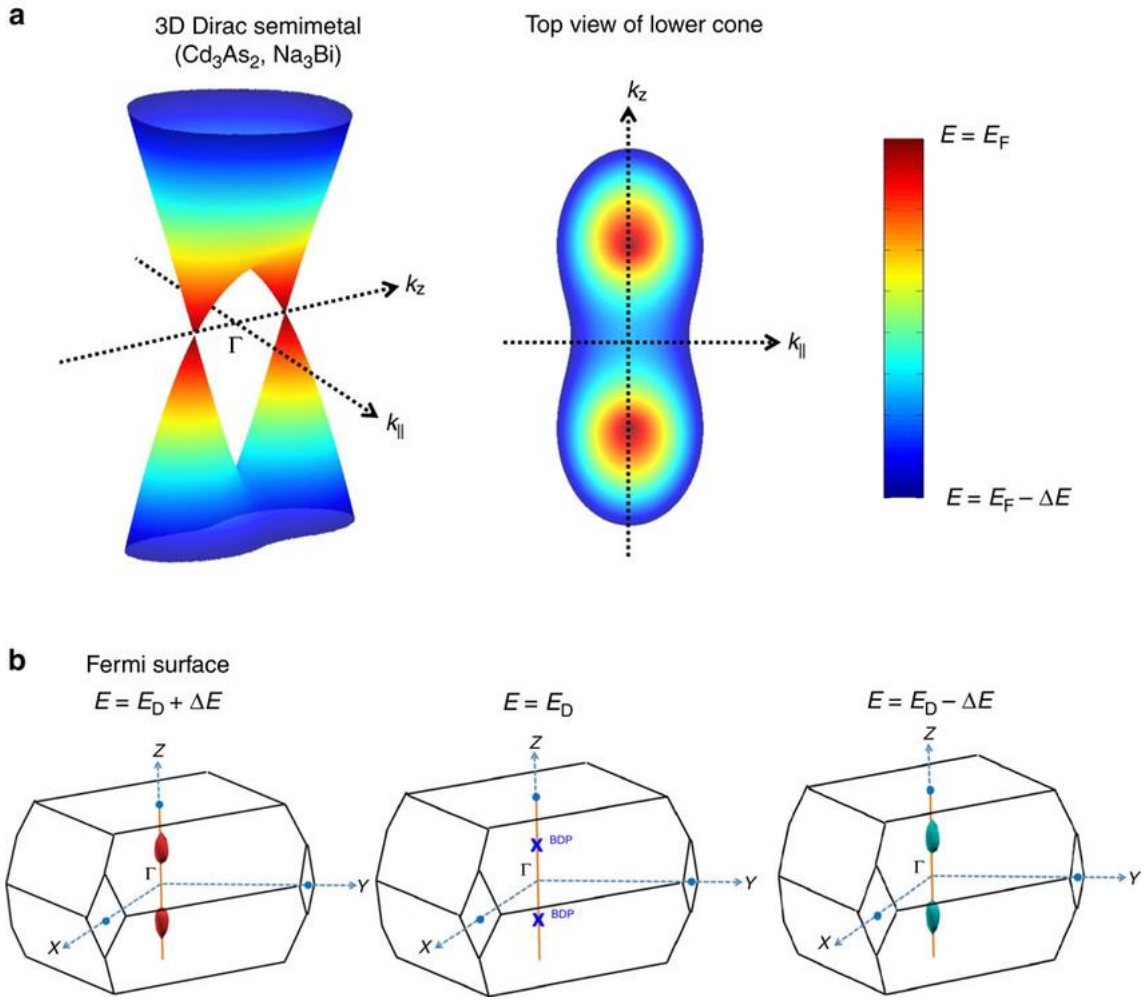

Neupane et al., Nat. Comm. (2014)

Dirac semimetal and Weyl semimetal

3D semimetals with linear dispersion

Weyl semimetal
(non-degenerated bands)

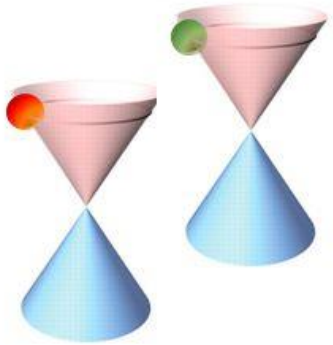

TaAs
NbAs
NbP
TaP

Dirac semimetal
(doubly degenerated bands)

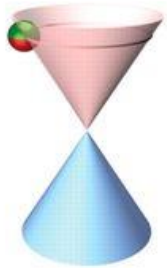

$ZrTe_5$
Na_3Bi,
Cd_3As_2

- The Dirac point can split into two Weyl points either by breaking the crystal inversion symmetry or time-reversal symmetry.
- In condensed matter physics, each Weyl point act like a singularity of the Berry curvature in the Brillion Zone – magnetic monopole in *k*-space

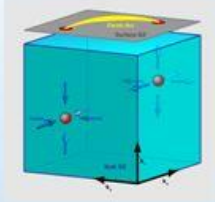

Dirac semimetal and Weyl semimetal

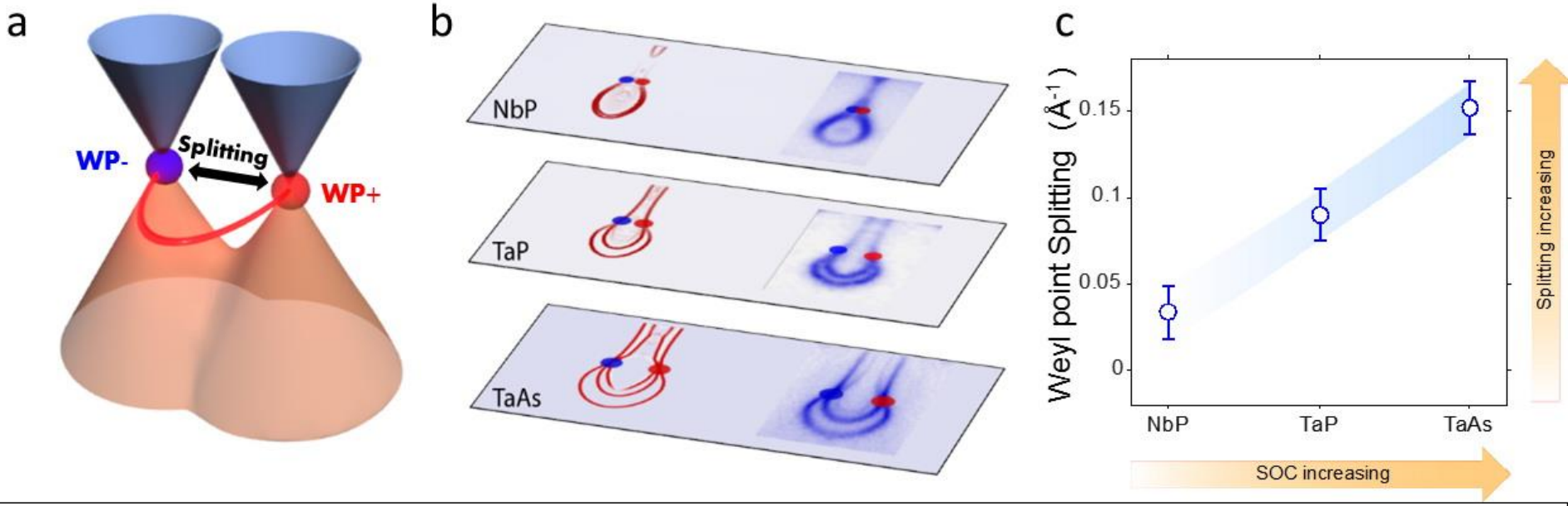

Liu et al., Nat. Mater. (2016)

Dirac semimetal and Weyl semimetal

Dirac semimetal | Magnetic semicond. | Weyl semimetal | Line node semimetal

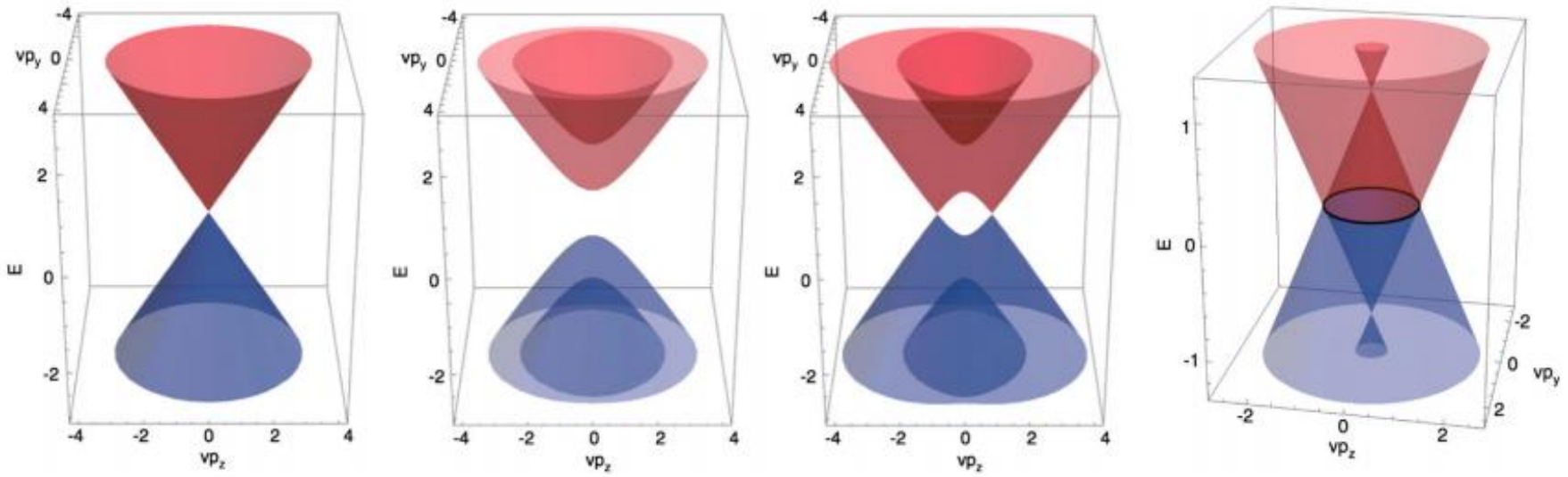

Armitage et al., RMP (2018)

Dirac semimetal Na_3Bi

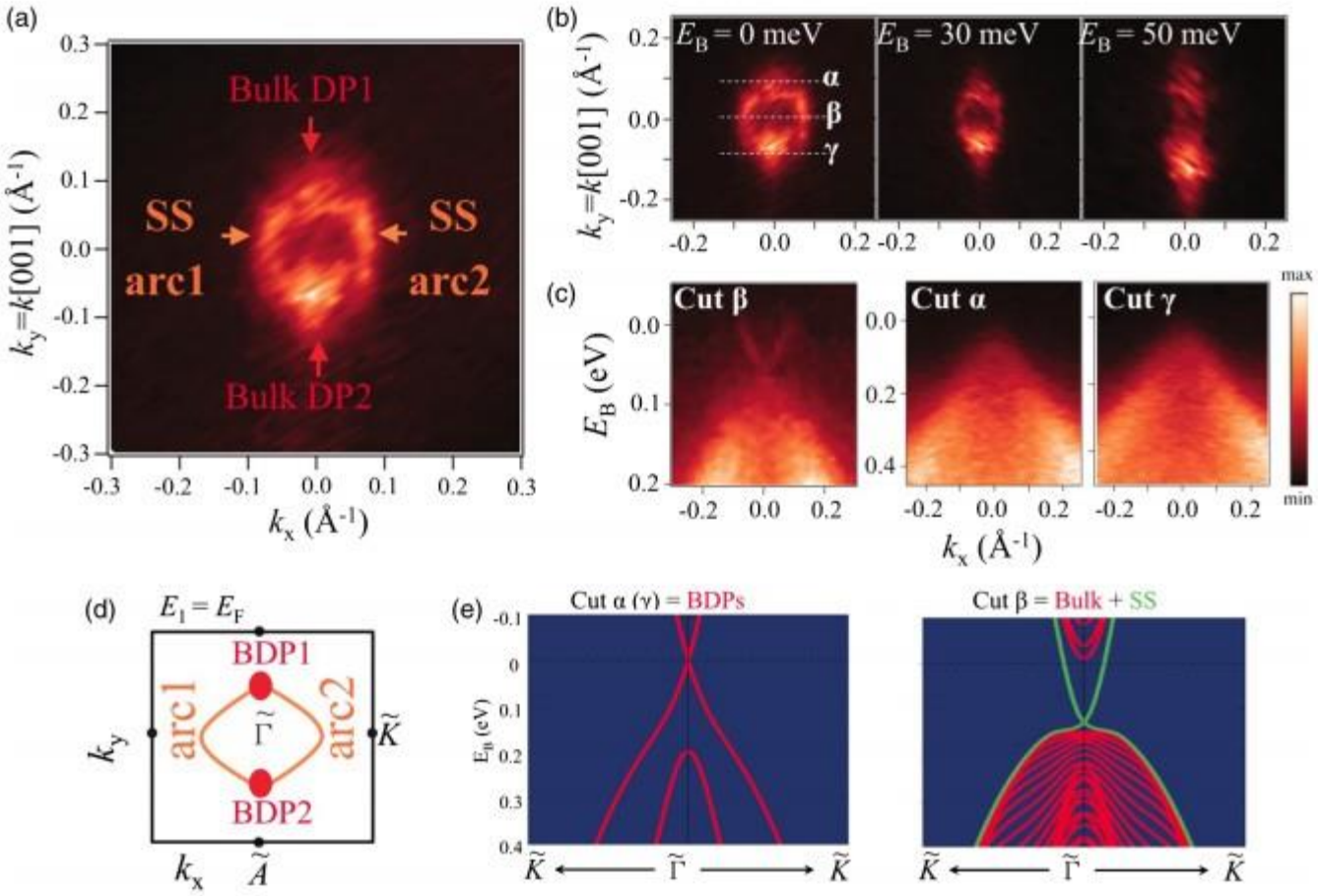

Armitage et al., RMP (2018)

Weyl semimetal TaAs

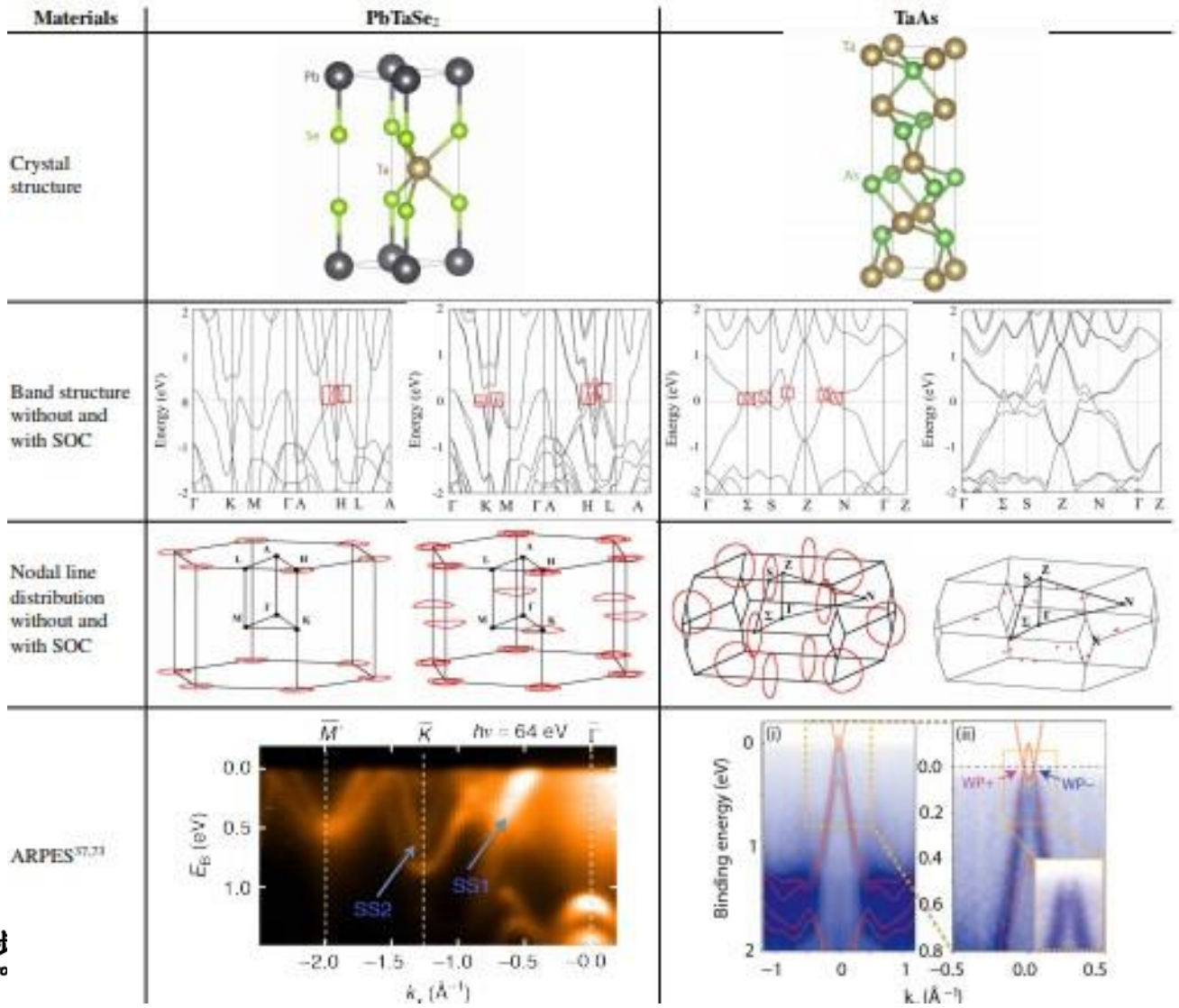

Yang et al., Advances in Physics :X (2018)

Summary of Dirac semimetal and Weyl semimetal

I : inversion symmetry
TR : time reversal symmetry

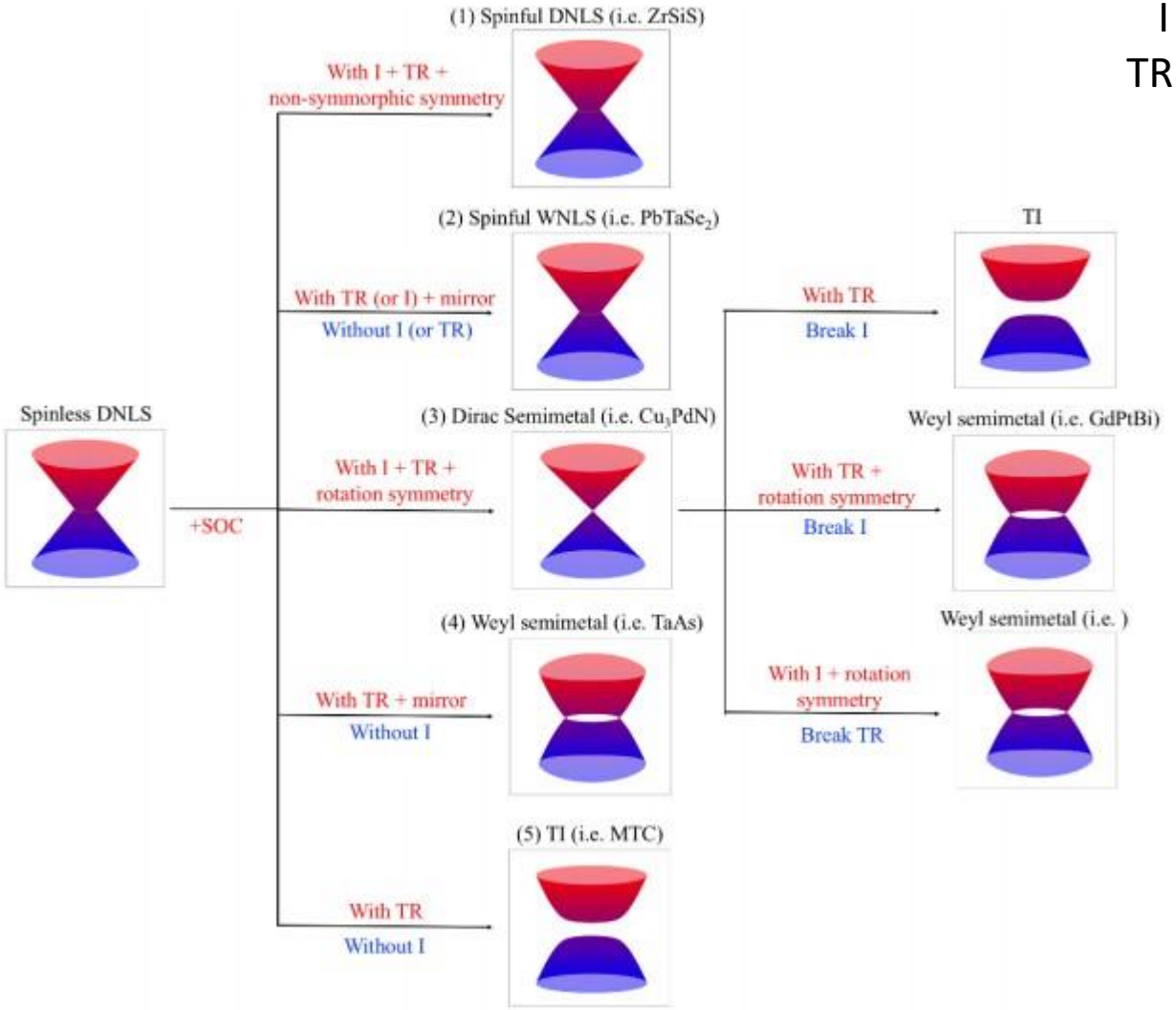

National Synchrotron Radiation Research Center

Yang et al., Advances in Physics :X (2018)

Graphene family

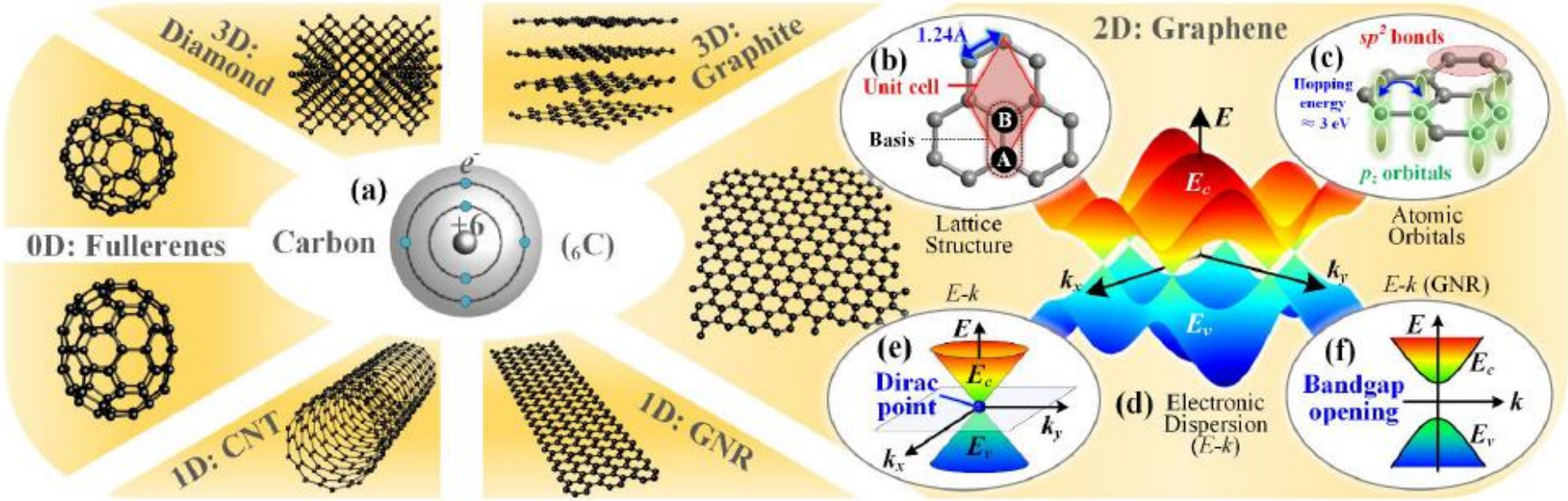

Figure 2. **(a)** Schematic of carbon atom and carbon allotropes, from 0D to 3D; **(b)** unit cell, basis and bond length of graphene; **(c)** atomic orbitals of graphene; **(d, e)** energy dispersion of graphene, where the energy dispersion is linear for low energies near the six corners (Dirac points) of the two-dimensional hexagonal Brillouin zone. **(f)** Energy dispersion of a semiconducting GNR, where a bandgap can be engineered by varying the width.

Kang et al., Proc. SPIE (2014)

Crystal structure of GNRs

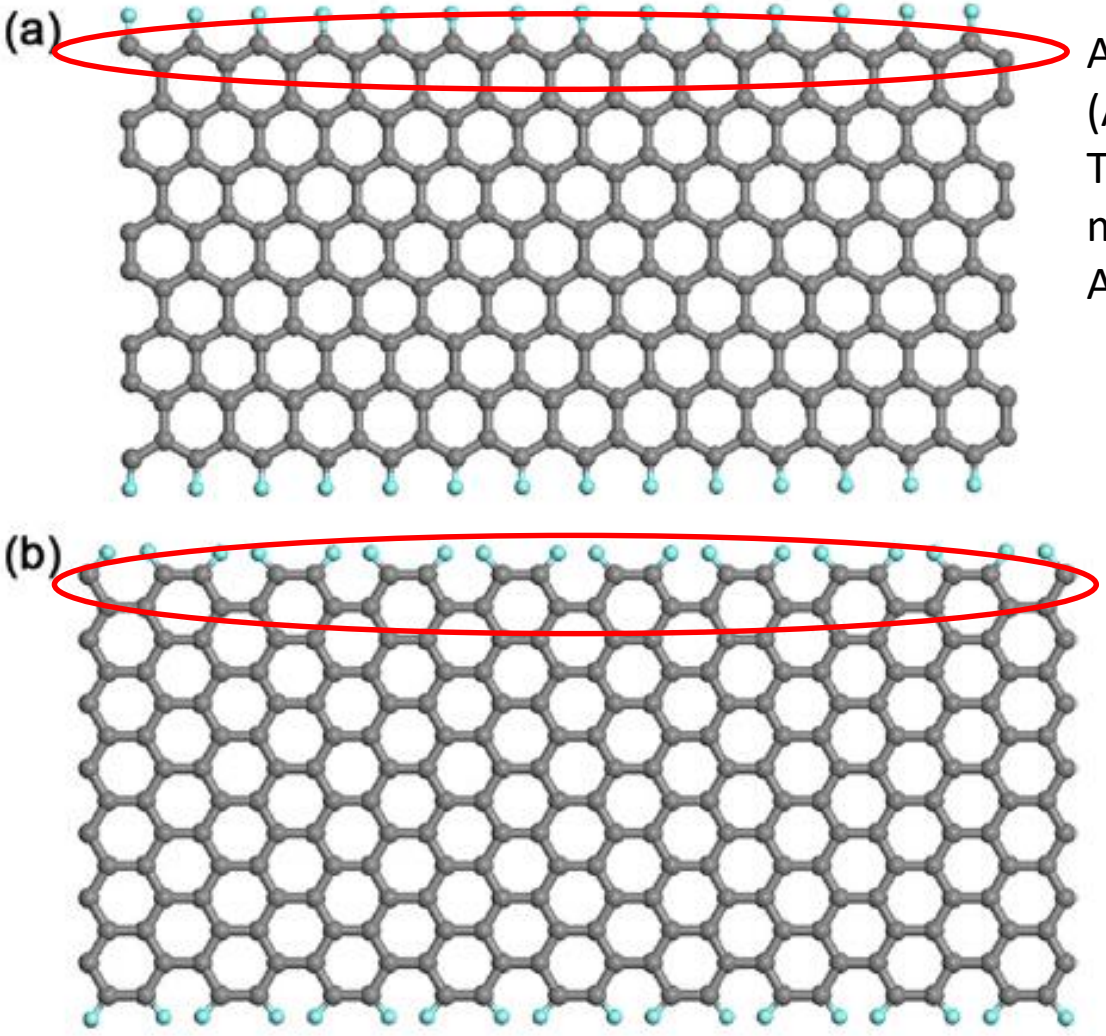

Armchair Graphene Nanoribbons (AGNRs)
TB simulation : semiconducting or metallic depending on the width of AGNRs

Zigzag Graphene Nanoribbons (ZGNRs)
TB simulation : metallic for all ZGNRs

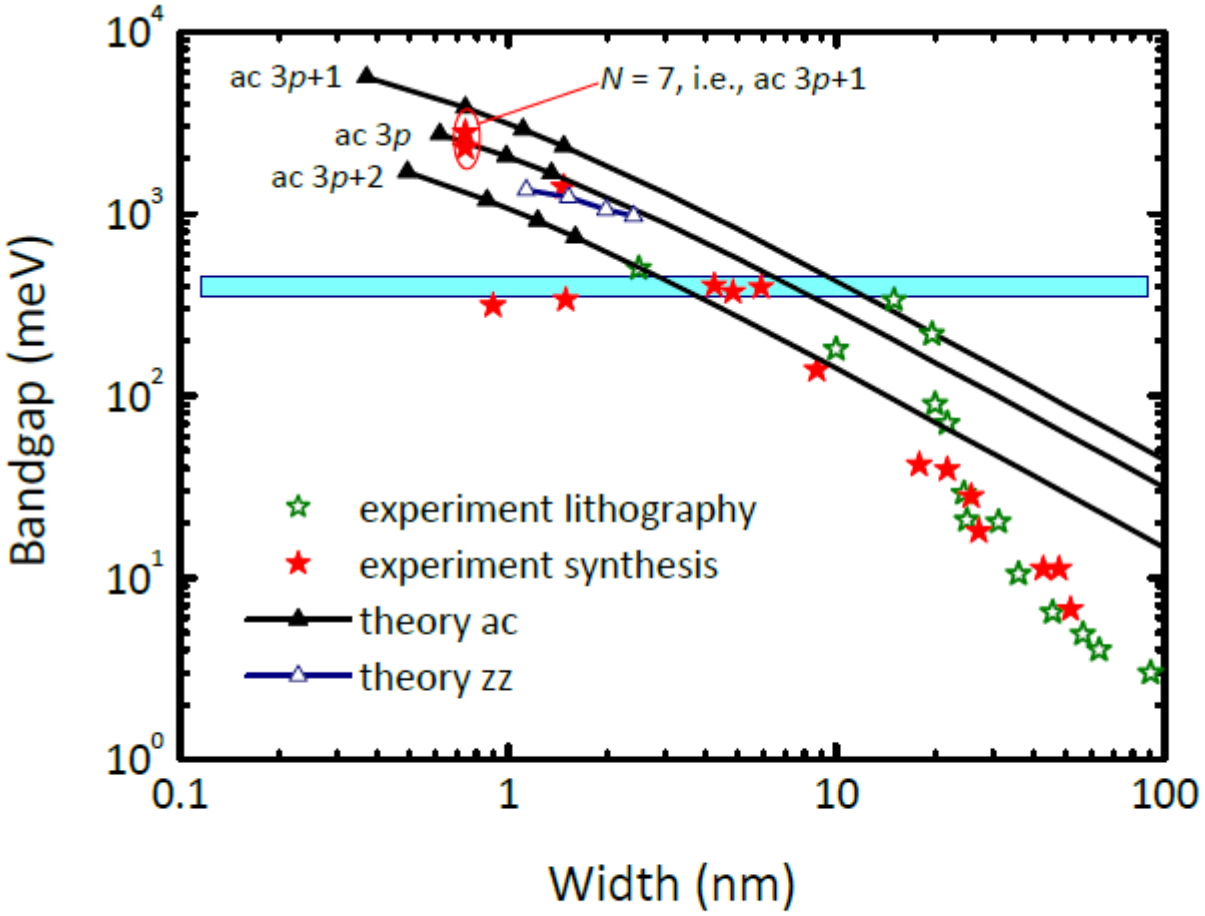

GNR bandgap vs width.

FS, Pezoldt, Granzner, Nanoscale 2015.

The bandgap of GNRs depends strongly on the ribbon width and the edge configuration!

Frank Schwierz, Nanoscale (2015)

Sample preparation for GNRs

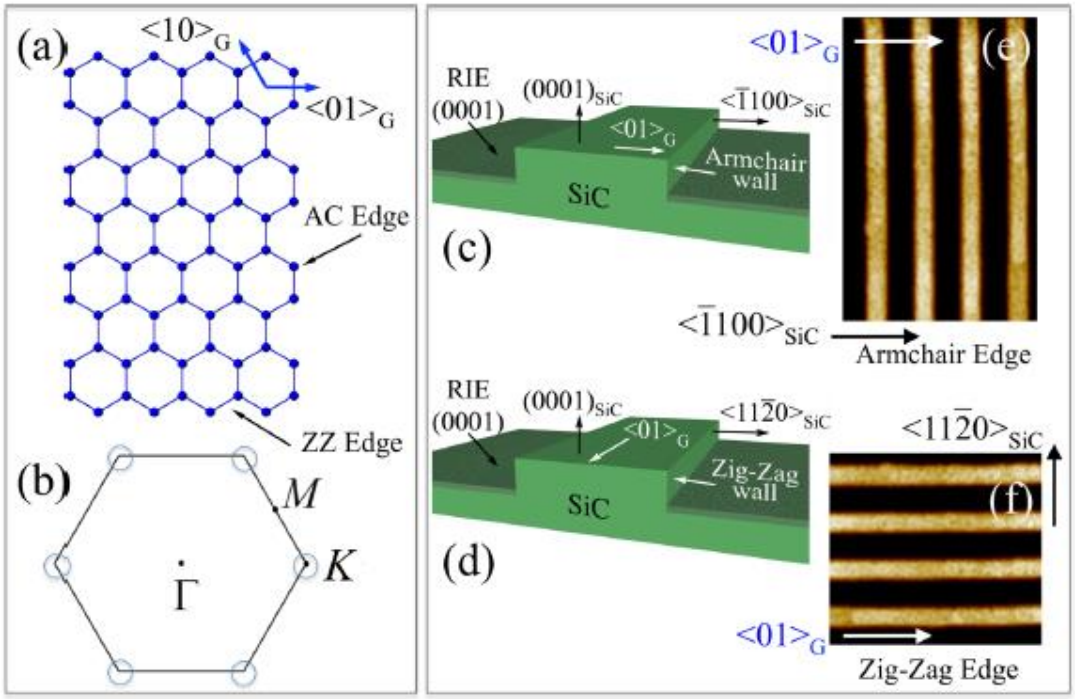

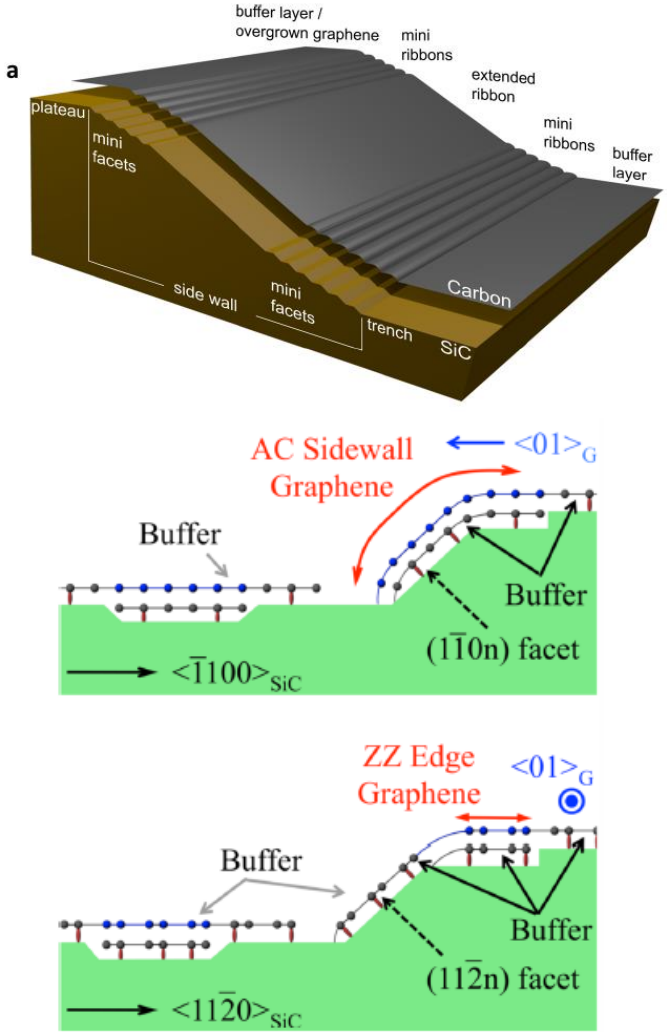

Nevius et al., Nano Lett. (2014)
Palacio et al., Nano Lett. (2014)

Using ARPES to probe GNRs/SiC

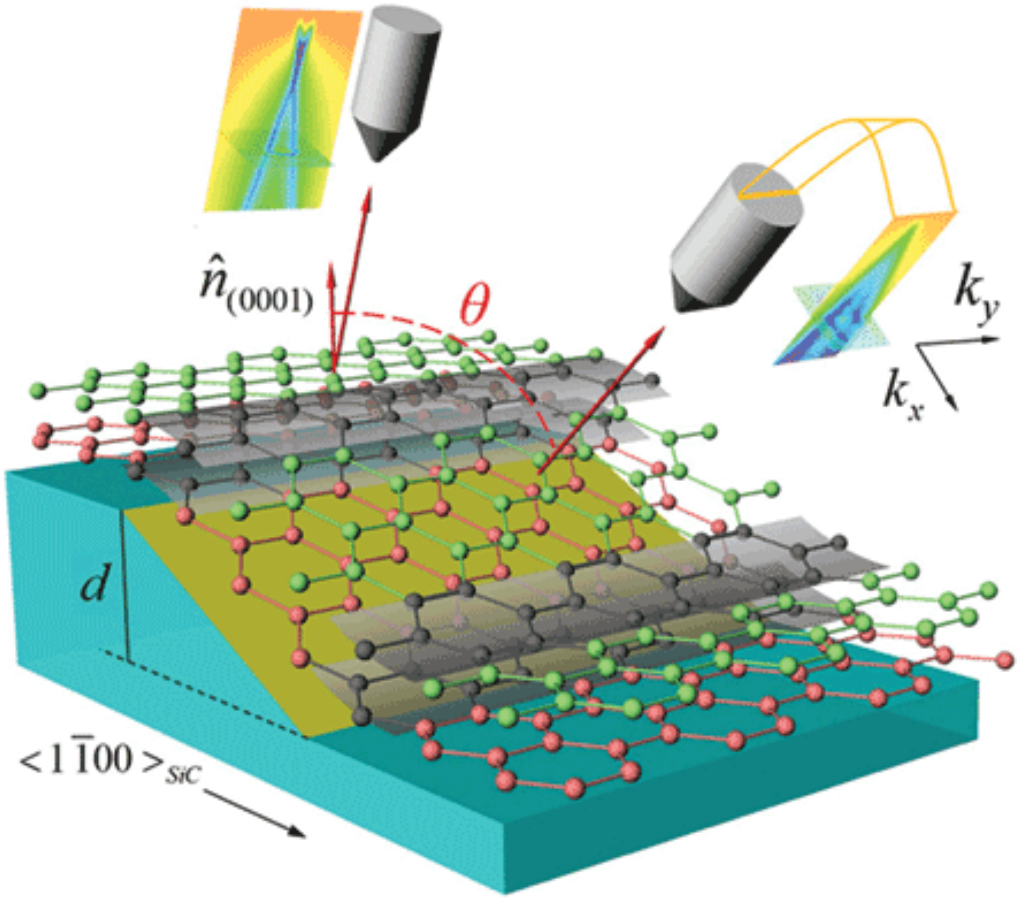

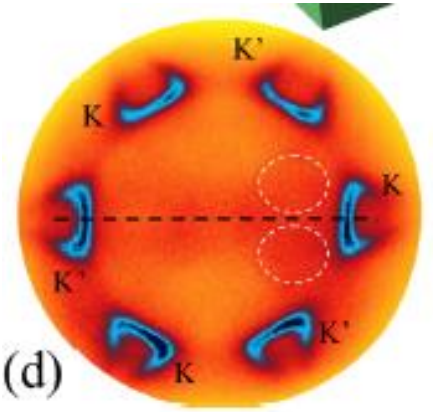

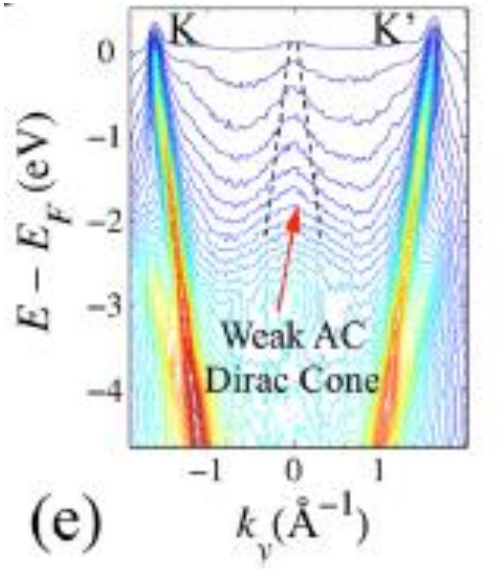

國家同步輻射研究中心
National Synchrotron Radiation Research Center

Nevius et al., Nano Lett. (2014)

2D Materials – An (Incomplete) Overview

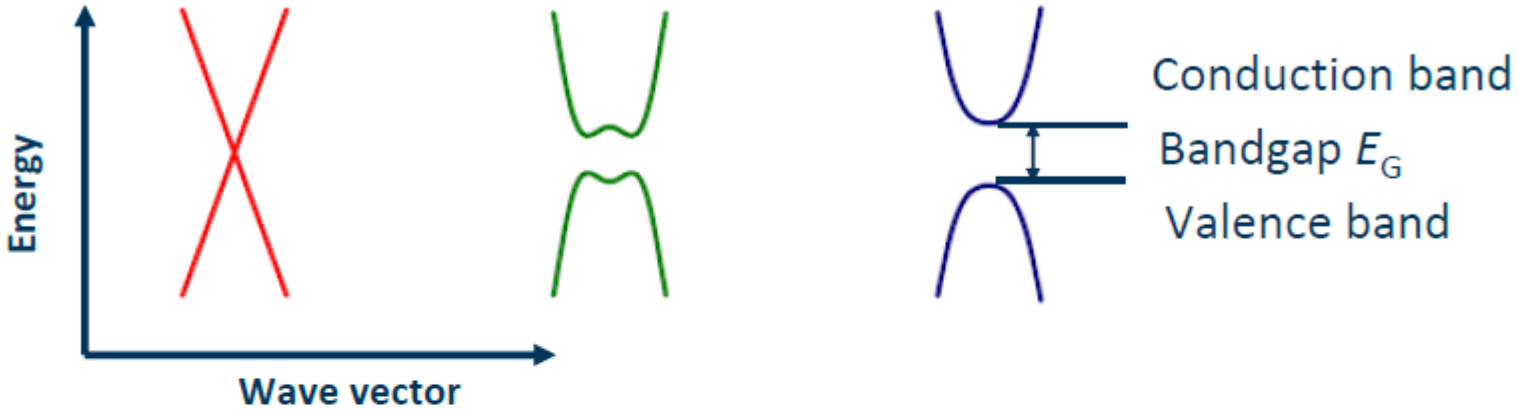

X-enes
- Graphene
- Silicene
- Germanene

No gap, E_G = 0! This is really a pitty, since the missing gap causes serious problems for transistors.

BLG

$E_G \leq 130$ meV
Too narrow for logic transistors.

X-enes
- Phosphorene
- Stanene
- GNRs

X-anes
- Graphane
- Silicane
- Germanane

MX-enes
- Sc_2CF_2
- $TiCO_2$

2D TMDs
- MoS_2, $MoSe_2$, $MoTe_2$
- WS_2, WSe_2, WTe_2

etc., etc.

Many of these materials have a gap E_G = 0.5... 2.5 eV, perfect for transistors.

Frank Schwierz, Nanoscale (2015)

2D materials :potential candidates for future applications

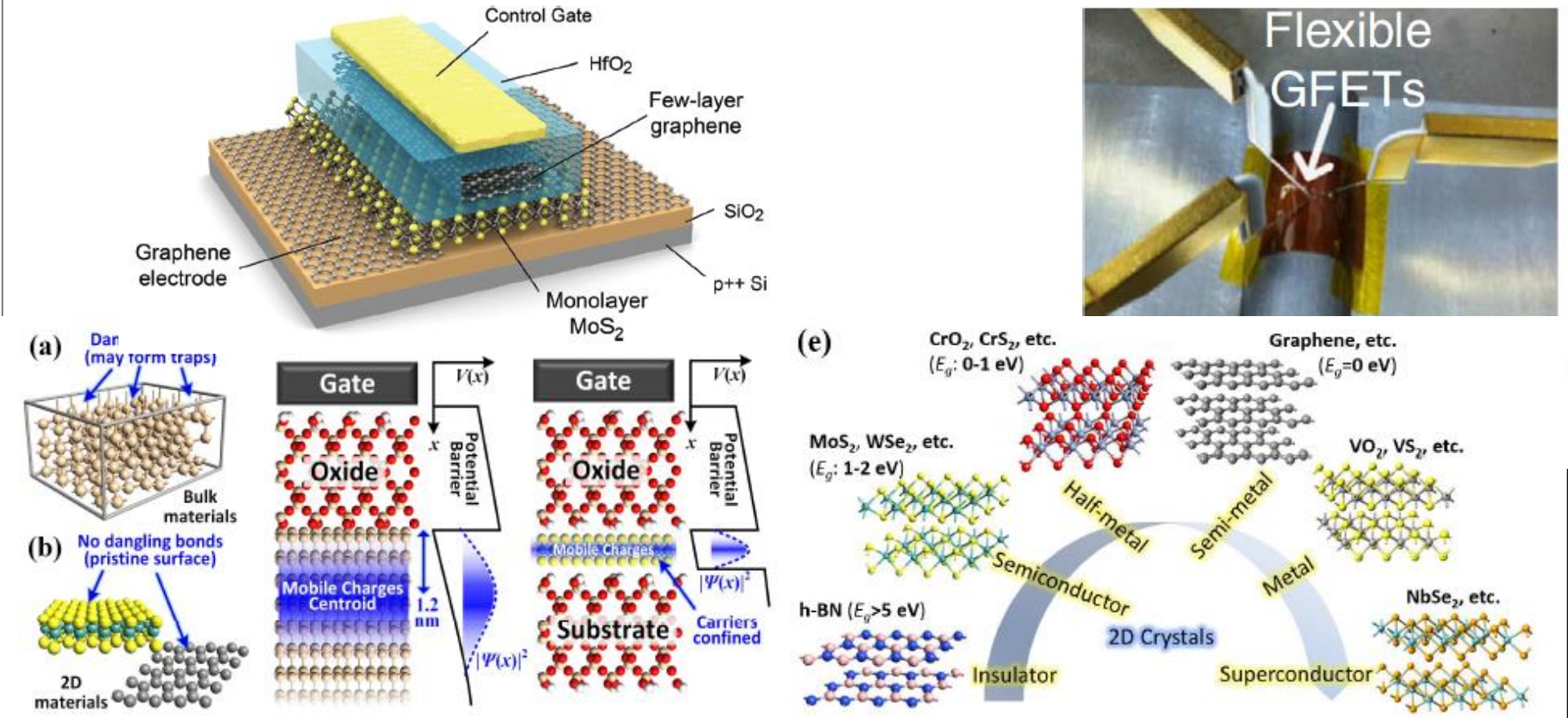

Figure 1. Schematic illustrating advantages of 2D materials: surfaces of **(a)** 3D and **(b)** 2D materials. The pristine interfaces (without out-of-plane dangling bonds) of 2D materials help reduce the interface traps. Mobile charge distribution in **(c)** 3D and **(d)** 2D crystals used as channel materials. The carrier confinement effect in 2D materials leads to excellent gate electrostatics. **(e)** Various types of 2D materials from insulator to superconductor. E_g denotes the band gap.

Kang et al., Proc. SPIE (2014)

2D materials :potential candidates for future applications

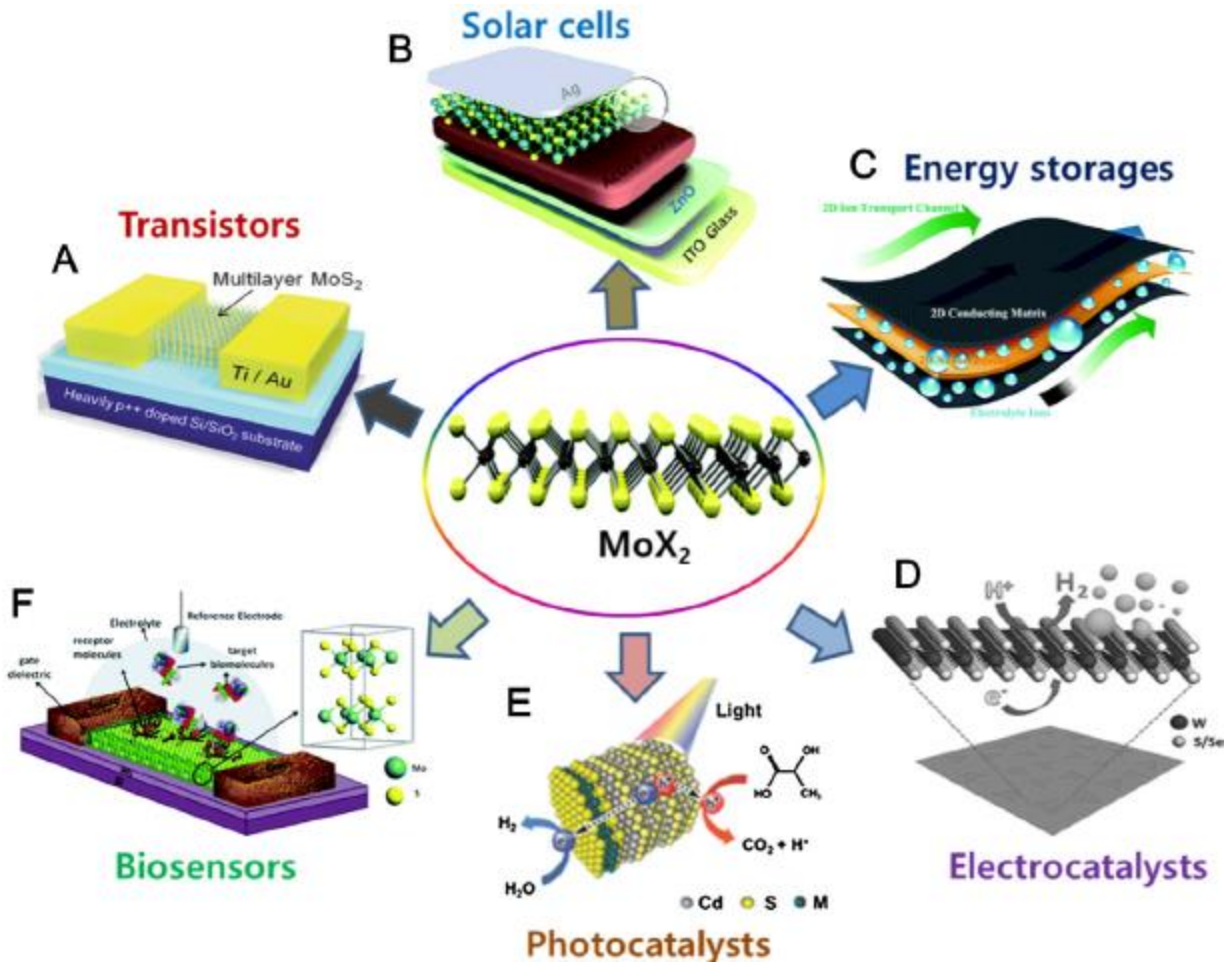

Tran et al., Progress in Materials Science (2018)

BBC Sign in | News | Sport | Weather | Shop | Earth | More | Search

NEWS

Home | Video | World | Asia | UK | Business | Tech | Science | Magazine | Entertainment & Arts | Health | More

Technology

Silicon rival MoS2 promises small, low-energy chips

8 March 2012 | Technology

The first computer chip made out of a substance described as a "promising" alternative to silicon has been tested by researchers.

The Switzerland-based team used molybdenite (MoS2) - a dark-coloured, naturally occurring mineral.

The group said the substance could be used in thinner layers than silicon, which is currently the most commonly used component in electronics.

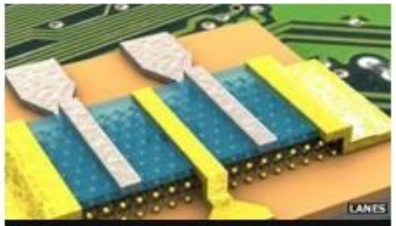

The researchers say molybdenite microchips would need less power than existing silicon-based circuits

It said MoS2 could make smaller, more flexible chips that used less energy.

Top Stories

Bad weather hits Japan quake survivors
Tens of thousands of people forced into shelters by two deadly tremors in Japan endure heavy rain and cold temperatures, as rescue efforts continue.
6 hours ago

Earthquake kills dozens in Ecuador
2 minutes ago

Rousseff in last-minute bid for support
6 hours ago

A demonstration of electric transistor fabricated with monolayer MoS_2 shows high current on/off ratios of > 10^8 . Even the mobility ~ 200 $cm^2V^{-1}s^{-1}$ is much lower than that in graphene. The large current on/off ratio originates from sizeable band gap in MoS_2.

Toward transistors with 1 nm gate lengths

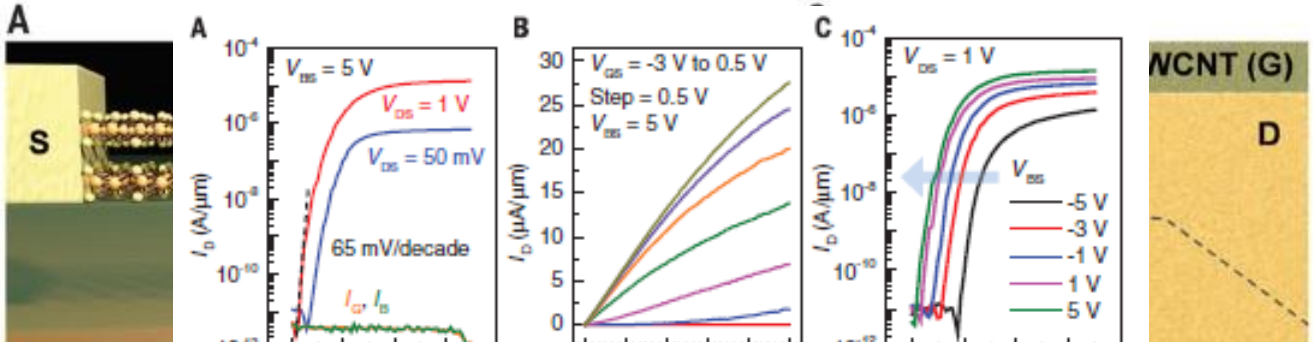

Using a 2D material called molybdenum disulfide (MoS2), Samsung believes it could scale logic technology even further. Samsung and others are exploring so-called MoS2 FETs. "We believe around 1nm is possible."

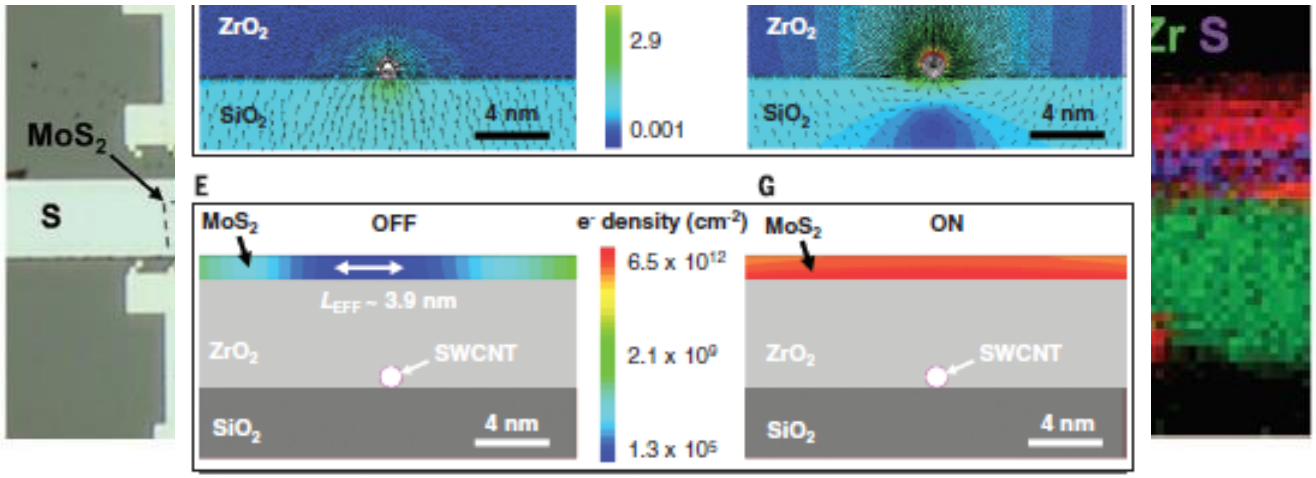

Desai et al., Science (2016)

The device structure of flexible OLED display with MoS_2-based backplane circuitry

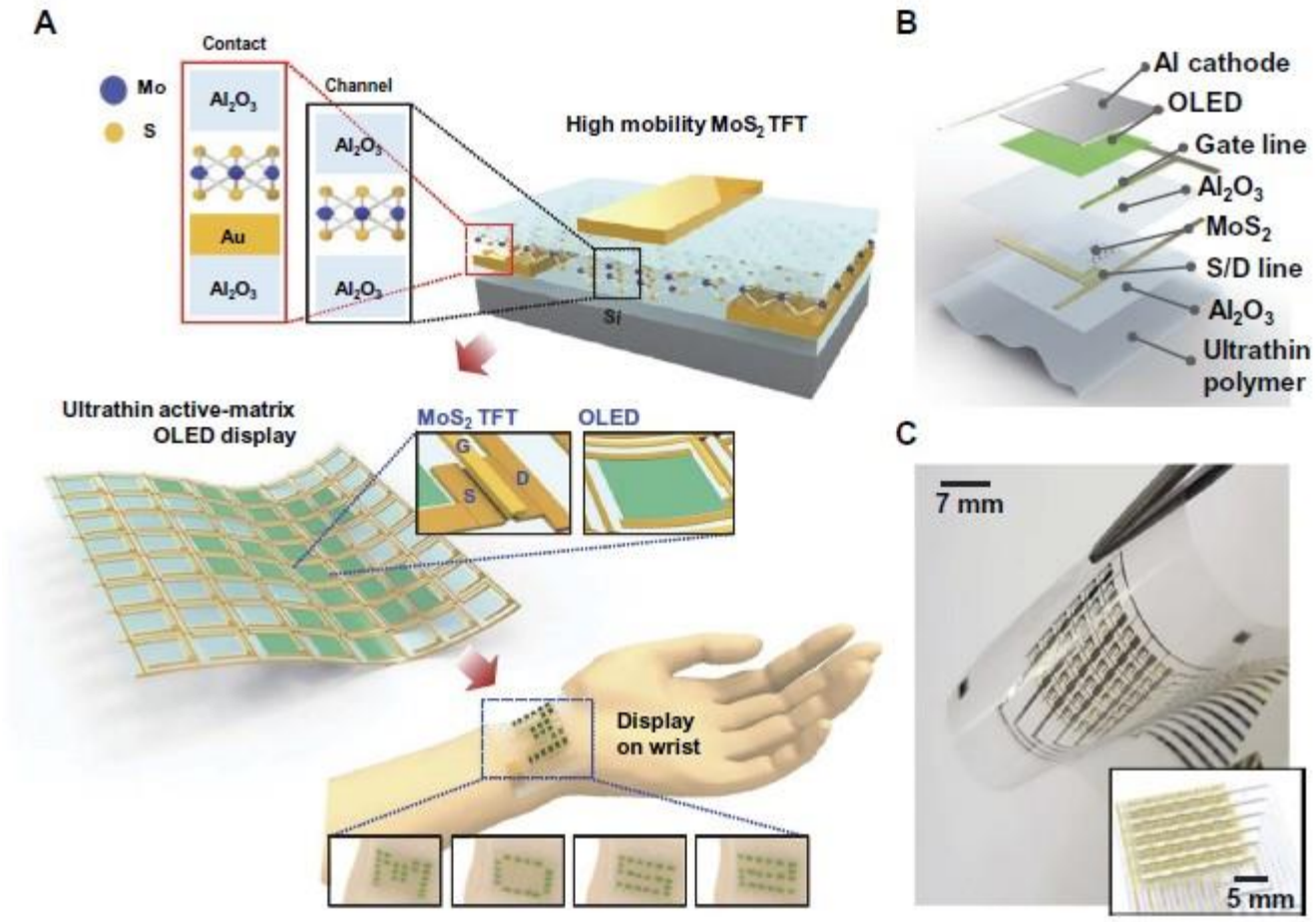

Choi et al., Science Advance (2018)

Benchmarks for display

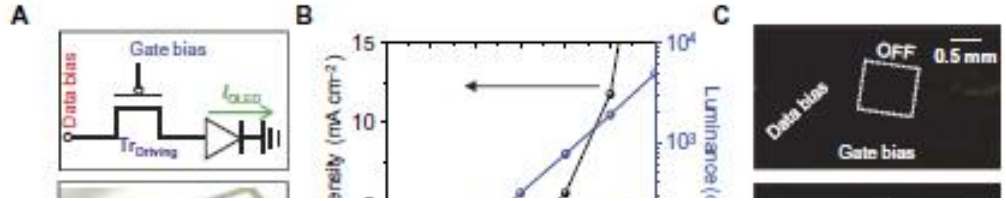

Benchmarks for display

	c-Si	poly-Si	a-Si	InGaZnO	Organic	Graphene	TMD
Band gap [eV]	1.12	1.12	2	3	~ 3	0	~ 1.8
Mobility	1600	450	2	20	10	>10,000	200~5000
Temp. [℃]	1000	600	200	R.T.	~ 100	R.T.	~ 600
Flexibility	X	X	X	X	OO	O	O
Clearness	X	X	X	O	O	O	O

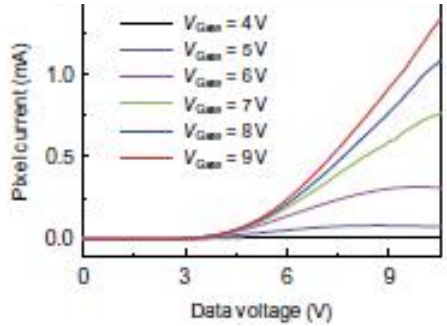

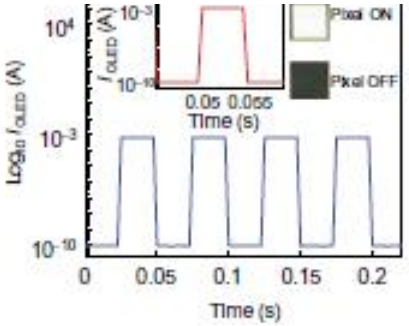

The band structure of MoS_2

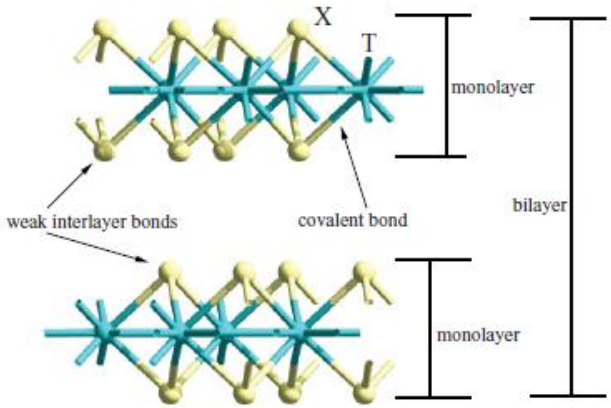

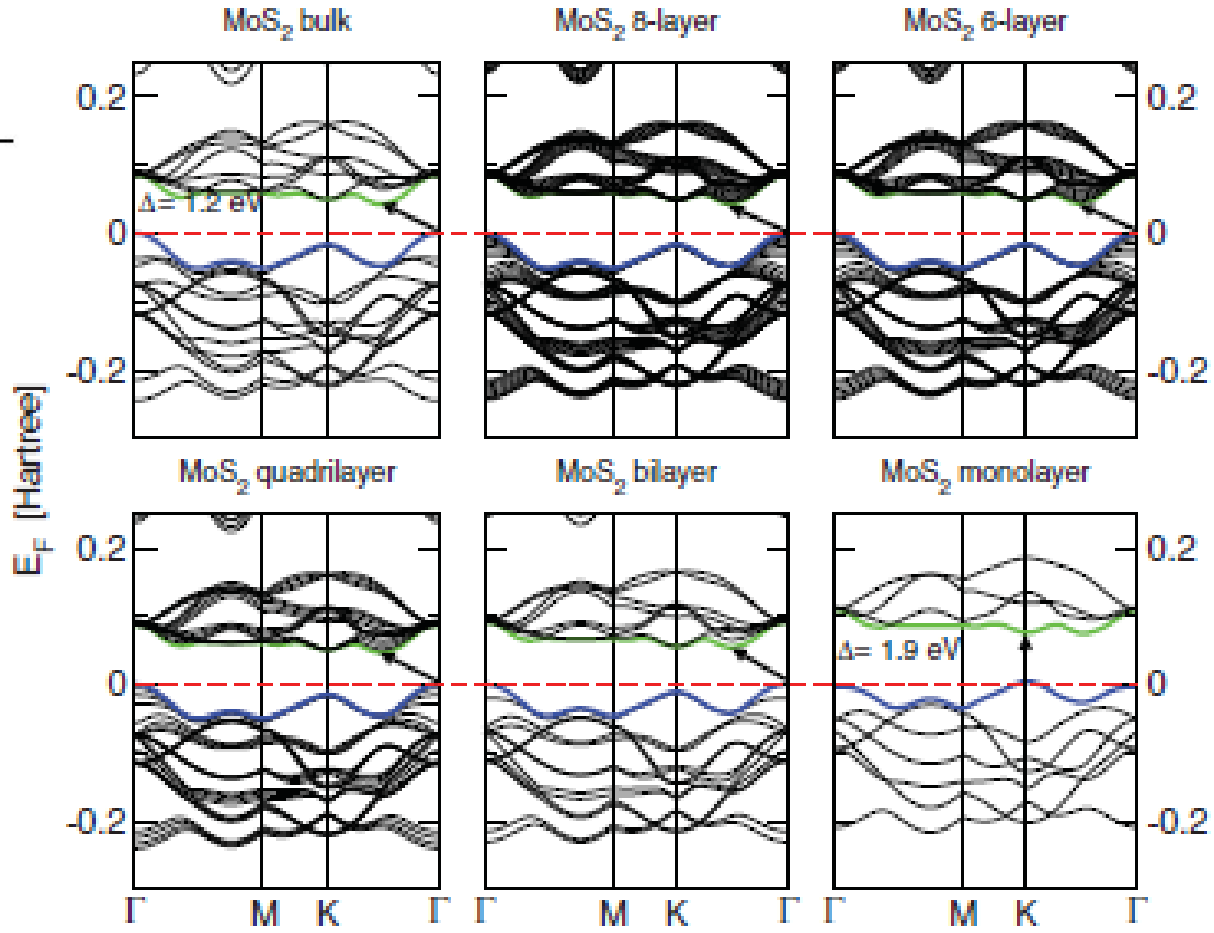

Kuc et. al., PRB (2011)

The electronic structure of $MoSe_2$

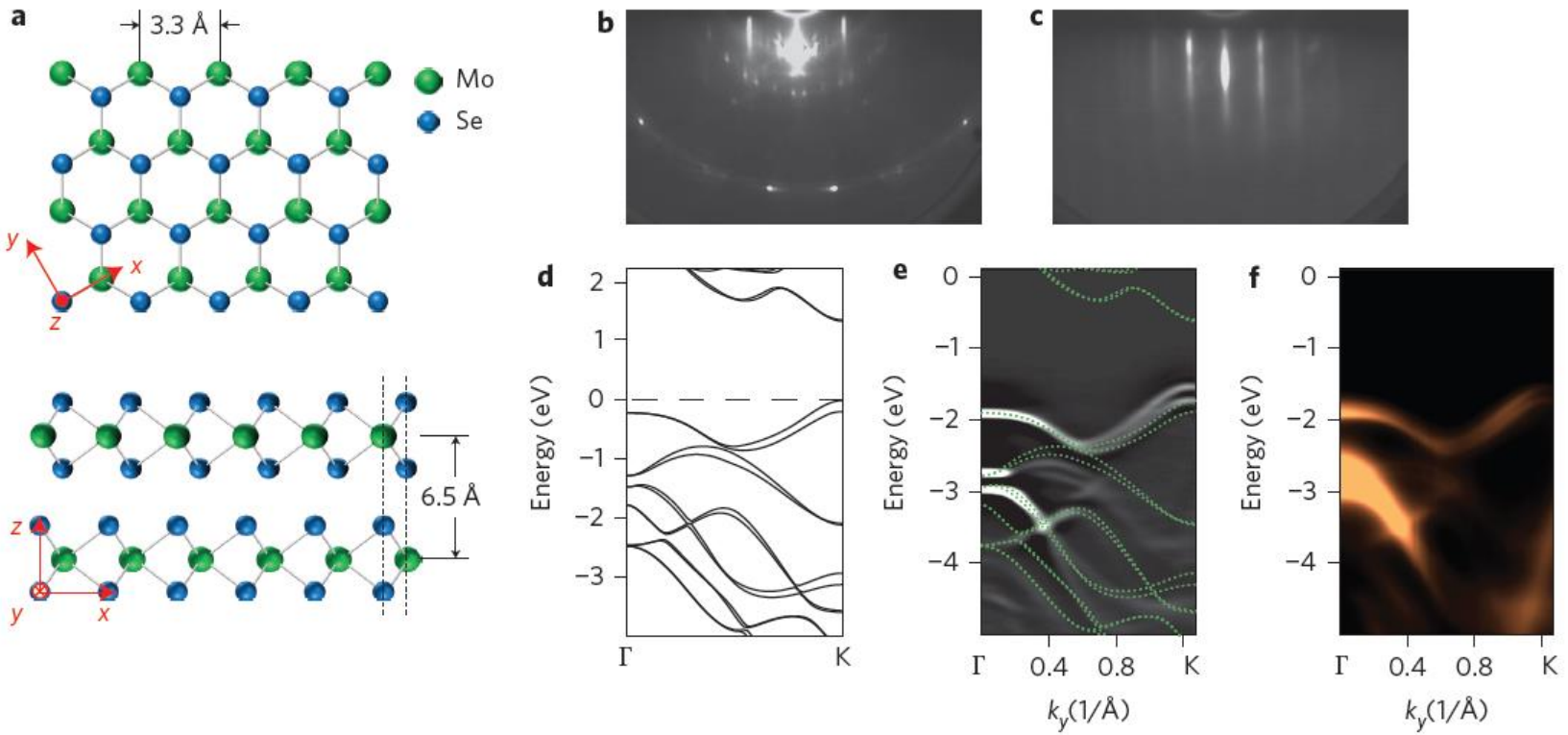

Zhang et al., Nat. Nano. (2013)

Alkali metal doped $MoSe_2$

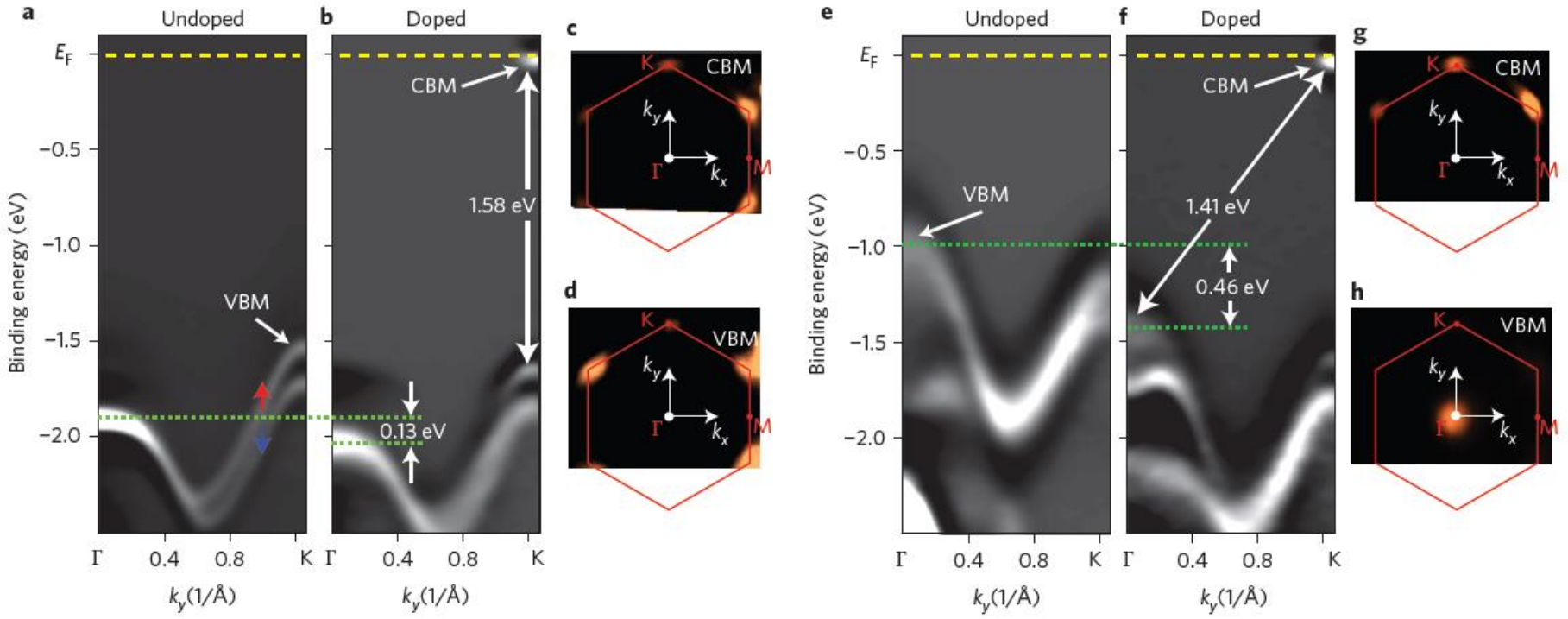

國家同步輻射研究中心
National Synchrotron Radiation Research Center

Zhang et al., Nat. Nano. (2013)

Black phosphorus (BP)

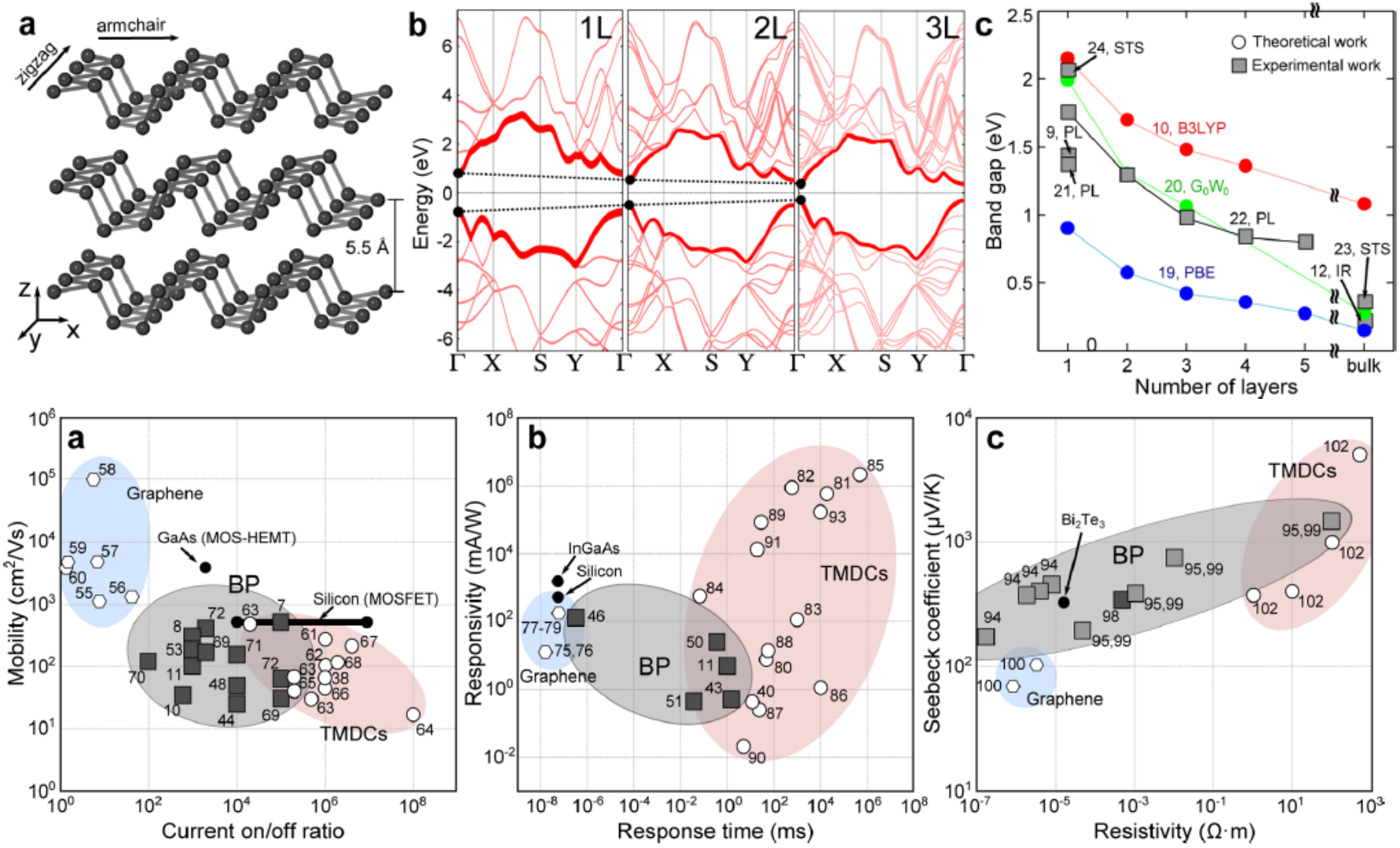

Catellanoas-Gomez, J. Phys. Chem. Lett. (2015)

The degradation of black phosphorus (BP)

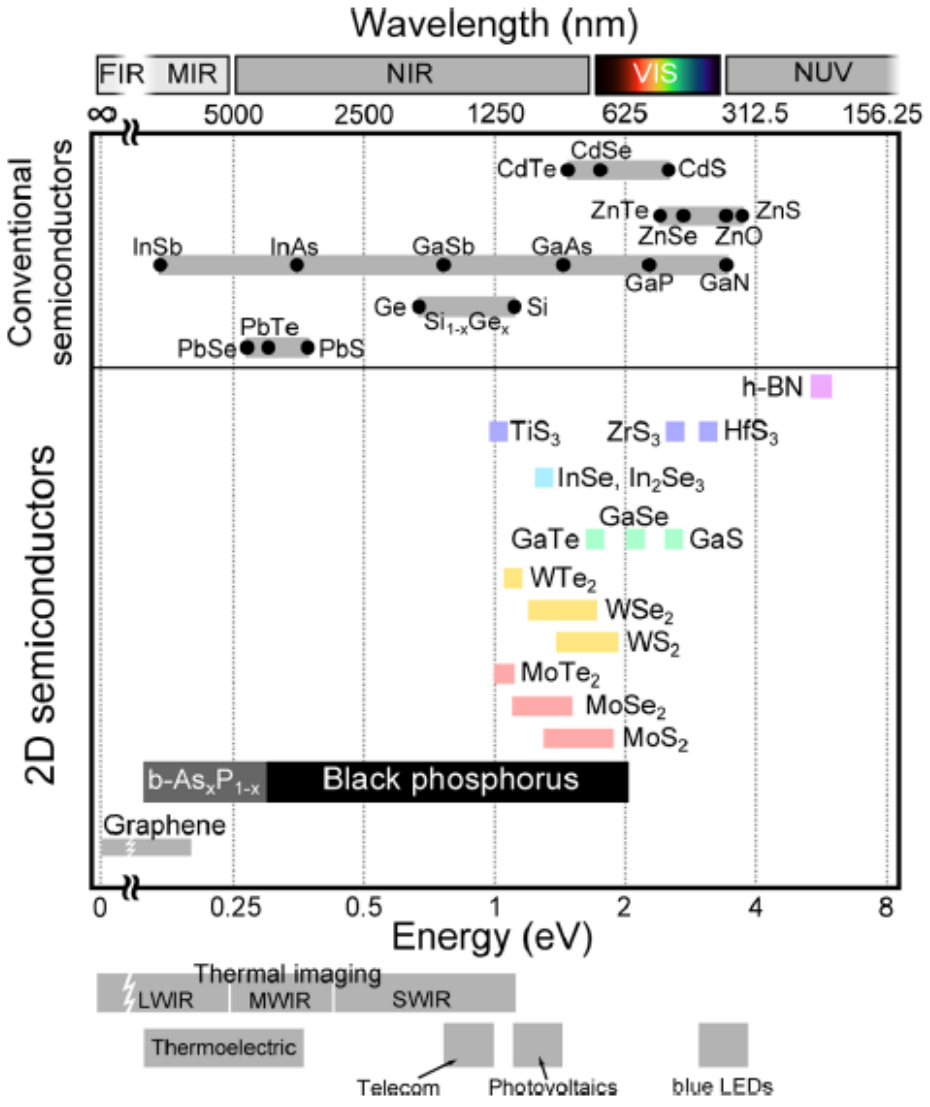

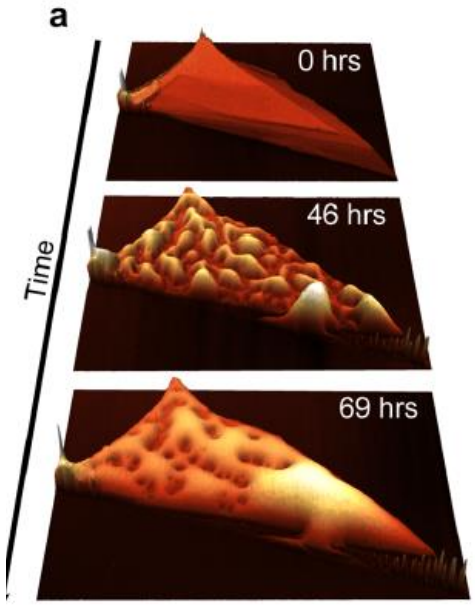

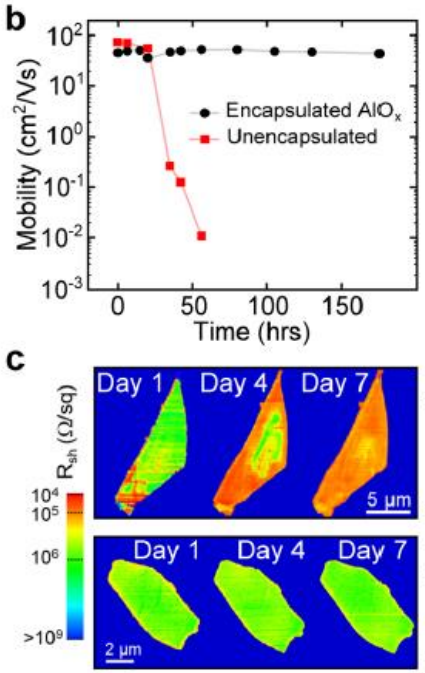

Catellanoas-Gomez, J. Phys. Chem. Lett. (2015)

Anisotropic Dirac semimetal state in BP

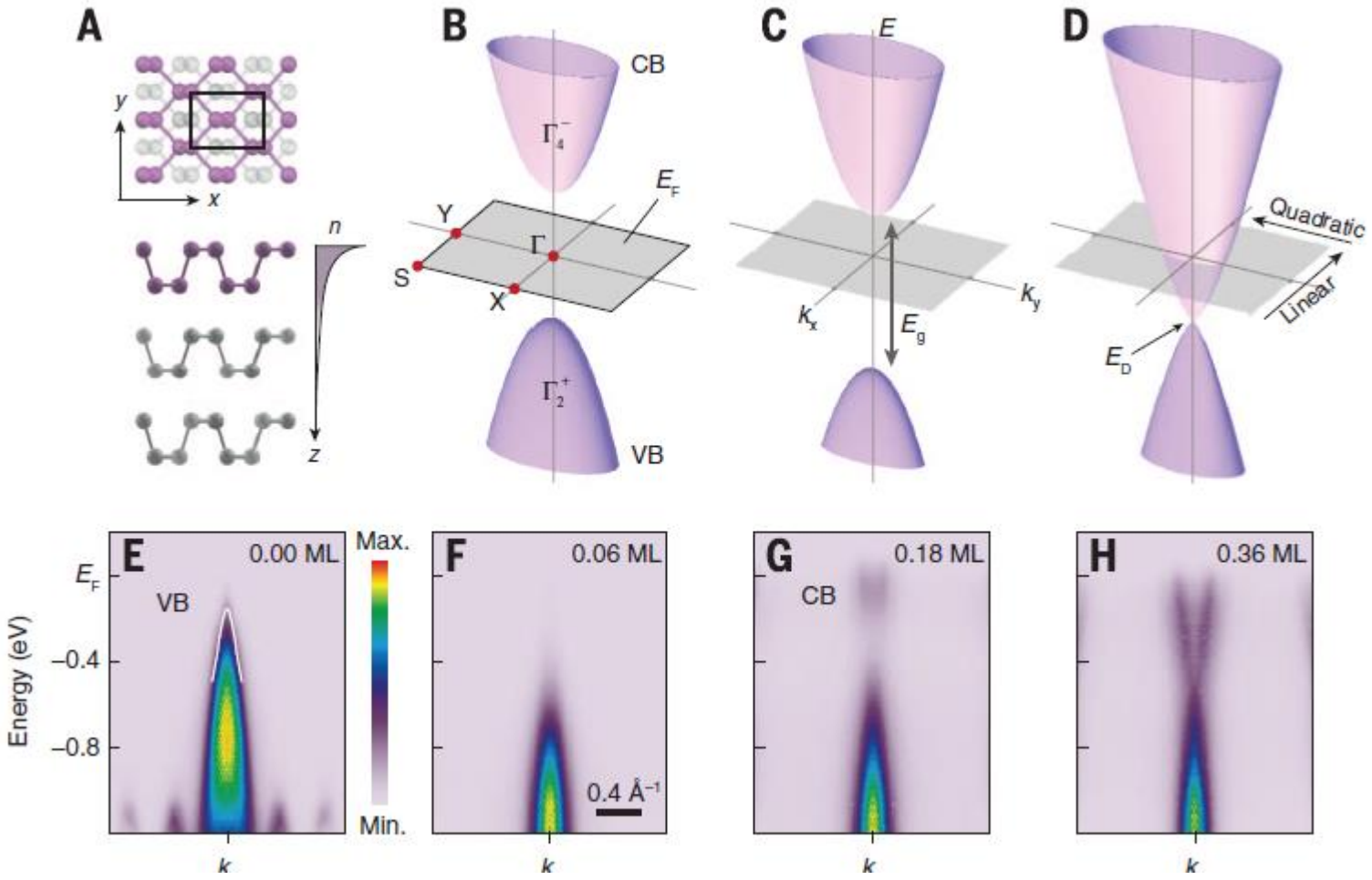

國家同步輻射研究中心
National Synchrotron Radiation Research Center

Anisotropic Dirac semimetal state in BP

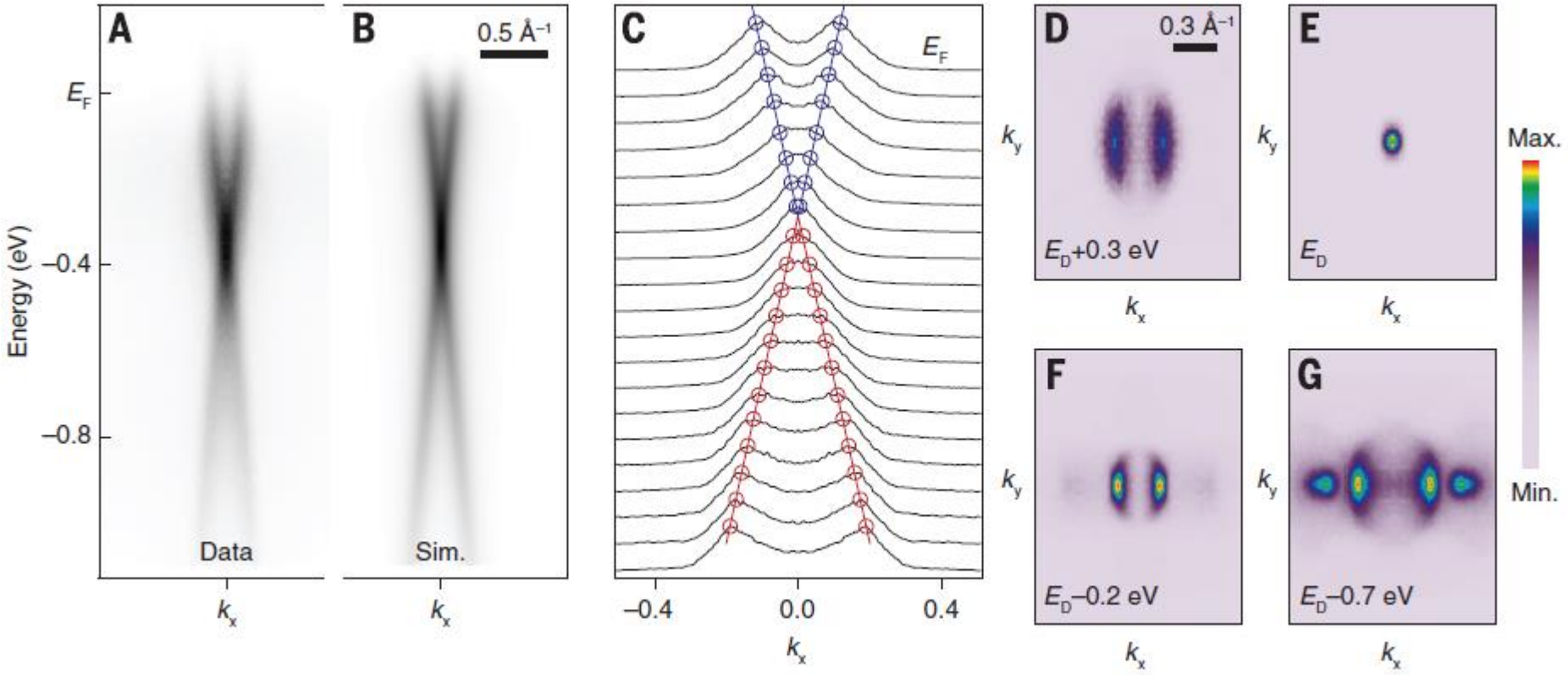

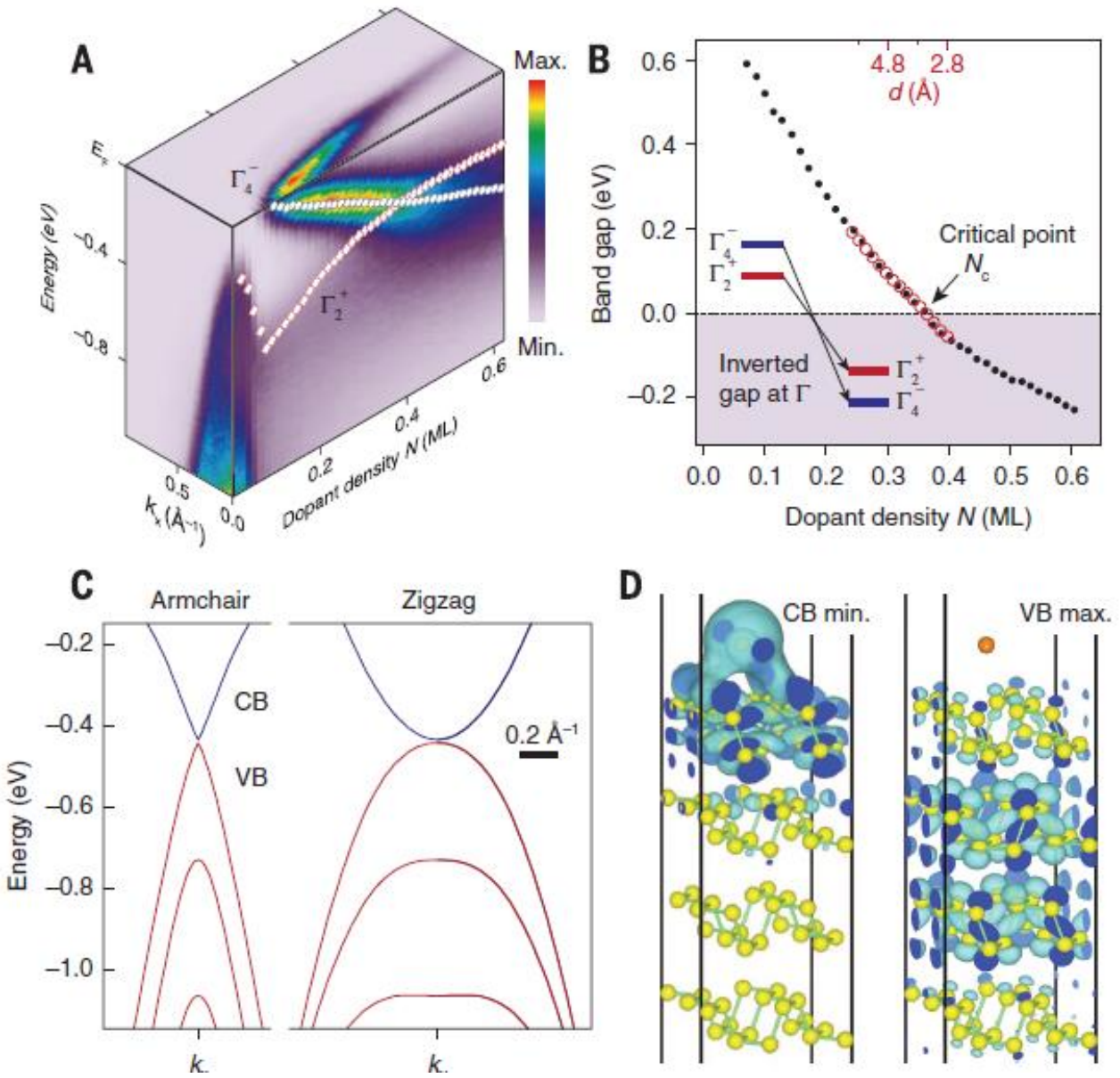
A
Max.
Min.
Energy (eV)
Γ_4^-
Γ_2^+
Dopant density N (ML)
B
4.8 2.8
d (Å)
Band gap (eV)
Critical point
N_c
Inverted
gap at Γ
Dopant density N (ML)
C
Armchair
Zigzag
CB
VB
0.2 Å⁻¹
Energy (eV)
D
CB min.
VB max.

Advanced Low-Dimensional Materials

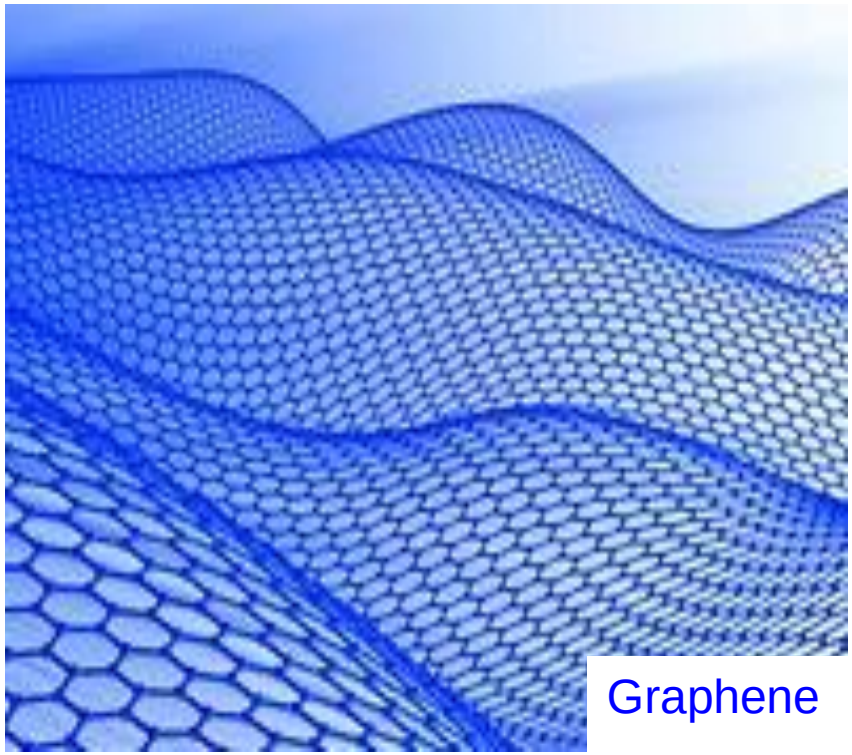

Graphene

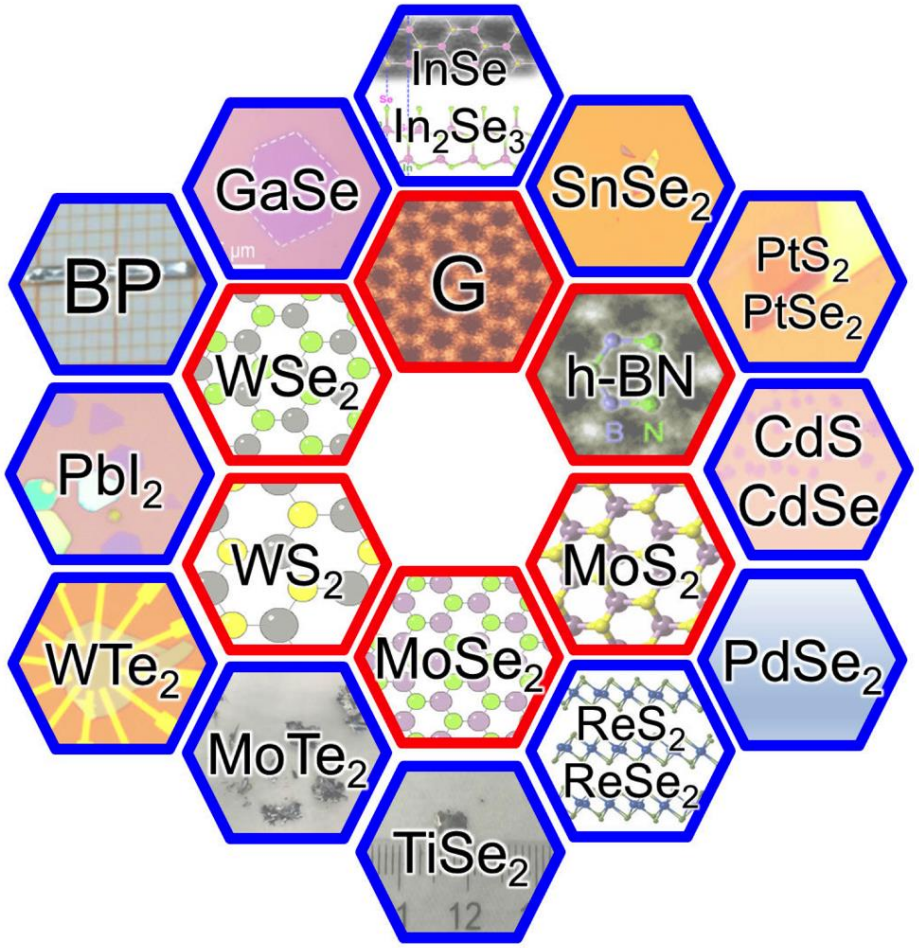

Collection of the 2D materials

Graphene is the first, but not ONLY

Advanced Low-Dimensional Materials

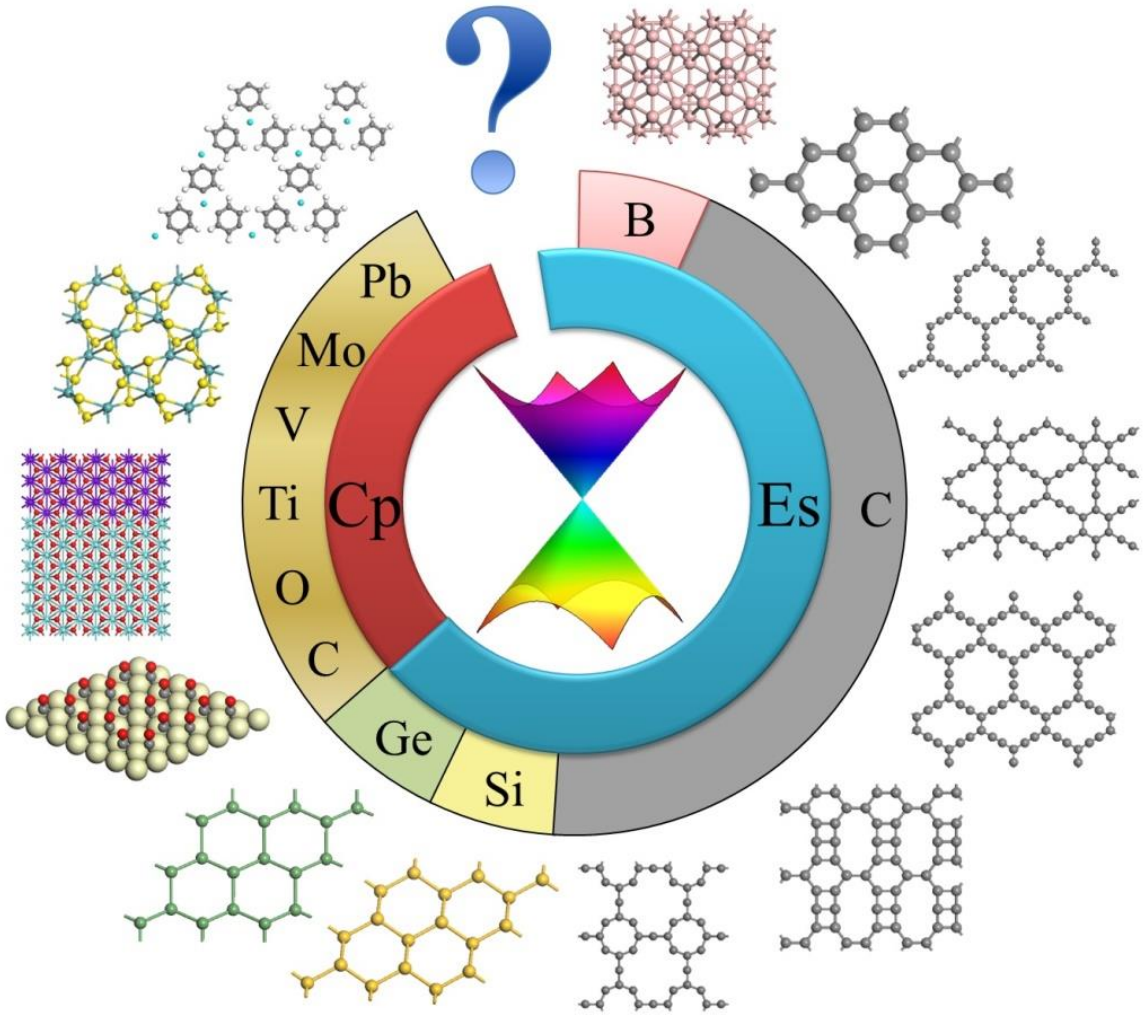

Advanced Low-Dimensional Materials

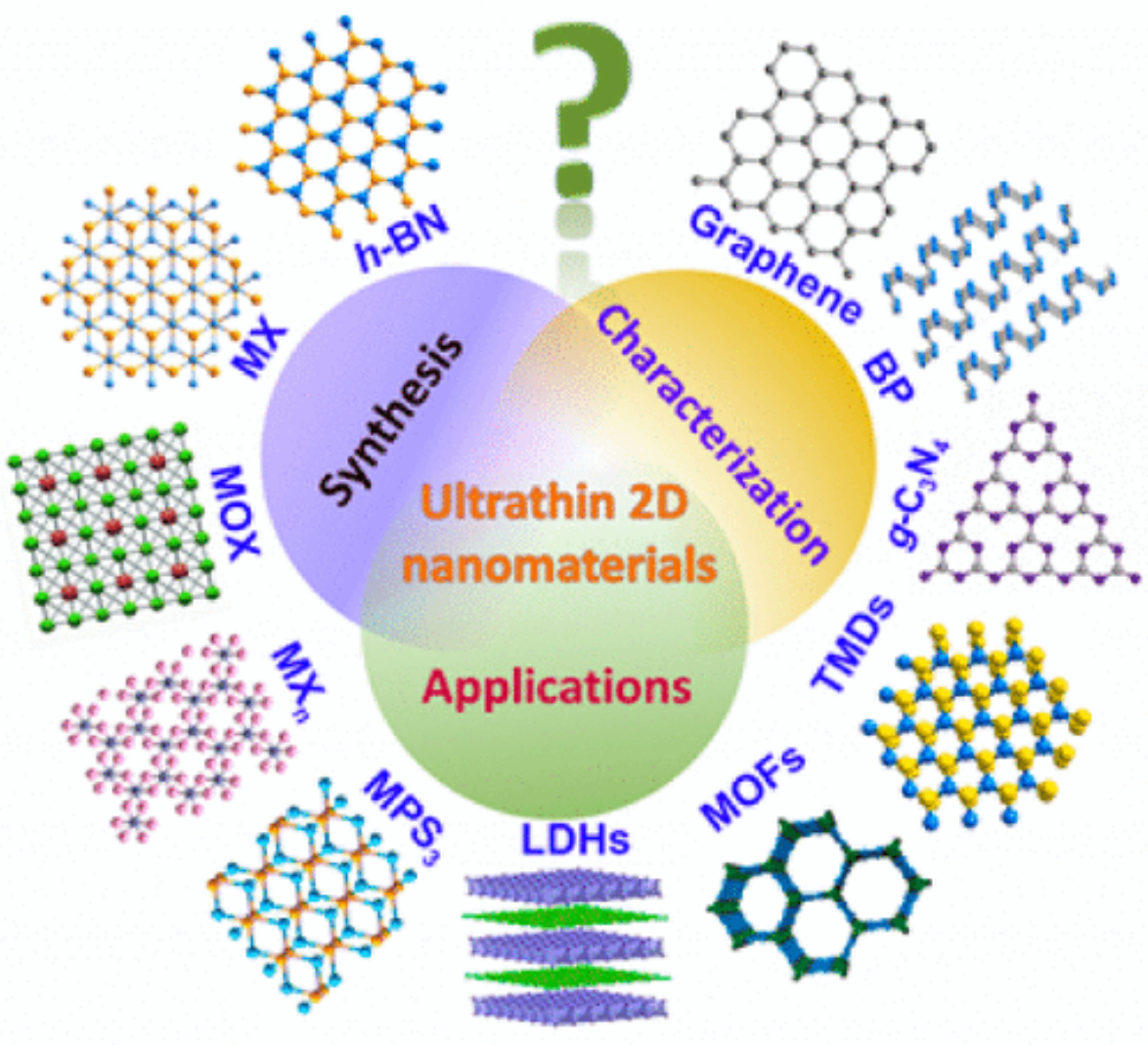

Nano Everywhere

Materials of interest often contain intrinsic, extrinsic, and designed nanoscale features.

Need rapid electronic structure mapping at the nanoscale

Large MgB_2 single crystal ~200 μm- available two years after discovery

10 μm - available shortly after discovery

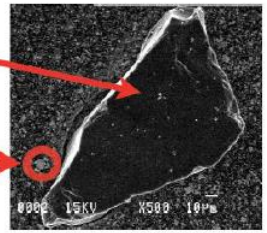

MgB_2 wire - available few months after discovery

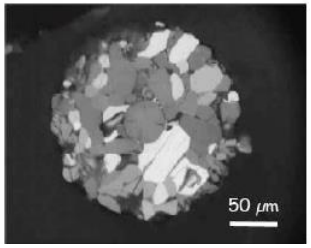

Multi-thickness domains existed in an exfoliated graphene flake

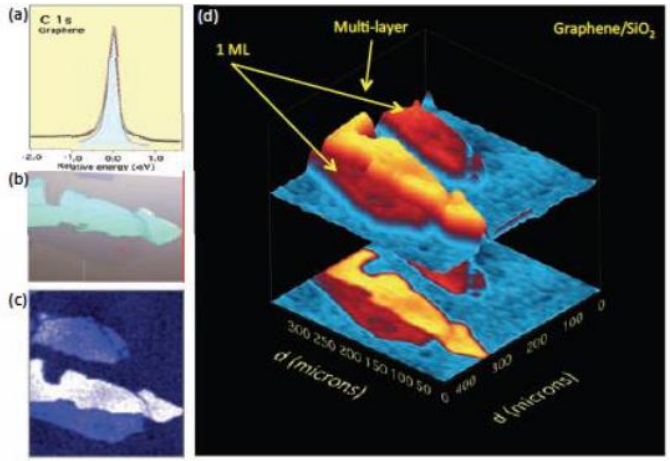

國家同步輻射研究中心
National Synchrotron Radiation Research Center

Ref : Avila, Synchrotron Radiation News (2014)

A crucial problem to understand the electronic of exfoliated graphene

Van der Waals heterostructures

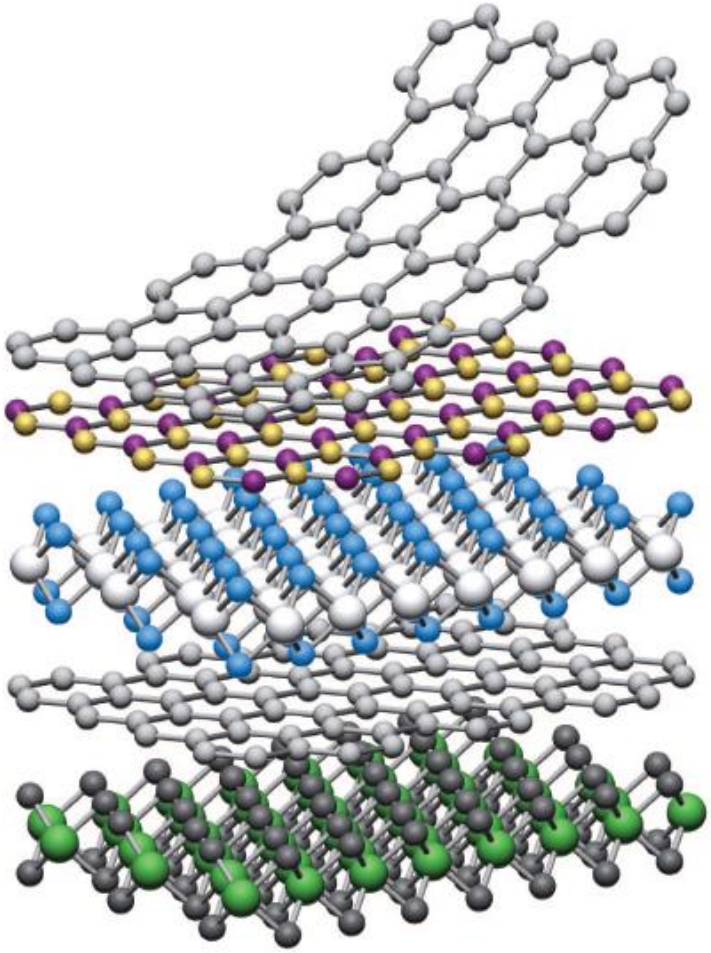

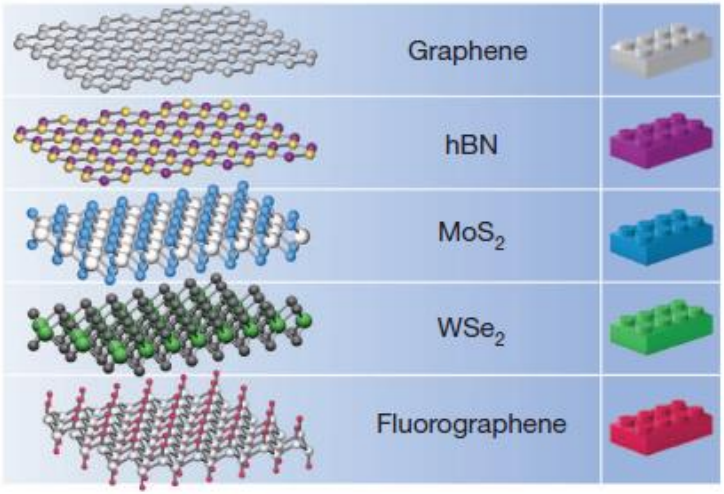

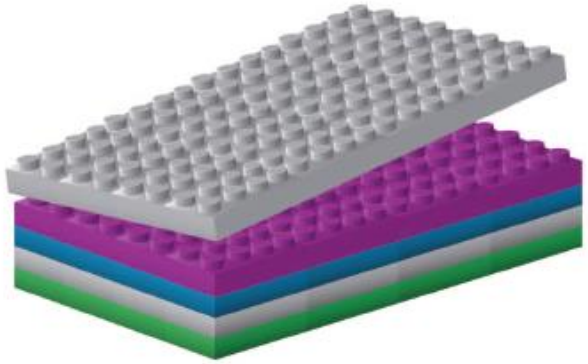

National Synchrotron Radiation Research Center

Geim, Nature (2013)

Van der Waals heterostructures

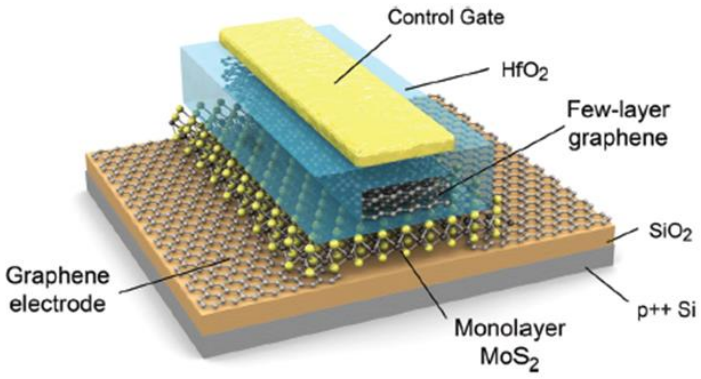

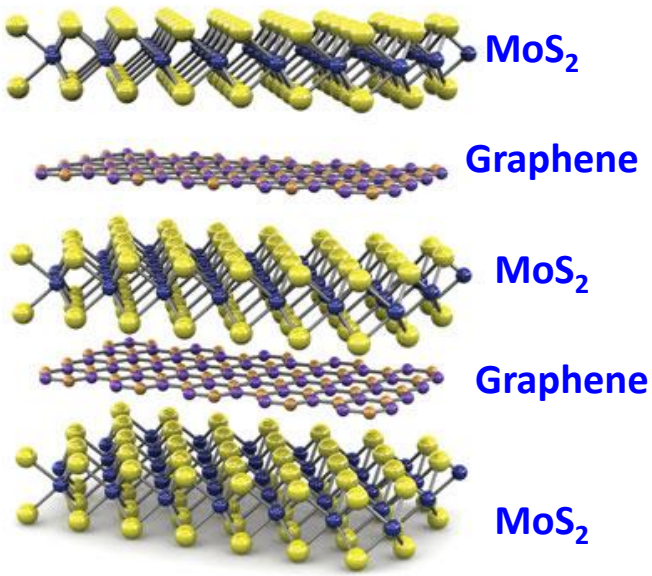

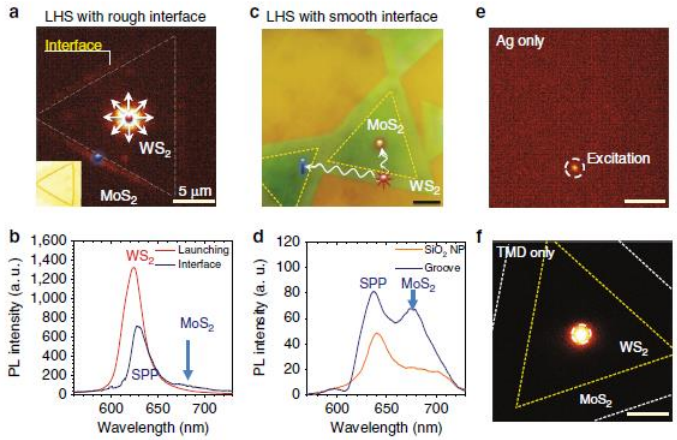

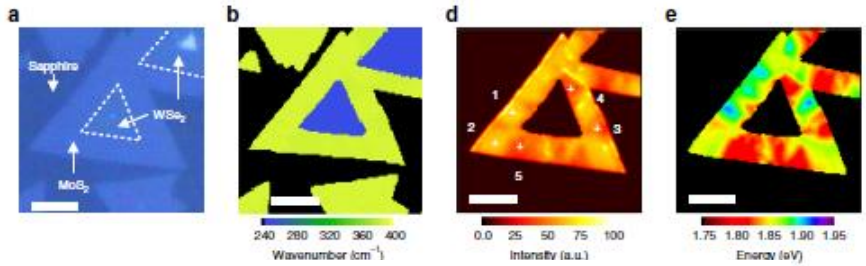

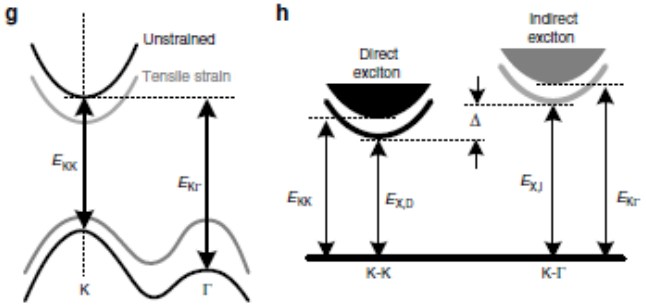

Ref : Shi et al., Nat. Comm. (2017)
Hsu et al., Nat Comm. (2017)

Material discovery

'Magic' Twist in Stacked Graphene Reveals Potentially Powerful Superconducting Behavior

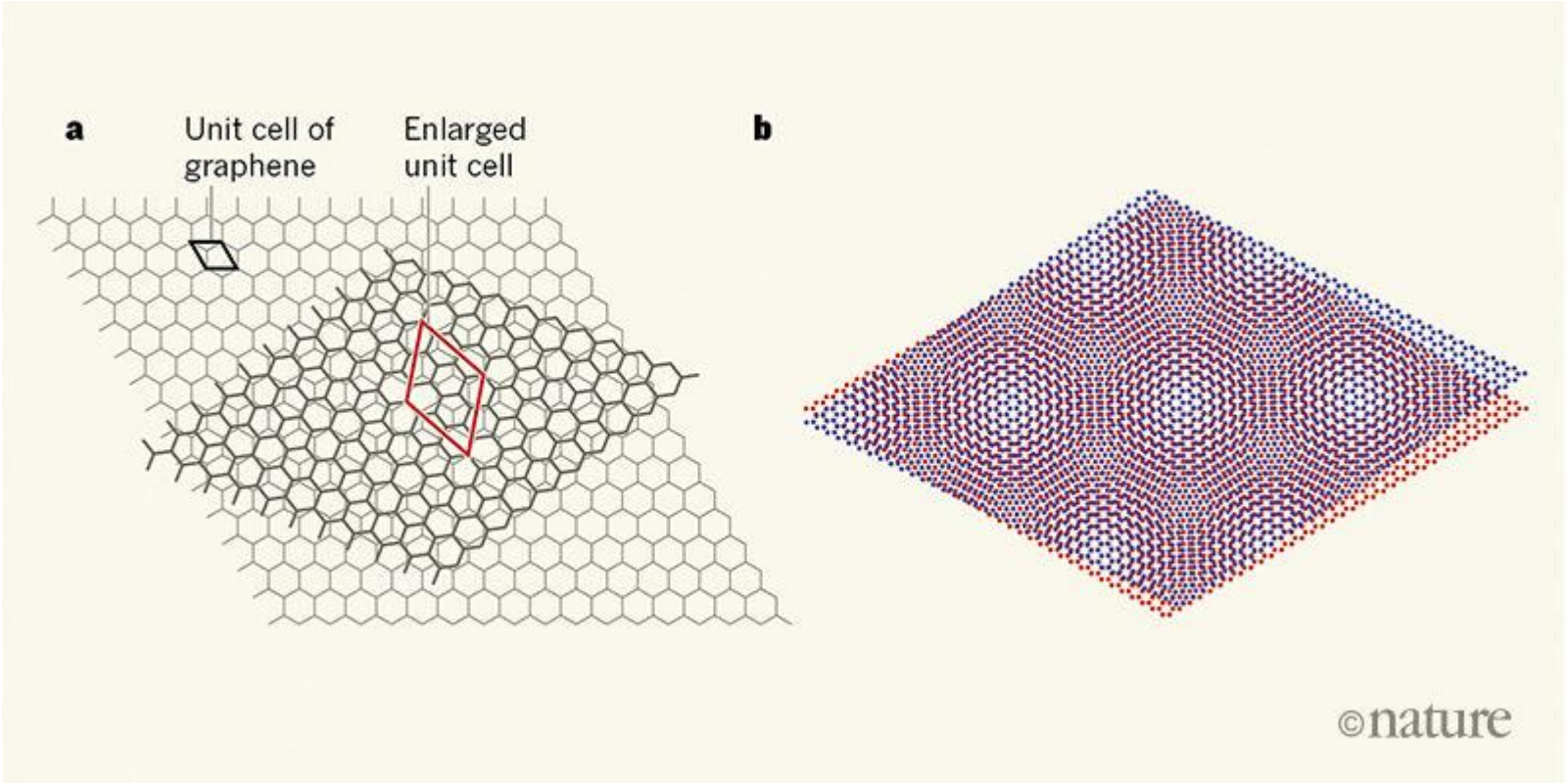

Comparison of X-ray microscopy

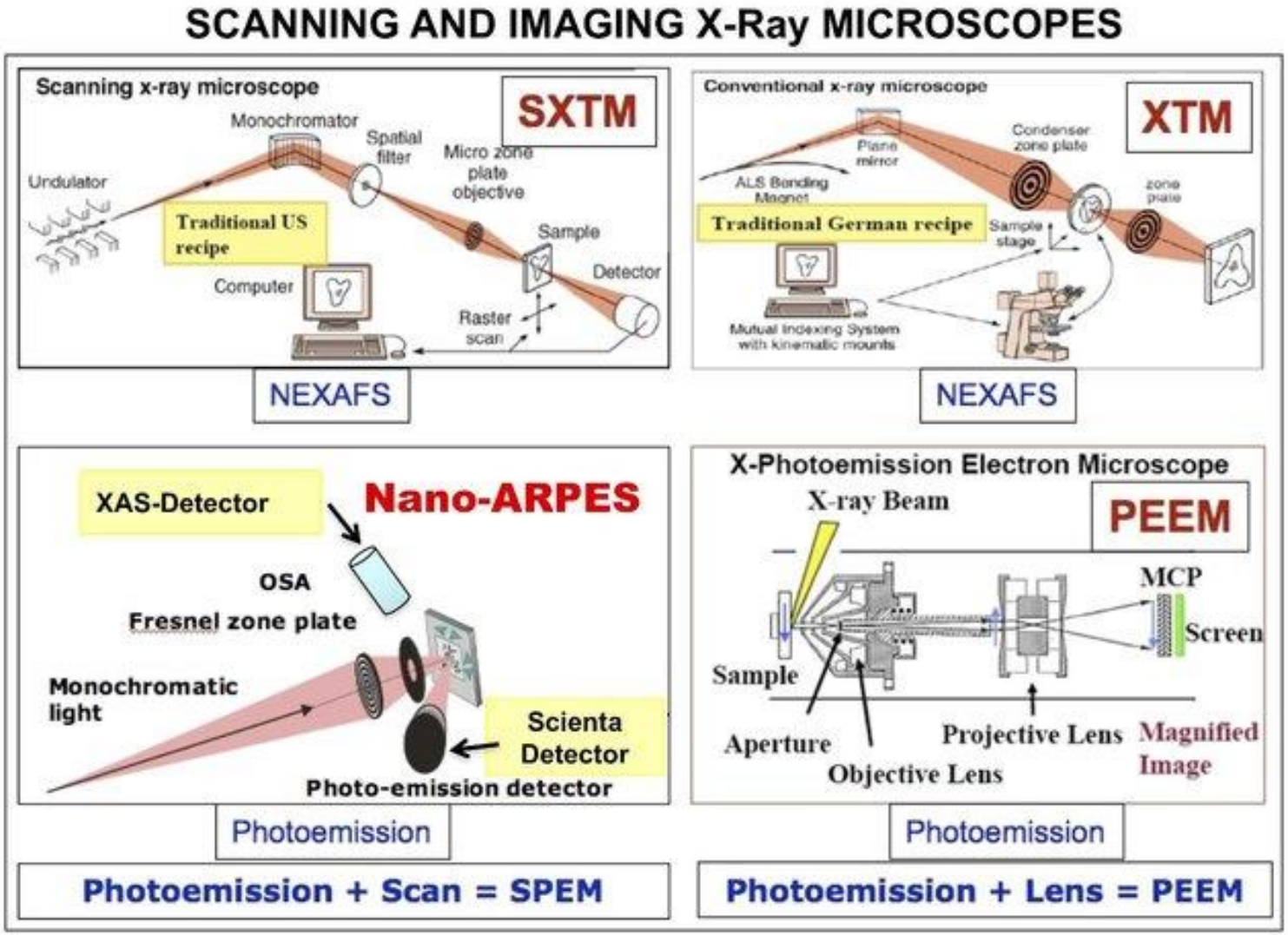

X-ray focusing optics

X-ray focusing optics:
zone plates, mirrors, capillaries

Zone Plate optics – circular grating with decreasing width: from ~ 200 to ~ 10000 eV
Monochromatic:
Resolution achieved 15 nm in transmission

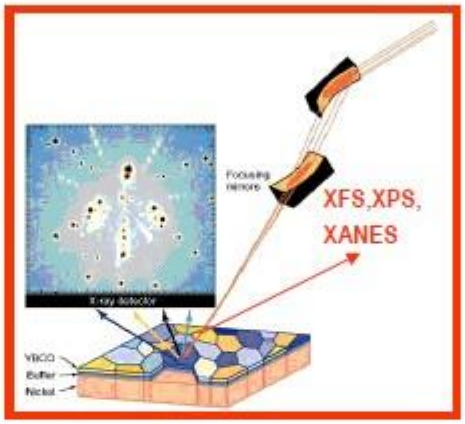

KP-B mirrors each focusing in one direction: soft & hard X-rays: ~ 100 nm
Soft & hard x-rays!
achromatic focal point, easy energy tunability, comfortable working distance
Resolution ≤ 100 nm

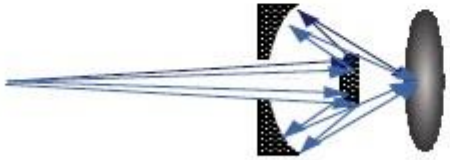

Normal incidence:
spherical mirrors with multilayer interference coating (Schwarzschild Objective)
Monochromatic, good for E < 100eV
Resolution: best ~ 100 nm

Capillary: multiple reflection concentrator

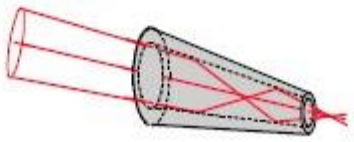

Hard x-rays ~ 8-18 keV
Resolution: > 3000 nm

Refractive lenses

Hard x-rays ~ 4-70 keV
Resolution: > 1000 nm

Capillary focusing method

- Many capillaries have a small mismatch between calculated and measured profiles near the tip.
- Cut a capillary in half and attempt to use differential deposition to smooth out inner surface.

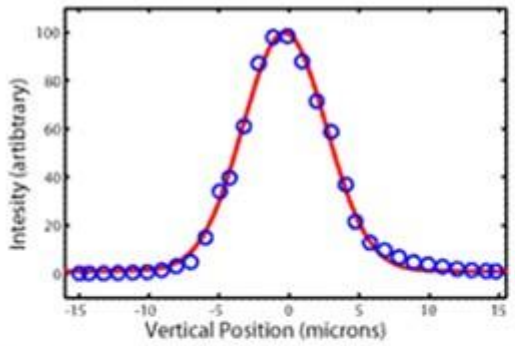

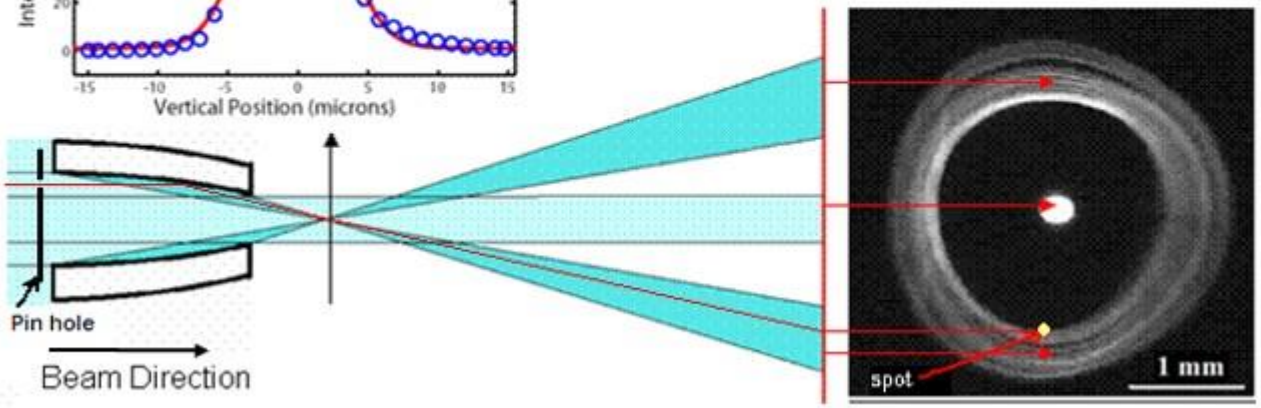

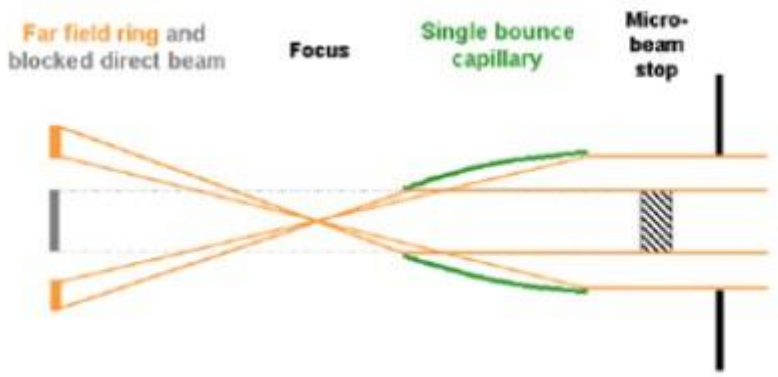

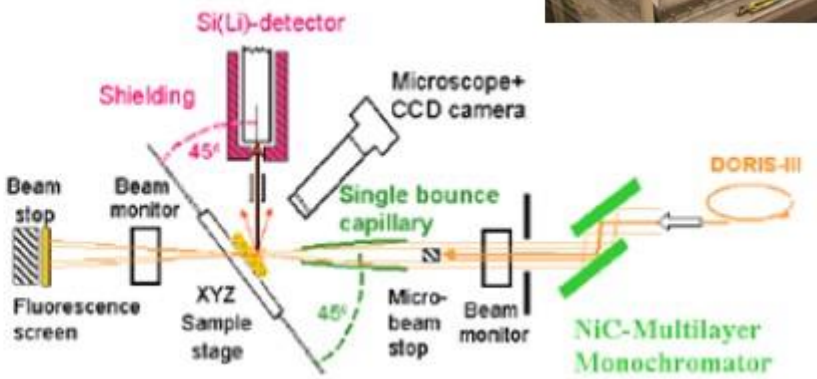

Fresnel Zone Plates

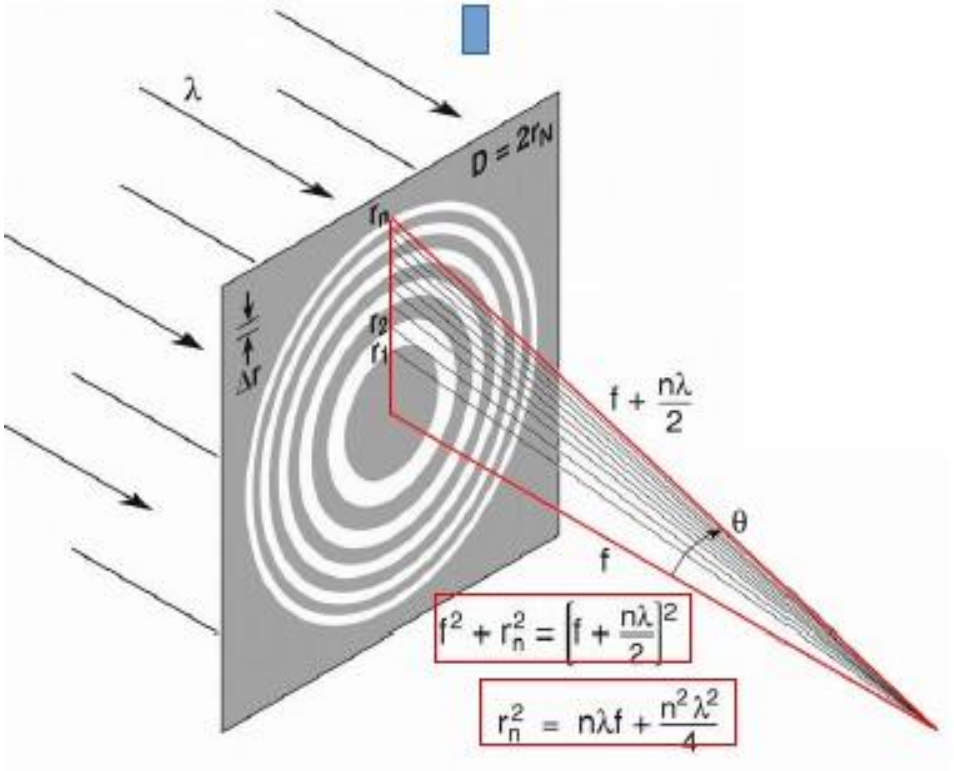

For f >> nλ/2, which corresponds to a small NA lens

$$NA = \sin\theta = \lambda/2\Delta r << 1$$

the radius of the nth zone is given by:

$$r_n \approx \sqrt{n\lambda f}$$

- A real first focus is achieved when successive zones increase in radius by $\sqrt{n}$
- FZP are highly chromatic

Fresnel Zone Plates

Relationships for f and D in terms of λ, Δr and N

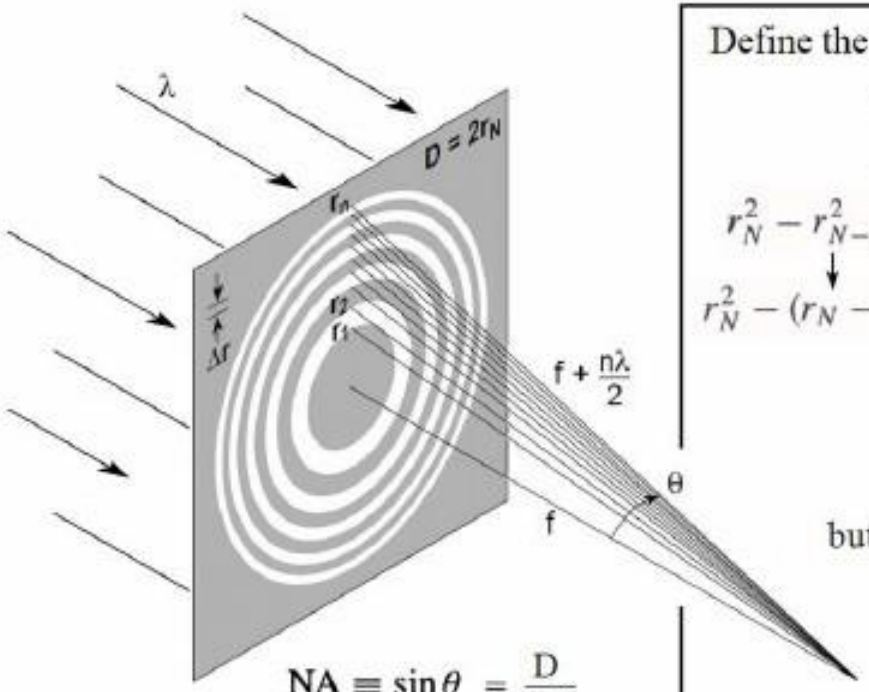

Define the outer zone width for n → N,

$$\Delta r \equiv r_N - r_{N-1} \qquad (9.11)$$

$$r_n^2 \simeq n\lambda f$$

$$r_N^2 - r_{N-1}^2 = N\lambda f - (N-1)\lambda f = \lambda f$$

$$r_N^2 - (r_N - \Delta r)^2 = 2r_N\,\Delta r - (\Delta r)^2 \simeq 2r_N\,\Delta r$$

$$2r_N\,\Delta r \simeq \lambda f$$

$$D\,\Delta r \simeq \lambda f \qquad (9.12)$$

$$\text{but } \lambda f = \frac{r_N^2}{N} = \frac{D^2}{4N} \quad \text{(from 9.10)}$$

$$\therefore\ D\,\Delta r \simeq \frac{D^2}{4N}$$

$$D \simeq 4N\,\Delta r \qquad (9.13)$$

and from (9.12) above

$$f \simeq \frac{4N(\Delta r)^2}{\lambda} \qquad (9.14)$$

$$\text{NA} \equiv \sin\theta = \frac{D}{2f}$$

$$\text{NA} \simeq \frac{\lambda}{2\,\Delta r} \qquad (9.15)$$

$$F^{\#} \equiv \frac{f}{D} \simeq \frac{\Delta r}{\lambda} \qquad (9.16)$$

Fresnel Zone Plates

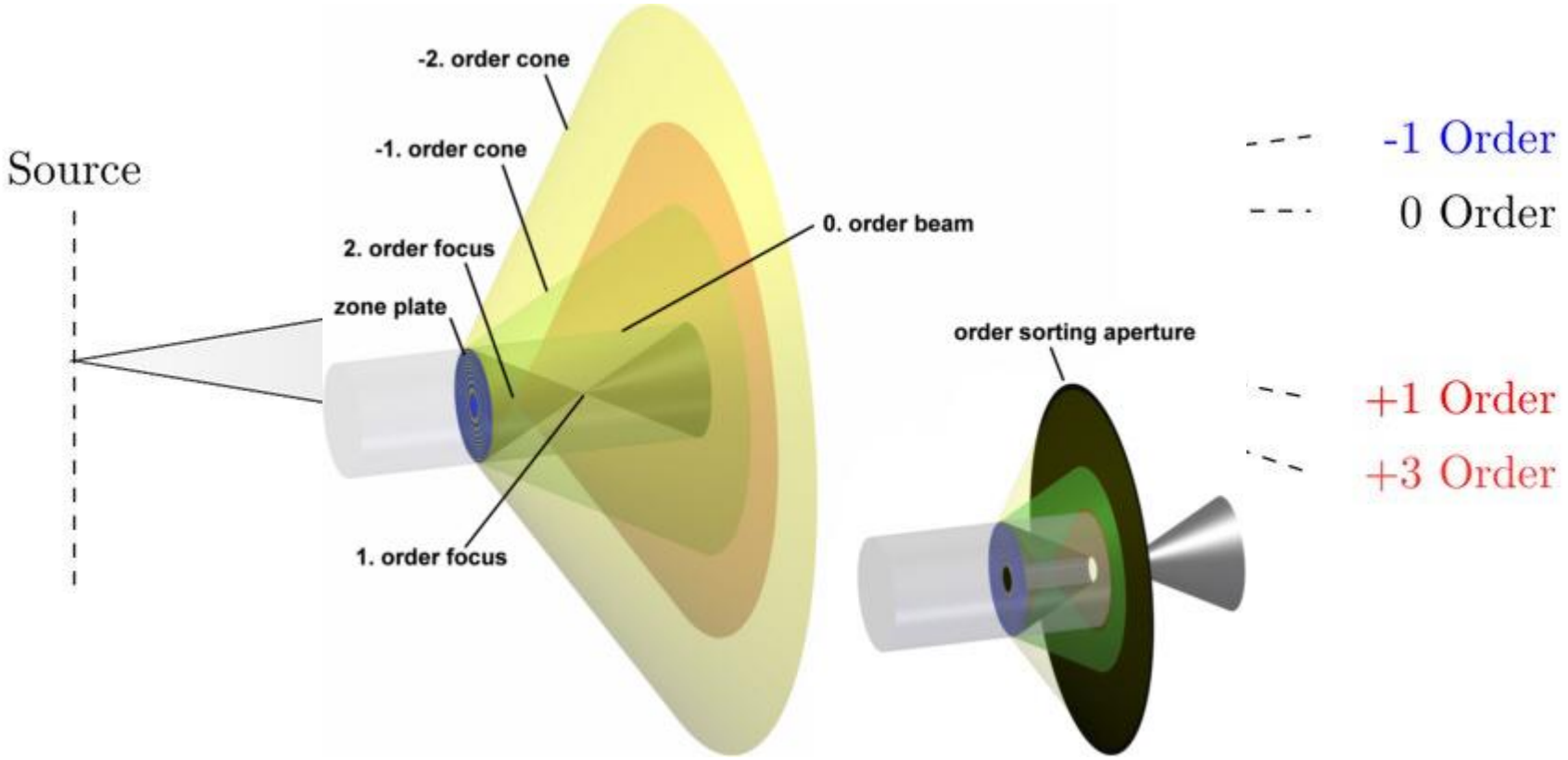

Fresnel Zone Plates

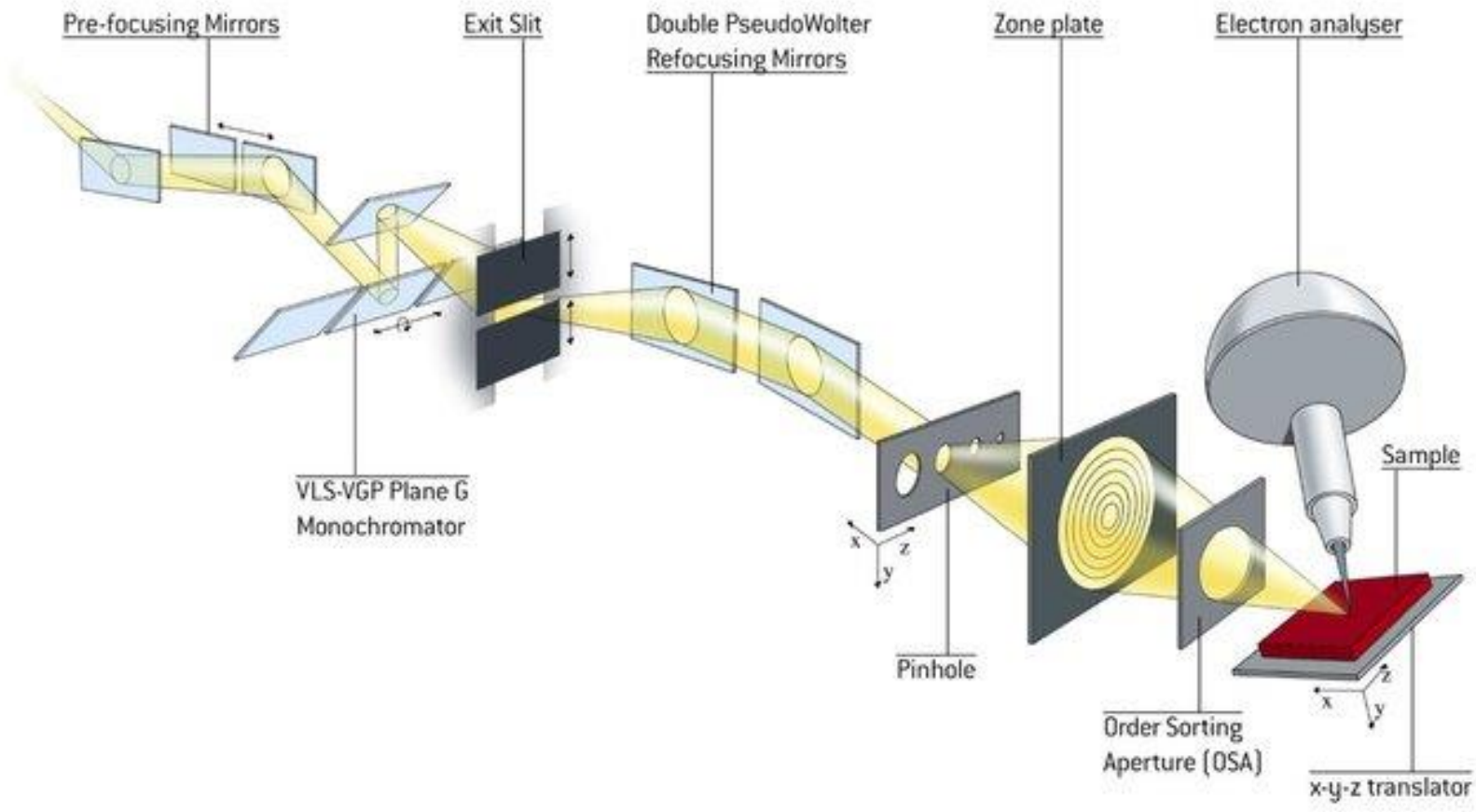

Beamlines in light sources worldwide for micro- or nano-ARPES

Light source	Micro- or nano-focusing	Energy range	Resolving power
ALS 1.9GeV MAESTRO Commissioning	KB μ-ARPES (10 x10 μm) FZP/Capillary- nanoARPES (goal 50 nm/200 nm)	60-600 eV for microfocusing	$3x10^4$ (10^4 for opt. flux)
SOLEIL 2.75GeV ANTARES	FZP (120 nm (opened for users))	95-300 eV with FZP	$2x10^4$(10-150 eV) 10^4 (>150 eV)
Diamond I05 Commissioning	FZP (700 nm)	60-150 eV	$2x10^4$
NSLS II 3GeV Construction	KB μ-ARPES (20 μm) (AP-XPS/SPEM)	15-1000 eV (200-2000 eV)	$10^5 – 10^4$
SSRF S^2-line (combination of Nano-ARPES and Spin-ARPES) (BL07U) Construction	undetermined	50 – 2000 eV	unknown

First NanoARPES facility, available at SOLEIL

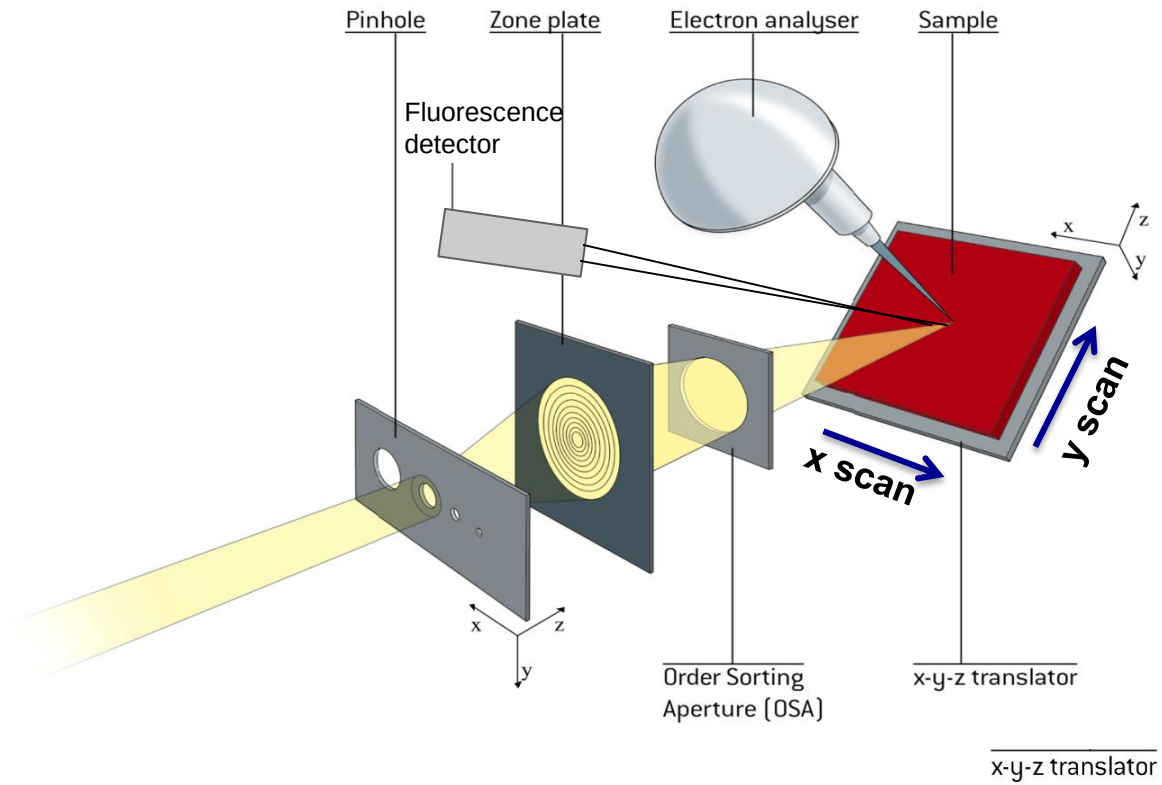

Avila, J. & Asensio, M. C. *Synchrotron Radiation News, 2014, 27, 24-30 & 2012, 25(5): 19-25*

- **Elemental specificity (Quantitative)**
- **Oxidation state Chemical information**
- **Valence Band with high momentum resolution**

Photon energy: 20 eV to 1000eV; ✔ lateral res. < 100 nm; ✔ energy res. < 0.9 meV; ✔ momentum res. @ 0.001 A^{-1} ✔

Comparison with similar leading beamlines II

MAESTRO:A a new facility for ARPES at the ALS

Aaron Bostwick

E. O. Lawrence Berkeley National Laboratory

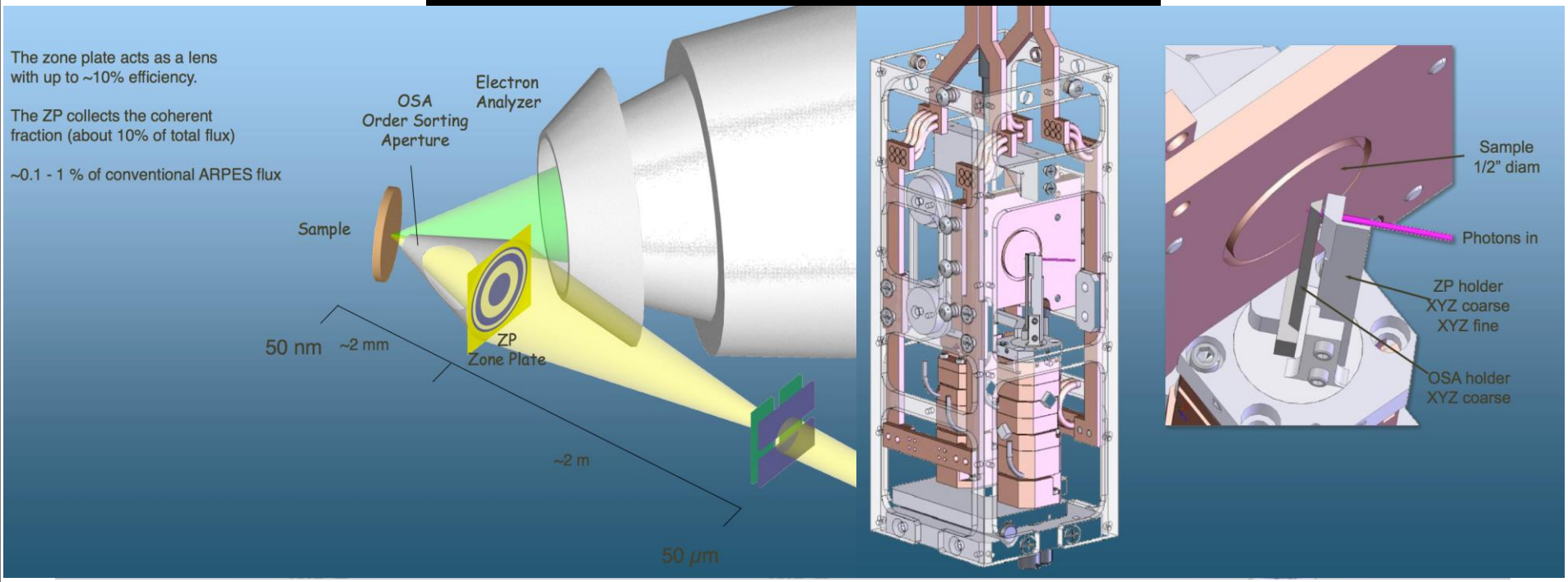

Source: Bostwick(ALS)

Comparison with similar leading beamlines III
I05 ARPES beamline at Diamond Light Source, UK

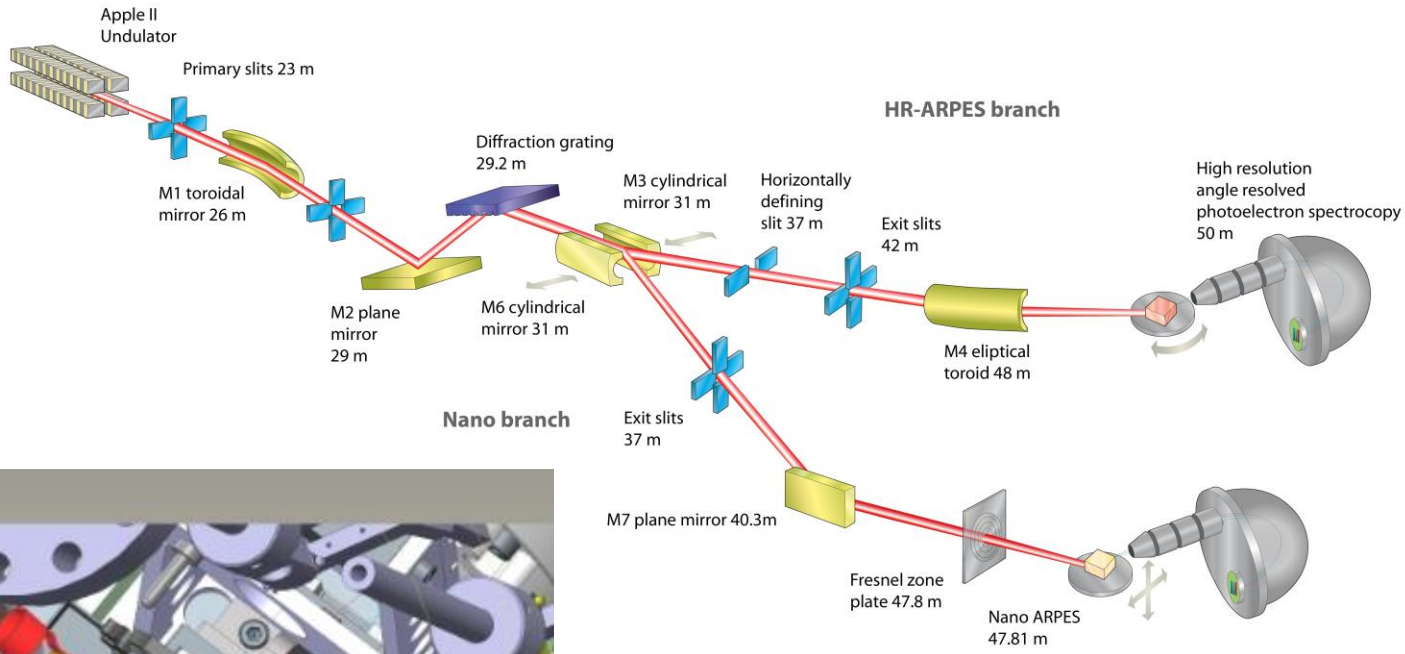

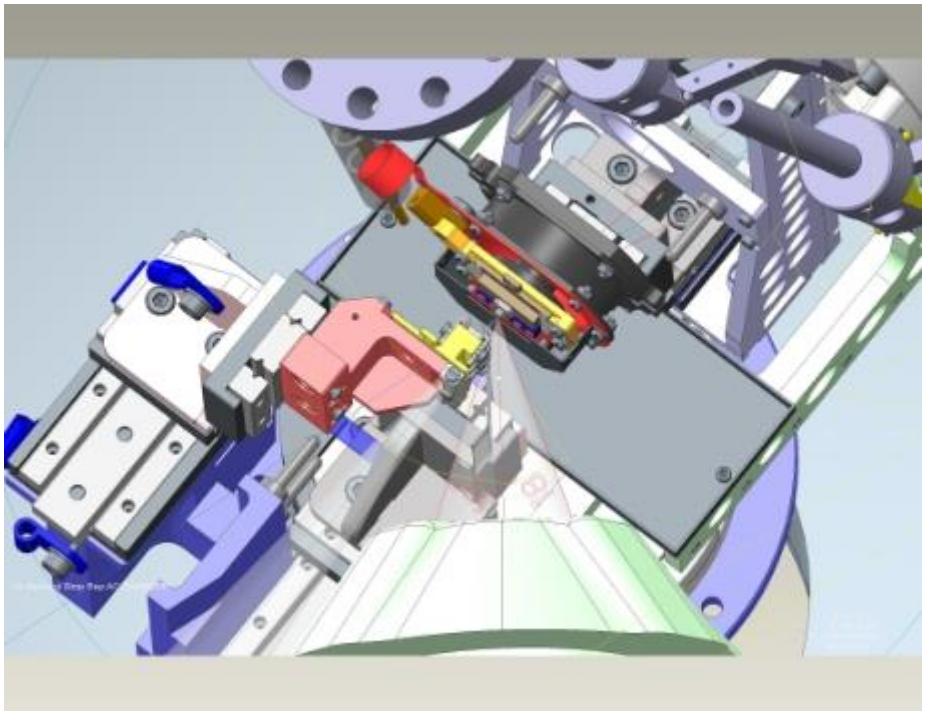

Graphene/hBN van der Waals heterostructures

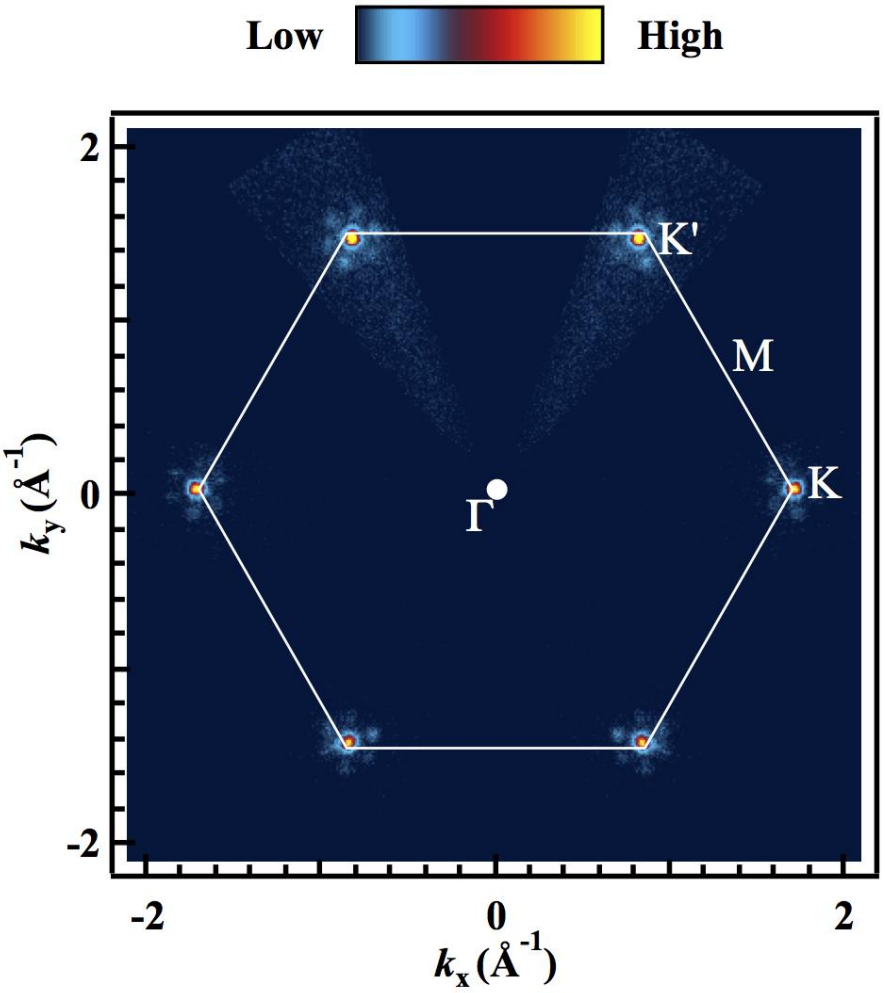

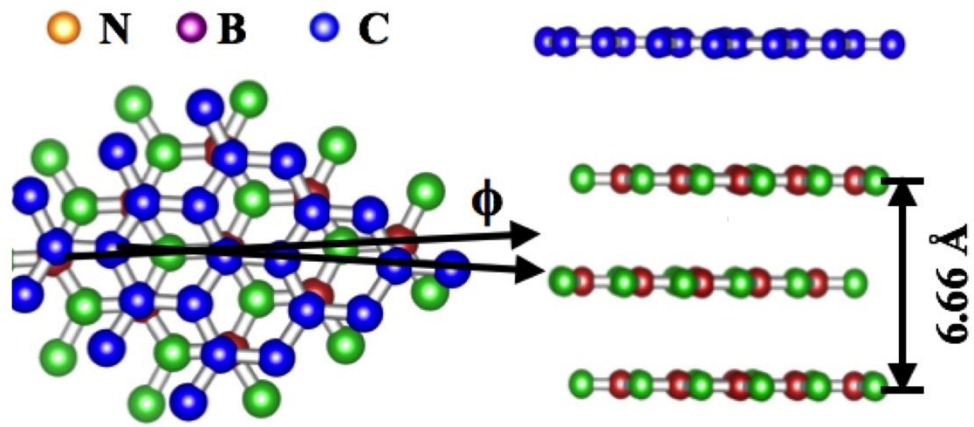

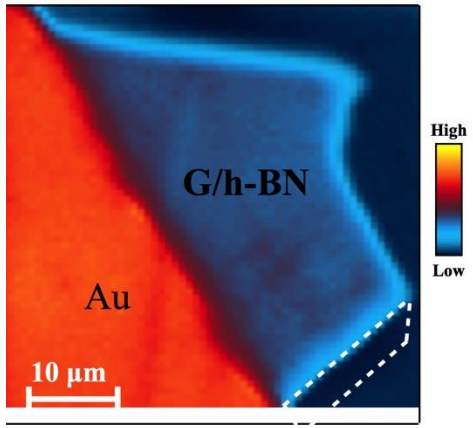

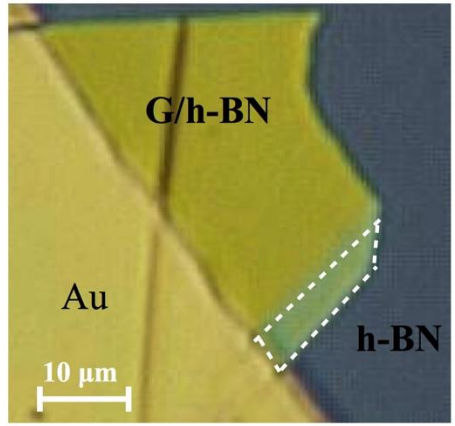

Graphene/hBN van der Waals heterostructures

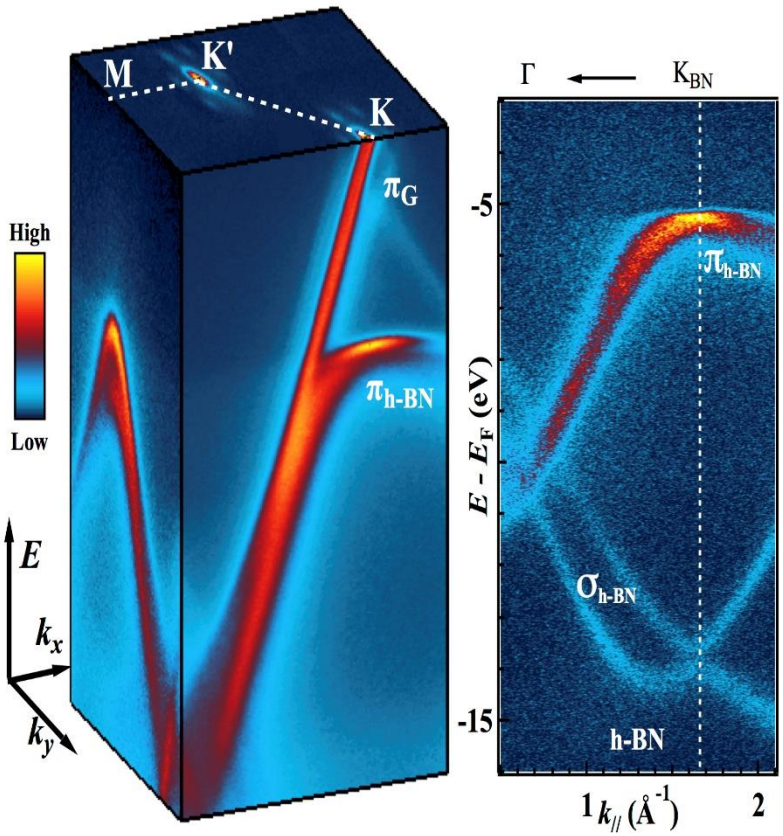

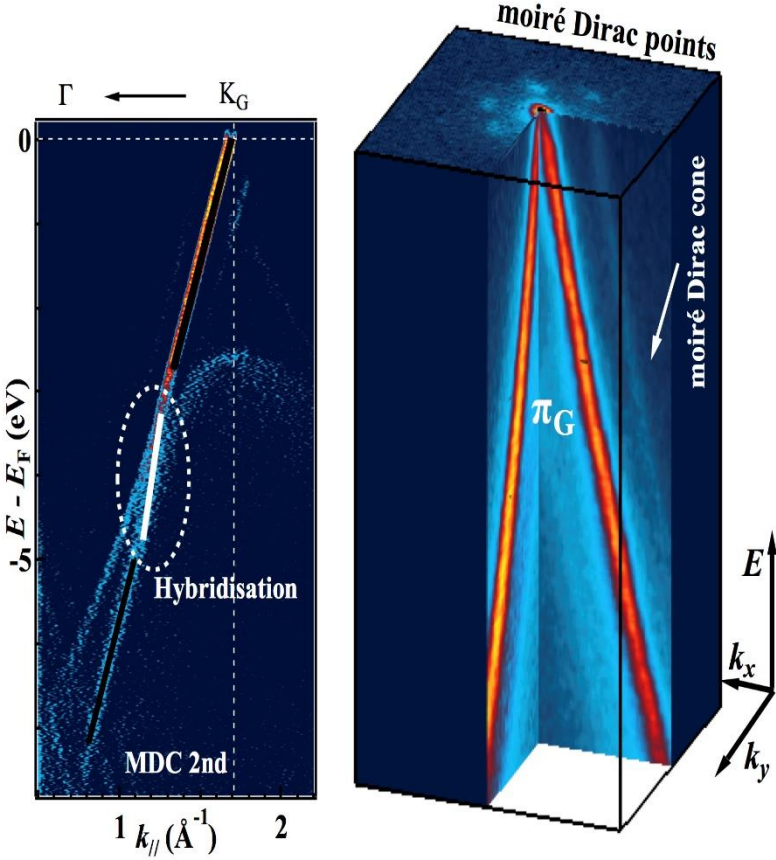

TPS 39A Nano-focus ARPES

Core techniques:

Probe the electronic structure of novel materials

- **μARPES :**
  Spatial resolution ~ 800 nm @20 eV/500nm for >50eV
- **nanoARPES (Zone plate branch)**:
  Spatial resolution ~ 50 nm

BL specification:

- Photon energy: 20 – 300 eV
- Resolving power $>10^5$
- Flux > 10^{12} ph/s with 10^4 resolving power

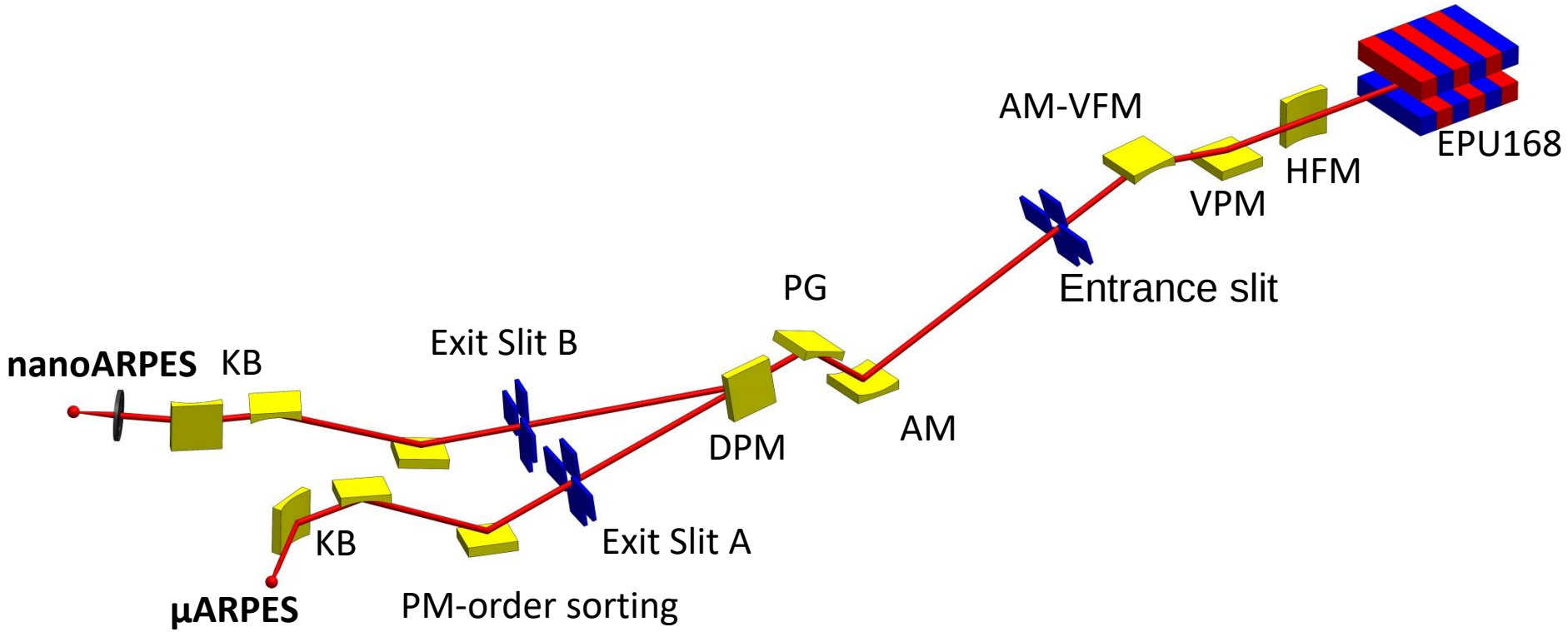

Table 1. Some typical laser light sources used in ARPES.

Laser catagory	Generation	Application	Pho. energy (eV)	Pulse width (ps, fs)	Rep. rate (kHz, MHz)	Max.Pho. flux (photons s^{-1})	Energy res. (meV)	Tem. Res. (fs)	References	Remarks
Quasi-CW	NLO crystal SFG+SHG	High-res ARPES	7	~10 ps	80 MHz	1.5×10^{15}	0.26 meV	/	Liu *et al* [21]	(a)
			6	~70 fs (seed)	100 MHz	$\sim10^{15}$	4.7 meV	/	Koralek *et al* [20]	(b)
			7	~10 ps	120 MHz	Unknown	0.025 meV	/	Okazaki *et al* [186]	(c)
			5.3–7	5 ps	76 MHz	$\sim10^{14}$	Unsecified	/	Jiang *et al* [87]	(d)
CW	NLO crystal SFG+SHG	High-res ARPES	6.05	Infinite	Infinite	1×10^{15}	0.01	/	Tamai *et al* [37]	(e)
			6.49	Infinite	Infinite	1.25×10^{15}	$\sim10^{-7}$ meV	/	Scholz *et al* [54]	(f)
Pulsed laser	NLO crystal SFG+SHG	Tr-ARPES	1.5,6	50 fs, 160 fs	80 MHz	Unspecified	<22 meV	163 fs	Sobota *et al* [41]	(g)
			1.5,6.04	35 fs, 55 fs	250 kHz	$\sim10^{13}$	40 meV	65 fs	Faure *et al* [40]	
			1.48, 5.92	170 fs,-	250 kHz	Unspecified	⩾10.5 meV	⩾240 fs	Ishida *et al* [149]	
HHG	Noble gas HHG	Tr-ARPES	1.58, 15–40	40 fs, 100 fs	10 kHz	3.6×10^{17}	90 meV@35.6 eV	125 fs	Frietsch *et al* [43]	(h)
			1.6, 22.1	30 fs, 11 fs	10 kHz	Unspecified	170 meV	13 fs	Rohde *et al* [42]	(i)
			1.57, 20.4	30 fs	1 kHz	Unspecified	Unspecified	30 fs	Petersen *et al* [31]	
Mod./ Reson. type HHG	Mixed rare gas	High-res ARPES	10.5	10 ps,	0.2–8 MHz	9×10^{12}	<1 meV	/	Berntsen *et al* [75]	(j)
			10.9	100 ps,	1–20 MHz	$\times10^{13}$	<2 meV	/	Yu He *et al* [76]	(k)
FEL	Long undulator	Tr-ARPES	26–300	30–150 ps	<10 Hz	Very high	300 meV	700 fs	Hellmann *et al* [59]	

Method to generate VUV light

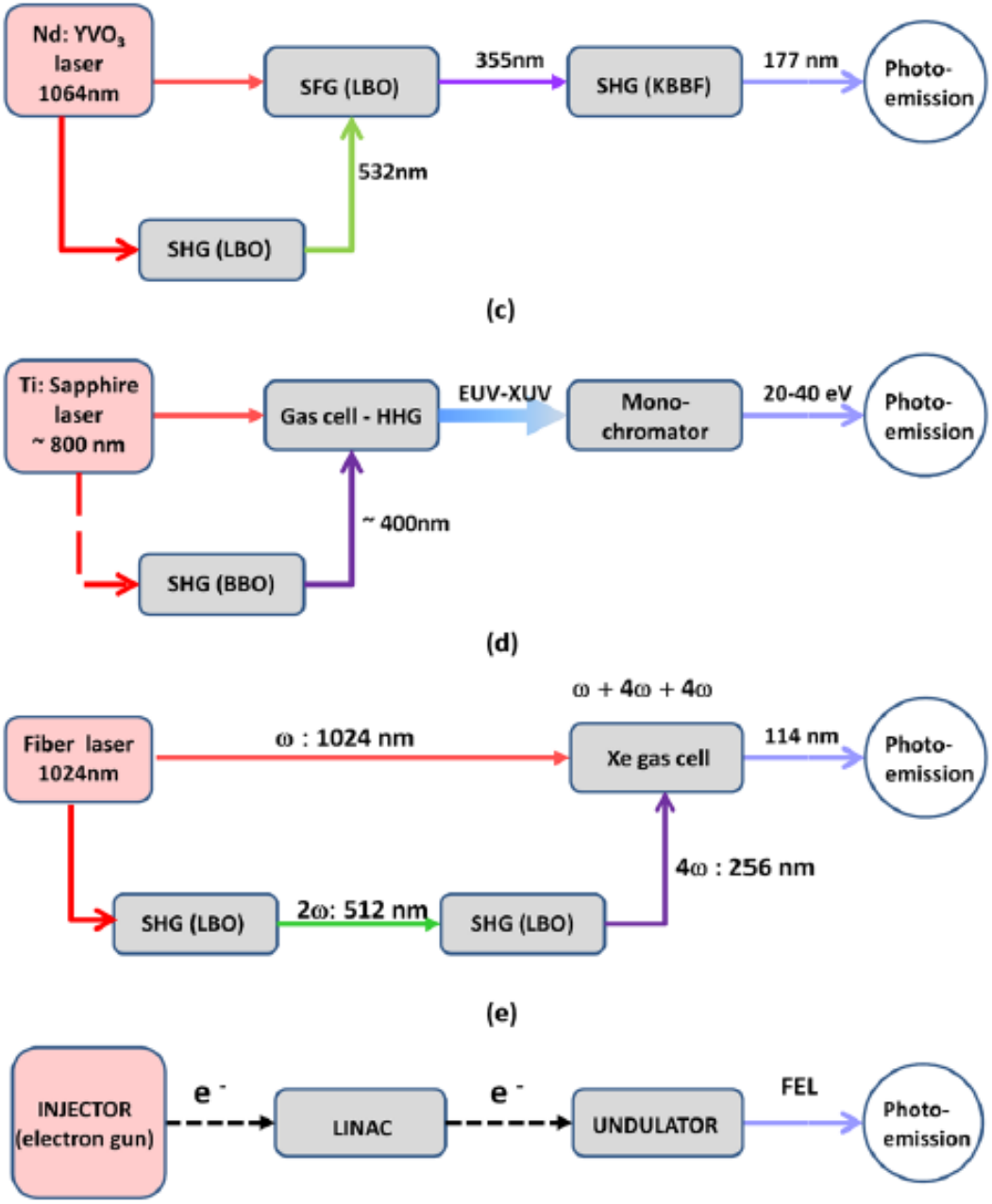

Tr-ARPES system in NSRRC

- Laser source:
  Turn key Yb:KGW laser, fundamental 1030 nm, 190 fs.
- **Probe**: Kr (6 kHz), photon energy 25.7-32.9 eV
  Ar (10 kHz) , photon energy 34.8-44.4 eV
  photon flux in the order of 10^9 photons/sec
  beam size: 100 micro in diameter
- **Pump**: 1.2 eV/ 2.4 eV
  variable power density 1-13 mJ/cm^2
- Variable **polarization LV/LH** for both pump and probe beam
- Temporal resolution ~ **230 fs**
- Energy resolution ~**90 meV at 300 K**

Tr-ARPES preliminary results

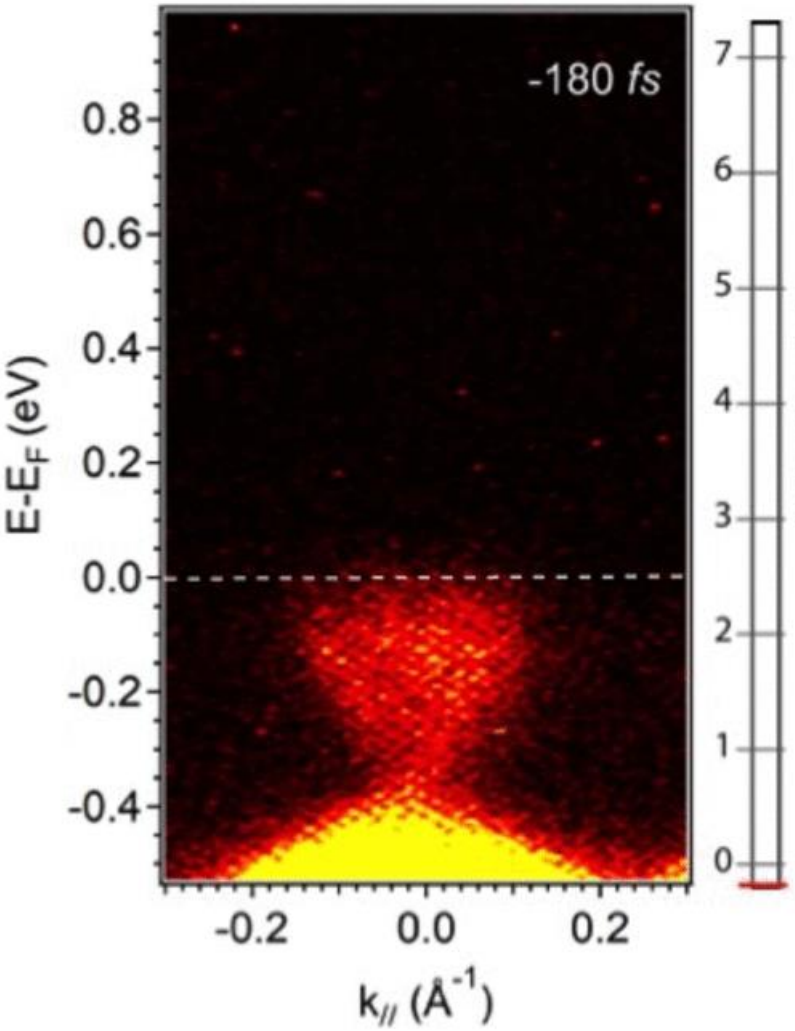

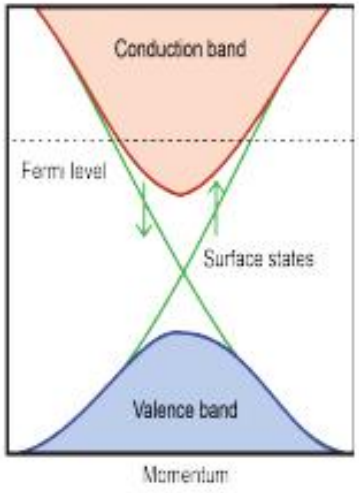

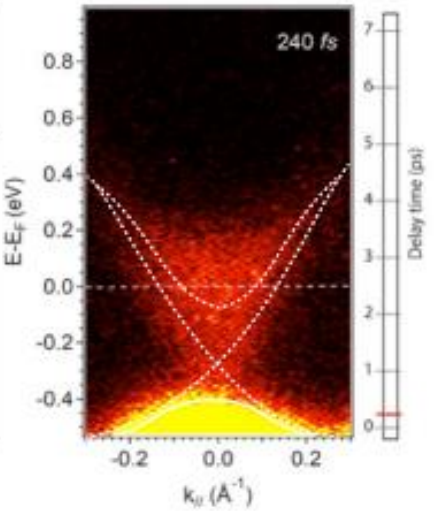

Summary

- ARPES can provide a deeper insight for the understanding of electronic property in 2D materials.
- A combination with other tools, such as XPS, XAS, STM, pump-probe experiment …etc., can establish better model to explain novel phenomena in emergent materials
- A cooperation with theorists is necessary for ARPES guys.
- Hungry for high quality single crystal or thin film


Thanks for your attention